Characterisation of *Leishmania major* metacaspase

Audrey Ambit

A thesis submitted in the fulfilment of the requirement for the degree of Doctor of Philosophy in the Faculty of Veterinary Medicine, University of Glasgow

Division of Infection and Immunity
Wellcome Centre for Molecular Parasitology
Glasgow Biomedical Research Centre
University of Glasgow
Scotland, United Kingdom

December 2006

Abstract

Metacaspases are distant orthologues of mammalian caspases and have been proposed to play a role in programmed cell death in yeast and plants, but little is known about their function in parasitic protozoa. In this study, I found that the single *MCA* gene of *Leishmania major* (*LmajMCA or MCA*) is expressed in actively replicating amastigotes and promastigotes, whereas expression level is significantly lower in non-dividing stationary phase promastigotes. In order to determine the role of the metacaspase during promastigote division, an analysis of the events of the *L. major* cell cycle was performed. Based on these findings, immunofluorescence experiments revealed the presence of LmajMCA in punctate structures throughout the cytoplasm of interphase cells and its accumulation in the kinetoplast (mitochondrial DNA) at the time of the organelle's segregation. LmajMCA also translocates to the nucleus during mitosis, where it associates with the mitotic spindle. *LmajMCA* null mutants could not be generated using standard gene deletion techniques. When LmajMCA was expressed from an episome, the only mutants that were viable were those expressing LmajMCA at physiological levels. Over-expression of LmajMCA in promastigotes leads to changes in ploidy and a severe growth retardation, associated with defects in kinetoplast segregation and nuclear division and an impairment of cytokinesis. Several LmajMCA variants lacking their N-terminal and/or C-terminal domains or with active site mutation(s) (C201G, C201-C202G, C202G, H147A) were expressed, with or without tags, in *L. major* promastigotes, in *Escherichia coli*, in the yeast *Pichia pastoris*, and using an *in vitro* translation kit. In all the systems used, the expression of most LmajMCA variants was barely detectable and was apparently toxic for the host cells. Some encouraging results were obtained using *P. pastoris*, with the expression and secretion in the culture medium of N- and C-terminally truncated LmajMCA. Thus, this system may facilitate production of sufficient enzyme for the characterisation of the biochemical properties of LmajMCA. Insights into the putative function of the different domains of LmajMCA were gained when it was observed, that the first 101 N-terminal amino acids of LmajMCA worked, in *L.major*, as a mitochondrion targeting signal. A potential role of the LmajMCA proline-, glutamine- and tyrosine-rich C-terminal domain in protein-protein interactions was also hypothesized. Together these data suggest that LmajMCA is essential for the correct segregation of the nucleus and kinetoplast and cytokinesis and that the tight regulation of the amount of LmajMCA within the cell is crucial for the development of *Leishmania* promastigotes.

Trypanosoma brucei possesses five metacaspase genes. Two of the encoded proteins, TbMCA1 and TbMCA4, possess substitutions at their putative active site residues and thus might lack peptidase activity. Therefore functional studies were

performed only on the three other metacaspases. Triple RNAi analysis showed TbMCA2, TbMCA3 and TbMCA5 to be essential in the bloodstream form, with induced parasites showing a delay in kinetoplast segregation and being blocked in pre-cytokinesis. Triple null mutants (*ΔTbmca2/3ΔTbmca5*) were found to be initially affected in their development, but recovered after several weeks of *in vitro* adaptation. The initial slow growth rate of the *ΔTbmca2/3ΔTbmca5* mutant was associated with a delayed entry in cytokinesis. This phenotype was similar, although less extreme, to that produced upon triple RNAi of *Tb*MCA2, *Tb*MCA3 and *Tb*MCA5. These data suggest that these metacaspases are essential for *T. brucei* bloodstream forms, but they have overlapping functions and their progressive loss can be compensated for by activation of alternative biochemical pathways. Analysis of *ΔTbmca2/3ΔTbmca5* revealed no greater or lesser susceptibility to stresses reported to initiate programmed cell death, such as treatment with prostaglandin D_2. These metacaspases co-localise with RAB11, a marker for recycling endosomes but variant surface glycoprotein (VSG) recycling processes and the degradation of internalised anti-VSG antibody were found to occur similarly in wild type, *ΔTbmca2/3ΔTbmca5* and triple RNAi-induced parasites. Thus the data provide no support for the direct involvement of *T. brucei* metacaspases in programmed cell death and suggest that the proteins have a function associated with RAB11 vesicles that is independent of known recycling processes of RAB11-positive endosomes.

As both the *L. major* and the *T. brucei* metacaspases appear to play crucial roles in cell cycle progression and because metacaspases are absent from the mammalian genome, these metacaspases have potential as novel drug targets.

Table of Contents

List of Tables

List of Figures

To my beloved parents and grandparents.

A mes bien-aimés parents et grands-parents.

Acknowledgements

First of all, I would like to warmly thank Professors Jeremy Mottram and Graham Coombs for giving me the opportunity of doing a PhD in their laboratory, by the way fulfiling one of my childhood dreams. I never thought I will be able to undertake such a Herculean task, but thanks to Jeremy and Graham's supervision, I reached final achievement. Also, I would like to thank my previous supervisors and colleagues at the Université de Bordeaux II, in France, Gilles Merlin, Frédéric Bringaud, Norbert Bakalara, and Derrick Robinson, for insinuating their passion of parasitology in me and sharing their inexhaustible knowledge. To all of them, thanks for believing in me.

My PhD but most generally my stay in Scotland was a great experience and even though I went through some tough times (like every PhD student does!), I learned a lot during these three years both at a spiritual and emotional level. First of all, I discovered that the sun so sorely missed in the Scottish sky is warmly present in the heart of every Scottish I met. For that and also for good time spend in the lab or in a pub, I would like to thank Lesley, Elaine, Caroline, Karen, Jim, Rod Walker, Alex, Richard, Chris, Annette, Liam and all the other Scots I forgot to cite. But I will not forget the kindness from Matt and Kirsteen, Kerry and Alex, Nick, Tansy, Cathy, Christina and Richard, Mike, Clare, Zoe, Saj, Pauline, Simon, Miriam, Mary... Thanks to Séverine, Svenja, Jane, Claire, Sylvia and Tomas for sharing their office with me, I enjoyed your company.

Being in the internationally renowned University of Glasgow, I also had the chance to meet exceptional people from all over the world. And even though I stayed in Glasgow I had the feeling that I travelled a lot and discovered many fascinating cultures and ways of life. I found that, when coming to Scotland, foreigners carry their sun with them. During the dark and rainy Glaswegian winters and the "wintery" summers, I greatly appreciated warmth shared around a nice meal or simply a drink with Alvaro and Veronica, Felipe and Vaso, Tomas and his family, Walide and his family, Lucio, Colin, Maria, and all the foreign students and friends that came in the lab. Thank to Sylke Muller and everybody from her lab as well as people from Graham's group. I also would like to thank the small group of "irréductibles Gaulois" from Christian Doerig's lab and also Marie and Marcello, Claire and Vincent, Leila and Mario, Hubert and Aobhinn, Nadia, Aude and Isabelle for giving me the feeling that home was never far!

Now I would like to give my eternal love and gratitude to my family for always being close to me even when we were thousand of kilometres apart and for always accepting my choices even when they meant being separated. I learned that the heart ties become stronger during difficult times and discovered how lucky I was to possess such a loving family. Merci à Dany et Jean-Pierre, Sabrina et Fabien, Christy, Valérie et toute sa famille ainsi que tous mes autres oncles, tantes, cousins, cousines, petit cousins et petites cousines pour leur soutien et encouragements. A Baptiste, merci d'être le meilleur petit frère qu'une grande soeur puisse avoir. Je suis fière de toi et serai toujours ta plus fervente admiratrice et supportrice. Je te souhaite tout le bonheur du monde avec ta charmante Aurélie. Merci à nos amis et à la famille de Sébastien pour ne pas avoir hésité à franchir des milliers de kilomètres pour passer de bons moments avec nous. J'espère que nous en partagerons beaucoup d'autres. En cette période d'accomplissement mes pensées vont à mes chers et tendres grands-parents qui nous ont quittés bien trop tôt et me manquent toujours cruellement. Par dessus tout, je tiens à remercier mes parents pour être les meilleurs parents dont on puisse rêver. Votre compréhension, soutien et amour sans limites sont mes forces. Vous êtes mes mentors et mes idoles. Je vous aime. Et enfin, dans les eaux tumultueuses que sont les années de thèse, je tiens à remercier mon phare, ma bouée de sauvetage, Sébastien qui m'a permis de garder la tête hors de l'eau et d'arriver à bon port en me sentant grandie de cette extraordinaire expérience. Ton soutien aussi bien au plan professionnel qu'affectif m'a été indispensable et je t'en serai à jamais reconnaissante. Du plus profond de mon être, je t'aime.

Author's Declaration

The research reported in this thesis is the result of my own original work, except where stated otherwise, and has not been submitted for any other degree.

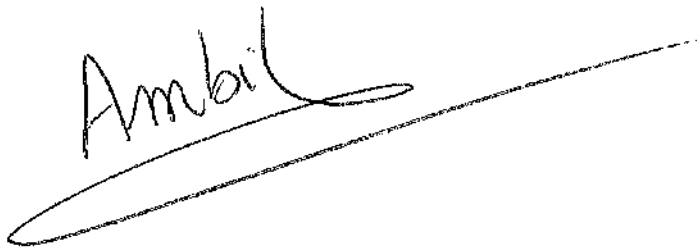

Audrey Ambit

December 2006

List of Abbreviations

AMC	7- amino-4-methylcoumarin
BSA	Bovine serum albumin
DABCO	4-diazabicyclo[2.2.2]octane
DAPI	4',6-diamidino-2-phenylindole
DMSO	Dimethyl sulphoxide
EDTA	Ethylenediaminetetraacetic acid
EGTA	Ethyleneglycol-bis(b-aminoethylether)-*N*,*N*,*N'*,*N'*-tetraacetic acid
ECL	Enhanced chemiluminescence
FITC	Fluorescein isothiocyanate
h(s)	hour(s)
HRP	Horseradish peroxidase
IgG	Immunoglobulin G
IPTG	Isopropyl-ß-D-thiogalactopyranoside
LB	Luria-Bertani medium
min(s)	minute(s)
PBS	Phosphate-buffered saline
PCR	Polymerase chain reaction
PVDF	Polyvinylidene Fluoride
SDS	Sodium dodecyl sulphate
SDS-PAGE	SDS-polyacrylamide gel electrophoresis
sec(s)	seconde(s)
SSC	Salt sodium citrate buffer
TRIS	Tris [hydroxymethyl] aminomethane
Triton X-100	t-Octylphenoxypolyethoxyethanol
Tween-20	Polyoxyethylene sorbitan monolaurate
X-Gal	5-bromo-4-chloro-3-indolyl-ß-[D]-galactopyranoside

Chapter 1:
Introduction

1.1. *Leishmania*

1.1.1. Leishmaniasis causative agent

Leishmania are parasitic protozoa belonging to the Kinetoplastidae order and the Trypanosomatidae family. They are the causative agent of leishmaniasis. More than 20 species and subspecies of *Leishmania* can infect humans. The induced symptoms, which are species-specific, range from self-healing skin ulcers to severe life-threatening disease. The leishmaniasis can be classified into 4 main clinical forms (**figure 1.1**):

1. Localised cutaneous leishmaniasis (LCL), the most common form, causes skin lesions which usually self-heal within a few months, but which leaves unsightly scars. In Asia and Africa, where it is mainly due to *Leishmania major*, this disease is commonly termed Baghdad ulcer, Delhi boil or Bouton d'Orient. *Leishmania mexicana* is mainly responsible for New World cutaneous leishmaniasis.

2. Mucocutaneous leishmaniasis (MCL) starts with skin ulcers but rapidly becomes a disfiguring affliction, causing massive destruction of the nose and mouth tissues. In the New World, it is due to *Leishmania braziliensis* subspecies: mainly *L. b. braziliensis*, but also *L. b. panamensis*, *L. b. guyanensis* and *L. b. peruviana*.

3. Diffuse cutaneous leishmaniasis (DCL) produces disseminated and chronic skin lesions comparable to those of leprosy and is particularly difficult to treat. It is a pathology observed with *L. amazonensis* and *L. aethiopica* infections, but which can also be attributed to *L. major*, *L. b. braziliensis* and *L. b. guyanensis* for immunodeficient patients.

4. Visceral leishmaniasis (VL) is the most serious form and is fatal in 90% of cases if left untreated. *L. donovani* is the primary cause of human visceral leishmaniasis (known as Kala azar) in the Indian subcontinent and East Africa. In the Mediterranean region and in the New World, *L. infantum* and *L. chagasi*, respectively, are responsible mainly for canine visceral leishmaniasis but also for some human disease.

Leishmaniasis is a worldwide disease, endemic in 88 countries: 72 of these are developing countries and 13 are amongst the least developed. More than 90% of cutaneous leishmaniasis cases occur in 7 countries: Afghanistan, Algeria, Brazil, Iran, Peru, Saudi Arabia and Syria. More than 90% of visceral leishmaniasis cases occur in 5 countries: Bangladesh, India, Nepal, Sudan, and Brazil (**figure 1.1**). Every year 1 to 1.5 millions cases of cutaneous leishmaniasis and 500 000 cases of visceral leishmaniasis are declared. But it is estimated that 12 million people are infected and 350 million people are at risk (www.who.int/tdr).

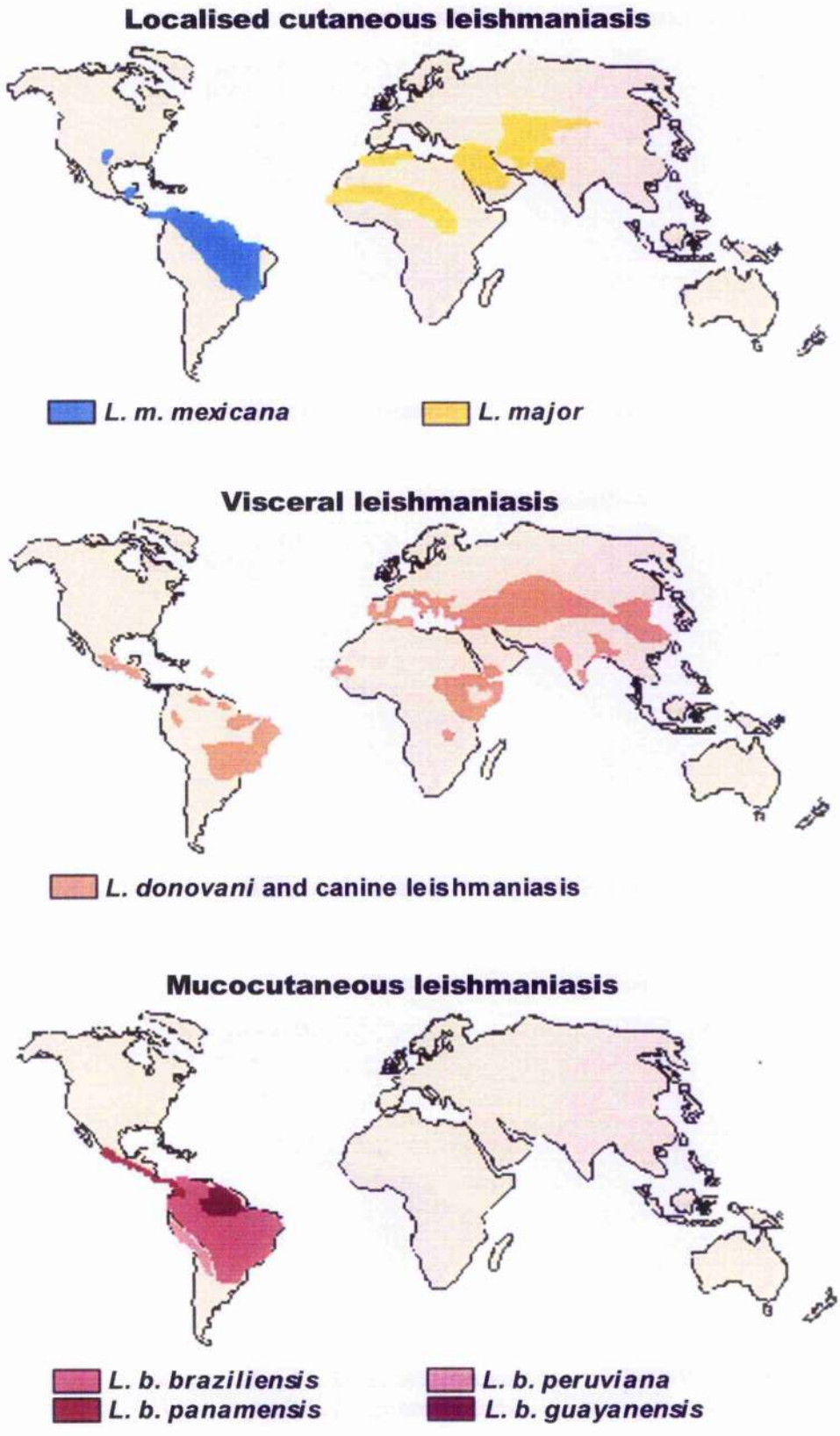

Figure 1.1: Causative agents of leishmaniasis around the world.

From World Health Organisation (WHO at www.who.int/tdr)

1.1.2. Life cycle

The *Leishmania* life cycle alternates between mammalian host and phlebotomine sandfly host. Humans contract leishmaniasis via the bite of *Leishmania*-infected female phlebotomine sandfly. As the sandfly feeds, promastigote forms of the *Leishmania* parasite enter the skin of the mammal via the proboscis. It has been reported that only ~16% of those promastigotes (called metacyclic promastigotes) are infectious and able of successfully entering a host macrophage directly or indirectly (Killick-Kendrick, 1990). Polymorphonuclear neutrophil granulocytes (PMN), the first immune cells present at the site of *Leishmania* infection, are also readily infected by the parasite and are used as a means of attracting and entering macrophages "silently" (van Zandbergen *et al.*, 2004). This "Trojan horse" strategy employed by the parasite maximises its survival and development in its final host cell, the macrophage. Once there, the metacyclic promastigote differentiates into a small aflagellated avoid cell called an amastigote. These latter forms will multiply inside the newly formed parasitophorous vacuoles until the cell eventually bursts, freeing the parasites and allowing them to infect other phagocytic cells. *Leishmania* parasites will remain as amastigote forms for the duration of the life cycle in the mammalian host (Handman and Bullen, 2002).

In one sandfly vector, *Lutzomyia longipalpis*, seven morphologically distinct forms of *L. amazonensis* were identified. The following occurred at different time points after infection: the amastigote, and several variations of a long body flagellated cell - the procyclic promastigotes, the nectomonad promastigotes, the leptomonad promastigotes, the metacyclic promastigotes, the haptomonad promastigotes (rarely seen) and paramastigotes (Rogers et al., 2002; Kamhawi, 2006) (**figure 1.2**). Only the procyclic promastigotes, in the sandfly abdominal midgut (bloodmeal phase) and the leptomonad promastigotes, in the sandfly thoracic midgut and foregut (sugarmeal phase) are replicatively active (Gossage *et al.*, 2003). Based on these finding, a life cycle for these *Leishmania* species is proposed and described in **figure 1.2.**

1.1.3. Leishmaniasis control

The chemotherapy currently available for leishmaniasis treatment involves mainly pentavalent antimonials (Croft and Coombs, 2003). Yet, resistance to these drugs is now common in some parts of the world, requiring the use of more toxic drugs, such as pentamidine or amphotericin B. Further more, most available drugs are costly, demanding long treatment and are becoming less effective, necessitating the discovery of new drugs (www.who.int/tdr/diseases/leish).

Currently, strategies piggybacking upon medicines used for anticancer and antifungal treatments are among the most successful approaches leading to the

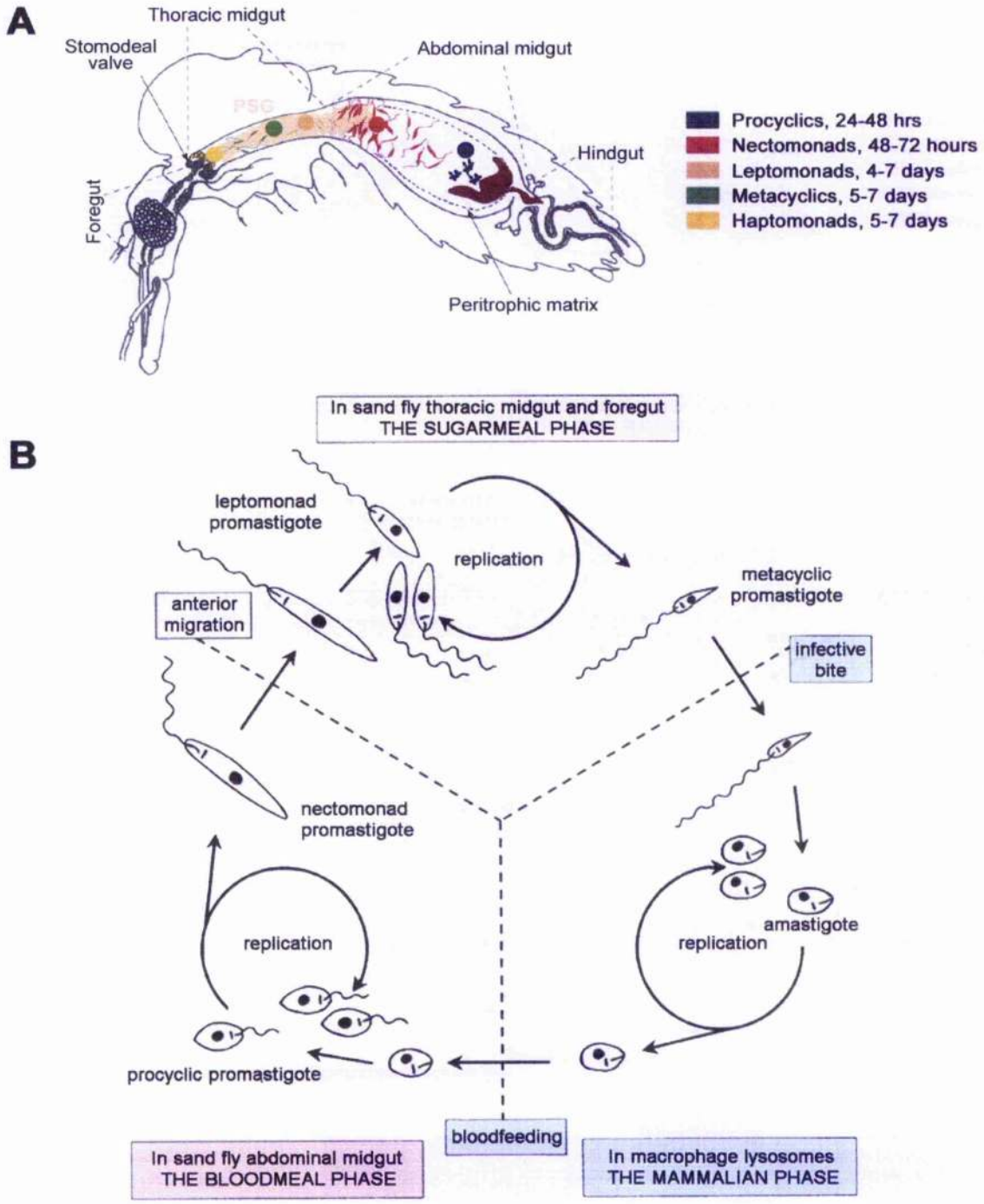

Figure 1.2: Life cycle of *Leishmania* species in *Lutzomyia longipalpis*.

From Kamhawi, 2006 and Gossage *et al.*, 2003
A) Schematic representation of a *Leishmania* infected phlebotomine sandfly. The diagram shows the time-dependant appearance of distinct morphological forms of promastigotes. Oesophagus and stomodeal valve are held open by promastigotes secreted gel (PSG). B) Digenetic life cycle of *Leishmania*. Only three forms of the parasites are able to replicate: i) the amastigotes in the parasitophorous vacuole (a type of phagolysosomes) of mammalian macrophages, ii) the procyclic promastigotes in the sandfly abdominal midgut, and iii) the leptomonad promastigotes in the sandfly thoracic midgut. The life cycle is completed by non-dividing stages.

identification of new candidate drugs against leishmaniasis. Indeed, miltefosine, an anticancer drug, has shown its efficiency as an oral treatment of LCL and *L. infantum* and *L. chagasi* VL and is now registered in India for the use against *L. donovani* VL (Croft *et al.*, 2003). Miltefosine is also a candidate drug for the treatment of canine leishmaniasis, a disease for which no drugs are currently potent enough. Effective treatment of canine leishmaniasis would not only affect dogs' well-being but also, and more importantly, reduce the number of *Leishmania* animal reservoirs. Current ways of controlling this *Leishmania* repository involve the culling of infected animals and the limitation of the size of the insect vector population via large scale spraying of insecticides.

Other antileishmanial drugs have been discovered and are at various stages of development e.g. sitamaquine (by GlaxoSmithKline) and paromomycin (by Walter Reed Army Institute of Research, USA), but problems remain for the future of antileishmanial treatment: i) the toxicity of theses drugs is not negligible ii) the modes of administration are often unpleasant (e.g. parenteral formulation).

Research for new drugs continues. Fundamental research into *Leishmania*-specific drug targets is one of the most promising fields being explored. Big advances in the identification and functional analysis of new virulence factors and other critical enzymes have been made thanks in part to the recently available entire genome content of several *Leishmania* species and powerful bioinformatic tools. Inter-strain genome comparisons will hopefully contribute to the characterisation of parasite factors responsible of tropism and disease pathology (Ivens *et al.*, 2005). As apparently early-branching eukaryotes (Coombs *et al.*, 1998), trypanosomatids possess a cellular organisation that is considerably different from that of mammalian cells (**see 1.1.4.**). Therefore, many of the parasite's proteins should be sufficiently different from anything in the mammalian host to be successfully exploited as drug targets or vaccine candidates. Unfortunately, to date there are no effective vaccines against *Leishmania*. Many strategies have been followed using live, killed or attenuated parasites, recombinant DNA, peptides or purified parasite antigens (Handman, 2001; Selvapandiyan et al., 2006). Recently, advances have been the creation of a promising multi-epitope subunit vaccine (Skeiky *et al.*, 2002) and of an increasing number of genetically altered parasites, which could constitute live attenuated vaccines (Alexander *et al.*, 1998; Papadopoulou *et al.*, 2002; Uzonna *et al.*, 2004). However, their protective efficiency in humans still remains to be determined.

There is a need for funds of the public and private sectors to shift towards neglected diseases such as leishmaniasis so that the discoveries made by fundamental research could be exploited to beneficit the field problems (Guerin *et al.*, 2002). The current situation of the death-threatening visceral leishmaniasis remains, in the 21st

century, purely unacceptable. Hopefully, the advent of the genomics and proteomics era will lead to a better understanding of *Leishmania* biology and to the development of new affordable drugs.

1.1.4. Ultrastructure

1.1.4.1. *Leishmania* amastigote and promastigote forms

Leishmania ultrastructure differs from that of other kinetoplastids and also between different *Leishmania* species and even, for a given species, between the two life stages of the parasite. The different forms of the *Leishmania* life cycle were initially classified by the observation of their overall dimensions, flagellar morphology, kinetoplast (mitochondrial DNA) position and basal body to nucleus distance (Clayton *et al.*, 1995).

The amastigote form is a small aflagellated ovoid cell of around 5 μm diameter occurring within acidic parasitophorous vacuoles of mammalian host macrophages (**figure 1.3**).

The promastigote form is a motile extracellular cell with a long thin body (approximately 5 by 20μm) with a flagellum of up to 20 μm, which is present inside the alimentary tract of the female sandfly vector (**figure 1.4**). Cell body and flagellum lengths are the main criteria used to distinguish the different forms of promastigotes found in the phlebotomine vector (**figure 1.2**).

1.1.4.2. Specialised organelles in *Leishmania*

Leishmania possesses many of the organelles found in higher eukaryotes, nevertheless they are characterised by a number of peculiarities. A cellular envelope called the glycocalyx, which is thin in amastigote forms and thick in infectious metacyclic promastigotes, can be observed. This envelope is made of glycolipids: the glycoinositol-phospholipid (GPI), its hyperglycosylated form, the lipophosphoglycan (LPG) (mainly present in *Leishmania* promastigotes) and its protein-associated form, the proteophosphoglycan (PPG) (McConville *et al.*, 2002). While LPG is essential for the infectivity of *L. major* promastigotes in both the insect and the mammalian host (Sacks *et al.*, 2000; Spath *et al.*, 2000), *L. mexicana* promastigotes lacking this molecule are still able to infect mice (Ilg, 2000; Turco *et al.*, 2001). *Leishmania* promastigotes also synthesize free GPIs which are 10-times more abundant ($5x10^7$ copies/cell) than LPG. *Leishmania* amastigotes lack the prominent surface glycocalyx of GPI or other GPI-anchored macromolecules. Both *Leishmania* promastigotes and amastigotes secrete large quantities of soluble PPGs. The PPGs, through their ability to form, individually or

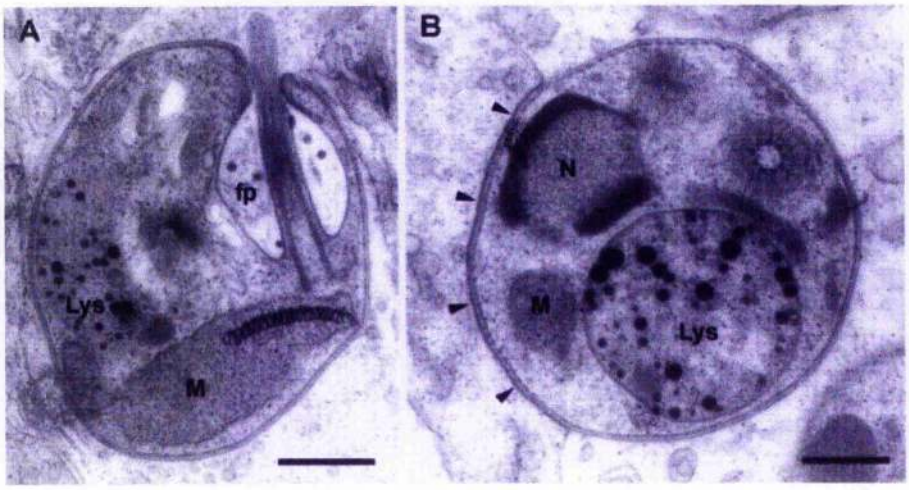

Figure 1.3: Ultrastructure of *Leishmania* amastigote seen by electron microscopy

Lys: lysosomes; fp: flagellar pocket; M: mitochondrion; N: nucleus; arrowheads: membrane of the parasitophorous vacuole.Scale bars: 500 nm. From Waller and McConville, 2002.

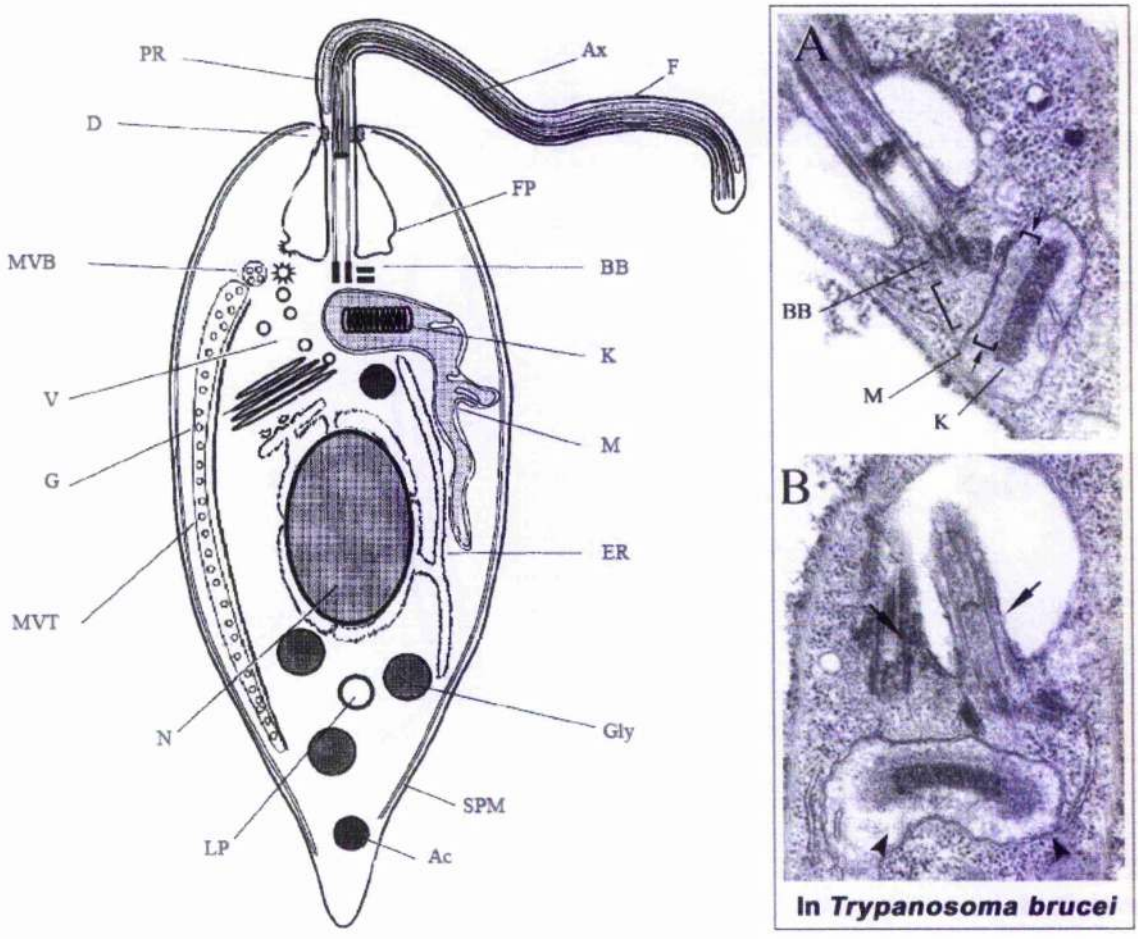

Figure 1.4: Ultrastructure of *Leishmania* promastigote.

On the left: schematic representation of *Leishmania* organelles (not to scale). Adapted from Clayton et al., 1995 and Waller and McConville, 2002. F: flagellum; Ax: axonemal

microtubules; PR: paraflagellar rod; D: desmosome junction; MVB: multivesicular bodies; V: vesicules; G: golgi; MVT: multivesicular tubule/lysosome; N: nucleus; LP: lipidic inclusion; Ac: acidocalcisome; SPM: sub-pellicular microtubules; Gly: glycosome; ER: endoplasmic reticulum; M: mitochondrion; K: kinetoplast; BB: basal bodies. FP: flagellar pocket. On the right: electron microscopy images showing the kinetoplast area of *T. brucei*. Adapted from (Ogbadoyi *et al.*, 2003) in an interphase (A) and a dividing cell (B). Large bracket: exclusion zone filaments; small bracket and arrow: unilateral filaments; arrow: flagellum; arrow head: fibrous lobe

after self-association, very large filamentous structures, mediate parasite aggregation and thus participate to the early stages of the invasion process. *Leishmania* promastigotes secrete a PPG-rich gel (PSG) in order to obstruct the digestive tract of the infected sandfly (Stierhof et al., 1999; Rogers et al., 2004). The *Leishmania* glycocalyx is also composed of several proteins (e.g. gp63) (McConville *et al.*, 2002). The gp63 glycoprotein is a metallo-peptidase, which is anchored into the *Leishmania* promastigote plasma membrane by a GPI molecule.

In the internal side of the plasma membrane, subpellicular microtubules (containing tubulin) that spiral around the cell form the cytoskeleton and are involved in the maintenance of the cell shape. This arrayed corset of microtubules converge in a closed structure at the posterior end of the cell while it remains open at the anterior end of the cell, giving rise to the flagellar pocket. Because the subpellicular microtubules block any vesicular exchanges between the extra- and intra-cellular environments, the flagellar pocket is the privileged location for endo- and exocytosis. This specialised invagination of the plasma membrane formed of cortical microtubules and desmosome junctions gives *Leishmania* its apical polarisation.

A flagellum arises from the flagellar pocket and is made of the traditional axonemal microtubules, as well as the trypanosomatid-specific paraflagellar rod (PFR). While giving to *Leishmania* promastigotes their motility, the flagellum also mediates attachment to the host cell (Killick-Kendrick et al., 1974a; Killick-Kendrick et al., 1974b). In addition the flagellum could act as an environment sensor and function in cell signalling (Bastin *et al.*, 2000). *Leishmania* amastigotes possess a shortened flagellum which, as it does not emerge from the flagellar pocket and is non-motile, can not mediate locomotion.

The *Leishmania* flagellum is anchored to the cell by a basal body, which is physically linked to the mitochondrion. Another basal body, which lies perpendicular to the major one, will develop during cell division. While, in *Trypanosoma brucei*, basal bodies take part in the kinetoplast division (Robinson and Gull, 1991), it has been reported that in *L. donovani* amastigotes the duplication and segregation of the kinetoplast can still occur in the absence of basal body replication (Selvapandiyan *et al.*, 2004).

The kinetoplast is an encapsulation of the condensed mitochondrial DNA. Composed of 10 to 30 maxicircles (20 to 40 Kbp) intertwined with between 1,000 and 10,000 minicircles (1 Kbp) (Simpson, 1987; Feagin, 2000), the kinetoplast represents 10 to 20% of the cellular DNA (Simpson, 1986). While the maxicircles have some of the functions of the mitochondrial DNA of higher eukaryotes and encode genes for the respiratory complexes, the minicircles encode guide RNAs that mediate the maturation of the non-functional pre-messenger RNAs produced by the maxicircles. This editing process, through insertion or deletion of a defined number of uridine residues at specific sites within the transcripts, contributes to the formation of start and stop codons, frameshifts and open reading frames within the cryptic maxicircle transcripts, thus rendering them functional and promoting their translation into proteins (Benne *et al.*, 1986). The cytosolic messenger RNAs are matured via polyadenylation and *trans*-splicing (LeBowitz *et al.*, 1993). In *T. brucei*, the kinetoplast is attached to the mitochondrion membrane via unilateral filaments and to the basal bodies through the exclusion zone filaments. This structure constitutes the tripartite attachement zone (TAC) (Ogbadoyi *et al.*, 2003) and mediate interactions between the cytoskeleton and the mitochondrion. The TAC is also likely to be present in *Leishmania*, although this remains to be confirmed.

Leishmania possess a single mitochondrion. While in logarithmic phase promastigotes the mitochondrion has a symmetrical circular shape with distension all over the cell body, non-dividing promastigotes possess a tubular mitochondrion that extends longitudinally within the cell (Simpson and Kretzer, 1997). In the amastigotes of *L. mexicana*, the mitochondrion is in the form of a complex network extending throughout the cell (Coombs et al., 1986). The mitochondrion produces part of the energy necessary for the cell's survival. Other energy is synthesized in a specialised organelle called the glycosome. Glycosomes are small spherical peroxisome-related organelles involved in *Leishmania* glycolysis. Other structures present are used for lipid storage (lipid inclusions), or for polyphosphates, magnesium, calcium and zinc storage (acidocalcisomes).

Leishmania also possess a single Golgi apparatus, located between the nucleus and the flagellar pocket. Endoplasmic reticulum (ER) and rough endoplasmic reticulum (RER) are mainly present around the nucleus. The ER provides part of the membranes necessary for the biosynthesis of endosomes and lysosomes. In stationary phase promastigotes the lysosomal compartment appears as a tubular structure and is termed the multivesicular tubule (MVT)/lysosome (Ghedin *et al.*, 2001; McConville *et al.*, 2002; Waller and McConville, 2002). In *Leishmania* amastigotes, the lysosomal system is more extensively developed and appears as one or several very large vesicles called megasomes (Coombs *et al.*, 1986; Ueda-Nakamura *et al.*, 2001). Megasomes contain

abundant highly active cysteine peptidases, but also arylsulfatase, β-glucuronidase, DNAse and RNase (Pupkis et al., 1986; Alberio et al., 2004). Cysteine peptidases have been shown to play major roles in the differentiation process (Williams *et al.*, 2006) as well as in parasite-host cell interaction and also in the survival of amastigote forms (Mottram *et al.*, 1998). Therefore, cysteine peptidases are considered as a potential targets for antiparasite drugs (Barrett *et al.*, 1999).

1.2. Cysteine peptidases

1.2.1. General

Enzymes that cleave polypeptide chains are named peptidases. When the excision site is present within the polypeptide chain, the enzyme is termed an endopeptidase, whilst when the cleavage occurs at the polypeptide ends the enzyme is called an exopeptidase (with aminopeptidase and carboxypeptidase cleaving N-terminal or C-terminal ends, respectively). Depending on the type of catalysis used for the peptide bond hydrolysis, peptidases are classified as serine, threonine, cysteine, aspartic, glutamic and metallo-peptidases. Peptidases using several catalytic mechanisms are termed "mixed" type peptidases. For their catalysis, most peptidases draw upon a nucleophile and a proton donor (very recently identified, glutamic peptidases employ a catalytic mechanism that remains obscure (Fujinaga *et al.*, 2004)). In the case of the serine and threonine peptidases, the role of the nucleophile is played by a reactive hydroxyl group (belonging to a serine or threonine residue, respectively) while in cysteine peptidase this function is undertaken by the sulfhydryl group of the active site cysteine. In aspartic and metallo-peptidases, the nucleophile attack of the peptide bond does not, like in serine and cysteine peptidases, depend directly on amino acid residues but on the activation of a molecule of water. The binding and activation of the catalytic water molecule can be mediated by either two aspartate residues or a metal ion (mainly zinc, but also cobalt or manganese) held in place by usually three amino acids, hence the respective names of the peptidases. The identity of the proton donor varies with the type of peptidase. This role is played by a histidine residue in cysteine peptidases (http://merops.sanger.ac.uk/about/about_9.htm) (Rawlings *et al.*, 2006).

In many cysteine peptidases the catalytic mechanisms by which the substrates are being hydrolysed are well understood. Mainly, they reside in the peptidase's ability to change the geometry of a substrate peptide bond (from a trigonal plane to a tetrahede), at a specific location within the peptide sequence (Stennicke and Salvesen, 1999). During its interaction with the peptidase, the substrate lies in the binding site of

the enzyme, with the scissile peptide bond positioned close to the catalytic residues. Indeed, while physically distant in the primary amino acid sequence, the active site residues are, within the tertiary structure of the peptidase, closely associated and together line the substrate binding pocket. Before or during catalysis, a nucleophile donates H-bonds to the substrate carbonyl oxygen thus polarizing the carbonyl group of the scissile bond and promoting the creation of a thiol ester intermediate with the substrate. Hydrolysis of the substrate will then occur by displacement of this ester and scission of the peptide bond. While the active site cysteine acts as the aforementioned nucleophile, the active site histidine promotes the formation of this nucleophile by acting as a base and removing the thiol- proton from the nearby active site cysteine. The de-protonation of the active site cysteine will then promote the creation of the thiol ester intermediate and the subsequent nucleophilic attack and protonation of the α-amino group of the substrate scissile bond, leading ultimately to the peptide bond proteolysis (Stennicke and Salvesen, 1999). Thus the active site cysteine is, in itself, essential for the catalytic activity of the cysteine peptidases. However, other conserved residues are important for the catalytic activity of some cysteine peptidases. A glutamine residue might participate to the formation of an oxyanion hole and thus to the stabilisation of reaction intermediates. Asparagine or aspartate residues might also orientate the imidazole ring of the active site histidine and facilitate the catalytic process.

Based on their primary and tertiary structural similarities, cysteine peptidases were assigned to families (Barrett and Rawlings, 2001). Families predicted to possess common evolutionary origin are grouped in clans. Each clan arose independently in evolution and only share its catalytic mechanism with the other clans. In regard of the conservation of the catalytic dyad residues, cysteine peptidases have been divided into 12 clans (http://merops.sanger.ac.uk) : clan CA, CD, CE, CF, CH, CL, CM, CN, C-, PA(C), PB(C), and PC(C) (**figure 1.5**). Initially identified by the presence of the catalytic cysteine-histidine dyad, some clans of cysteine peptidases (CA, CE, CF, CH, CM and PA(C)) function actually with a catalytic triad. Furthermore, it has to be noted that the tertiary fold around the active site cysteine differ significantly between different clans and thus underpins variations in substrate specificity. Clan PA(C) and PB(C) contain mixed-type peptidases. Respectively resembling chymotrypsin-like and threonine peptidase, they both contain active site mutations which might modify their catalytic properties.

Amongst the ~ 500 types of peptidases currently indexed in the human genome (http://merops.sanger.ac.uk), many cysteine peptidases were characterised to play a vital function or to be involved in disease processes and are under investigation as drug

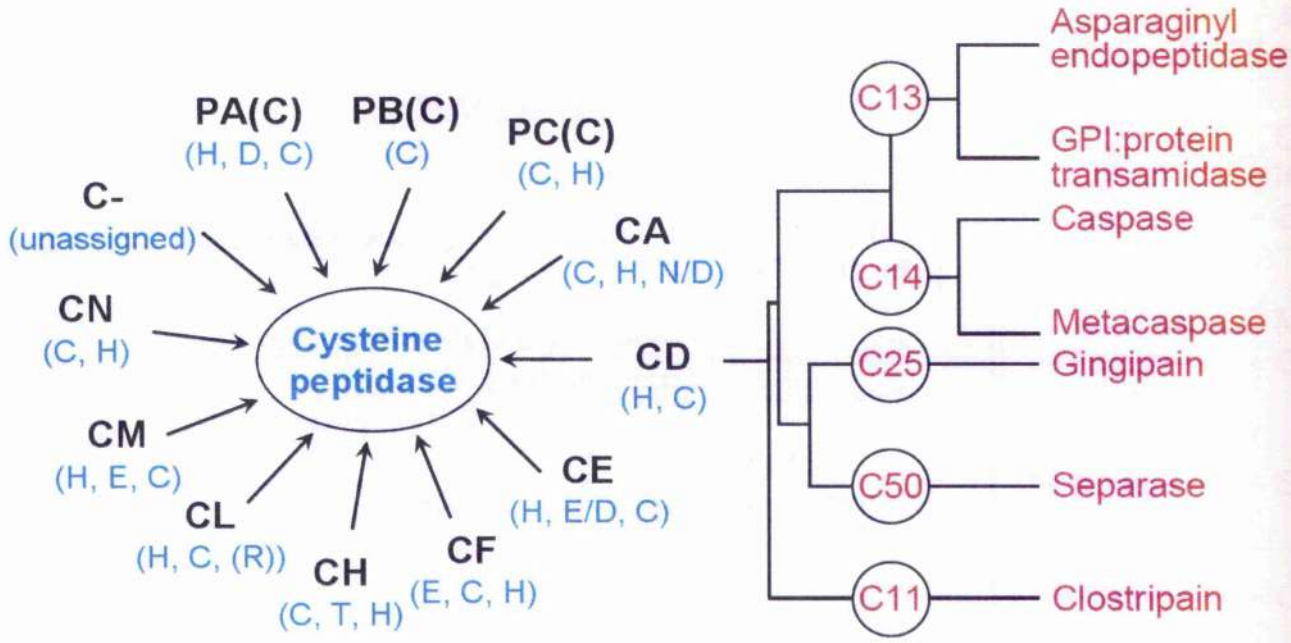

Figure 1.5: Clans of cysteine peptidase and the CD families.

Adapted from Mottram *et al.*, 2003. Each clan (in black) is indicated by a black arrow. Important catalytic residues as well as their order in the protein sequence are written in green. The phylogenetic relationship between different families (in open circles, red) of clan CD peptidases is shown. Abbreviations: C, cysteine; D, aspartic acid; E, glutamic acid; GPI, glycosylphosphatidylinositol; H, histidine; N, asparagine; R, arginine; T, threonine.

targets (Lecaille *et al.*, 2002). Cysteine peptidases belonging to clans CA and CD are the most studied.

Clan CA is defined around the largest subfamily of cysteine peptidases, papain-like, also known as thiol-dependent cathepsin, and belonging to the C1 family. Papain-like cysteine peptidases are widely represented in eukaryotic cells, but are also present in viruses and bacteria. Papain-like cysteine peptidases were shown, in mammals, to mediate extracellular matrix turnover, antigen presentation, and processing events. Furthermore, they might constitute potent drugs targets for osteoporosis, arthritis, immune-related diseases, atherosclerosis, cancer, but also for numerous parasitic infections (Lecaille *et al.*, 2002). Indeed, when compared to the human enzymes, the parasite papain-like cysteine peptidases cluster in three major groups: cathepsin B-like, cathepsin L-like and cathepsin F-like. In *Leishmania*, cathepsin B-like (also called CPC) and cathepsin L-like (CPA and CPB) cysteine peptidases were found to mediate cell growth and differentiation (Mottram et al., 1996b; Williams et al., 2006) but also, through their functions in host-parasite interactions, to act as virulence factors (Alexander *et al.*, 1998; Lecaille *et al.*, 2002).

1.2.2. Clan CD cysteine peptidases

The analysis of the amino acid sequences, protein structures and biochemical properties of these enzymes clearly demonstrate that they are distinct from those of the others clans (Mottram *et al.*, 2003). For example, it appears that clan CD cysteine peptidases are much stricter in their substrate specificity (especially at the S1 sub-site) than clan CA cysteine peptidases. Consequently, clan CD cysteine peptidases are not inhibited by E-64 (L-trans epoxysuccinyl-leucylamido-(4-guanidino)-butane), the much used clan CA cysteine peptidase inhibitor. But, in contrast, various clan CD cysteine peptidases are inhibited by aza-epoxides while clan CA enzymes are not (Asgian *et al.*, 2002). Another interesting feature of the clan CD cysteine peptidases is that whereas most of the cysteine peptidases require a catalytic triad for the hydrolysis of peptide bonds, they appear to be functional with only a catalytic dyad (Mottram *et al.*, 2003). Furthermore, while clan CA cysteine peptidases can either be endo- or exo-peptidases, the clan CD enzymes characterised so far are all cleaving within the peptide sequence.

Clan CD peptidases sharing relative amino acid sequences similarities are classified in 5 families: C11, C13, C14, C25 and C50 (**figure 1.5**) (Chen *et al.*, 1998). Nevertheless, some members of the different families possess very different biological functions and mechanisms of action.

For example, in the C13 family, the asparaginyl endopeptidase, present in plants and animals, has been identified as a lysosomal cysteine peptidase that specially cleaves after asparagine residues, playing, in mammals, an important role in antigen processing and immune disorders (Li *et al.*, 2003). Whereas the GPI:protein transamidase, a cysteine peptidase that also belongs to the C13 family and is found in eukaryotes, adds preformed glycosylphosphatidylinositol (GPI) anchors to polypeptides that form in *L. mexicana* and *T. brucei* the parasite's surface (Ellis *et al.*, 2002; Lillico *et al.*, 2003). The C25 family is represented by a *Porphyromonas gingivalis* cysteine peptidase, known as gingipain. This bacterial pathogen of human mucosal surfaces is known to produce two individual cysteine peptidases of this type, Arg-gingipain (R) and Lys-gingipain (K), with, respectively, arginine and lysine specificities at the S1 sub-site, but both causing tissue damage in periodontal disease (Curtis *et al.*, 2001). The clostripain (C11 family) is also involved in bacterial infection and also has Arg-gingipain specificity. Another arginine-specific endopeptidase is found solely in eukaryotes: the separase (C50 family). This enzyme was shown to play a major role in mammalian cells in chromosome division during mitosis (Nasmyth *et al.*, 2000; Uhlmann, 2001). Separase exercises this precise function via the cleavage of cohesin, a protein tying together, at the centromere, the sister chromatids of each chromosome. Separase becomes active

when the sister chromatids are accurately connected to the mitotic spindle microtubules and upon degradation of its complexed inhibitor, securin. While the gene coding for an apparent homologue of the separase is present in *L. major* (Mottram *et al.*, 2003), the genome of the parasite lacks securin, suggesting that separase might be involved in alternative mechanisms. The final family, C14, is described in detail in the section below.

1.3. Clan CD cysteine peptidases, the C14 family

The C14 family of the clan CD cysteine peptidases is composed of three sub-families: the caspases, the paracaspases and the metacaspases.

Until recently, metazoa were thought to be the only organisms to possess caspases, because no homologous caspase genes were found in the genomes of yeast or parasitic protozoa. But in their attempt to characterise sequences with distant but statistically significant similarity to caspases, doing database searches, Uren *et al.* managed to distinguish two groups of caspase-like proteins (Uren *et al.*, 2000). Paracaspases were identified from their low sequence identity with caspases while metacaspases were found through their distant similarity with paracaspases. Within eukaryotes, paracaspases are found in metazoa and *Dictyostelium discoideum*, whereas metacaspases are only found in plants, fungi, and protozoa.

The primary sequences as well as the secondary structure of these two families share similarity with human caspases but they also possess specific features (**figure 1.6**).

1.3.1. Caspases

The caspases, *C*ysteine *ASP*artate specific prote*ASES*, are a family of more than 15 members of which about two-thirds are involved in apoptosis (a form of programmed cell death) in mammalian cells (Earnshaw *et al.*, 1999). Caspases are associated with inflammatory disorders and neurodegenerative diseases such as stroke, Alzheimer's and Parkinson's (Cohen, 1997; Thornberry and Lazebnik, 1998; Barrett and Rawlings, 2001; Dickinson, 2002; Mottram et al., 2003).

All the caspases contain a conserved QACXG (where X is R, Q or G) active site motif which gives them a very strict specificity for aspartate residue at the P1 position of their targets. Because of their lethality for the cell, caspases are synthesized and stored as inactive proenzymes. The zymogens comprise an N-terminal peptide (prodomain) along with one large (~20 kDa) and one small (~10 kDa) sub-unit (**figure 1.7A**). Some caspases have specific features at their N-terminus e.g. large prodomains containing protein-protein interaction modules such as the caspase recruitment domain

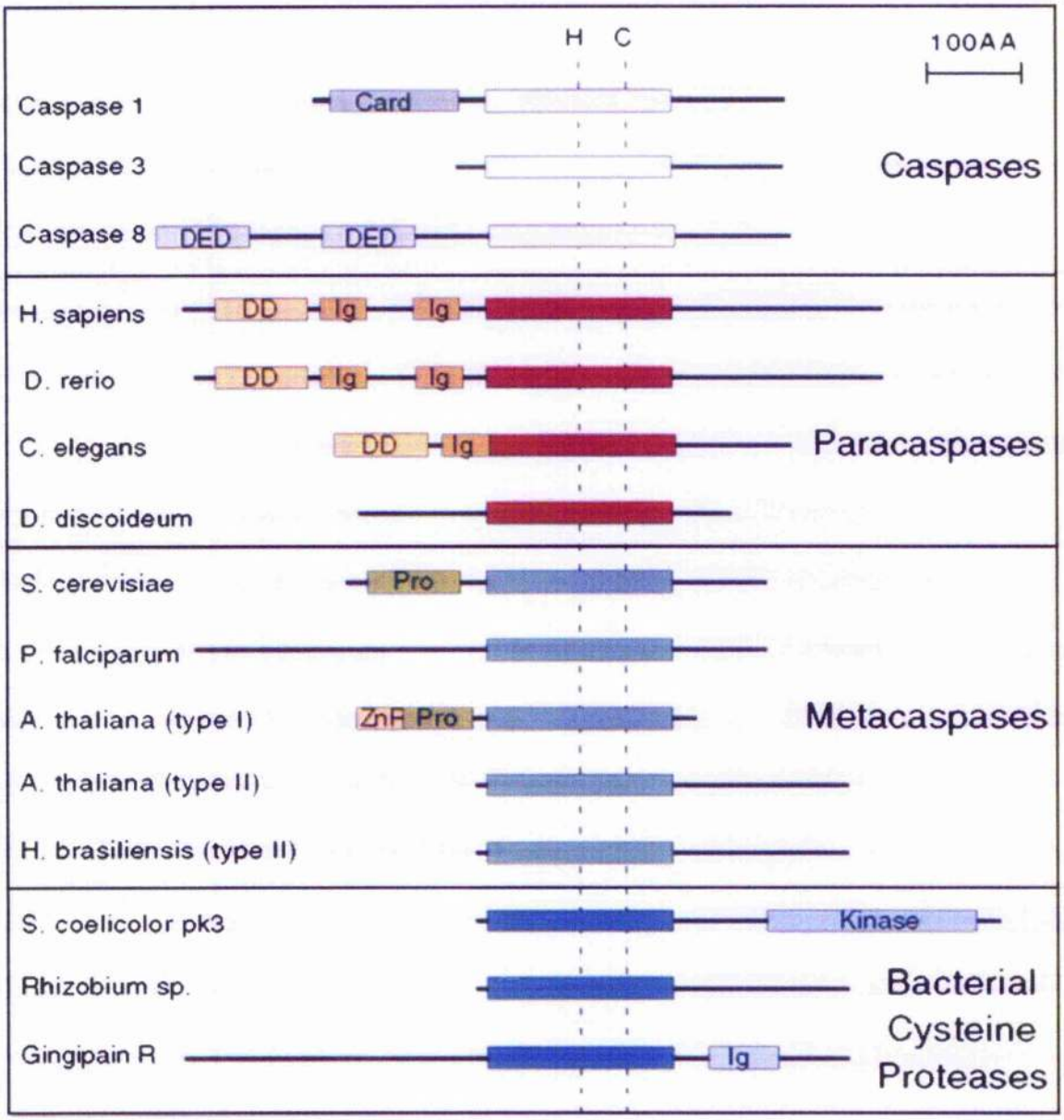

Figure 1.6: Domain structure of caspases, paracaspases, and metacaspases.

From Uren *et al.*, 2000. Caspases possess a caspase domain (p20, empty box) and in some case a prodomain with CARD or DED oligomerization motifs. Paracaspases, metacaspases, and several bacterial cysteine peptidases are predicted to possess a caspase-like proteolytic domain. The prodomains of the metazoan paracaspases are generally composed of a death domain ("DD") and one or two Ig domains. According to their sequence and structural similarities, the metacaspases are divided in two groups, type I and type II. In plants and fungi, the type I metacaspases have prodomains with proline-rich repeat motif ("Pro"). A zinc finger motif ("Zn") similar to those of the plant hypersensitive response protein lsd-1 can also be observed in the plant type I metacaspases. Meanwhile, the plant type II metacaspase, which lacks a prodomain, has an insertion of approximately 200 amino-acids close to their C-terminus. *Streptomyces coelicolor* pk3 possess both a caspase-like and a protein kinase domain. All the sequences are presented as their unprocessed zymogen forms.

(CARD) (caspase-1) or death effector domain (DED) (caspase-8). Caspases with large prodomains are generally involved in the initiation phase of apoptosis and are called initiator caspases. Caspases with shorter N-terminal domains (caspase-3, -6 and -7) are termed effector caspases and are generally activated by initiator caspases. Another group of caspases comprise those with a potential involvement in the control of inflammation (caspase-4, -5 and -13) (Fuentes-Prior and Salvesen, 2004). Meanwhile, caspase-2 and caspase-14 are difficult to classify. More details about the caspase-dependant programmed cell death and its regulation in mammals can be found in **section 1.4.**

The crystal structure of caspase-1 and caspase-3 showed that the active enzyme is a dimer, containing two small and two large sub-units. The activation of the caspase zymogens is mediated by at least two cleavages, one removing the N-terminal domain, the other separating the large and small subunit. Cleavages occur after specific D-X bonds, with the removal of the inter-sub-unit linker apparently preceding the one of the N-terminus. The catalytically active dimer results from either proteolytic autoprocessing or cleavage by other caspases, followed by self-association and translocation of the activation loop to the neighbouring molecule (Earnshaw et al., 1999). The resulting enzyme contains two active sites at the opposing ends of the dimer (**figure 1.7A**).

The caspase active site is composed of residues belonging to both the large and the small sub-units. The aspartate at the P1 position of the substrate is buried in a deep pocket in the caspase active site (S1 site) which is lined by R179, H237, Q283, C285 and R341 (**figure 1.7B**). The residue lining the S2, S3 and S4 pockets all belong to the small sub-unit.

The caspase proteolytic activity can be of different natures depending on the identity of its substrate and the precise position of the cleavage site. In most cases, cleavage by caspases results in loss of biological function. However limited proteolysis can also occur leading, in that case, to a gain of function of the substrate by removal of inhibitory domains or sub-units (e.g. Bid). The cleaved product can also antagonise the function of the non-processed full length product (e.g. Bcl-2) (Hengartner, 2000).

Caspases cleave a wide variety of substrates from single polypeptide chain enzymes (e.g. polyADP-ribose polymerase (PARP)) to complex macromolecular structures (e.g. lamin network). So far, more than 280 caspase substrates have been characterised (Fischer *et al.*, 2003). Caspases are able to cleave major structural elements of the cytoplasm, nucleus and cytoskeleton, components of the DNA repair machinery and several kinases and thus play important roles not only in the cellular dismantling associated with apoptosis execution but also in cellular differentiation

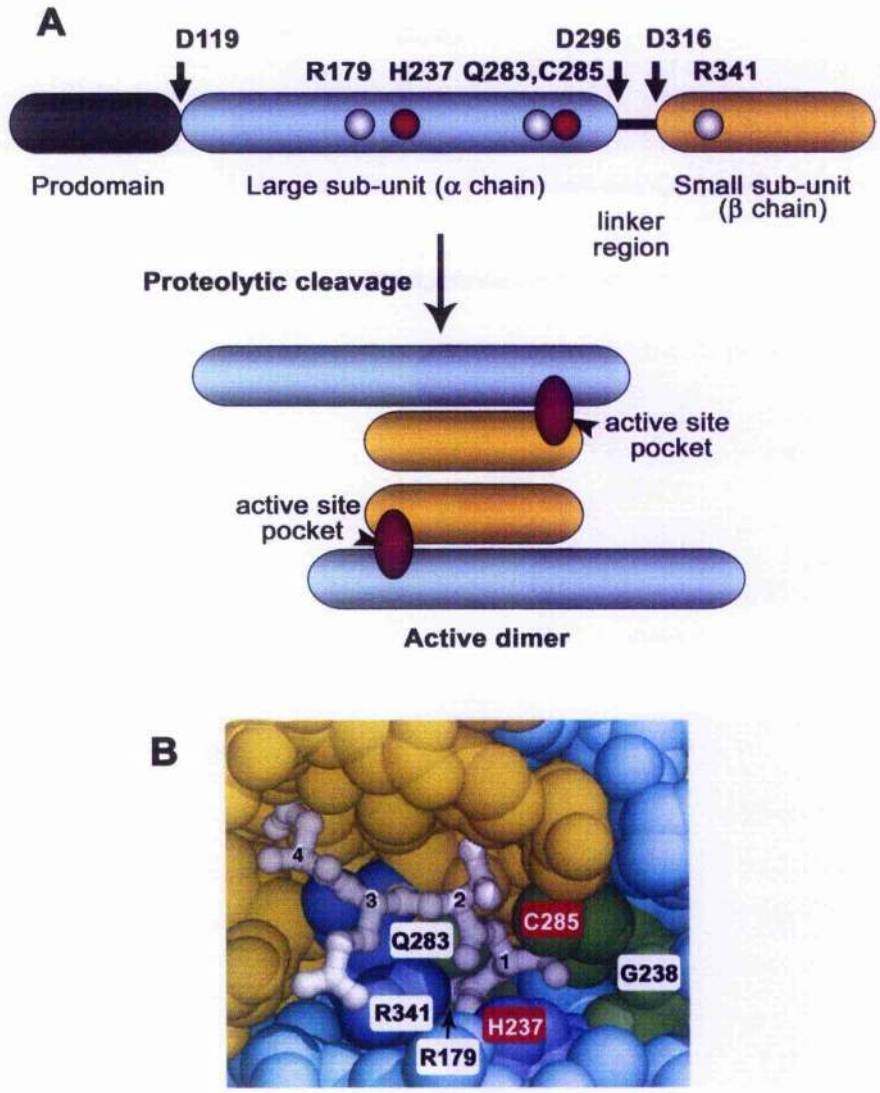

Figure 1.7: Domain organisation of caspases

A) All caspases possess an N-terminal segment with a length varying from 3 kDa (caspase-3 and -6) to 24 kDa (caspase-8 and -10). Unlike other cysteine peptidases where the prodomains represent an activation peptide, the removal of the caspase N-terminal region does not always result in activation. The large (17 to 21 kDa) and the small (10 to 13 kDa) subunits that form the catalytic domain of the enzyme are represented. These two regions are separated by a linker segment of 12 to 39 kDa. Removal of this segment generally results in the peptidase activation. Residues important for catalysis (C285 and H237), maturation (D119), activation (D296, D316), and the S1 substrate binding pocket (Q283, R179 and R341) are shown. Activation of the zymogens depends of the translocation of the activation loop into the accepting pocket of the neighboring dimer. For initiator caspases, latent monomers are activated by dimerisation. For executioner caspases, zymogens exist as preformed dimers and activation is enabled by removal of the inter-sub-unit linker (Boatright and Salvesen, 2003). B) Space-filling representation of the substrate-binding pocket of caspase 3 (by standard crystallographic convention, residue numbers correspond to those in caspase-1) around its bound tetrapeptide aldehyde inhibitor Ac-DEVD-CHO (P1-P4, right to left, white). Taken from Earnshaw *et al*, 1999.

(Zermati et al., 2001; Fernando et al., 2002; Mogi and Togari, 2003) and cell cycle progression (Kim et al., 2005; Hsu et al., 2006).

1.3.2. Paracaspases

Metazoan paracaspases possess a prodomain composed of a death domain (DD) followed by either one or two immunoglobulin domains (Ig) (**figure 1.6**). Paracaspases also possess a caspase-like domain containing the universally conserved catalytic cysteine and histidine dyad required for catalysis by cysteine peptidases. However, no peptidase activity has been reported yet (Uren et al., 2000; Snipas et al., 2004). The paracaspase also possesses an ubiquitin E3 ligase domain in its C-terminus. The ubiquitinin E3 ligase activity of the paracaspase was shown to be involved in NF-κB activation following T-cell receptor ligation (Ruefli-Brasse *et al.*, 2003). NF-κB enters the nucleus and switches on the expression of genes that are essential for the proliferation and function of activated T cells (van Oers and Chen, 2005). Because of its involvement in the subsequent increased in lymphocyte proliferation and survival which is responsible for mucosa-associated lymphoid tissue (MALT) lymphoma, the human paracaspase was also termed MALT1. There is so far no evidence that MALT1 directly participates in the execution of cell death.

Dictyostelium discoideum possesses one paracaspase (*pcp*) but no caspase or metacaspase (Roisin-Bouffay *et al.*, 2004). The *D. discoideum* paracaspase does not possess the death domain and the immunoglobulin domains found in the metazoan paracaspases. Cell death can be observed in *D. discoideum in vivo*, upon starvation, and can be mimicked *in vitro*. However, in this organism, deletion of the paracaspase gene had no effect, both *in vivo* and *in vitro*, on the execution of developmental cell death. Furthermore, *D. discoideum* development was apparently not impeded by the paracaspase inactivation. Therefore it seems that *D. discoideum* does not require paracaspase or caspase-related molecules for the execution of developmental cell death.

Paracaspases are more closely related to caspases than to metacaspases (Roisin-Bouffay *et al.*, 2004). Paradoxically, the *Dictyostelium* paracaspase is not apparently involved in cell death, while the yeast metacaspase is (Madeo et al., 2002b). It still remains to be seen if other metacaspases behave the same way.

1.3.3. Metacaspases

1.3.3.1. General

Genome database searches and sequence analyses have proven the presence of metacaspases in many of the non-metazoan eukaryotic cells (plants, fungi and protozoan). Thus it might be considered that they are the functional homologues of the metazoan caspases and might therefore be involved in programmed cell death (Uren *et al.*, 2000).

Metacaspases from yeast and some plants contain, in their prodomain, a proline-rich region preceded by a zinc finger motif (type I metacaspase). This motif is, by amino acid sequence, very close to those present in plant proteins involved in hypersensitive response pathways (e.g. LSD1 protein). This plant hypersensitive response is a defence mechanism triggered upon infection of plants by a pathogen, which prevents the spread of these pathogens from the inoculation site to the neighbouring cells by activating a programmed cell death pathway (PCD). The cell death involved in this case has morphological similarities with animal apoptosis, suggesting that cell death mechanisms might be closely related between plant and animal (Aravind *et al.*, 1999).

While a special form of animal programmed cell death, apoptosis, is regulated by caspases, caspase-like proteolytic activities were detected in tobacco tissues that were developing hypersensitive response - after infection with tobacco mosaic virus (TMV)- suggesting that caspase-like plant peptidases participate to the cell death associated with the hypersensitive response (del Pozo and Lam, 1998). A cysteine peptidase with the specificity of the mammalian caspase-6 (called VEIDase) was implicated in plant programmed cell death (Bozhkov *et al.*, 2003). VEIDase activity has also been detected in yeast during hydrogen peroxide- or aged-induced apoptosis, and attributed to the yeast Yor197w protein, which apparently functions as a caspase, and so called yeast caspase-1 (YCA1), even though it actually is a metacaspase (Madeo et al., 2002b). Hydrogen peroxide- and nitric oxide-induced cell death in *Arabidopsis* were abolished by addition of caspase-1 inhibitor, suggesting that there might be another caspase-like activity involved in plant programmed cell death (Clarke *et al.*, 2000). In addition to this evidence that there are plant and yeast cysteine peptidases involved in cell death that are able to cleave fluorogenic tetrapeptidic substrates that mimic caspase substrate recognition sites, other data suggest that natural caspase substrates (such as PARP) might also be processed during programmed cell death (Tian *et al.*, 2000). Furthermore the functionality of natural caspase inhibitors (e.g. IAP and p35) in these systems underpins the concept that peptidases with caspase-like specificities are

present and actively involved in programmed cell death in plant and yeast (Hansen, 2000; Snipas et al., 2001; Lincoln et al., 2002; Danon et al., 2003).

Although some cathepsin-like cysteine peptidases have caspase-3-like activity (Zangger et al., 2002), the metacaspases were, until recently, considered responsible for the caspase-like activities detected during the execution of programmed cell death. However, the silencing and biochemical characterisation of the Norway spruce (*Picea abies*) metacaspase (mcII-Pa) recently established that although the metacaspase was involved in programmed cell death during plant embryogenesis, it did not possess a caspase-like activity (Bozhkov et al., 2005). Instead, it was observed that mcII-Pa had a preference for substrates with an arginine residue in P1 (Bozhkov et al., 2005). Interestingly, similar observations were made with the *Arabidopsis* metacaspases (Vercammen et al., 2004; Watanabe and Lam, 2005).

1.3.3.2. Plant metacaspases

There are many genes coding for plant metacaspases, but only a few have been studied. A metacaspase gene (*LeMCA*) was characterised in *Lycopersicon esculentum* (tomato) (Hoeberichts *et al.*, 2003). Alignment with various full length metacaspase protein sequences revealed that LeMCA is 67% identical to one of the type II *A. thaliana* metacaspases (AtMCA8) and 14% identical to *S. cerevisiae* metacaspase. *Botyris cinerea* is a fungal pathogen that induces cell death in several plant species by activating the hypersensitive response (HR) pathway. Hoeberichts *et al.* showed that the *LeMCA* gene is expressed only during *Botyris cinerea*-induced PCD. Interestingly, chemically-induced PCD does not lead to *LeMCA* gene expression, suggesting that this gene is expressed only under very specific circumstances.

A type II metacaspase gene, *mcII-Pa*, in Norway spruce, was shown to be involved in somatic embryogenesis, which is one model system of developmental PCD in plants (Suarez *et al.*, 2004). The hypothesis was risen that this metacaspase gene may encode a functional homologue of animal caspase-6 (VEIDase), because silencing of *mcII-Pa* resulted in a significant reduction of VEIDase activity in the cells, an activity that was strongly associated with the initial execution phase for this plant developmental PCD (Bozhkov *et al.*, 2003). However, it was later established that mcII-Pa preferentially cleaved its substrates after arginine residues and was not directly responsible of the VEIDase activity detected during PCD (Bozhkov *et al.*, 2005). Nevertheless, it was observed that in terminally differentiated cells mcII-Pa translocates from the cytoplasm to the nucleus and mediates their elimination by triggering the nuclear phase of the PCD process (Bozhkov *et al.*, 2005).

Recently, by characterizing two type II *A. thaliana* metacaspases, Vercammen *et al.* demonstrated that the plant's caspase-like activities reported earlier were not associated with these metacaspases. In the *A. thaliana* genome, nine metacaspases genes (*AtMCA1-9*) were identified. AtMCA1-3, which possess a proline- or glutamine-rich N-terminal extension with or without a Zinc finger domain, were classified as type I metacaspases while AtMCA4-9 were classified as type II metacaspases. Production of recombinant AtMCA4 and AtMCA9 in *Escherichia coli* resulted in cysteine-dependent autocatalytic processing of the proform into large and small subunits, in analogy to animal caspases (Vercammen *et al.*, 2004). A detailed biochemical characterization, with a broad range of synthetic oligopeptides and several peptidase inhibitors, showed that both AtMCA4 and AtMCA9 are arginine/lysine-specific cysteine peptidases and did not cleave caspase-specific synthetic substrates (Vercammen *et al.*, 2004). Later, Watanabe and Lam consolidated this finding and extended it to a type I *A. thaliana* metacaspase. By heterologous expression in yeast, it was observed that a type I and type II *A. thaliana* metacaspases were able to induce programmed cell death in this organism, in response to oxidative stress and ageing, presumably through activation of downstream peptidases with caspase-like activities (Watanabe and Lam, 2005). Recently, the tetrapeptide Val-Arg-Pro-Arg (VRPR) was found to be the favoured *in vitro* substrate of AtMCA9 (Vercammen *et al.*, 2006). Intriguingly, two hybrid screening revealed that a serine peptidase inhibitor, AtSerpin, was a suicide inhibitor of this metacaspase.

1.3.3.3. Yeast and fungi metacaspases:

Saccharomyces cerevisiae possess a single metacaspase gene, *YCA1* or *ScMCA* or *YOR197w*. Deletion or overexpression of the metacaspase gene doesn't lead to any obvious phenotype (Szallies *et al.*, 2002). Nevertheless, hydrogen peroxide-induced apoptosis (as attested by chromatin condensation and DNA fragmentation) could be completely abrogated or strongly stimulated after, respectively, disruption or overexpression of *ScMCA* (Madeo et al., 2002b). Overexpression of dead *ScMCA* (C296A) showed a reduced induction of apoptosis, compared to overexpression of the native *ScMCA*, but less survival than the wild type cells. It was also observed that ScMCA was autocatalytically processed between domains similar to the caspases' large and small sub-units. As caspase-like activities were previously detected, in yeast, during hydrogen peroxide-induced PCD, various biochemical experiments were performed to assess whether these activities could be attributed to ScMCA. A 26 hours overexpression of *ScMCA* did not result in any increase of catalytic activity toward caspase-6 (VEID-AMC) and caspase-8 (IETD-AMC) substrates, however, addition of hydrogen peroxide to the

culture medium of *ScMCA* overexpressing cells increased significantly the proteolytic activity toward these same substrates. Intriguingly, hydrogen peroxide strongly augmented the caspase-like activities but not the processing of ScMCA in the overexpressor cells (Madeo et al., 2002b). The authors suggested that the metacaspase processing might be rate-limited.

In contrast, another group, using yeast as a PCD model to study the function of two plant metacaspases, found that the yeast metacaspase was, in the presence of low doses of hydrogen peroxide, not able to cleave caspase-like substrates but instead preferentially processed substrates with an arginine/lysine residue at their P1 position (Watanabe and Lam, 2005). It was thus considered that the caspase-like activities detected in yeast, during hydrogen peroxide-induced PCD, were not due the metacaspase itself but to other peptidases. However, as the caspase-like activities detected during hydrogen peroxide-induced PCD were significantly reduced upon ScMCA deletion, it seems that the metacaspase is involved in the activation of these peptidases and thus plays an important role in the PCD signalling cascade. This role is particularly important in ageing yeast cells. Indeed, in the absence of ScMCA and thus PCD, ageing cells progressively lost their ability to regrow on fresh medium. Although the lack of PCD seems to be advantageous for the clone, the absence of removal of the damaged cells and their prolonged utilisation of the restricted nutrient supplies were ultimately detrimental for the development of the population (Herker et al., 2004). Later it was established that ScMCA was involved in PCD induced by various stresses (Wadskog et al., 2004; Ivanovska and Hardwick, 2005; Flower et al., 2005; Khan et al., 2005; Silva et al., 2005) or some defects in biological functions (Bettiga *et al.*, 2004; Mazzoni *et al.*, 2005).

In the fungi *Aspergillus nidulans*, overexpression of the single metacaspase gene *(casA)* inhibited *A. nidulans* growth and induced morphological changes typical of apoptosis (Cheng *et al.*, 2003). However, *casA* was not involved in phytosphingosine-induced apoptosis.

1.3.3.4. *Plasmodium falciparum* metacaspase

Putative metacaspase (PfMCA, PF13_0289) and metacaspase-like (PfMCA-like, PF14_0363) genes are present in the *Plasmodium falciparum* genome. Alignment with caspases shows that PfMCA retains the typical catalytic dyad histidine and cysteine residues, conserved in all proteolytically-active caspases. Nevertheless, it has considerable sequence differences around the active site, when compared to vertebrate caspases and human paracaspase, suggesting that this distinct configuration could reflect a parasite-specific substrate preference (Wu *et al.*, 2003). Unfortunately, no

further work has been done yet to give some clues about the plasmodial metacaspase expression and its function in the malaria causative agent.

1.3.3.5. Metacaspases in trypanosomatids:

Please refer to chapter 4 for a detailed presentation of the structural and biochemical properties of these metacaspases.

1.4. Programmed Cell Death and cysteine peptidases

In mammals, up to 11 pathways of cell death can be distinguished. Amongst them, 10 are genetically programmed (Melino *et al.*, 2005). Programmed Cell Death (PCD) is a physiological process of cell suicide, genetically regulated, that is essential to the development and homeostasis of multicellular organisms. Some examples of PCD include: the apoptotic form (caspase-mediated and caspase-independent (Lukovic et al., 2003; Lockshin and Zakeri, 2004b)), the autophagic form (Bursch *et al.*, 2000; Lockshin and Zakeri, 2004a), the non-apoptotic form (Sperandio *et al.*, 2000) and the necrosis form (Bursch et al., 2000; Gozani et al., 2002; Knight, 2002; Lukovic et al., 2003; Nicholson and Thornberry, 2003; Edinger and Thompson, 2004; Assuncao and Linden, 2004).

As the different cell death types are mostly defined by morphological criteria, without a clear reference to precise biochemical mechanisms, a unification of the criteria and terminologies used was recently proposed by the Nomenclature Committee on Cell Death (Kroemer *et al.*, 2005).

1.4.1. Apoptosis in multicellular organisms

The classification of apoptosis as a form of cell death distinct from necrosis was initially based on morphological observations (Kerr *et al.*, 1972). Necrosis is apparently not genetically programmed and mainly occurs in response to severe toxic damage or physical insults. It results, amongst others, in breakdown of the plasma membrane, vacuolisation of the cytoplasm, loss of homeostasis (Choi, 1988), disruption of the cytoskeleton (Hall *et al.*, 1997), swelling of various organelles (e.g. mitochondrion, ER, golgi) and inhibition of ATP synthesis (Edinger and Thompson, 2004). The subsequent release of the cellular content into the surrounding environment induces local inflammation and might damage the neighbouring cells.

In contrast to necrosis, cells dying by apoptosis are not lysed but are eliminated by phagocytosis, thus preventing the development of an inflammatory response and making apoptosis the most common type of physiological cell death. Apoptosis is characterised by budding of the plasma membrane, chromatin condensation, nuclear

DNA fragmentation, mitochondrial membrane potential changes and formation of apoptotic bodies (Melino *et al.*, 2005). These latter structures consist of organelles and/or nuclear material surrounded by an intact membrane. Exposing phosphatidylserine on their surfaces, these apoptotic bodies are rapidly engulfed by macrophages or neighbouring cells. Unlike necrosis, apoptosis is an active process that necessitates ATP hydrolysis, the expression of degradative enzymes and the activation of complex signalling pathways (Edinger and Thompson, 2004). Apoptosis was initially defined as playing a "complementary but opposite role to mitosis" in that it regulates cell proliferation by a controlled elimination of cells no longer required by the organism or impaired in their function (Kerr *et al.*, 1972).

It appears that genes encoding the apoptotic machinery as well as the morphological and biological features of apoptosis are conserved in vertebrates (e.g. mammals), nematodes (e.g. *Caenorhabditis elegans*) and insects (e.g. *Drosophila melanogaster*) (Hengartner, 2000; Meier *et al.*, 2000)

In mammalian cells, apoptosis is executed through two major pathways, which in some cases might operate together and amplify each other. The first induces mitochondrial membrane permeabilization and the other involves the proteolytic activation of the caspases. A simplified succession of events leading to apoptosis is exemplified in **figure 1.8** (Hengartner, 2000). The death cascade starts with either an external stimulus or an internal defect (here DNA damage). When death receptors such as CD95 are triggered, the initiator caspase-8 is recruited by the adaptor molecule FADD and subsequently activated. Hence the caspase pathway starts. The extrinsic and intrinsic cell death pathways converge at the mitochondrion, with the permeabilisation of the outer membrane and the release in the cytosol of proteins initially present in the mitochondrial intermembrane space. This process mainly involves proteins of the Bcl-2/Bax family. When activated, the pro-apoptotic members of this family such a Bax, Bad, Bim and Bid are translocated from the cytosol to the mitochondrion. Activation can be achieved by either dephosphorylation or proteolytic cleavage. For example, Bid is processed by the activated caspase-8. However, cross-talks between the death receptor and the mitochondrial pathway remain minimal at this point. Meanwhile other members of this family, Bcl2 and Bcl-XL, which are constitutively present in the mitochondrial membrane, play a protective role and anti-apoptotic functions. The pro- and anti-apoptotic Bcl-2 family members enter in competition, at the mitochondrion membrane to regulate the exit of cytochrome c and Smac/Diablo which will then induce the activation of the caspase pathway or of AIF which will subsequently involve caspase-independent pathways of cell death. After its release from the mitochondrion, the cytochrome c associates with many proteins amongst which Apaf-1 and the procaspase-9 to form the apoptosome. This complex will then mediate the activation of the

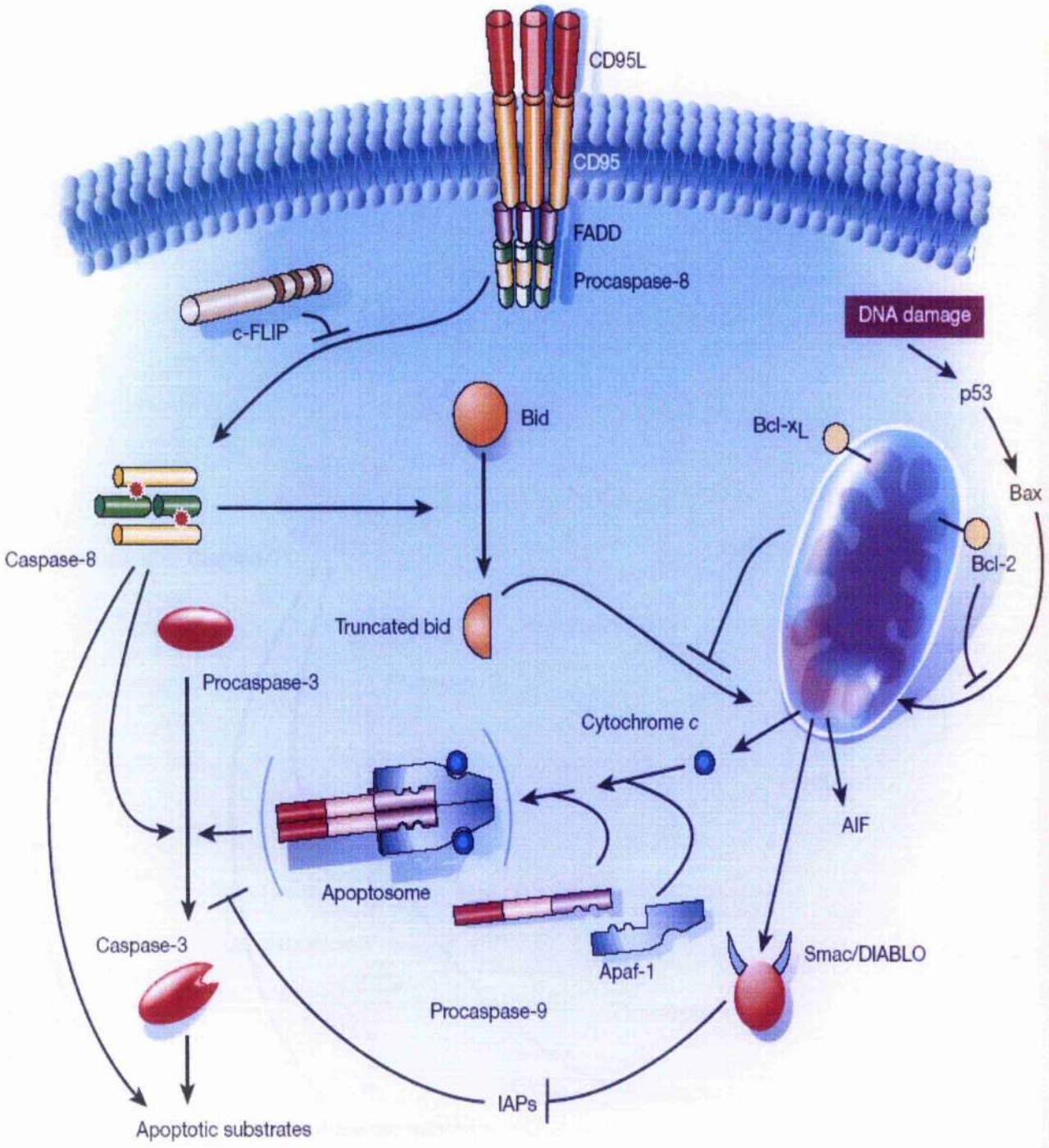

Figure 1.8: Two major apoptotic pathways in mammalian cells.
From Hentgartner, 2000. Refer to text for details.

executionner caspase-3. In parallel, Smac/Diablo, recently freed from the mitochondrion, antagonizes the caspase-3 inhibitor, IAP. The extrinsic and intrinsic cell death pathways then follow the same chronological events. The activated caspase-3 propagates the apoptotic cascade though the cleavage of many cellular substrates, ultimately resulting in the dismantling of the cell and its removal.

The regulation of caspase activity can be mediated by cellular inhibitors such as IAP. However other regulatory mechanisms exist. For example, some anti-apoptotic members of the Bcl-2/Bax family and other cellular polypeptides such as the degenerate caspase isoform FLIP (also termed c-FLIP) are able to block the proximity-induced activation of certain procaspases. In addition, the control of the caspase activation is mediated by the regulation of caspase zymogen gene transcription (Earnshaw *et al.*, 1999).

In mammalian cells, the activation of caspases is essential for the nuclear phase of apoptosis through its involvement in chromatin condensation and internucleosomal DNA fragmentation. However, in those cells, the execution of apoptosis can use caspase-independent pathways (Lockshin and Zakeri, 2004b). Indeed, it was observed that the effects of caspase deletion on the execution of apoptosis were varying with the type of caspase targeted, the type of cell manipulated and the type of triggering stimuli used (Earnshaw *et al.*, 1999). In contrast, PCD in *C. elegans* and *D. melanogaster* can not be accomplished without caspase activation. Therefore, it was suggested that the cell death machinery has evolved since the origin of the metazoa and that the caspases might be the initial ancestral effectors of PCD (Ameisen, 1996; Aravind *et al.*, 2001).

It was initially proposed that PCD only arose with multicellularity and would have been counter selected in unicellular organisms. However, on the evolution tree, PCD is likely to have appeared before the origin of metazoa as attested by the presence of caspase-like molecules in the prokaryotes (Koonin and Aravind, 2002). Furthermore, several forms of PCD have now been described in various single-celled eukaryotes, among which are the kinetoplastid protozoa *Trypanosoma cruzi*, *T. brucei*, and *Leishmania* (see below for details). In *Peridinium gatunense*, execution of PCD seems to be mediated by cysteine peptidases that are sensitive to the clan CA inhibitor E-64 (Vardi *et al.*, 1999). In *Dictyostelium discoideum*, developmental PCD does not require the paracaspase (Roisin-Bouffay *et al.*, 2004). Therefore, althought PCD pathways seems to be present in lower eukaryotes they differ significantly from the ones present in higher eukaryotes and little is yet known about the nature of the molecules involved and their exact mechanisms of action.

1.4.2. Programmed cell death (PCD) in trypanosomatids

Initially, because of the occurence of some form of PCD in prokaryotes (Lewis, 2000; Engelberg-Kulka et al., 2006), it was hypothesised that the presence of the PCD machinery in trypanosomatids was only a remnant from the eukaryotic cell evolution and was a process without a defined function (Nguewa *et al.*, 2004). However, in view of recent findings, it has been proposed that PCD plays an active role in the development of trypanosomatid by enhancing their biological fitness. Indeed, by selecting for the fitter cells or specific developmental forms within the population, by optimally regulating the cell number to adapt to the environmental constraints, and by tightly controlling the cell cycle and the cell differentiation, PCD could potentially maximise the infectivity of parasites and their survival in the host.

Inside the gut of the sandfly vector, the *Leishmania* promastigote forms multiply and differentiate into several intermediate forms until the ultimate infectious metacyclic form is generated. Metacyclic promastigotes are the form best able to establish an infection in the mammalian host. They do not divide and will differentiate into amastigotes only once in the host cell. It is known that only a small percentage of the promastigotes differentiate into metacyclic promastigotes (see **section 1.1.2.**). It has been proposed that the procyclic forms remaining in the insect gut will undergo PCD to limit the utilisation of the restricted supplies of nutrients to promote the survival of the forms better suited to transmit the disease (Debrabant and Nakhasi, 2003). More recently, it was observed that apoptotic-like promastigotes are necessary for *Leishmania* virulence *in vivo* and the establishment of the infection (van Zandbergen *et al.*, 2006). Apparently, the high ratio of apoptotic-like promastigotes present in the virulent inoculum allows the immune-silencing of the phagocytic process. Inside the mammalian host, PCD of the intracellular *Leishmania* amastigotes could also mediate the silencing of the host immune response, and especially during the chronic phase of the disease (Zangger *et al.*, 2002). PCD could also be activated to maintain clonality within the population (Lee *et al.*, 2002; Madeo *et al.*, 2002a).

In kinetoplastids, PCD appears in most cases to share nuclear and cytoplasmic features with mammalian apoptosis and is morphologically characterised by the observation of chromatin fragmentation, internucleosome-like DNA fragmentation, phosphatidylserine exposure on the outer leaflet of the plasma membrane, mitochondrial permeabilisation and loss in transmembrane potential (Moreira et al., 1996; Ameisen et al., 1996; Welburn et al., 1997; Arnoult et al., 2002). Such peculiarities were detected in *T. brucei* procyclic forms during tsetse fly infection (Welburn *et al.*, 1989; Welburn and Maudlin, 1997) or *in vitro* during concanavalin A

treatment (Welburn et al., 1999; Pearson et al., 2000) and oxidative stress (Ridgley *et al.*, 1999). Meanwhile very few examples of PCD have been characterized in *T. brucei* bloodstream forms (Figarella et al., 2005; Tsuda et al., 2005; Figarella et al., 2006). Features of apoptosis-like PCD were also observed in *T. cruzi* epimastigotes during *in vitro* differentiation into trypomastigotes (Ameisen *et al.*, 1996), upon treatment with fresh human serum (Piacenza et al., 2001; Piacenza et al., 2002; Kosec et al., 2006) or *Bothrops jararaca* venom (Deolindo *et al.*, 2005). In *Leishmania*, apoptotis-like PCD was triggered *in vitro* by heat shock (Raina and Kaur, 2006; Alzate et al., 2006), nitric oxide (Holzmuller et al., 2002; Raina and Kaur, 2006; Holzmuller et al., 2006), hydrogen peroxide (Mukherjee et al., 2002; Das et al., 2004), staurosporine (Arnoult *et al.*, 2002), amphotericin B (Lee *et al.*, 2002), camptothecin (Sen et al., 2004a; Sen et al., 2004b; Sen et al., 2006b), miltefosine (Chowdhury *et al.*, 2003; Verma and Dey, 2004), antimonial (Sereno *et al.*, 2001) or other drug treatments (Mittra et al., 2000; Jayanarayan and Dey, 2005; Singh et al., 2005; Sen et al., 2006a; Sen et al., 2006c) but also under physiological conditions (e.g. in cells subject to serum deprivation, in late stationary phase cultures (Lee *et al.*, 2002)) and in amastigotes within antileishmanial drug-treated macrophages (Sudhandiran and Shaha, 2003) (Debrabant *et al.*, 2003).

However, the mechanisms involved in the parasite PCD remains poorly described at the molecular level. In *T. cruzi* epimastigotes, the translocation of the elongation factor 1-alpha (EF1α) from the cytoplasm into the nucleus of the dying cells is suspected to mediate transcriptional processes that regulate cell death genes (Billaut-Mulot *et al.*, 1996). In the same parasites, arginine metabolism was found to inhibit human serum-induced PCD via production of polyamines that favours cell growth (Piacenza *et al.*, 2001; Piacenza *et al.*, 2002). In *T. brucei rhodesiense* procyclic forms, prohibitin, an orthologue of a mammalian proto-oncogene and RACK, a receptor for activated protein kinase C were found to be up-regulated during lectin-induced cell death (Welburn and Murphy, 1998). In *T. brucei brucei* procyclic forms, it was observed that the PCD induced by reactive oxygen species (ROS) was Ca^{2+}-dependent but could not be prevented by the expression of the mouse anti-apoptotic protein Bcl-2 (Ridgley *et al.*, 1999). Another group found that, again in *T. brucei brucei* procyclic forms, co-expression of the human anti-apoptotic Bcl-XL with the human pro-apoptotic Bax was sufficient to inactivate the Bax-induced mitochondrion fission (Esseiva *et al.*, 2004). In addition, it appeared from this study that the early phases of the PCD mitochondrial pathway were comparable to the mammalian system. In bloodstream form parasites, prostaglandin D_2 (and, more precisely, its J series metabolites) was found to induce PCD through production of ROS but in a caspase-independent manner (Figarella *et al.*, 2005; Figarella *et al.*, 2006).

In *Leishmania*, although PCD has been more extensively studied, very few reports actually contribute to the molecular characterization of the external and internal stimuli controlling apoptosis-like PCD. Surprisingly, most of them point to stage-specific mechanisms of PCD. In addition, apoptosis-like PCD seems to be triggered in response to a cell cycle block. While deletion of centrin, a Ca^{2+}-binding cytoskeletal protein involved in duplication of basal bodies, had no visible effect on promastigotes growth, *Leishmania* amastigotes failed to duplicate this organelle, could not enter cytokinesis, and lost their infectivity *in vivo*. The G2/M cell cycle block induced in amastigotes by centrin removal was shortly later accompanied by caspase-3/-7 activities, loss of membrane integrity and nuclear DNA fragmentation - which are features commonly observed during apoptosis-like PCD execution (Selvapandiyan *et al.*, 2004).

In amastigotes, the cytoplasmic Silent Information Regulator 2 (SIR2), a NAD-dependent deacetylase, was found to possess a fundamental role in cell proliferation. Partial gene deletion or specific inhibition (with Sirtinol) of this molecule resulted in amastigotes growth arrest and PCD induction (Vergnes et al., 2005a; Vergnes et al., 2005b). Overexpression of SIR2 decreased the amastigotes susceptibility to Sirtinol-induced PCD (Vergnes *et al.*, 2002). While *SIR2* gene knock-out was not achievable in promastigote forms, the growth of the heterozygote parasites was not affected *in vitro* (Vergnes *et al.*, 2005a) and Sirtinol treatment had no effect of the wild type promastigote development (Vergnes *et al.*, 2005b). Nevertheless, overexpression of SIR2 significantly increased the promastigotes survival under starvation conditions (Vergnes *et al.*, 2002).

Present only in the kinetoplast in promastigotes but distributed throughout the mitochondrion in amastigotes, the differentially-expressed peroxiredoxin, a mitochondrial enzyme involved in peroxide detoxification, participates to the stabilisation of the mitochondrial membrane potential. In the parasite, its overexpression has a protective role against hydrogen peroxyde-induced PCD (Harder *et al.*, 2006). Also, expression of high levels of peroxiredoxin might aid the survival of the amastigote forms which are exposed to high oxidative stress during their stay in the macrophage.

It was reported that promastigotes lacking the GPI-anchored metallo-peptidase gp63 (leishmanolysin), their major surface protein, are more susceptible to apoptosis-like PCD induced by antimicrobial peptides (Kulkarni *et al.*, 2006). Because of the protective role of gp63 against the sandfly immune system, but also its role as a promastigote virulence factor (Joshi *et al.*, 2002), apoptosis-like PCD appears to control the infectivity of the parasite population.

In this chapter I have conveyed the notion that PCD in trypanosomatids resembles mammalian apoptosis by use of the term "apoptosis-like PCD". Indeed, these

parasites can be killed in a way that provides morphological features of mammalian apoptosis and notably the activation of caspase-like activities. Also, because of their distant relationship with caspases and in the absence of better candidates, the trypanosomatid metacaspases were assumed to be responsible for the detected caspase-like activity and the nuclear phase of the apoptotic-like PCD (Kosec *et al.*, 2006).

However, when compared to apoptosis in higher eukaryotes (e.g. mammalian cells), there clearly are differences in the apoptosis-like PCD of parasitic protozoa, exemplified by *L. donovani* (Lee *et al.*, 2002) and *L. major* promastigotes (Arnoult *et al.*, 2002). In these parasites, the permeabilisation of the plasma membrane seems to occurs simultaneously with the activation of caspase-like activity, rather than following it like in mammals; no apoptotic bodies are formed; the caspase-like activities are only partially inhibited by caspase inhibitors, underpinning the involvement of other cysteine peptidases (Arnoult *et al.*, 2002; Lee *et al.*, 2002). It was also suggested that in *L. major* and *L. mexicana* the nuclear phase of the apoptosis-like PCD was likely to be mediated by uncharacterised nucleases and apparently not directly by caspase-like peptidases (Zangger *et al.*, 2002). Most importantly, in the strain initially used for the sequencing of the *Leishmania* genome, *L. major*, the vast majority of the proteins involved in the mammalian PCD are absent (Uren *et al.*, 2000). Notably, most representatives of the mitochondrial pathways are lacking (e.g. Bcl-2, Bid, Bax, Bcl-XL, Smac/Diablo, AIF), all the caspases and the PCD regulators such as cell death receptors (CD95/L, FADD), FLIP, IAP or Apaf-1.

In conclusion, although PCD appears to exist in trypanosomatids and in some cases has features comparable to mammalian apoptosis, the molecules involved remain mostly uncharacterised and the function of the metacaspase is still a big unknown.

1.5. Aims of my thesis project

My thesis project aimed to answer the following questions:

1) Is the *Leishmania major* metacaspase expressed? Is it constitutively expressed or only under stress conditions?
2) Is the *L. major* metacaspase an active enzyme? What are its biochemical properties?
3) Is the *L. major* metacaspase involved in PCD or does it play a different role within the cell?
4) Why does *L. major* have only one metacaspase, yet *T. brucei* has five?

Chapter 2:
Material and Methods

MATERIAL

2.1. Cell lines used in this study

2.1.1. Trypanosomatid cells

Leishmania major (MHOM/JL/80/Friedlin) amastigotes, freshly extracted from mouse lesions, were transformed into promastigote forms by cultivation in the appropriated medium. Stabilates of the freshly differentiated and virulent promastigote cells were made and used for the rest of the study (WUMP3888).

Trypanosoma brucei strain *427* (WUMP4496) was used for the genetic knockouts in the bloodstream forms (BSF). For the RNAi study, the bloodstream form 427 pLew13 pLew90-6 cell line was used (Wirtz et al., 1999). The Δ*Tbmca2*/3Δ*Tbmca5* (WUMP4499) and the *TbMCA2*, *TbMCA3* and *TbMCA5* triple RNAi (WUMP4148 and WUMP4149) bloodstream form cell lines were generated by Matthew J. Helms (Helms, 2004). The *MOB1* RNAi bloodstream form cell line (WUMP4674) was produced by Tansy C. Hammarton (Hammarton *et al.*, 2005).

2.1.2. Bacterial cells

Host strain: *Escherichia coli* XL1- Blue (*recA1 endA1 gyrA96 thi-1 hsdR17 supE44 relA1 lac* [F'*proAB lacI*^{q}*lacZ*Δ*M15 Tn10* (Tet^r)]) (Stratagene) or *E. coli* DH5α (F$^-$ φ80*lacZ*ΔM15 Δ(*lacZYA-argF*)U169 *recA1 endA1 hsdR17*(r_k^-, m_k^+) *phoA supE44 thi-1 gyrA96 relA1* λ$^-$) (Invitrogen). The *lacZ*ΔM15 marker provides α-complementation of the β-galactosidase gene encoded by the pGEMT cloning vector, allowing white/blue screening of vector-bearing colonies, on plates containing X-gal.

Expression strain: *E. coli* BL21(DE3) (F$^-$ *ompT hsdSB*(r_B^- m_B^-) *gal dcm* (DE3)) (Novagen). (DE3) strains are lysogenic for a λ prophage that contains an IPTG-inducible T7 RNA polymerase and are specially designed for protein expression from pET vectors. Alternatively, *E. coli* BL21(DE3)pLysS (F$^-$ *ompT hsdSB*(r_B^- m_B^-) *gal dcm* (DE3) pLysS (Cam^R)) (Novagen) cells were used. This strain carries a pACYC184-derived plasmid that encodes the T7 lysozyme, a natural inhibitor of the T7 RNA polymerase, which allows the repression of the background expression of target genes.

2.1.3. Yeast cells

The methylotrophic yeast *Pichia pastoris* was used as the host for high-level recombinant protein expression in the *Pichia* Expression System. In the absence of glucose, *Pichia pastoris* uses methanol as a carbon source. The alcohol oxidase (*AOX1*)

promoter controls expression of alcohol oxidase, which catalyzes the first step in methanol metabolism. Typically, 30% of the total soluble protein in methanol-induced cells is alcohol oxidase. The pPIC9 *Pichia* expression vector take advantage of the powerful *AOX1* promoter and use methanol to induce high-level expression of your gene of interest.

Expression strain: *Pichia pastoris* KM71 (*his4, aox1::ARG4, arg4*) (Invitrogen). The *Pichia* host strain KM71 has a mutation in the histidinol dehydrogenase gene (*his4*) which prevents them from synthesizing histidine (His^-). The parent strain of KM71 has a mutated argininosuccinate lyase gene (*arg4*) that prevents it from growing in the absence of arginine but, in the KM71 strain, the wild-type *ARG4* gene was used to disrupt *AOX1* thus reastoring their ability to grow without arginine (Arg^+). The loss of the *AOX1* gene, and thus a loss of most of the cell's alcohol oxidase activity, results in a strain that is phenotypically methanol utilization slow (Mut^S). This results in a reduction of the cells' ability to metabolize methanol and they therefore exhibit poor growth on methanol medium. Thus, cells are grown to high density and concentrated, before induction, to increase the total cell mass.

In addition to the expression strain, a GS115 (*his4*) control stain was provided in the *Pichia* expression kit (Invitrogen). The GS115/albumin (His^+ Mut^S) was used as the control for secreted expression and the Mut^S phenotype when screening *Pichia* transformants. The gene for serum albumin was cloned with its native secretion signal, then integrated into *Pichia* at the *AOX1* locus. This strain secretes albumin (67 kDa) into the medium at levels > 1 gram per liter.

2.2. Cell cultivation

2.2.1. *Leishmania major* promastigotes

The wild type *Leishmania major* Friedlin promastigotes cells were grown in HOMEM medium (For 500 ml of medium: 5.29 g S-MEM, 1 g glucose, 0.15 g $NaHCO_3$, 0.055 g sodium pyruvate, 0.5 mg Para Amino Benzoic Acid, 0.05 mg biotin, 2.98 g HEPES, 5 ml MEM-essential aminoacids (50x), 5 ml MEM-non essential aminoacids (100x) (Invitrogen, ref 041-946-99M)) + 10-20% (v/v) of heat inactivated Foetal Calf Serum (Labtech International, cat No 4-101-500) at 25°C in a phenolic-style cap flask. In order to maintain the cells alive a sub-passage in fresh medium was done twice a week. The required antibiotics were added to the cultures of generated transgenic cell lines typically as follows: hygromycin B (Calbiochem) at 50 mg ml^{-1}; phleomycin (Cayla) at 10 mg ml^{-1}; puromycin (Calbiochem) at 10 to 100 mg ml^{-1}; blasticidin S (hydrochloride, Calbiochem) at 10 mg ml^{-1}; and neomycin (G418, Geneticin, Calbiochem) at 15 to 50 mg

ml^{-1}. Stabilates were made by diluting 500µl of cells with 500µl of HOMEM + 20% FCS+ 10% DMSO in a 1.5 ml cryotube and then were stored at -80°C overnight and then in liquid nitrogen.

2.2.2. *Trypanosoma brucei* bloodstream forms

Bloodstream form (BSF) 427 *T. brucei* were cultured at 37°C with 5% CO_2 in HMI-9 medium (Hirumi and Hirumi, 1989) supplemented with 10% (v/v) of heat inactivated FCS and 10% (v/v) serum plus. For the BSF *TbMCA2*, *TbMCA3* and *TbMCA5* RNAi cell lines and *MOB1* RNAi cell line, antibiotic pressure was maintained by addition of hygromycin (Calbiochem) at 5 µg ml^{-1}, neomycin (Calbiochem) at 2 µg ml^{-1} and phleomycin (Cayla) at 2.5 µg ml^{-1}. When needed, blasticidin (Calbiochem) and puromycin (Calbiochem) were used at 2 µg ml^{-1}. RNAi was induced with 1 µg ml^{-1} tetracycline hydrochloride when the cells were at a density of $1x10^5$ cells ml^{-1}.

2.2.3. *Escherichia coli* cells

Cells were transformed with the desired vector which, with either the *β-lactamase* or *kan* genes, would confer resistance to ampicillin or kanamycin, respectively. Selection of the transformants was performed with 100 µg ml^{-1} ampicillin (100 mg ml^{-1} stock solution in 50% ethanol) or 25-50 µg ml^{-1} kanamycin (25 mg ml^{-1} stock solution in 50% ethanol). Cells were culture in liquid LB medium (Lennox Both base, 10 g l^{-1} bacto-tryptone, 5 g l^{-1} yeast extract, 10 g l^{-1} NaCl), complemented with the relevant selective antibiotics, at 37°C. Transformant clones were obtained after spreading on a LB-agar plate (LB medium, 15 g l^{-1} bacto-agar) with antibiotics.

2.2.4. *Pichia pastoris* cells

The wild type KM71 (Mut^S, Arg^+, His^-) strain grows on complex medium such as YPD (Yeast extract Peptone Dextrose medium, 1% yeast extract, 2% peptone and 2% dextrose (glucose)) and on minimal media supplemented with histidine (Minimal Dextrose Histidine medium, MDH, 1.34% YNB, 4 x 10^{-5}% biotin, 2% dextrose, 0.004% histidine). Until transformed, KM71 cells do not grow on minimal medium alone as they are His^-. All expression plasmids carry the *HIS4* gene which, after introduction into the host cell, complements the host *his4* and allow the selection of the transformants by their newly acquired ability to grow on histidine-deficient medium. Spontaneous reversion of KM71 to His^+ prototrophy is less than 1 out of 10^8. The growth temperature of *Pichia pastoris* is 28-30°C for liquid cultures and plates. Growth above 32°C during induction can be detrimental to protein expression and can even lead to cell death.

The doubling time of log phase Mut^S *Pichia* in YPD is ~2 hs and ~18 hs in methanol-containing medium. During methanol induction, methanol was added every day, to the culture medium, to compensate for loss due to evaporation or consumption. Cells were stored for weeks to months on YPD medium or YPD agar plates at 4°C. For longer storage cells were stored at -80°C in YPD containing 15% glycerol. After long-term storage at 4°C or -80°C, the His$^+$ transformants were checked for correct genotype and viability by streaking them on Minimal Dextrose plates (MD medium, 1.34% YNB, 4 x 10^{-5} % biotin, 2% dextrose), before using again.

2.3. Vectors used in this study

2.3.1. Subcloning vectors

The pGEM-T vector (Promega) was used for the cloning of PCR fragments amplified with the *Taq* DNA polymerase (NEB). For PCR fragment generated with proof reading DNA polymerases such as the *Pfu* Turbo (Stratagene) or the *Taq* Plus Precision polymerase mixture (Stratagene), the blunt-ended pPCR-Script vector (Stratagene) was favoured. Both plasmids confer ampicillin resistance to the host strain and, when transformed into *E. coli* XL1 Blue cells, allow a white/blue screening of the vector-bearing bacteria. The sub-clonings were performed following the manufacturer's protocol.

2.3.2. Expression vectors

2.3.2.1. For *E. coli*: pET28a(+) (Novagen)

The pET-28a (+) vectors carry an N-terminal His-Tag/thrombin/T7-Tag configuration plus an optional C-terminal His-Tag sequence. This vector was used to generate N- or C-terminally His tagged protein. The vector contains strong transcription signals for the control of the T7 RNA polymerase of the *E. coli* BL21 host. Expression of the target gene is induced upon addition of IPTG to the culture medium of the vector-bearing BL21 cells. MCA, MCA^{C201G}, MCA$^{C201-202G}$, MCA^{C202G}, and MCA^{H147A} were cloned into the pET28a(+) to give the pGL1421 to pGL1425, respectively.

2.3.2.2. For *P. pastoris*: pPIC9 (Invitrogen)

This vector allows multicopy integration of the gene of interest thus potentially leading to a higher expression of the protein of interest in *P. pastoris*. The pPIC9 carries an *AOX1* promoter for high-level inducible expression, a *HIS4* gene for identification of

transformants, 5' and 3' *AOX1* gene fragments for targeted integration into the *Pichia* host genome and the α-factor secretion signal to target recombinant protein expression to the growth medium (**figure 2.1**).

The pPIC9 is linearised by *Sac*I to allow insertion at the 5' of the *AOX1* region and generate a His^+ Mut^S phenotype when transformed into the *Pichia* KM71 strain. MCA, ΔproMCA, ΔeproMCA, ΔeproMCAΔCterm, MCAΔCterm and ΔproMCAΔCterm were cloned into the pPIC9 (pGL1426) to give the pGL1112, 1113, 1419, 1420, 1427 and 1428, respectively.

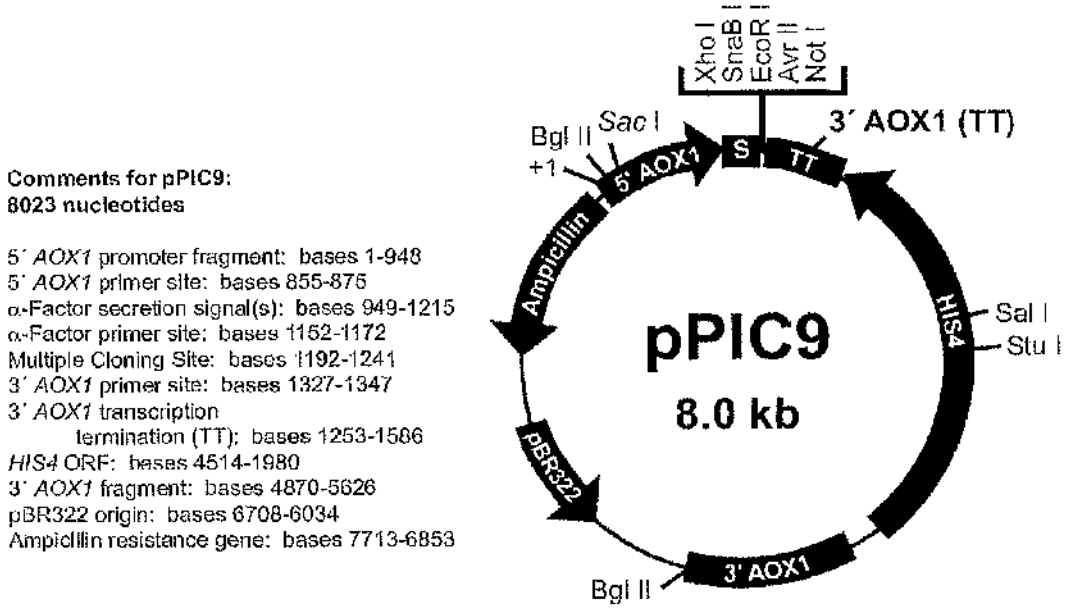

Figure 2.1: Schematic of the pPIC9 *Pichia* expression vector

2.3.2.3. For *Leishmania major*

2.3.2.3.1. pNUS vectors

It is known that, in trypanosomatids, 5'-trans-splicing signals and poorly defined regions within the 3'-untranslated regions of genes are required for optimal expression of genes. Based on the pUC18 vector, the pNUS vectors also possess intergenic region of the *Crithidia fasciculata* phosphoglycerate kinase (*PGK*) genes A and B, which allows polyadenylation of the target gene and spliced leader addition to the selectable marker gene. Part of the intergenic region of the *PGK* locus was added upstream of the target gene to permit its trans-splicing. A 3'-untranslated sequence from the *C. fasciculata* glutathionylspermidine synthetase (*GSPS*) was also added to allow the polyadenylation

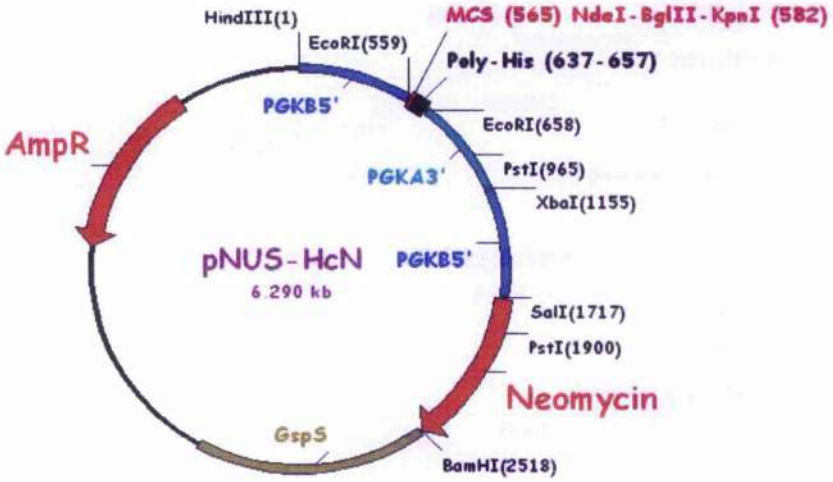

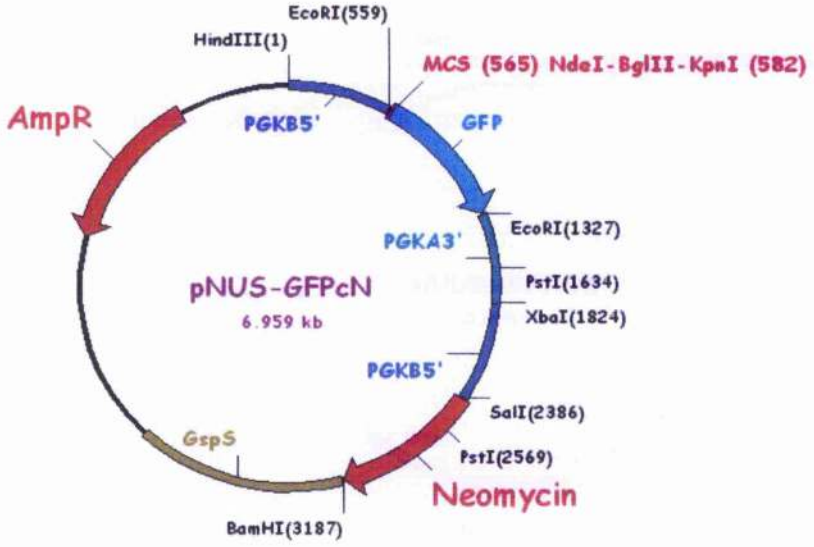

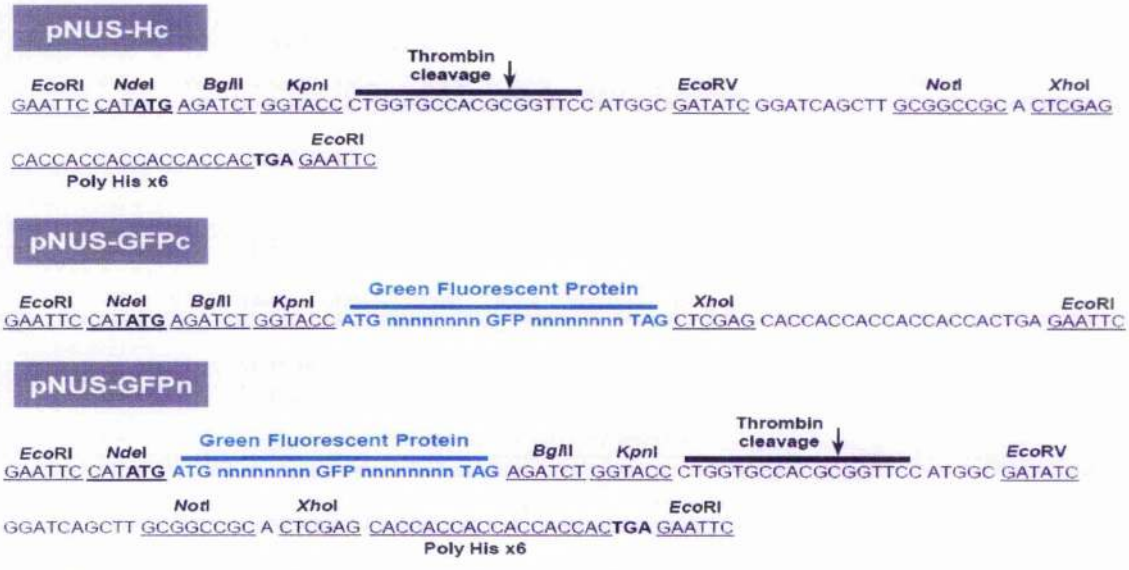

Figure 2.2: Schematic of the pNUS *Leishmania* expression vectors and their multiple cloning sites

Maps were obtained from http://www.ibgc.u-bordeaux2.fr/pNUS/

of the selectable marker gene. Genes can be readily inserted using a multiple cloning site and can be expressed as a fusion protein with a poly-histidine sequence or with the *Aequorea victoria* green fluorescent protein (GFP), at either the N- or C-terminus (Tetaud *et al.*, 2002). The vectors used in this study were the pNUS-HcN (pGL1137), the pNUS-GFPcN (pGL1132) and the pNUS-GFPnN (pGL1135) (**figure 2.2**) (kindly provided by Dr E. Tetaud). They all possess a neomycin resistance marker. For a detailed list of the vectors generated please refer to **section 2.5.**

2.3.2.3.2. pTEX

Based on the pBlueScript vector, this shuttle vector possesses, in addition, the intergenic and flanking regions of the two *Trypanosoma cruzi* glyceraldehyde 3-phosphate dehydrogenase (*GAPDH*) genes (**figure 2.3**). The two tandem GAPDH genes themselves have been replaced by a multicloning site and a selectable marker gene. The cloned target gene and the neomycin resistance gene will therefore be properly trans-spliced and polyadenylated and thus optimal expressed **(Kelly et al., 1992)**. MCA, MCA^{C202G}, ΔproMCA, ΔproMCA^{C202G}, MCA^{C201G}, MCA$^{C201-202G}$ and MCA^{H147A} were cloned into the pTEX (pGL83) to give the pGL1128, 1129,1130, 1131, 1294, 1296 and 1406, respectively.

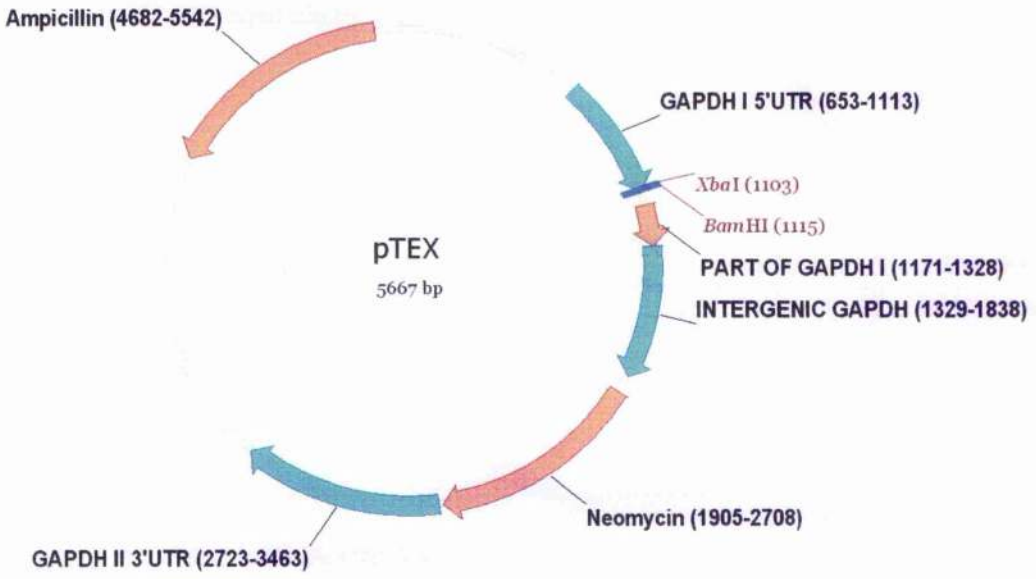

Figure 2.3: Schematic of the pTEX *Leishmania* expression vector

2.3.2.3.3. pRIB

Based on the pFW31 vector (Benzel *et al.*, 2000), the pRIB vector allows gene addback and heterologous expression studies (Garami and Ilg, 2001). This vector uses the 5'-trans-splicing signals and 3'- polyadenylation sites of the *L. major* dihydrofolate reductase-thymidylate synthase (*DHFR-TS*) gene to allow the optimal expression of the

target gene (**figure 2.4**). Once excised by *Pac*I and *Pme*I, the linearised integration cassette, containing the 5' and 3' untranslated regions of the 18S ribosomal RNA small subunit gene (*18S rRNA*), will recombine into the ribosomal locus of *Leishmania*, and allow the expression of the target gene under the control of the rRNA promoter. This promoter is known to lead to high level expression not only in promastigote but also in amastigote forms (Misslitz *et al.*, 2000). MCA and MCA^{H147A} were cloned into the pRIB (pGL631) to give the pGL1399 and 1400, respectively.

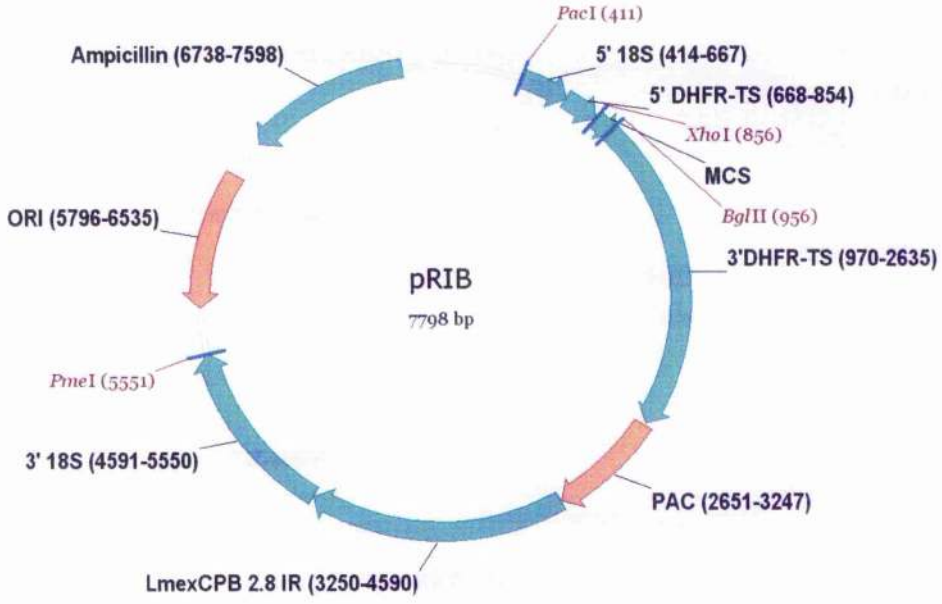

Figure 2.4: Schematic of the pRIB *Leishmania* expression vector

2.3.3. Gene knock-out vector for *Leishmania*

The backbone vector used here is the pGL896 (Besteiro *et al.*, 2004). The recombination cassettes containing the 5' and 3'UTRs of *L. mexica ICP* can be easily replaced by the ones of the gene of interest by *Hin*dIII/*Sal*I and *Xma*I/*Bgl*II digestions, respectively (**figure 2.5**).

For antibiotic selection, this vector contains a blasticidin resistance cassette flanked by the 5' and 3'UTR of *DHFR-TS*. Once excised by *Hin*dIII and *Bgl*II, the linearised integration cassette, containing the 5' and 3' UTRs of the gene of interest, will allow homologous recombination into the chromosomal locus of the gene of interest, therefore achieving a knock-out.

The 5' and 3' flanking regions of *MCA* were cloned into pGL792 to give pGL842. The selectable marker cassette (*Spe*I/*Bam*HI) was then replaced by either a hygromycin (pGL849) or a bleomycin (pGL1033) resistance gene. Alternatively the 5' and 3' of *MCA*

itself were used as recombination cassettes (pGL968 and 971 with blasticidin and hygromycin resistance genes, respectively)

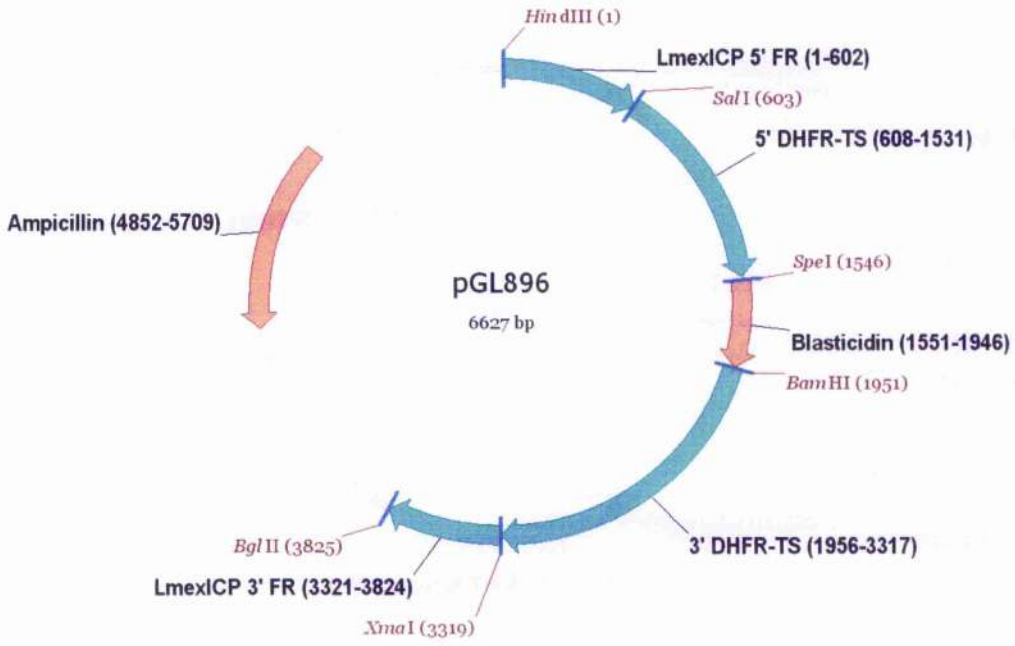

Figure 2.5: Schematic of the pGL896 *Leishmania* knock-out vector

2.4. Oligonucleotides used in this study

Sequences are written in 5' → 3' sense. The orientations of the primers are indicated in brackets after theirs names (5' for forward and 3' for reverse). When the oligonucleotides contain restriction sites, their sequences are underlined and the corresponding cleaving enzymes are named in brackets. Oligonucleotides removing the natural stop codon of MCA to allow the fusion of a C-terminal tag are pointed by the mention "stop deleted". Oligonucleotides designed to be in frame with the start codon of an N-terminal tag are indicated by the mention "α-factor". For the active site mutagenesis, the codon that has been modified is underlined, the mutated nucleotide(s) indicated in bold and the resulted mutation written in brackets.

OL1188 (5'):	aac gaa CTC GAG ATG GCA GAC CTT TTT GAT	(*Xho*I)
OL1189 (3'):	acg ttc GGA TCC ATC TTA GCC AGG CGG GAG	(*Bam*HI)
OL1190 (5'):	gag cga AAG CTT TGA TCC TCT CAA GAA GGT	(*Hind*III)
OL1191 (3'):	tcg ttt GTC GAC TAT AGT ATT ACG CGT ATT	(*Sal*I)
OL1192 (5'):	gtg gag CCC GGG ATG TTT TGG CAC CGG TTC	(*Xma*I)
OL1193 (3'):	ccg ctg AGA TCT GCT TGA ACA CAC GCT TGT	(*Bgl*II)

OL1215 (5'):	tgg tca CCA TGG CAG ACC TTT TTG ATA TTT	(*Nco*I)
OL1216 (3'):	tga tgt CTC GAG GCC AGG CGG GAG TGG GCT	(*Xho*I, stop deleted)
OL1304 (5'):	GCT TGG AGA TAT CGA CTG AT	
OL1305 (3'):	CG AGT AGA CAC GAG CTG AAG	
OL1396 (5'):	gaa atc CAT ATG GCA GAC CTT TTT GAT ATT	(*Nde*I)
OL1397 (5'):	cgg gtc CAT ATG AAT GCC GGA AGG CGG CTC	(*Nde*I)
OL1398 (3'):	tga tgt GGT ACC GCC AGG CGG GAG TGG GCT	(*Kpn*I, stop deleted)
OL1399 (5'):	aac gaa TCT AGA ATG GCA GAC CTT TTT GAT ATT	(*Xba*I)
OL1400 (5'):	aaa cgg TCT AGA ATG AAT GCC GGA AGG CGG CTC	(*Xba*I)
OL1401 (5'):	TGC GTC TTT GAC TGC GGT CAC TCA GCC AGC ATG	(C201G)
OL1402 (3'):	CAT GCT GGC TGA GTG ACC GCA GTC AAA GAC GCA	(C201G)
OL1446 (5'):	aac gaa GGA TCC ATG GCA GAC CTT TTT GAT ATT	(*Bam*HI)
OL1447 (5'):	aaa cgg GGA TCC ATG AAT GCC GGA AGG CGG CTC	(*Bam*HI)
OL1570 (3'):	gta ctg GGT ACC CAC GCA ATG CAT CAT	(*Kpn*I, stop deleted)
OL1571 (5'):	aac gaa TAC GTA ATG GCA GAC CTT TTT GAT	(*Sna*BI)
OL1572 (5'):	cgg gtc TAC GTA AAT GCC GGA AGG CGG CTC	(*Sna*BI, α-factor)
OL1573 (3'):	acg ttc CCT AGG ATC TTA GCC AGG CGG GAG	(*Avr*II)
OL1774 (5'):	ACG TGC GTC TTT GAC GGC TGT CAC TCA GCC AGC	(C202G)
OL1775 (3'):	GCT GGC TGA GTG ACA GCC GTC AAA GAC GCA CGT	(C202G)
OL1841 (5'):	ACG TGC GTC TTT GAC GGC GGT CAC TCA GCC AGC AT	(C201-202G)
OL1842 (3'):	CAT GCT GGC TGA GTG ACC GCC GTC AAA GAC GCA CGT	(C201-202G)
OL2005 (5'):	aac tac TAC GTA ATG CGC AAC GCA CTG CGT	(*Sna*BI, α-factor)
OL2006 (3'):	GAG GAT CAT ATG CTC GCT AAT CGG GAA GGA	(*Nde*I)
OL2007 (5'):	ACC AGC CTC GAG GTG CAG AAC GGC GGC CAC	(*Xho*I)
OL2008 (3'):	CGA AGG GAG CTC TTA GCC AGG CGG GAG TGG	(*Sac*I)
OL2064 (5'):	CAC TCC AGA CGG TGG GCA	
OL2065 (3'):	CAC CTA CAG CTA CCT TGT	

2.5. Plasmids generated

Schematics of the MCA constructs generated are shown in **figures 2.7 and 2.8.**

Active site mutagenesis

pGL1429: pPCR-Script + *MCA* OL1215/1216 (*Xba*I/*Xho*I)

pGL1231: pPCR-Script-OL1400/1189 (*Xba*I/*Xho*I) + *C202G* cassette (*Xba*I/*Xho*I from pGL1421)

pGL1291: pGL1231 (*Xba*I/*Xho*I) + *C201G* cassette OL1174/1175 (*Xba*I/*Xho*I)

pGL1292: pGL1231 (*Xba*I/*Xho*I) + *C201-202G* cassette OL1841/1842 (*Xba*I/*Xho*I)

Expression in pET28a(+)

MCA-His

pGL1421: pET28a(+) AMP (*XbaI/XhoI*) + *MCA* (*XbaI/XhoI* from pGL1429)

MCA^{C201G}-His

pGL1422: pET28a(+) AMP (*XbaI/XhoI*) + MCA^{C201G} (*XbaI/XhoI* from pGL1291)

$MCA^{C201-202G}$-His

pGL1423: pET28a(+) AMP(*XbaI/XhoI*) + $MCA^{C201-202G}$ (*XbaI/XhoI* from pGL1292)

MCA^{C202G}-His

pGL1424: pET28a(+) AMP (*XbaI/XhoI*) + MCA^{C202G} (*XbaI/XhoI* from pGL1231)

MCA^{H147A}-His

pGL1425: pGL1422 (*NruII/XhoI*) + MCA^{H147A} (*NruII/XhoI* from pGL1401)

Expression in pPIC9

Backbone plasmid

pGL1426: pPIC9 vector for inducible expression in *Pichia* (multicopy + secretion in medium)--Invitrogen K171001

MCA with α-factor signal in N-terminus

pGL1112: pPIC9 (*SnaBI/AvrII*) + *MCA* OL1571/1573 (*SnaBI/AvrII*)

ΔproMCA with α-factor signal in N-terminus

pGL1113: pPIC9 (*SnaBI/AvrII*) + *ΔproMCA* OL1572/1573 (*SnaBI/AvrII*)

ΔeproMCA with α-factor signal in N-terminus

pGL1419: pPIC9 (*SnaBI/AvrII*) + *ΔeproMCA* OL2005/1573 (*SnaBI/AvrII*)

ΔeproMCAΔCterm with α-factor signal in N-terminus

pGL1420: pGL1419 digested by *MluI/AvrII*, filled in with Klenow and ligated on itself to remove the C-terminal extension of MCA

MCAΔCterm with α-factor signal in N-terminus

pGL1427: pGL1112 digested by *MluI/AvrII*, filled in with Klenow and ligated on itself to remove the C-terminal extension of MCA

ΔproMCAΔCterm with α-factor signal in N-terminus

pGL1428: pGL1113 digested by *MluI/AvrII*, filled in with Klenow and ligated on itself to remove the C-terminal extension of MCA

Expression in pNUS vectors

MCA-His

pGL981: pNUS-HcN (*NdeI/KpnI*) + *MCA* (*NdeI/KpnI* from pPCR-Script-OL1396/1398)

MCA^{C202G}-His

pGL982: pNUS-HcN (*NdeI/KpnI*) + MCA^{C202G} (*NdeI/KpnI* from pPCR-Script-OL1396/1398 C202G)

ΔproMCA-His

pGL983: pNUS-HcN (*NdeI/KpnI*) + *ΔproMCA* (*NdeI/KpnI* from pPCR-Script-OL1397/1398)

ΔproMCA^{C202G}-His

pGL984: pNUS-HcN (*NdeI/KpnI*) + *ΔproMCA^{C202G}* (*NdeI/KpnI* from pPCR-Script-OL1397/1398 C202G)

MCA^{H147A}-His

pGL1401: pGL981 (*NruI/MluI*) + *H147A* cassette (*NruI/MluI* from pGL 1406)

MCA-GFP

pGL985: pNUS-GFPcN (*NdeI/KpnI*) + *MCA* (*NdeI/KpnI* from pPCR-Script- OL1396/1398)

MCA^{C202G}-GFP

pGL986: pNUS-GFPcN (*NdeI/KpnI*) + *MCA^{C202G}* (*NdeI/KpnI* from pPCR-Script-OL1396/1398 C202G)

ΔproMCA-GFP

pGL987: pNUS-GFPcN (*NdeI/KpnI*) + *ΔproMCA* (*NdeI/KpnI* from pPCR-Script-OL1397/1398)

ΔproMCA^{C202G}-GFP

pGL988: pNUS-GFPcN (*NdeI/KpnI*) + *ΔproMCA^{C202G}* (*NdeI/KpnI* from pPCR-Script-OL1397/1398 C202G)

Cterm-GFP

pGL1108: pGL985 digested by *NdeI/MluI* , filled in with Klenow and ligated on itself to remove the rest of MCA ORF. ATG in frame naturally presents.

proregion-GFP

pGL1109: pGL985 digested by *Nru/Acc65I*, filled in with Klenow and ligated on itself to remove the rest of MCA ORF.

MCAΔCterm-GFP

pGL1110: pNUSGFPcN (*NdeI/KpnI*) + *MCAΔCterm* OL1396/1570 (*NdeI/KpnI*)

ΔproMCAΔCterm-GFP

pGL1111: pNUSGFPcN (*NdeI/KpnI*) + *ΔproMCAΔCterm* OL1397/1570 (*NdeI/KpnI*)

MCA^{C201G}-GFP

pGL1293: pGL985 (*BglII/MluI*) + *C201G* cassette (*BglII/MluI* from pGL1291)

MCA$^{C201-202G}$-GFP

pGL1295: pGL985 (*BglII/MluI*) + *C201-202G* cassette (*BglII/MluI* from pGL1292)

MCA^{H147A}-GFP

pGL1402: pGL985 (*NruI/MluI*) + *H147A* cassette (*NruI/MluI* from pGL 1406)

eNterm-GFP

pGL1403: pNUS-GFPnN (*NdeI*) + *eNterm* OL1396/OL2006 (*NdeI/NdeI*)

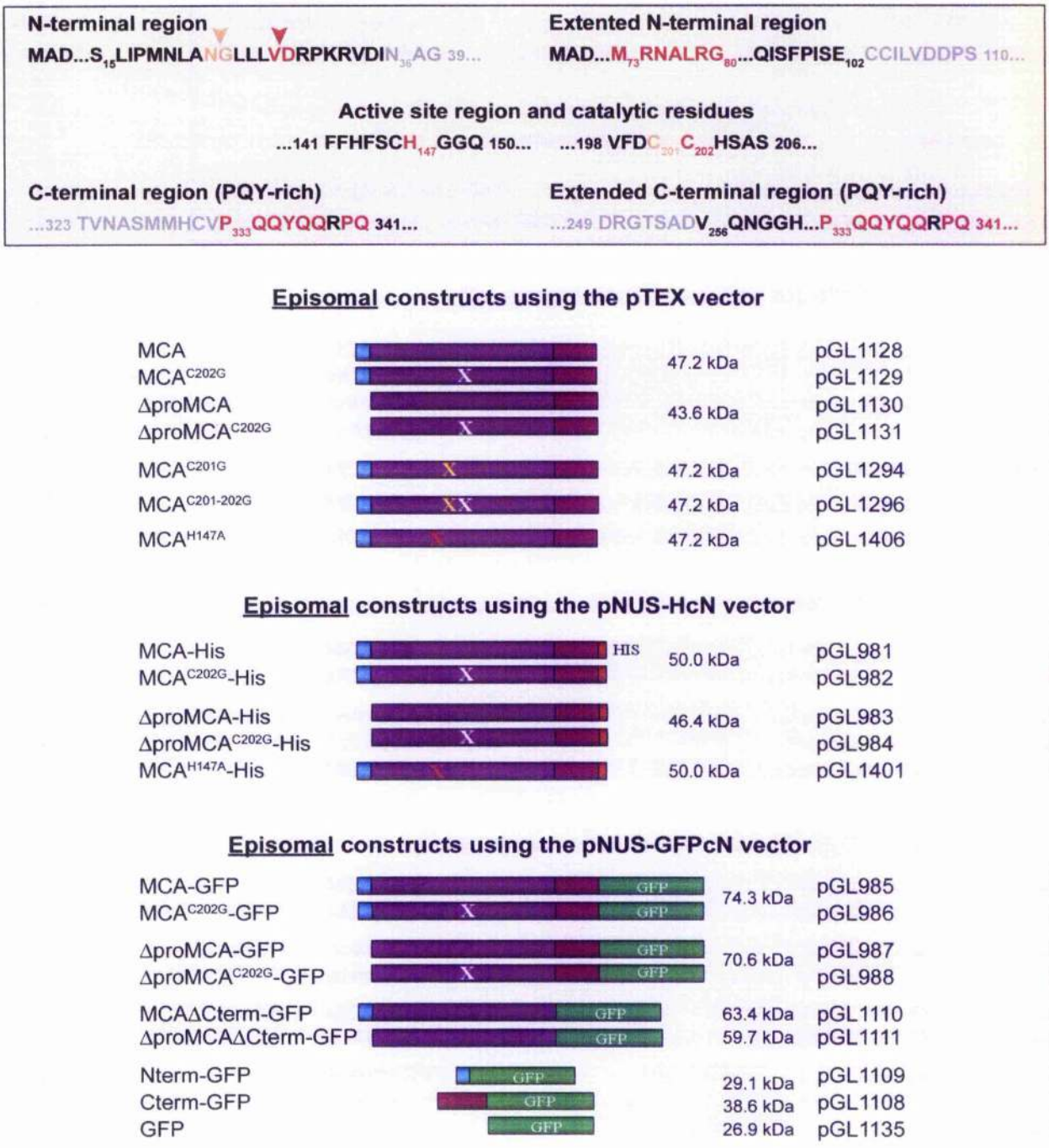

Figure 2.6: Schematic representation of the MCA constructs generated for this study (part A).

Upper panel: key regions of MCA. Regions of interest and important amino acids are shown in black and red, respectively. The numbers indicate their positions in the MCA sequence. Lower panel: Schematics of the various constructs created. All the constructs represented here were expressed (except pGL1406) in *L. major*, *E. coli* or *P. pastoris* (see part B in **figure 2.7**). The protein encoded, its molecular weight and the corresponding plasmid used for the expression (pGL numbers) are indicated. For the legend of the color code please refer to **figure 2.7**.

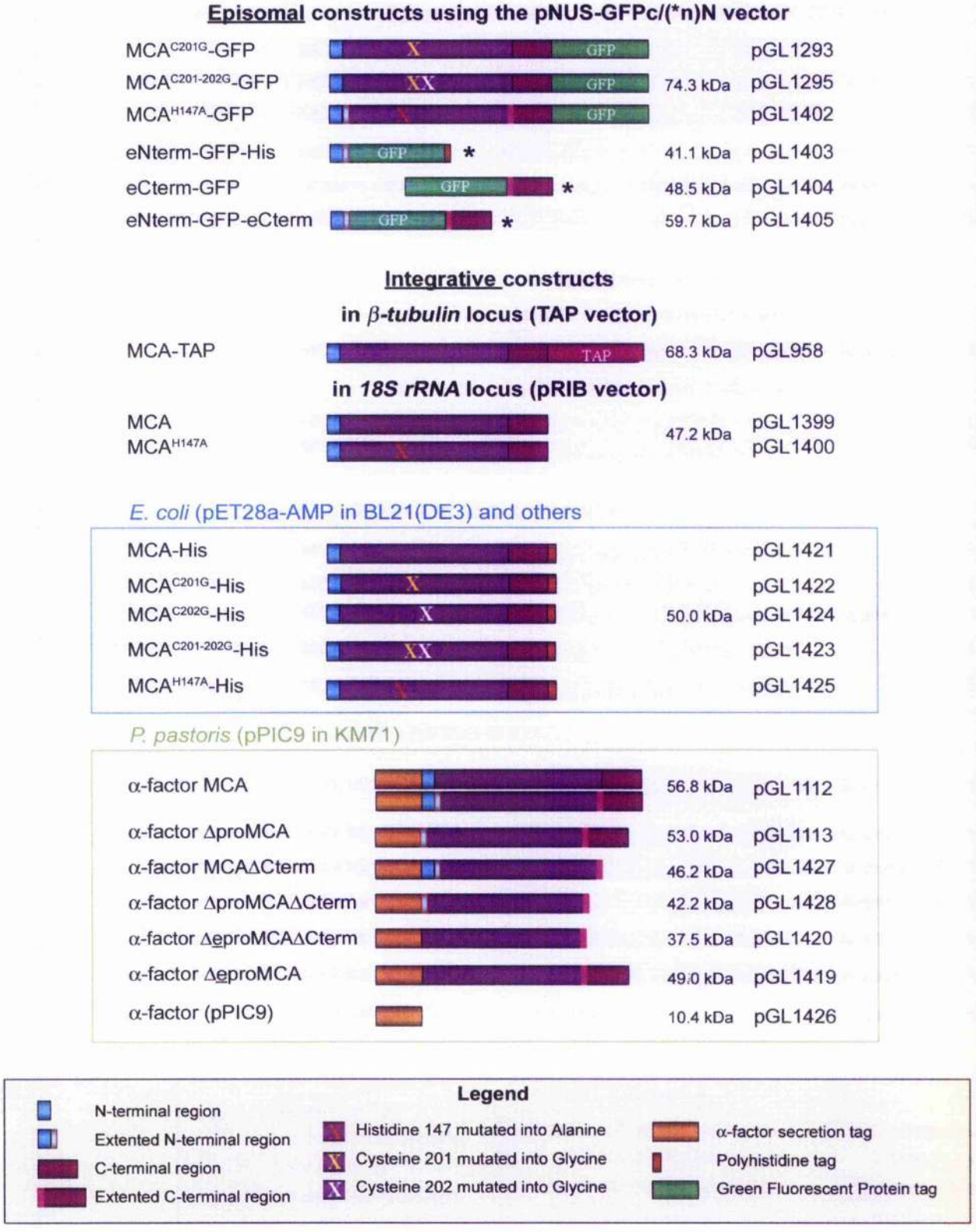

Figure 2.7: Schematic representation of the MCA constructs generated for this study (part B).

The asterisks indicate constructs designed using the pNUS-GFPnN.

GFP-eCterm

pGL1404: pNUS-GFPnN (*XhoI*/*SacI*) + *eCterm* OL2007/OL2008 (*XhoI*/*SacI*)

eNterm-GFP-eCterm

pGL1405: pGL1403 (*XhoI*/ *SacI*) + *eCterm* OL2007/OL2008 (*XhoI*/*SacI*)

Expression in pTEX

MCA

pGL1128: pTEX (*XbaI*/*BamHI*) + *MCA full* (*XbaI*/*BamHI* from pPCR-Script- OL1399/1189)

MCA^{C202G}

pGL1129: pTEX (*XbaI*/*BamHI*) + *MCA^{C202G}* (*XbaI*/*BamHI* from pPCR-Script-OL1399/1189 C202G)

ΔproMCA

pGL1130: pTEX (*XbaI*/*BamHI*) + *ΔproMCA* (*XbaI*/*BamHI* from pPCR-Script-OL1400/1189)

ΔproMCA^{C202G}

pGL1131: pTEX (*XbaI*/*BamHI*) + *ΔproMCA^{C202G}* (*XbaI*/*BamHI* from pCR-Script-OL1400/1189 C202G)

MCA^{C201G}

pGL1294: pGL1128 (*BglII*/*MluI*) + *C201G* cassette (*BglII*/*MluI* from pGL1291)

MCA$^{C201-202G}$

pGL1296: pGL1128 (*BglII*/*MluI*) + *C201-202G* cassette (*BglII*/*MluI* from pGL1292)

MCA^{H147A}

pGL1406: pGL1128 (*NruI*/*BstEII*) + *H147A* cassette (*NruI*/*BstEII* from pESC-His + *MCA^{H147A}* (from Iveth Gonzales (Nicolas Fasel's lab))

Expression in pRIB

Integration of MCA into ribosomal locus

pGL1399: pRIB (*XhoI*/*BglII*) + *MCA* OL1188/OL1189 (*XhoI*/*BamHI*)

Integration of MCA^{H147A} into ribosomal locus

pGL1400: pGL1399 (*NruI*/*BstXI*) + *H147A* cassette (*NruI*/*BstXI* from pGL 1406

MCA knock-out

Gene replacement

pGL842: pGL896 (blasticidin selection marker) + 5'FR *MCA* OL1190/OL1191 (*HindIII* /*SalI*) + 3'FR *MCA* OL1192/OL1193 (*XmaI*/*BglII*),

pGL849: pGL842 (*SpeI*/*BamHI*) + hygromycin selection marker (*SpeI*/*BamHI*) from pGL720

pGL1033: pGL842 (*SpeI*/*BamHI*) + bleomycin selection marker (*SpeI*/*BamHI*) from pGL726

Gene disruption

pGL967: pGL842 (*Bst*EII/*Bgl*II) + new 3' region (*Bst*EII/*Bam*HI from pPCR-Script-OL1188/OL1189)

pGL968: pGL967 (*Hin*dIII/*Sal*I) + new 5' region (*Hin*dIII/ *Sal*I from pPCR-Script OL1397/OL1216)

pGL970: pGL967 (*Spe*I/*Bam*HI) + hygromycin selection marker (*Spe*I/*Bam*HI) from pGL849 (cl1 23/09/03).

pGL971: pGL970 (*Hin*dIII/*Sal*I) + new 5' region (*Hin*dIII/ *Sal*I from pPCR-Script OL1397/OL1216).

METHODS

2.6. Preparation of genomic DNA from *Leishmania major*

Around $5x10^7$ cells were washed twice in PBS, resuspended in 500 µl of TELT (50 mM Tris-HCl pH 8, 62.5 mM EDTA pH 8, 2.5 M LiCl, 4% Triton X-100) with 10 µl of RNAse A (Sigma, 10 mg ml^{-1} stock) and incubated at room temperature for 5 mins. Two phenol extractions were then performed followed by two chloroform (24:1 with isoamylic alcohol) extractions. DNA was subsequently ethanol-precipitated by addition of 2 volumes of 100% ethanol and 10% 3 M NaAc pH5.2 and incubation at -20°C for at least 30 mins prior to centrifugation at 20,000 g for 30 mins. The DNA pellet was then washed twice with chilled 70% ethanol. Once air-dried the genomic DNA pellet was resuspended in 50 µl TE (10 mM Tris-HCl, 1 mM EDTA pH=8) or water. Alternatively, genomic DNA was prepared following the "cultured animal cells" protocol of the DNeasy tissue kit (Qiagen). DNA was quantified by measuring the absorbance of a 1:10 dilution, in water, at a wavelength of 260 nm. Genomic DNA concentration was deduced from the Beer-Lambert Law: Concentration (µg/ml) = $Abs_{\lambda=260nm}$ x sample dilution x 50µg ml^{-1} (where 50µg ml^{-1} represent the concentration of DNA necessary to obtain 1unit of absorbance at λ=260nm).

2.7. Southern blot

2.5 µg of genomic DNA were digested for 18 hs with 30 units of the appropriate restriction enzymes under the temperature and buffer conditions mentioned by the manufacturer (NEB). The various fragments of the digested genomic DNA were then separated by electrophoresis through a 0.8 % agarose gel (SeaKem LE Agarose, BMA) in

0.5xTBE. The agarose gel was then immersed in a depurination solution (0.25 M HCl) for 15 mins then in a denaturing solution (0.5 M NaOH, 1.5 M NaCl) for 30 mins and then twice 15 mins, in a neutralisation solution (0.5 M Tris-HCl pH 8, 3 M NaCl). Between each of those steps, the agarose gel was washed with distilled water. After 5 mins incubation in a 20x SSC solution (3 M NaCl, 3 M trisodium citrate), the agarose gel was transferred to a positively charged nylon membrane (Hybond N+, Amersham Pharmacia biotech) by upward capillarity (Sambrook J. and Russell D.W., 2001)

On the following day the membrane was rinsed in 2 x SSC, air dried and then the DNA were fixed to the membrane by UV exposure (UV Stratalinker: 2 times "autocross link"). The membrane was then incubated in 10 ml of hybridation solution (1 M NaCl, 10% SDS and 10 μg ml^{-1} salmon sperm DNA) for 1 h at 65°C. The membrane was then probed at high stringency (65°C), overnight, with the ^{32}P radiolabelled probe (prepared by random primer labelling with the Prime-It II kit (Stratagene) according to the manufacturers instructions). 20 mins washes were then performed at 60°C with 2x SSC, 0.1 % SDS and then with 0.2x SSC, 0.1% SDS. A ^{32}P sensitive screen was then exposed to the radioactive membrane and revealed using the storage phosphor acquisition parameter (Typhoon Image Control) of a PhospholImager (Typhoon 8600, Amersham Bioscience Labcrew). The data were then analysed using the ImageQuant 5.1 software (Molecular Dynamics).

2.8. Polymerase Chain Reactions (PCRs)

PCR reactions were, depending on the requirements, performed using either the *Taq* DNA polymerase (AB gene or NEB) or the high-fidelity *Taq* Plus Precision polymerase mixture (Stratagene).

For analytic PCRs, 100 ng of DNA were hybridised with 100 ng of each oligonucleotide and amplified by 0.5 units of *Taq* polymerase in a final volume of 20 μl. For the polymerase to be fully active, 2 μl of 10x PCR mix (1.13 mg ml^{-1} BSA, 450 mM Tris pH 8.8, 110 mM ammonium sulphate, 45 mM $MgCl_2$, 68.3 mM β-mercaptoethanol, 44 μM EDTA pH 8.0, 10 mM dCTP, 10 mM dATP, 10 mM dGTP, 10 mM dTTP, water) were included in the reaction tube. Amplifications were ultimately performed in a PCR Express machine (Hybaid) during the following successive steps: 95°C 5 mins, 50°C 30 secs, 72°C y mins) x1 then (95°C 30 secs, 55°C 30 secs, 72°C y mins) x25 and finally 72°C for 10 mins.

For proof-reading amplification from genomic DNA, PCRs were usually performed in 100μl reaction with 150 ng of DNA, 250 ng of each oligonucleotide, 5 units of *Taq* Plus Precision polymerase mixture, 0.8 mM of dNTP and 10 μl of 10x *Taq* Plus Precision buffer (Statagene). PCRs were performed using the following program: (95°C 1 min) x1

then (95°C 1 min, 55°C 1 min, 72°C y mins) x25 and finally 72°C 10 mins. The elongation time (y) was estimated from the size of the fragment to be amplified, knowing that a typical DNA polymerase synthesises around 1 Kb per min.

2.9. DNA gel electropheresis and gel extraction

Day to day analysis was performed using 0.8% agarose (Gibco) in 0.5x TRIS borate EDTA buffer (TBE, 20 mM Tris, 20 mM boric acid, 0.5 mM EDTA pH 7.2). For gel destined for DNA extraction or Southern blot, low melting point extra-pure agarose was used (SeaKem). Ethidium bromide (Sigma) was added to the agarose gel, at a final concentration of 0.5 μg ml^{-1}, to later allow the visualisation of the DNAs by exposure to UV light (Gel Doc 2000 (BioRad)). A 1 kb ladder molecular weight marker (Invitrogen) was used at a concentration of 0.5 μg per lane to determine the size and concentration of the analysed DNAs (e.g. in those conditions the 1.6 Kb marker band is composed of 50 ng of DNA, therefore, fragment of similar size and similar intensity are at the same concentration). For PCR sample analysis, 10 μl of the reaction were mixed with 1 μl of 10x DNA loading buffer (50% (v/v) glycerol, 0.25% (w/v) bromophenol blue in TBE).

Following PCR reactions or enzymatic digestion, DNA fragments of interest were isolated and purified using the Gel Extraction Kit (Qiagen) as specified in the manufacturer's instructions. To be concentrated or when used for transfection, the DNA was ethanol-precipitated as described earlier. The obtained DNA pellet was then re-suspended in a suitable volume of sterile water and kept at -20°C until required.

2.10. Cloning of PCR products

2.10.1. Ligations

PCR products generated, as described previously, with the *Taq* DNA polymerase or the high fidelity *Taq* Plus Precision polymerase mixture were ligated into the pGEM-T (Promega) or pPCR-Script (Stratagene) vectors, respectively, following the manufacturer's guidelines.

For ligation into the final cloning vector, the digested insert and 100-200ng of digested vector were, after gel purification, mixed together at a molecular ratio of 10:1 and incubated with 40 units of T4 DNA ligase (NEB) and 1 μl of 10x T4 DNA ligase buffer (NEB) in a final volume of 10 μl, overnight at 16°C.

These ligations were then used to transform heat-shock competent *E. coli* XL-1 blue cells and transformants were selected on LB agar plates supplemented with the appropriate antibiotics.

2.10.2. Generation of heat-shock competent *E. coli* strains

The strain of interest was first plated on an LB agar plate without any antibiotic (or containing tetracycline in the case of XL1 cells). One colony was then used to inoculate 10 ml of LB medium, overnight at 37°C. The overnight culture was then diluted 1:100 in 50 ml of LB medium and grown at 37°C, until reach of an OD=0.7 (at 600 nm). Cells were then transferred to a 50 ml tube and put on ice for 10 mins before centrifugation at 350 g for 15 mins. The cell pellet was then resuspended in 16 ml of RF1 buffer (100 mM rubidium chloride, 50 mM $MnCl_2$ 4 H_20, 30 mM potassium acetate, 10 mM $CaCl_2$, 15% glycerol, with a final pH of 5.8, adjusted with 0.2 M acetic acid) and incubated on ice for 15 mins. The suspension was then centrifugated 15 mins at 540 g. The cell pellet was then resuspended, with careful pipetting, in 4 ml of RF2 buffer (10 mM MOPS ph 6.8, 10 mM rubidium chloride, 75 mM $CaCl_2$, 15% glycerol, with a final pH of 6.8, adjusted with NaOH) and incubated on ice for 1 h. Heat-shock competent cells were then aliquoted and deep-freezed with dry iced. Aliquots were subsequently stored at -80°C.

2.10.3. Heat-shock transformation

Frozen heat-shock competent *E. coli* cells were placed on ice to defrost. The DNA of interest was then added to the cells and incubated with them, still on ice, for 15 mins. Transformation was then performed by incubation of the cells-DNA mix at 42°C for 45 secs. The suspension was then placed on ice for a further 15 mins before being spread on LB agar plate containing the relevant antibiotic. Alternatively, LB medium was added to the transformed cells to allow their recovery, 1 h at 37°C, before plating.

2.11. Colony screening by PCR

When using the pGEM-T or the pPCR-Script vectors, addition of 0.5 mM IPTG and 80 $\mu g\ ml^{-1}$ X-gal to the transformant plates allowed white/blue screening of the colonies and the identification of cells potentially containing the DNA insert. However when the number of positive colonies was too important, to exclude false positives or when the system used did not allow such primary screening, the presence of the insert was assessed by PCR on colonies. Bacterial colonies were taken from their plate with a sterile 200 µl pipette tip and resuspended in 20 µl of sterile distilled water. 10 µl of this suspension were then used as template DNA for the *Taq* DNA polymerase mediated PCR reaction (see above). For screening the presence of insert in the pGEM-T or pPCR-Script, the SP6 / T7 and T3 / T7 primer couples were used, respectively. When using different plasmid, the couples of oligonucleotides used were determined using the Vector-Nti

map of the contructs and the "research motif" function of this software (Vector-Nti Advance 10, Invitogen). Only the primers with a level of homology superior to 80% were used.

PCR products were analysed on an agarose gel as described previously. The clones of interest were then selected and the 10 µl of bacterial suspension left were used to inoculate 10 ml of LB medium. After an overnight incubation at 37°C, 1 ml of the culture was pipetted, mixed with 1 ml of a 2% (w/v) peptone 40% (v/v) glycerol solution, and placed at -20°C or -80°C for cryopreservation and long term storage.

2.12. Plasmid preparation

The 9 ml of bacterial culture left were then processed with a MiniPrep kit (Qiaspin miniprep, Qiagen), following the manufacturer's guideline, to allow the extraction of the plasmid DNA. The plasmid DNA was eluted in water or TE and stored at -20°C until needed. When larger amount of DNA were required, particularly in preparation for transfection of *Leishmania* cells, 50 ml of bacterial culture were grown and the DNA was extracted using either several miniprep column or a MidiPrep kit (Qiagen). The obtained DNA was then ethanol-precipitated as described before.

2.13. Plasmid generation

Transfer of DNA insert from one vector to the other was unable by the use of single-cutter restriction enzymes. To do so, the relevant restriction sites were added in the 5' end of the oligonucleotides used for the PCR amplifications. Thus, after sequencing and verification of its conformity, the obtained DNA fragment was easily freed from the sub-cloning vector by enzymatic digestion. Restriction enzymes (NEB) were used at 10 units per µg of DNA in the appropriate reaction buffer (NEB) and following the manufacturer's recommendations.

Most of the enzymes used were generating 5' or 3' overhangs. However, when, during the preparation of the vector DNA, there was no other possibility than to use restriction enzymes creating blunt-ends fragment, the calf intestinal alkaline phosphatase (CIP from NEB) was used, as indicated by the manufacturer, to dephosphorylate the digested DNA and forbid the linearised plasmid from relegating on itself.

When the number of possible single-cutting sites was limited, isoschizomers, enzymes that recognize the same DNA sequences but cleave at different positions within it, were used (e.g. *Kpn*I and *Acc*65I). Alternatively, enzymes with compatible cohesive ends were used (e.g. *Bam*HI and *Bgl*II for pGL1399). Also, the DNA Polymerase I, Large (Klenow) Fragment (NEB) was used for its 5'-3' exonuclease activity and its

ability to fill-in 5' overhangs and generate blunt end fragments. Doing so, the C-terminal extension of MCA was conveniently removed following a *MluI/AvrII* digestion (e.g. pGL1420).

2.14. DNA sequencing and analysis

DNA sequencing was performed by the University of Glasgow Molecular Biology Support Unit (MBSU), using an ABI automatic sequencer. Electrophoregrams were then edited and compiled into contigs using AlignX (a module of Vector Nti Advance 10, Invitrogen).

2.15. Sequences alignments and phylogenetic analyses

Amino acid sequences were imported either from the GeneDB (www.genedb.org) or the National Center for Biotechnology Information (NCBI) (http://www.ncbi.nlm.nih.gov/) websites and into Vector NTI Advance 10. Alternatively, the amino acid sequences were obtained from translation of nucleotide open reading frames (in Vector NTI Advance 10). Alignments were performed using the Clustal W algorithm of the Align X program (included in the Vector NTI Advance 10 package, http://www.informaxinc.com/). The set of data could be exported as a multiple sequence file (MSF) format and used to build a phylogenetic tree with the MEGA 3.1 software (Kumar *et al.*, 2004). The tree was made using the Neighbor-Joining method and Poisson-corrected amino acid distance was used. The reliability of clustering patterns in the tree was tested by bootstrapping (1000 pseudoreplicates).

2.16. Transfection of *Leishmania major* cells

2.16.1. Plasmid DNA preparation

For the knock out or integrative constructs, 45 μg of plasmid were linearised by digestion with the appropriated restriction enzymes (see molecular constructs for details). The digested DNA fragments were then separated by electrophoresis on an ethidium bromide-free 0.5x TBE / 0.8% agarose gel (SeaKem LE Agarose, BMA). The migrated DNA fragments were then revealed by immersion of the agarose gel in a methylene blue solution (approximately 1 ml of a 0.065% (w/v) methylene blue stock in 50 ml water). The band corresponding to the fragment of interest was purified using the Qiaquick gel extraction kit (QIAGEN) and then ethanol- precipitated.

For the episomal constructs, 20 μg of circular plasmid was directly precipitated with ethanol. The last washing step would be done under a sterile hood. The

precipitated DNA would then be resuspended in 20µl of sterile water and used for transfection of $4x10^7$ *Leishmania*.

2.16.2. Electroporation and cloning

Promastigote cells at a density of around $0.5\text{-}1.5x10^7$ cells ml^{-1} were preferentially used. $4x10^7$ *Leishmania* and 20µg of purified (linearised or not) plasmid DNA (in 20µl water) were necessary for the transfection. After counting, the appropriate volume of cells was centrifuged 10 mins at 540 g at 4°C and washed with ElectroPoration Buffer (EPB, 20 mM HEPES pH 7.4, 135 mM NaCl, 5 mM KCl, 1 mM sodium phosphate buffer pH 7.4, 0.12% glucose). The washed cell pellet then was resuspended in 400µL of EPB ($1x10^8$ cells ml^{-1}) and incubated with the plasmid DNA, in a sterile ice-cold screw cap eppendorf tube, for 15 mins, on ice. The cells/DNA mix was transferred to an ice-cold 2 mm gap cuvette (Gene Pulse, Biorad) and left an additional 5 mins, on ice, before proceeding to the electroporation. The electroporation was done with a BIORAD Gene Pulser II apparatus by application of a 450 Volts-500 µFarads pulse to the cuvette. The transfected cells were kept on ice for 15 mins, then transferred into a phenolic-style cap $25cm^2$ flask (Corning) containing 5 ml of HOMEM medium + 20% FCS and left to recover overnight at 25°C. The following day, cells were aliquoted into a flask (1 ml of cells), a 24 (2 ml) and a 96 (2 ml) well plates containing, respectively, 4 ml, 22 ml or 8 ml of HOMEM medium + 20% FCS + antibiotics (see **section 2.2.1**). Alternatively, 5 ml of HOMEM medium + 20% FCS + 2x antibiotics could be added to the 5 ml overnight culture. Thus, after using twice the previously indicated volumes of cells for the aliquoting, the remaining 4 ml were centrifuged 10 mins at 540 g, resuspended in 200 µl of HOMEM and finally spread on two plates of 0.7% low melting point agarose (Seaplaque) in HOMEM medium + 20% FCS + antibiotics.

2.16.3. Cell extracts

Leishmania, growing in HOMEM medium + 10-20% FCS +/- antibiotics, were counted, centrifuged 5 mins at 540 g, washed with 15ml PBS, and the pellet stored at -20°C. Cells are then resuspended at $1x10^7$cells $10\mu l^{-1}$ in a peptidase inhibitors mix (10x solution: 0.1 mg ml^{-1} leupeptin, 1 mM phenantroline, 0.5 mg ml^{-1} Pefabloc SC, 5 µg ml^{-1} Pepstatin A and 0.1 mg ml^{-1} PMSF) + 2% SDS + 1x SDS-PAGE loading buffer (5x: 250 mM Tris-HCl pH 6.8, 10% (w/v) SDS, 50% (v/v) glycerol, 0.5% (w/v) bromophenol blue, 500 mM β-mercaptoethanol). Cells extracts were stored at -20 or -80°C.

2.16.4. Preparation of cytoskeleton

The first method used was based the one used in mammalian cells and previously applied to *L. tropicana* (Kratzerova et al., 2001). Cells were lysed with 0.5% Triton X-100 in microtubule-stabilising buffer (MSB, 20 mM Mes, pH 6.9, 2 mM EGTA, 2 mM $MgCl_2$) and in the presence of a cocktail of peptidase inhibitors for a 15 mins at RT. The lysates were then centrifuged at 20,000 g for 15 mins and the soluble fractions (S) were collected. The insoluble fractions (I) were washed twice with MSB buffer and ultimately resuspended a volume of 0.5% Triton X-100 in MSB corresponding to the one of the equivalent soluble fractions.

The second method used was adapted from the ones used for the purification of *T. brucei* cytoskeleton (Woods et al., 1989; Robinson et al., 1991; Broadhead et al., 2006). Promastigote cells were lysed in 0.5% Nodinet P40 in PEME buffer (100 mM Pipes, pH 6.9, 2 mM EGTA, 1 mM $MgSO_4$, 0.1 mM EDTA, Woods et al), on ice for 5 mins. A few microliters of the total extract (T) were kept before proceeding to the centrifugation of the rest of the sample at 250 g for 30 mins at 4°C. The soluble fraction (S) was collected and the insoluble pellet was washed twice in PEME before being finally resuspended in 0.5% NP40-PEME (I, insoluble fraction).

The T, S and I fractions were separated by SDS-PAGE in a 12% (w/v) acrylamide gel. The quantity of protein within the T, S or P fraction groups was normalised after BCA protein quantification (Pierce) and Coomassie staining. The samples were then processed for immunoblotting.

2.17. Production of recombinant MCA

2.17.1. In *E. coli*:

Heat-shock competent cells of *E. coli* BL21 were transfected with the appropriate plasmids. After selection on ampicillin LB agar plates, a single colony was grown in LB medium until reaching an OD=0.8. Recombinant protein expression was then induced by addition of 1 mM of IPTG for at least 2 hs at 37°C (or alternatively 16°C for a longer period). Cells were then placed on ice for 10 mins and centrifuged 10 mins at 350 g (4°C). The pellet was then resuspended in 2% SDS, sonicated (tune 40% total time 1.5 mins, on ice) and centrifuged 30 mins at 20,000 g. The soluble (supernatant) and the insoluble (pellet) fractions (induced or not) were then analysed by Western Blot. Alternatively, when nickel-affinity purification of the produced His-tagged proteins was needed, the cell pellets were resuspended in 5 ml (for an initial 100 ml culture) of 1x

Binding buffer +/- urea (see **section 2.19.1** for composition) and either processed immediately or stored at -80°C.

2.17.2. In *P. pastoris*

These protocols are based or extracted from the *Pichia* expression kit manual (Invitrogen, catalog no. K1710-01).

Various versions of the MCA were cloned into the pPIC9 *Pichia* expression vector (refer to **section 2.5**). Prior to transfection, the plasmids were amplified in DH5α *E. coli* cells to allow the obtention of "clean" DNAs and thus increase the transfection efficiency. 15 μg of the DNAs were then linearised by *Sac*I digestion, purified by phenol-chloroform extraction, ethanol-precipitated and resuspended in sterile water. Electrocompetent *P. pastoris* KM71 cells (made following the *Pichia* expression kit manual) were then transfected with the digested DNA by electroporation using a MicroPulser (Biorad) (one pulse at 2 kVolts in a 0.2 cm cuvette). Cells were immediately resupended in 1 ml ice-cold 1M sorbitol and then spread on RDB plates (100, 200 or 350 μl per plate, Regeneration Dextrose medium, 1 M sorbitol, 2% dextrose, 1.34% YNB (yeast nitrogen base with ammonium sulfate and without amino acids), $4x10^{-5}$% biotin, 0.005% amino acids, 20 g l^{-1} agar). Transformants started to be visible on the plates after about 4-6 days at 30°C. A few transfectants were then choosen and grown in liquid MD medium. Genomic DNAs of these transfectants were then extracted and analysed by PCR for integration in the *aox1::ARG4* locus of the *Pichia* KM71 genome. Transfectants with the correct integration were then selected for induction of the expression of the recombinant protein. Transfectants were grown, at 30°C in a shaking incubator (260 rpm), in liquid BMGY medium (Buffered Glycerol-complex Medium, 1% yeast extract, 2% peptone,100 mM potassium phosphate pH 6.0, 1.34% YNB, $4x10^{-5}$% biotin, 1% glycerol) until reaching an OD of around 8 and were then centrifuged, washed with sterile water and resuspended in BMMY medium (Buffered Methanol-complex Medium, BMGY where the glycerol has been replaced by 0.5% methanol) to induce the expression of the protein of interest. Induction was then maintained for up to 10 days by adding each day methanol at a final concentration of 0.5% to the culture. Culture sample were taken every 24 hs and centrifuged. The culture medium supernatant, containing the secreted recombinant protein, was separated from the cells pellet and both were stored at -20°C or -80°C. The medium samples were then directly analysed by SDS-PAGE and western blot for presence of the secreted desired recombinant protein. Alternatively, the cell pellets were lysed with Y-PER buffer (Pierce) following the manufacturer's protocol, before conducting similar analyses to assess the expression and potential retention within the cells.

2.18. *In vitro* translation

Alternatively, recombinant MCA was produced by in vitro translation, using plasmid DNA as template (EasyXpress Protein Synthesis Mini Kit, Qiagen). The matrix vector was pET28a(+)-MCA (pGL1421), thus allow the expression of C-terminally His-tagged MCA. Proteins were produced and purified following the manufacturer protocol. Basically, the reactions were performed in a final volume of 50 µl containing: 20 µl of EasyXpress reaction buffer, 2.5 µl of RNase-free water, 17.5 µl of *E. coli* extract, 0.8 µg of pGL1421 or 2.5 µl of the positive control plasmid, 1 mM of IPTG, sterile water. The reactions were then placed at 37°C for 1 h and finally stopped by placing on ice and proceeding with the sample purification and analysis. The His-tagged proteins were purified using Ni-NTA Superflow resin (Qiagen) under native conditions. Shortly, 100 µg of Ni-NTA agarose slurry was washed with 1 ml of Binding buffer, in a 1.5 ml column. 5 µl of the *in vitro* translation samples were reserved while the remaining 45 µl were mixed with 400 µl of ice-cold Binding buffer and placed on the washed resin. His-tagged proteins were allowed to bind the resin for 2 hs at 4°C on a rotating shaker. The bottom cap of the column was then removed and the flow-through collected and saved, before proceeding to a 500 µl wash (with Washing buffer) and elution of the His-tagged proteins twice with 50 µl of Elution buffer. Note that to facilitate the elution of small volumes a 30 secs spin at 6,000 g was performed. Samples from the total, flow-through, wash and elution fractions were then analysed by SDS-PAGE and Western blot using anti-His antibodies. Please refer to next section for the recipe of the buffers used in this experiment.

2.19. Protein purification (and enzymatic assays)

2.19.1. His-tagged proteins

Induced bacteria cell pellets were frozen on dry ice and defrosted several times to facilitate cell lysis. Cells were then sonicated for 1 min at 40% amplitude. The lysate were then spun 20 mins at 10,000 g. The pellets were then resuspended in 5 ml of 1x Binding buffer, incubated on ice for 15 mins, sonicated again and centrifuged as above. When purification in denaturing conditions was necessary, this step was successively repeated with 4 M, 6 M and finally 8 M urea. Every time, both the supernatant and pellet fractions were kept for further analysis. Samples were then analysed by SDS-PAGE followed by a Coomassie staining and a Western blot. Upon determination of the

optimal solubilisation conditions, the experiment was repeated and the Nickel-affinity purification of the His-tagged proteins carried over.

A 10 ml polypropylene column (Pierce) was loaded with 2 ml 50% Ni-NTA agarose and equilibrated with 10 ml of 1x Binding buffer +/- urea. The samples were then added and the His-tagged proteins were allowed to bind the resin for 2 hs at 4°C. After washing with around 40 ml of 1x Washing buffer +/- urea (10 fractions), the proteins were eluted in 10 fractions of 1.5 ml with 1x Elution buffer +/- urea. The various fractions were then further analysed. The Ni-NTA column was rinsed with 1x Washing buffer and kept in 1x Binding buffer at 4°C, for later use.

Concentrated stock solutions of the various buffers were made and stored at 4°C. 8x Binding buffer: 40 mM imidazole, 4 M NaCl, 160 mM Tris-HCl ph 7.9. 8x Washing buffer: 480 mM imidazole, 4 M NaCl, 160 mM Tris-HCl pH 7.9. 4x Elution buffer: 4 M imidazole, 2 M NaCl, 80 mM Tris-HCl pH 7.9. For purification under denaturing conditions, urea was added, at the appropriate concentration to the 1x buffers.

2.19.2. TAP-tagged proteins

The protocol used was the one described by O. Puig for the yeast model (Puig et al., 2001)

2.20. Peptide synthesis and antibodies production

A peptide corresponding to the C-terminal 15 amino acids of the predicted MCA sequence (QPPPAQYTFSPLPPG) was synthesized (Seqlon) and used to immunize animals (Seqlon). The rabbit antiserum was then affinity-purified. Affinity purified rabbit antibodies raised against the TbMCA2 and TbMCA3 active site region ([DAKPGD...(68)...MDLPFT]) were previously produced in the laboratory (Helms *et al.*, 2006).

2.21. Affinity purification of antibodies

In a 5 ml polypropylene column (Pierce), 1 mg of MCA peptide (QPPPAQYTF SPLPPG) was covalently linked to 500 µl of Aminolink Coupling Gel (Pierce) following the manufacturer protocol. The peptide/aminolink resin was then equilibrated with 10 ml of IgG binding buffer (0.14 M NaCl, 8 mM sodium phosphate buffer pH=7.5, 2 mM potassium phosphate buffer pH 7.5, 0.01 M KCl). 2 ml of anti- MCA rabbit antisera (rabbit 3122, 3^{d} bleed) were then diluted by half in IgG binding buffer and incubated 3 hs at room temperature with the peptide/aminolink resin. The resin was washed with 20 ml of IgG binding buffer before eluting the bound antibodies with multiple

500 µl fractions of Immunopure IgG elution buffer (Pierce). Note that 25 µl of 1M Tris-HCl pH 9.5 were present in the collection tube to instantly equilibrate the acidic pH of the elution buffer and thus ensure the stability of the eluted antibodies. The proteins in the various elution fractions were then quantified by measurement of their OD at λ=280nm. The fractions having the highest OD were pooled and concentrated on a Vivaspin 2 ultrafiltration unit (regenerated cellulose 10,000 MWCO, Vivascience), at 3000g. The filter was then washed 3 times with 2 ml of IgG binding buffer, and a last time with 2 ml of IgG binding buffer + 0.05% sodium azide. 200 µl of concentrated antibodies were finally recovered by turning the Vivaspin 2 column upside-down and spinning 5-15 mins at 3000g. The purified antibodies were stored at -20°C (in aliquots).

2.22. SDS-PAGE, Coomassie staining and Western blot

After denaturation at 100°C for 5 mins, cell lysates or recombinant protein extracts were loaded on a 12% bis-acrylamide SDS-PAGE gel. This gel was cast and run according to the protocol from "Molecular cloning, a laboratory manual" (Sambrook J. and Russell D.W., 2001) and using the Mini-PROTEAN III system (Biorad). After migration at 200 Volts (for two gels), the gels were processed for direct visualisation of the total proteins (Coomassie stain) or for immunodetection (Western blot).

Coomassie staining of the gels was performed by immersion in a solution of 0.25% (w/v) coomassie blue, 45% ethanol, 9.2% acetic acid for 1 h at room temperature. A maximum of staining background was then removed by several washes with destain solution (30% ethanol, 5% acetic acid). Gels were then washed in water and air-dryed between two sheets of gelatine using a drying frame (Easy breeze, Hoefer Scientific instrument).

To proceed for the Western blot method, the gels were firstly incubated 10-15 mins in transfer buffer to equilibrate (48mM Tris, 39mM Glycine, 20% ethanol). A semi-dry transfer of the gels on PVDF membranes (previously activated in absolute ethanol, Perkin Elmer Life Science) was then performed with a Trans-blot SD Semi-Dry transfer cell (Biorad) for 30 mins at 20 volts (constant) or 10 volts for 1 gel. The membranes were then saturated with PBS + 0.05% Tween + 5% milk for 10-15 mins, before incubating, from 1 h (at room temperature) to overnight (at 4°C) with the appropriated antibodies.

The affinity purified rabbit antibodies against MCA and TbMCA2/3 were used at 1:50 and 1:10,000 dilutions, respectively. Monoclonal anti-tetra HIS (Qiagen) and anti-TbEF1α (Upstate) antibodies were used at 1:1000 and 1:20,000, respectively. *L. major* cysteine synthase (Williams,R.A.M and Coombs, G.H., unpublished data) and *L. mexicana* transketolase (Veitch *et al.*, 2004) specific rabbit antibodies were used at

1:1,000. Mouse IgG2b anti-β-tubulin (KMX-1, (Birkett *et al.*, 1985)) and rabbit anti-TbRAB11 (Jeffries et al., 2001) antibodies were used at 1: 10,000.

After at least six washes of 5 mins each with PBS + 0.05% Tween + 5% milk, the western blot membranes were incubated with goat anti-mouse, goat anti-rabbit or donkey anti-sheep Horse Radish Peroxidase (HRP) conjugated antibodies at 1:2000, 1:2000, 1:5000 respectively, for 1 h at room temperature. After washes, the western blots were revealed using an ECL kit (SuperSignal West Pico Chemoluminescent Substrate, PIERCE).

2.23. Direct fluorescence analysis

Slides were examined under UV light on a Zeiss Axioplan microscope, and images were processed using a Hamamatsu ORCA-ER digital camera and Openlab version 3.5 software.

2.23.1. 4,6-Diamidino-2-phenylindole (DAPI) staining

1 ml of cells were centrifuged 5 mins at 250 g, washed with PBS, resuspended in 200 µl of PBS + 10 µg DAPI (10 mg ml^{-1} stock) and incubated 5 mins in the dark. After a wash in PBS, the cells were then resuspended in 20µl of PBS on spread on a Twin frosted 76x26mm microscope slide (BDH) with a 22x64mm coverglass (BDH).

Alternatively 0.5% of 1,4-diazabicyclo[2.2.2]octane (DABCO) was added to the slide as anti-fading agent. The fluorescence was observed with the DAPI filter (λ=480nm) of the UV light microscope and pictures were taken with an exposure time of 50 ms. Phase was observed against bright visible light and pictures were taken with an exposure time of 50 ms.

2.23.2. Green Fluorescent Protein (GFP)

1 ml of cells were washed in PBS and resuspended in 20 µl of PBS or PBS + 2% formaldehyde and prepared as described before. The GFP fluorescence was observed with the FITC filter (λ=540nm) of the UV light microscope and pictures were taken with an exposure time of 300 ms.

2.23.3. FM4-64 labelling

500 µl of promastigotes were pelleted, washed with 1.5 ml of HOMEM and resuspended in 100µl of HOMEM + 0.5 µl of FM4-64 (16 mM stock in dimethyl sulfoxide [DMSO]; Molecular Probes) and incubated 30 mins at 25°C. Cells were then washed with HOMEM and resuspended in 1 ml HOMEM to perform a 1h chase at 25°C. Cells were then

washed with PBS and prepared as exposed before. The FM4-64 fluorescence was observed with the Rhodamine filter (λ=580nm) of the UV light microscope and pictures were taken with an exposure time of 50 ms.

2.23.4. Lysotraker labelling

500 µl of promastigotes were pelleted, washed with 1.5 ml of HOMEM, resuspended in 100µl of culture medium + 1 µl of LysoTraker Red DND-99 (1mM stock in DMSO; Molecular Probes) and incubated 30 mins at 25°C. Cells were then washed with PBS and prepared as exposed before. The Lysotraker fluorescence was observed with the Rhodamine filter (λ= 580nm) of the UV light microscope and pictures were taken with an exposure time of 50 ms.

2.23.5. Mitotraker labelling

1 µl of a 1 µM stock solution of Mitotraker Red CMXRos (Molecular probes, M7512, in DMSO) was added to 1 ml of promastigotes and incubated for 2-5 mins at 25°C. Alternatively, 1 µl of a 1mM stock solution of Mitotraker Green FM (Molecular probes, M7514, in DMSO) was used. 1µl of DAPI at 10 mg ml^{-1} was added at the same time. The cells were then centrifuged at 1,000 g for 30 secs, washed with cold PBS and resuspended in 20 µl PBS or 15 µL PBS + 5 µl of 4% formaldehyde. Finally, the cells were mounted between slide and coverslide and sealed with nail varnish. The Mitotraker Red CMXRos and the Mitotraker Green FM fluorescences were observed with the Rhodamine filter (λ= 580 nm) or the FiTC filter (λ= 540 nm) of the UV light microscope, respectively. Pictures were taken with an exposure time of 100 ms.

2.24. Immunofluorescence analysis (IFA)

2.24.1. Fixation

Leishmania were washed twice in PBS while *T. brucei* BSFs were washed in trypanosome dilution buffer (TDB: 20 mM Na_2HPO_4, 2 mM NaH_2HPO_4, 80 mM NaCl, 5 mM KCl, 1 mM $MgSO_4$, 20 mM glucose, pH 7.4) before fixation in 200 µl of 1% formaldehyde/PBS for 30 mins at RT. The cells were then permeabilised by addition of 20 µl of 1% Triton X-100/PBS for 10 mins. 20µl of 1M glycine/PBS were added to neutralise the free aldehyde bonds resulting from the formaldehyde fixation, in order to diminish any background fluorescence. The cells were incubated a further 10 mins. In the meanwhile, glass slides were washed with 70% ethanol before being coated with 0.01% poly-L-lysine (0.1% stock, Sigma) for 5 mins and air dried. A small square-shaped

border of nail varnish was drawn on the surface of the slide in order to limit the spreading of the cells and later of the antibody solutions. The treated cells were then pipetted on these poly-L-lysine-coated slides and left to sediment and adhere to the surface for 15-30 mins in a dark box containing PBS-soaked tissues, to prevent the cells from drying.

2.24.2. Immunofluorescence

The primary antibodies diluted in 0.1% Triton X-100, 0.1% BSA (TB) were added to the slide and incubated with the cells for at least 1 h at RT or alternatively overnight at 4°C. The cells were then washed with 10ml of PBS, and the maximum of the remaining liquid was removed by applying a tissue to a corner of the slide. The Alexa Fluor 488 (green) or Alexa Fluor 594 (red) - conjugated secondary antibodies (Molecular Probes), diluted at 1/1000 in TB, were then added to the cells and incubated in the dark for 1h at RT. 0.5μg ml^{-1} of DAPI (Sigma) was then added for 1 min before proceeding to a 10ml PBS wash. A maximum of liquid was removed, as well as the nail varnish frame, and a mounting solution (2.5% DABCO in 50% glycerol) was applied to the coverslip before its application to the slide. The fluorescence was observed with the "DAPI" (λ=480nm), "FITC" (λ=540nm) or "Rhodamine" (λ=580nm) filters of the UV light microscope. Cells were viewed with a Zeiss UV microscope, and images were captured by an Orca-ER camera (Hammamatsu) and Openlab software version 4.0.3 with deconvolution module (Improvision). Images were prepared for presentation using Adobe Photoshop CS.

2.25. VSG recycling

Bloodstream form (BSF) *T. brucei* were harvested at mid-log phase and after three washes with ice-cold TDB (see above), the cell density was adjusted to $1x10^8$ cells ml^{-1} and the cells were incubated with 1 mM sulfo-NHS-SS-biotin (Pierce) for 10 mins on ice. 10 mM Tris-HCl, pH 7.5, was added to stop the reaction. After three washes with of ice-cold TDB, parasites were re-suspended to density of $1x10^7$ ml^{-1} in pre-warmed HMI-9 and endocytosis allowed for 5 mins at 37°C. Endocytosis was stopped and sulfo-NHS-SS-biotin removed from the cell surface by addition of ice-cold stripping-solution (HMI-9, 10% (v/v) FCS, 50 mM glutathione, pH 9) and a further 30 mins incubation on ice. Parasites were subsequently washed a further three times in ice-cold TDB before returning them to HMI-9 at 37°C. Samples were taken at 5 and 10 mins for analysis by immunofluorescence and processed as previously described. Biotin was detected using either a streptavidin-Texas Red conjugate (Molecular Probes) at 1:5000.

2.26. Anti-VSG antibodies degradation

BSF parasites expressing VSG221 were harvested at mid-log phase and labelled with anti-VSG221 antibodies at 4°C for 30 mins in HMI-9 at a concentration of $1x10^7$ parasites ml^{-1}. Parasites were then washed three times in ice cold serum-free HMI-9 and incubated, in pre-warmed, serum-free HMI-9, at 37°C for 10 or 30 mins. Following this incubation period, samples were prepared for immunofluorescence as previously described. Rabbit anti-VSG IgG was detected directly using an anti-rabbit IgG-FITC conjugate (Molecular Probes) at 1:5000.

2.27. Prostaglandin D_2 treatment

A 4 mM stock of prostaglandin D_2 (P5172, Sigma, MW: 352.5 g mol^{-1}) was made by resuspension of 1 mg of powder in 700 µl of ethanol. 0, 2.5, 5 and 7.5 µM of PGD_2 were added to the BSF at a density of $2x10^6$ cell ml^{-1} and cell count were made at different time points.

2.28. Partial cell cycle synchronisation of *L. major* cells

Promastigote cells at $0.5x10^7$ cells ml^{-1} were partially synchronised in G1/S phase by treatment with 5 mM hydroxyurea (HU, MW:76.06 g mol^{-1}) for 12 hs at 25°C (Soto *et al.*, 2004). Semi-synchronisation in G2/M phase could be achieved by treatment with 2.5 µM flavopiridol (MW: 401.84 g mol^{-1}) for 12 hs at 25°C (Hassan *et al.*, 2001). Both solutions were used fresh. Cells were then released from the specific phase block by washing them twice in PBS and resuspending them in the same volume of pre-warmed HOMEM + 10% FCS. Aliquots of the cells were taken at several time points to perform Western blot and FACS analysis.

2.29. DNA content analysis

2.29.1. Cells preparation

Mid-log phase promastigotes were spun at 250 g, 4°C for 5 mins, then washed with PBS, centrifuged again and finally resuspended in 1 ml of 70% methanol/PBS. Cells were then stored at 4°C for at least an hour or overnight. Prior to analysis, the cells were centrifuged at 350 g, 4°C for 5 mins, washed with 1 ml PBS once, spun , resuspended in 1ml of PBS with 10 µg ml^{-1} propidium iodide (Sigma) and 10 µg ml^{-1} RNAse A (Sigma), and finally incubated at 37°C for 45 mins, in the dark.

2.29.2. Fluorescence Activated Cell Sorting (FACS) analysis

FACS analysis was performed with a Becton Dickinson FACSCalibur using the FL2-A (fluorescence intensity at 585/642nm, note $\lambda_{emission}$ Propidium Iodine = 620 nm under an $\lambda_{excitation}$ = 488nm (blue, Uniphase Argon Ion laser)), the Forward Scatter (FSC, relative cell size) and the Side Scatter detectors (SSC, cell granulometry or internal complexity). Introduction of the prepared samples into the cytometer was automated with a FACS Loader (Worklist manager and Loader manager softwares). For each sample, 10 000 events (cells) were analysed. Data were interpreted using the CellQuestPro software (BD Bioscience).

Chapter 3:

Cell cycle of *Leishmania major* promastigotes

3.1. General presentation of the cell cycle in eukaryotes

The duration of the cell cycle varies greatly from one cell type to another. The time during which the cell divides is termed M phase. The M phase is divided between the nuclear division (mitosis) and cell fission (cytokinesis). The whole of M phase covers only a small fraction of the total cell cycle. The period between one mitosis and the next is called interphase.

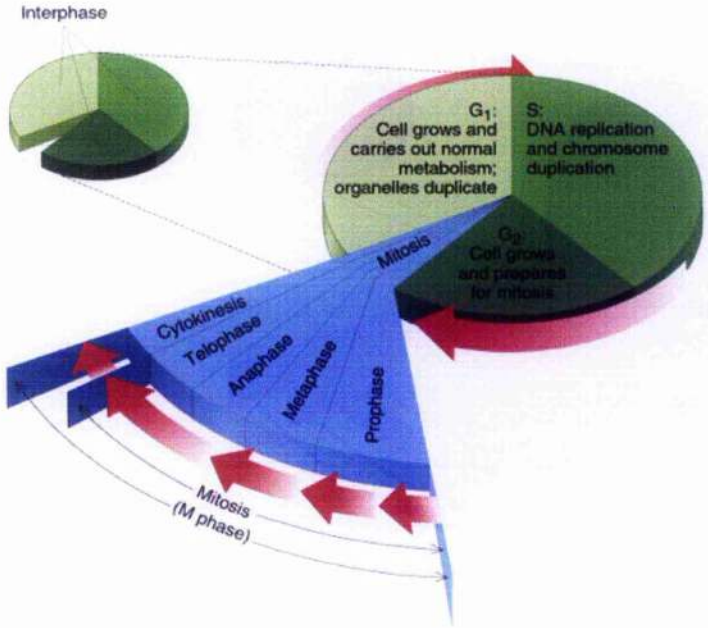

Figure 3.1: The successive phases of a standard eukaryotic cell cycle
From http://fig.cox.miami.edu/~cmallery/255/255mitos/cycle.jpg

Interphase is a period during which preparations for cell division are occurring in a closely ordered sequence. First, the organelles start to duplicate and as a result the cell increases its volume (G1 phase). Then the nuclear DNA replicates (S phase). And finally the cell ensures that DNA replication is complete and finishes the doubling of its mass before mitosis, during the "safety" gap G2 (G2 phase) (**figure 3.1**).

Mitosis is a crucial period of the cell cycle during which the nuclear envelope breaks down, the content of the nucleus condense into visible chromosomes and the cellular microtubules reorganise to form the mitotic spindle that will separate the chromosomes (prophase and prometaphase, **figure 3.2a,b**) (Scholey et al., 2003). During progression into mitosis, the cell seems to briefly pause in metaphase, when duplicated chromosomes align on the mitotic spindle, halfway between the spindle poles (metaphase plate, **figure 3.2c**). The immobilised chromosomes will remain so until the metaphase-to-anaphase transition checkpoint has controlled that the cell is

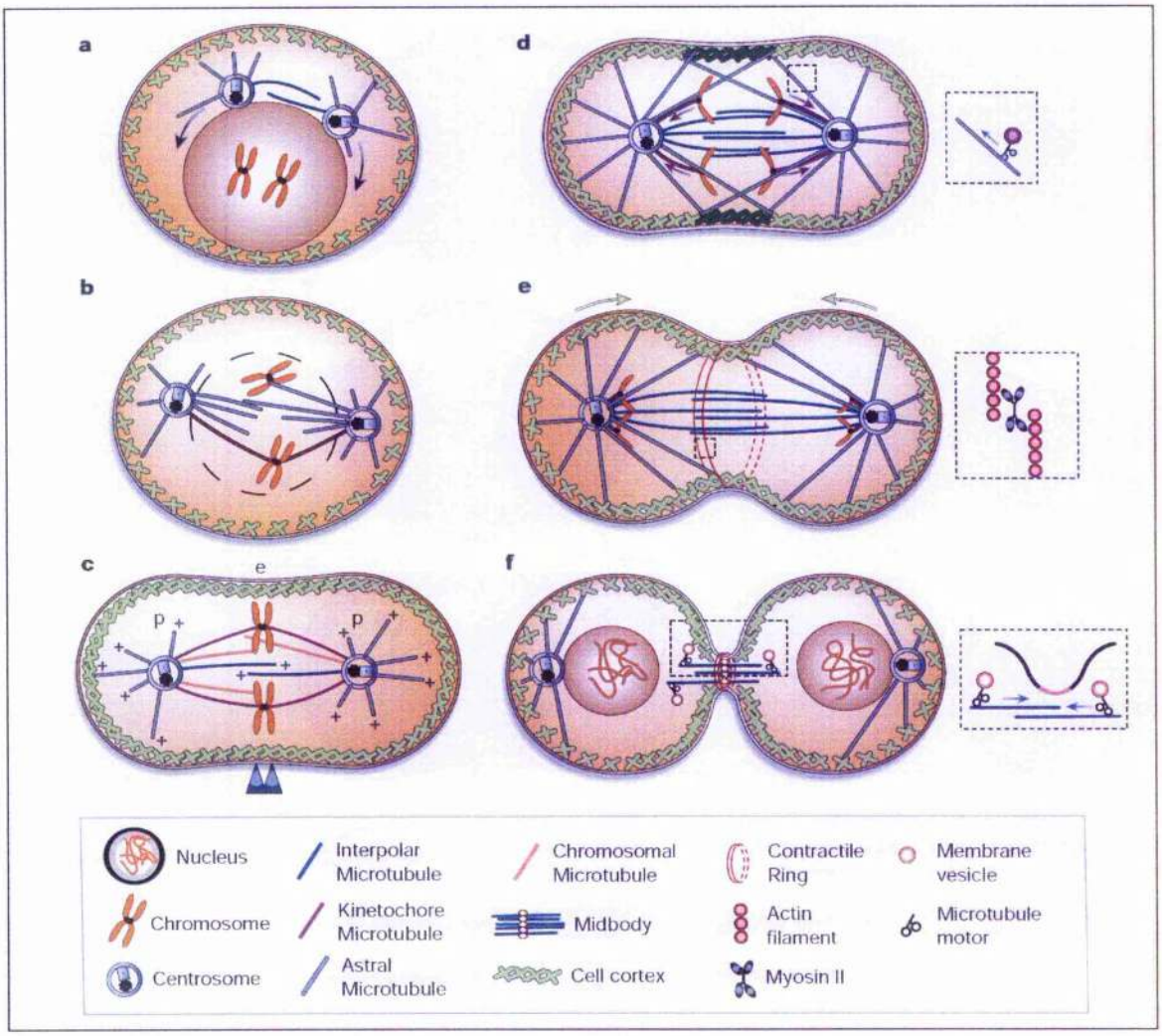

Figure 3.2: The six stages of cell division

From Scholey *et al.*, 2003.

a) Prophase. The duplicated centrosomes, each composed of two centrioles, migrate around the nucleus, nucleating the assembly of microtubules (MTs) and organising the spindle poles. b) Prometaphase. The nuclear envelope breaks down. The spindle MTs can now capture the chromosomes and move them to the equator (e). c) Metaphase. The pairs of sister chromatids (double arrowheads) face opposite spindle poles (p). MTs are oriented with their plus ends distal to the poles, and are organized into the astral MTs, which link spindle poles to the cell cortex; chromosomal MTs, which link chromosome arms to poles; kinetochore MTs, which link poles to kinetochores; and interpolar MTs (ipMTs), which link the two poles. d) Anaphase A. The sister chromatids cohesion is lost and they are moved to opposite poles. The spindle delivers message to the cell cortex to indicate the position and orientation of the forming contractile ring. e) Anaphase B. The spindle poles move further apart. The actin-myosin II contractile ring (inset) begins to ingress and forms the cleavage furrow. f) Telophase/cell-cell scission (or abscission). The nuclear envelopes reassemble around the sets of decondensing sisters chromatids. Meanwhile, the furrow ingression has created a barrier between the daughter cells and progressed until only a small bridge remained (midbody). This structure contains the remnants of the ipMTs, which were initially lying between separated chromatids. The contractile ring then disassemble and the two daughter cells plasma membranes are sealed and separated by a mechanism thought to involve vesicle transport/exocytosis (inset) (e.g. Rab11-mediated).

ready to enter anaphase. Once this point is passed, the cell will carry on to the end of mitosis (anaphase and telophase, **figure 3.2d, e, f**) through cytokinesis and into a new interphase.

During cytokinesis, the cytoplasm divides by a process called cleavage. Although nuclear and cytoplasmic division are generally linked, they are separable events and in some cases like embryogenesis, nuclear division is not followed by cytokinesis. However, in typical cells, cytokinesis accompanies every mitosis, beginning in anaphase and reaching completion at the end of the telophase, when the following interphase starts. The cleavage is carried out by the contraction of a thin ring composed mainly of an interconnected array of actin and myosin filaments. This contractile ring determines the cleavage furrow (**figure 3.2e, f**). The cleavage first appears during anaphase when the plasma membrane starts to furrow. The furrowing invariably occurs in the plane of the metaphase plate, at right angle to the axis of the elongated mitotic spindle. It ensures the cleavage between the two groups of dividing chromatids and the distribution of identical copies of the genome to the two daughter cells. It is established that the mitotic spindle microtubules determine the position of the cleavage furrow within the dividing cell (Field et al., 1999; D'Avino et al., 2005).

In addition to the previously described anaphase-to-metaphase checkpoint, which regulates the exit from mitosis, there are at least two others cell cycle checkpoints, one at the transition between the G1 and S phase (G1/S), which triggers the DNA replication machinery, and one at the transition between the G2 and M phase (G2/M) activating the mitosis machinery. This system of control is represented as a clock that turns, triggering essential processes when it passes specific points on the dial (4pm, tea time!). The processes controlling the cell cycle are mainly based on interactions between cyclin-dependent kinases (Cdks) and cyclins. There are two main classes of cyclins, the mitotic cyclins, which bind to Cdks during the G2 phase and mediate the entry into mitosis, and the G1 cyclins that associate with the Cdks during the G1 phase and are required for the entry into S phase. Cdk activation is stopped by a proteasome-mediated degradation of the cyclins.

The organisation of mitosis in fungi and protozoa differs significantly from that of animals and plants (Field *et al.*, 1999). Cell division in *Leishmania* and *Trypanosoma* harbours many features that are unique to single-celled organisms but also possesses particularities which are species- and stage-specific.

3.2. State of current knowledge on the cell cycle of trypanosomatids

As described in **chapter 1 section 1.1.4.**, the ultrastructure of a trypanosomatid cell resides around a nucleus, a single mitochondrion with its kinetoplast DNA and a flagellum. The flagellum emerges from the flagellar pocket and is linked to the kinetoplast through the basal body and the microtubules/filaments of the tripartite attachment complex (Ogbadoyi *et al.*, 2003). For the cell cycle to progress, these various organelles will have to be replicated with accuracy and then divided with precision. Trypanosomatids possess cell cycle peculiarities compared to mammalian cells. First, while the replication (S phase) of the nuclear and kinetoplast DNAs starts almost synchronously, their other phases of the cell cycle are separated in time. Second, the chromosomes do not visibly condense and the nuclear envelope remains intact during mitosis (Ogbadoyi *et al.*, 2000). Thirdly, there are no structural equivalents to the mammalian spindle poles bodies (centrosomes) in kinetoplastids. However, the centrioles of the flagellar basal bodies are directly involved in the partitioning of the mitochondrial genome (Robinson and Gull, 1991). In the dividing nucleus, chromosome segregation involves not only kinetochores, but also interpolar microtubules (Ersfeld and Gull, 1997; Ersfeld *et al.*, 1999). And finally, the extensive remodelling during cytokinesis that occurs in mammalian microtubular cytosketelon has not yet been observed. Furthermore, the mechanisms involved in the plasma membrane furrowing are still obscure.

Meanwhile, the chronology of the cell cycle events remains poorly characterised in trypanosomatids. One exception is for the procyclic form of *T. brucei* (Sherwin and Gull, 1989; Woodward and Gull, 1990).

It is well established that in these parasites progression throughout the cell cycle is dependent on microtubule-mediated events. Indeed, those cells possess several microtubule-based structures. The cytoplasmic microtubules of the sub-pellicular corset define the shape of the cell, while flagellar microtubules form the axoneme and intranuclear microtubules mediate the creation of the mitotic spindle. Microtubular structures are also densely packed in the area of the kinetoplast, such as in the basal bodies (Ogbadoyi *et al.*, 2003). Interfering with microtubule polymerisation/ depolymerisation was shown to affect basal body duplication, kinetoplast segregation, flagellar axoneme growth, mitosis, cell growth and cytokinesis of trypanosomes (Robinson and Gull, 1991; Robinson et al., 1995; Ploubidou et al., 1999). Interestingly, the parasite tubulin shows a different level of sensitivity to antimicrotubule agents than mammalian cells, indicating that it might constitute a good drug target (Robinson and

Gull, 1991). Through the inhibition of specific cell cycle events it was possible to establish, with a satisfactory accuracy, their order and duration during the growth of *T. brucei* procyclic forms (Woodward and Gull, 1990; Ploubidou et al., 1999; McKean, 2003). While the sub-pellicular microtubules are constantly dynamic along the duration of the complete procyclic form cell cycle (8.5 hours), the maturation and duplication of the basal bodies are some of the first events taking place. These processes are tightly linked with the generation and growth of a daughter flagellum (**figure 3.3a**). Meanwhile, the nuclear and kinetoplast DNAs enter their respective S phases and duplicate their genomic content. The segregation of the kinetoplast, driven mainly by the separation of the basal bodies, then starts and achieves completion before the triggering of nuclear mitosis. The generated daughter nucleus subsequently migrates between the two kinetoplasts. Cytokinesis finally starts at the anterior end of the cell and the helical progression of the cleavage furrow along the cell body determines accurate organelle partitioning and ultimately leads to cell scission.

In mammalian cells, the cleavage furrow is formed by the contraction of an actin/myosin-based ring. Also, it has been shown that the cytoskeleton of those cells is complexly composed of intertwined arrays of microtubules, actin and intermediate filaments. The cross-talk between these various networks mediates essential cellular processes such as vesicle and organelle transport, cell division and signal transduction (Goode et al., 2000; Rodriguez et al., 2003; Chang and Goldman, 2004). In trypanosomes, while the existence of intermediate filaments remains obscure, little is known about the cellular functions of actin filaments. Apparently, in procyclic forms, actin is distributed throughout the cell (Garcia-Salcedo et al., 2004). Interestingly, silencing of this protein by RNA interference, while slightly modifying the morphology of the cell body, nucleus and kinetoplast, did not affect cell growth and division. Also it was suggested that, in the *in vitro*-cultured insect stages, actin might either play non-essential functions or could be compensated for by others proteins. Surprisingly, actin was found to be essential for bloodstream form growth and via its association with the endocytic pathway, for vesicular traffic from the flagellar pocket. Thus, although the potential involvement of actin in cleavage furrow formation remains elusive, these data indicates that actin likely possesses stage-specific roles.

Other proteins, while present in both bloodstream and procyclic forms, were found to harbour discrete functions. Indeed, studies of cyclin- dependent kinases and their cyclin partners revealed differences, between the different life stages, in many aspects of cell cycle control (Hammarton *et al.*, 2003). As exemplified with the RNAi of the cyclin CYC6, which in procyclic forms inhibited mitosis but not cytokinesis when blocking both processes in bloodstream forms, the mechanisms behind cell division and its control present many stage-specific features.

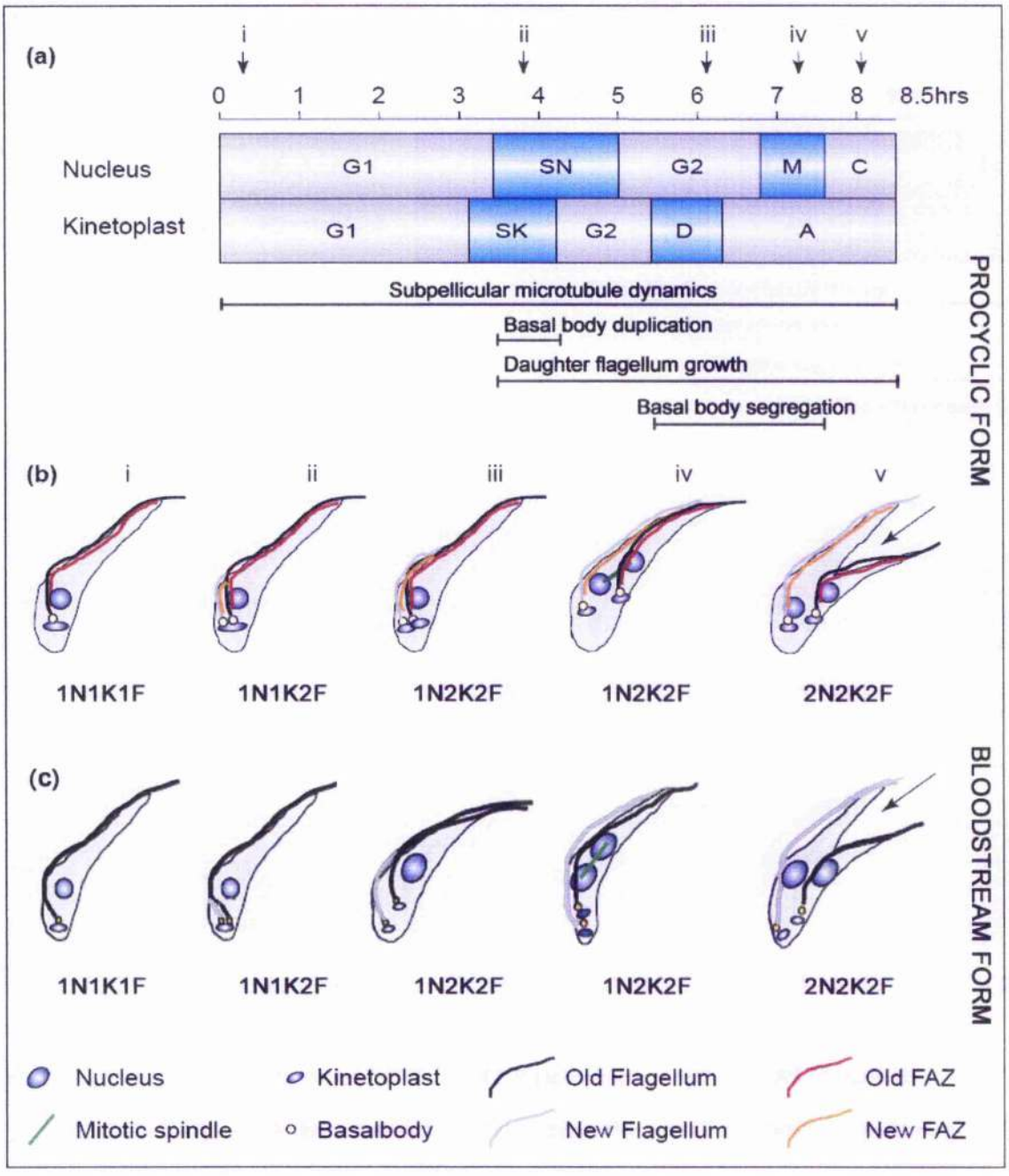

Figure 3.3: Representation of the major morphological events of the *T. brucei* cell cycle

Adapted from McKean, 2003 and based on the data in Woodward and Gull, 1990.
a) Chronology of the nuclear and kinetoplast phases of the procyclics cell cycle. The microtubules-mediated events are indicated below. Even if the nuclear and kinetoplast S phases (SN and SK, respectively) are overlapping, the SN is longer than the SK. The division of the kinetoplast (D) is completed before the start of the segregation of the duplicated nucleus (mitosis, M). The basal bodies continue to move apart even once the kinetoplast division is terminated (apportioning, A). Cytokinesis starts upon completion of the mitosis. **b-c**) Schematic representations of the morphological events leading to cell division in procyclic (b) and bloodstream (c) forms. N: nucleus, K: kinetoplast, F: flagellum. The black arrow points the direction and position of the cleavage furrow.

Although less is known about the chronology of the events leading to cell division in bloodstream forms, the cell shape and growth rate differences between the two life stages of the parasite indicate that the basic biology of the cell cycle might have variations. And indeed, whereas the bloodstream forms possess a short and thick cell body, the insect stages have an elongated shape. It is estimated that the PCF and BSF complete their cell cycles within around 13 and 8.5 hours, respectively. One other major peculiarity was observed after mitosis, when the parent and daughter nuclei of the bloodstream form cell remain juxtaposed while, in procyclics, the latter migrates between the two kinetoplasts (**figure 3.3b, c**). Also, in G1 phase, the bloodstream form kinetoplast is closely associated with the nucleus, while in the insect stage it is positioned approximately midway between the posterior part of the cell and its nucleus (Robinson et al., 1995). However, both stages share many cell cycle features, with the division of the kinetoplast occurring before nuclear segregation. While the *Leishmania* cell cycle remains even more obscure, it seems that, in this trypanosomatid, mitosis happens before the kinetoplast separation (Milligan, 1996; Havens et al., 2000). But apparently, some species of *Leishmania* (e.g. L. tarentolae) undergoes these two processes in reverse order (Simpson, 1968). Like in trypanosomes, microtubule-mediated events plays major roles in cell cycle progression (Jayanarayan and Dey, 2002; Borges et al., 2005; Jayanarayan and Dey, 2005). Indeed, treatment with anti-microtubule agents of *in vitro*-cultivated *Leishmania* promastigotes resulted in the inhibition of nuclear mitosis and cytokinesis and a disturbance of the accurate positioning of the kinetoplast within the cell (Havens et al., 2000).

So far, there has been no published report of descriptive or quantitative analyses of the morphological events associated with *Leishmania* cell cycle progression. Thus, I attempted to generate a chronological map of the processes during the promastigote cell cycle by using microscopic observations and immunofluorescent labelling.

3.3. Chronological events leading to *L. major* division

A major requirement for the analysis of the *L. major* cell cycle was the ability to follow the dynamics of the kinetoplast and nucleus. As the flagellum is tightly associated with the kinetoplast DNA through a microtubular structure comprising the basal bodies, the presence and length of the newly synthesized flagellum is an indicative parameter for progression of kinetoplast segregation (Robinson *et al.*, 1995). Simultaneously, anti-β-tubulin immunofluorescence coupled to DAPI staining was used to visualise the appearance and further elongation of the intranuclear mitotic spindle and monitor the progression of nuclear mitosis (Ogbadoyi *et al.*, 2000). These two morphological markers were theoretically enough to position the cell precisely within its

division cycle. However, another antibody raised against *T. brucei* RAB11, a characterised constituent of recycling endosomes in this parasite (Jeffries *et al.*, 2001), has unexpectedly showed its utility in the visualisation of kinetoplast segregation in *L. major*.

In interphase promastigotes, the anti-β-tubulin antibody mainly labelled the sub-pellicular microtubules (**figure 3.4A**). However, the fluorescent staining rapidly evolved during cell cycle progression, indicating the highly dynamic nature of this cytoskeletal structure. Cells with a wider nucleus and cell body and probably in S phase had only the microtubules of their posterior end labelled (**figure 3.4B**). However, for a more precise assignment of these cells to the S phase of the cell cycle, a more comprehensive study based, for example, on 5-bromo-2-deoxyuridine (BrdU) incorporation is needed (Woodward and Gull, 1990). At the onset of mitosis, a bright fluorescent β-tubulin signal accumulated at the centre of the nucleus, in a rhomboid structure excluded from the DAPI staining (**figure 3.4C, D**). This structure became bigger with time, until the parent and daughter genomic contents started to migrate apart and the structure elongated (**figure 3.4E, F**). A characteristic mitotic spindle was then observed. Interestingly, this structure was able to form along either the longitudinal or lateral axis of the dividing nucleus (thus being respectively perpendicular (**figure 3.4E**) or parallel (**figure 3.4F**) to the kinetoplast). The orientation of the mitotic spindle would later define the orientation of the dividing nucleus within the cell. After completion of mitosis, the fluorescent signal progressively returned to the sub-pellicular microtubules. At that stage, the divided nuclei were positioned laterally within the cell, thus ensuring their distribution on both sides of the division plane and their accurate allocation to the parent and daughter cells. In one particular instance, β-tubulin was also found to occur in a structure that resembled the mammalian contractile ring (**figure 3.4G cr**). Later during cytokinesis, the β-tubulin fluorescent signal became brighter in the proximity of the cleavage furrow and especially during cell-cell scission (**figure 3.4H cr**).

In *T. brucei*, RAB11 is present on endosomes involved principally in recycling processes (Jeffries et al., 2001; Hall et al., 2005). Within the *L. major* genome, a gene (LmjF10.0910) encoding a putative RAB11 protein, with a predicted molecular mass of 23.4 kDa, was identified. Because of it has 78% sequence identity with its *T. brucei* orthologue (TbRAB11), the expression of RAB11 in *L. major* promastigotes was assessed by Western blot using an anti-TbRAB11 antibody (**figure 3.5**). A protein with a size close to the predicted molecular mass for LmajRAB11 was detected (**figure 3.5 red arrow head**). An additional protein of about 27 kDa, however, was also revealed (**figure 3.5 black arrow head**). Interestingly, in *T. cruzi* insect forms, an antibody raised against TcRAB11 recognised a protein of 26kDa rather than the predicted 24 kDa protein

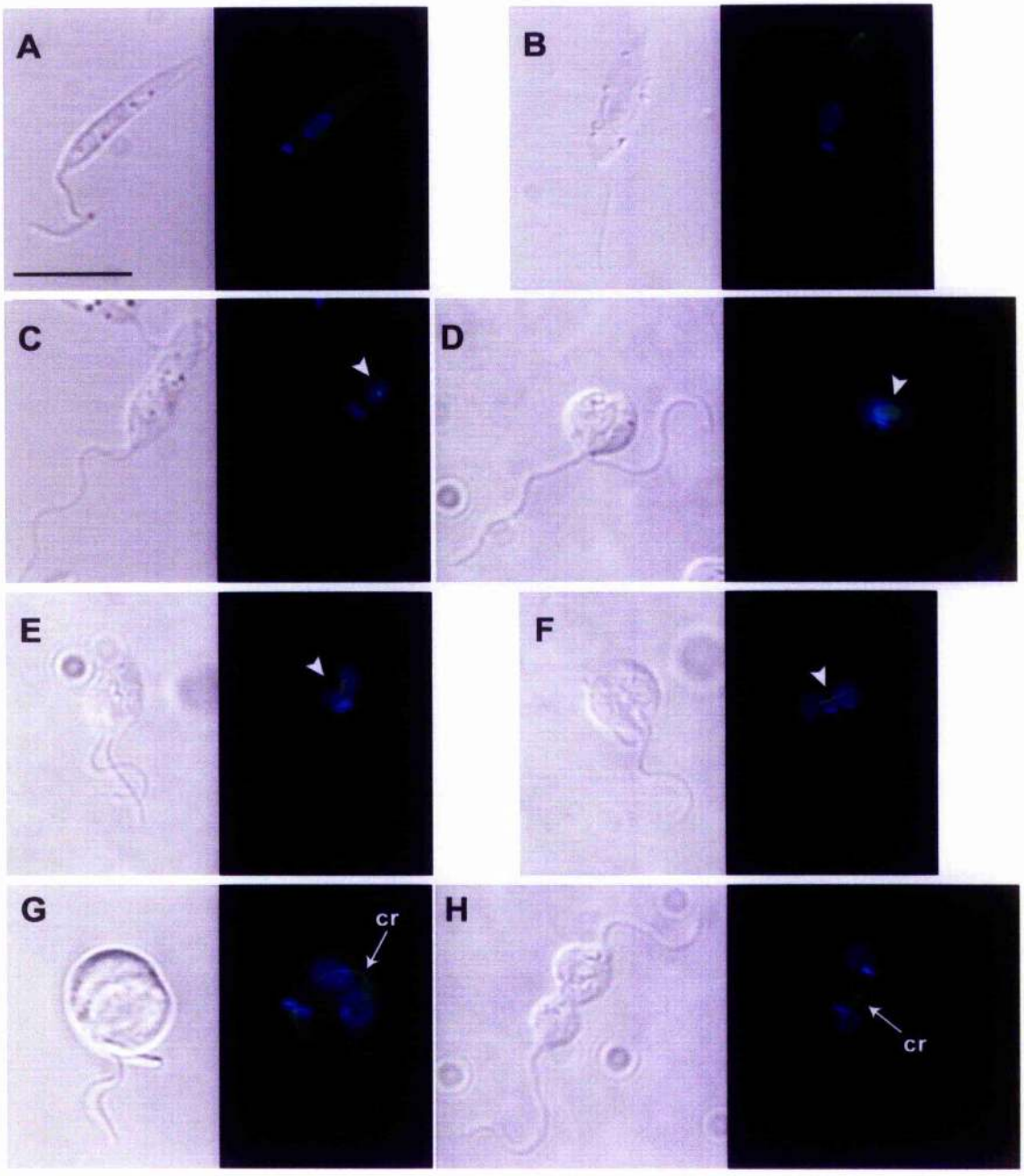

Figure 3.4: Immunofluorescence analysis of β-tubulin location during the cell cycle

Fixed cells were labelled with mouse anti- β-tubulin (KMX, (Sasse and Gull, 1988)) and Alexa 488-conjugated anti-mouse antibodies (green). The nuclear and kinetoplast DNA was stained with DAPI (blue). Left: merge pictures of the β-tubulin labelling and DAPI staining. Right: Corresponding DIC pictures. The white arrow heads indicate the microtubules of the mitotic spindle. cr: contractile ring. Representative pictures are shown except in G, where a single cell out of the 130 examined had such a developed ring-like labelling. Scale bar = 10 μm.

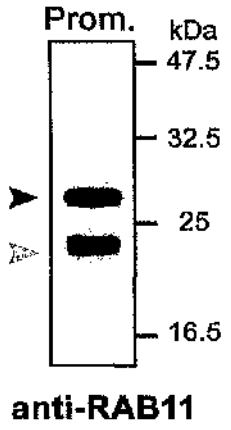

Figure 3.5: RAB11 expression in *L. major* promastigotes

The equivalent of 10^7 promastigotes were loaded per lane of a 12% (w/v) SDS-PAGE gel before electrophoresis and transfer to a PVDF membrane. The blot was then hybridised with anti-TbRAB11 at a 1:10,000 dilution in PBS + 0.05% Tween + 5% milk and then revealed with HRP-conjugated anti-rabbit antibodies (1:2,000) and an ECL kit. The expected size protein is shown by a red arrow head. The black arrow head indicates an additional protein of unknown identity.

(Mauricio de Mendonca et al., 2000). The authors then hypothesised that this larger protein might represent a geranylgeranyl modified TcRAB11 as this post-translational modification is required for membrane anchoring of RAB proteins (Calero et al., 2003; Leung et al., 2006). The prediction software PrePS (Prenylation prediction site, http://mendel.imp.ac.at/sat/PrePS, (Maurer-Stroh and Eisenhaber, 2005)) revealed that LmajRAB11 potentially possess a geranylgeranylation site in its C-terminus. The 27 kDa protein, therefore might result from geranylgeranyl modification of LmajRAB11 and its association with lipids. Although less likely, it can not yet be excluded that this cross-reacting protein might possess a different identity. Despite this observation, immunofluorescence experiments were performed in *L. major* promastigotes using the anti-TbRAB11 antibody.

In interphase cells the antibody labelled a compartment composed mainly of a structure at the base of the flagellum but also of a two pronged forked structure, positioned between the first structure and the kinetoplast and coming in close proximity to the mitochondrial membrane (**figure 3.6Aa, B1**). This observation was most surprising as none of the endosomal compartments characterised so far in trypanosomatids have a similar shape. However, co-localisation with concanavalin A (at 4°C) showed that the main structure of the RAB11-positive compartment was actually corresponding to the flagellar pocket while the two pronged forked structure was coming from it, thus confirming that this compartment belonged to the endosomal system (Besteiro, S, unpublished data). This RAB11-positive compartment was closely

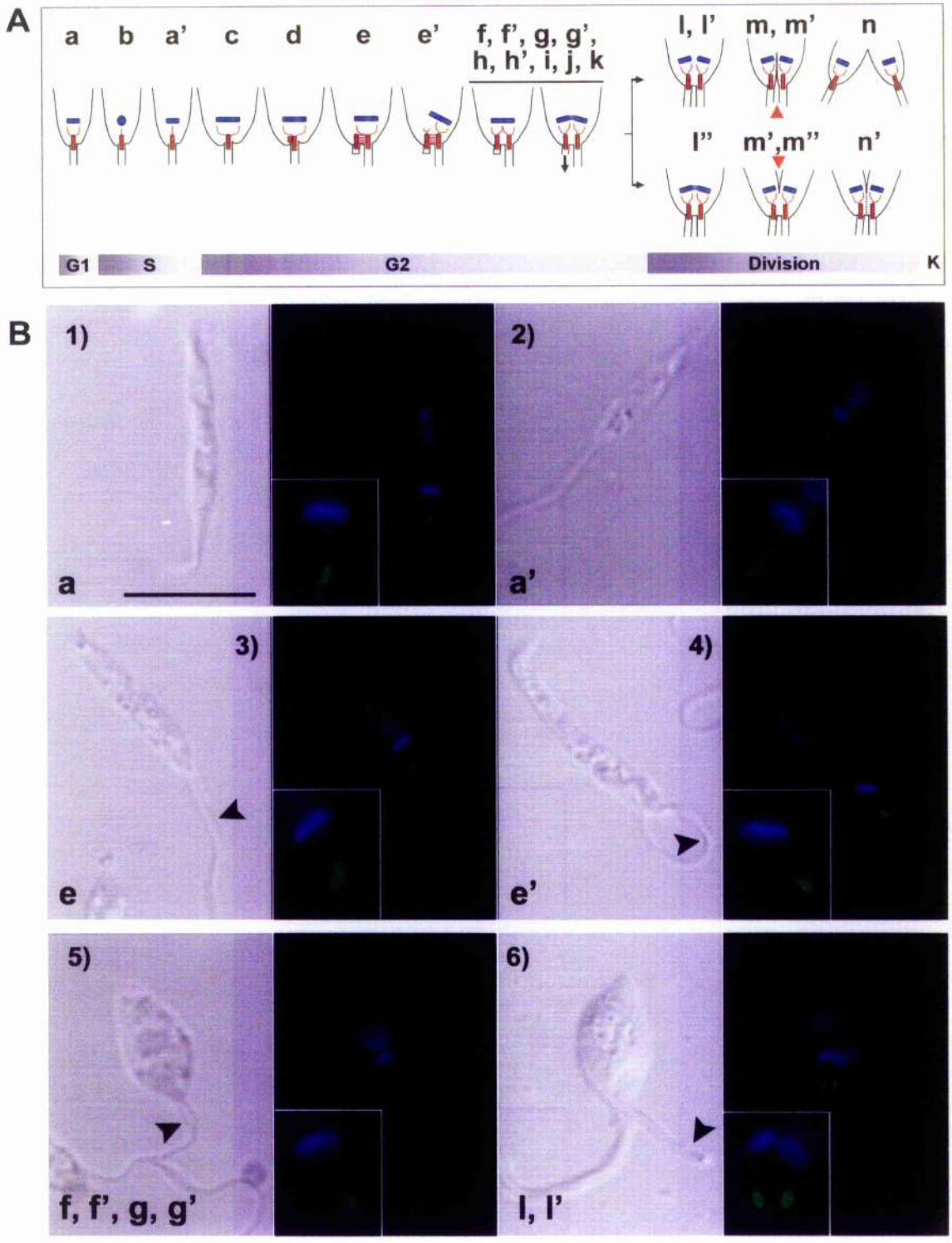

Figure 3.6: Analysis of Rab11 localisation during the kinetoplast division

A) Schematic of the various signals observed using anti-RAB11 antibodies. The letters also refer to **figure 3.8** and indicate cells with 1N1K1F or 1N*1K*1F (a, a', b, c, d), 1N*1K*2F (e, e'), 1N*^{M}1K*2F (f, f', g, g', h, h', i, j, k), 1N*^{M}2K2F (l, m), 2F2K2F (l', m', n, n') or 2N1K*2F (l'', m''). B) Immunofluorescence pictures illustrating the observations presented in A. Rabbit anti-TbRAB11 (Jeffries *et al.*, 2001) and Alexa 488-conjugated anti-rabbit (green) antibodies were used to label the fixed cells. Nucleus

and kinetoplast are shown in blue (DAPI staining). The insets pictures are 2x enlargement of the kinetoplast area. Scale bar = 10 μm.

associated with the kinetoplast and its morphology evolved with the kinetoplast division cycle. During the early events of the cell cycle the RAB11-positive compartment had a two-pronged fork-like form in the majority of the cells (**figure 3.6Aa, B1**). Nevertheless, for a small proportion of the cells, the compartment was modified and it possessed only one fork (**figure 3.6Aa', B2**). It was noted that this particular morphology was more abundant in cells blocked in S-phase (data not shown). As the parasites moved through the cell cycle the shape of the RAB11-positive compartment evolved. Firstly, at the base of the flagellum, a small additional structure appeared next to the existing one, suggesting the creation of the daughter flagellar pocket (**figure 3.6Ad-e', B3, B4**). Next, the two-pronged forked structure progressively extended from the newly synthesized flagellar pocket. Meanwhile, the duplicated kinetoplast had apparently slightly rotated on its axis, as if to make some space for the synthesis of the new RAB11-positive structure (**figure 3.6Ae', B4**). In addition, the existing RAB11-positive compartment had shifted its position so that instead of being closely associated with the two sides of the kinetoplast, one of its prongs was now placed midway along the longitudinal axis of the mitochondrial DNA. The elongation of the newly synthesized fork structure was found to be concomitant with the daughter flagellum outgrowth. Ultimately, both the old and new compartments appeared to associate with the same elongated kinetoplast (**figure 3.6Af-k, B5**). From that point, it seemed that the extension of the daughter flagellum was driving the segregation of the kinetoplast (**figure 3.6Al-n', B6**).

The division of the kinetoplast finished when the parent and daughter flagella had reached similar lengths. Ingression of the cleavage furrow and subsequent cytokinesis was then triggered. In most cases, the completion of kinetoplast division was achieved before the end of mitosis, as shown by the continued presence of the mitotic spindle (**figures 3.7l, 3.8l**). In that configuration, the subsequently formed cleavage furrow would progress from the anterior part of the cell, between the duplicated flagellar pockets, toward the posterior end (**figures 3.7n, 3.8n**). However, in some cells, the timing of kinetoplast segregation and nuclear separation was either reverted or almost synchronous. These alternative sequences of events could account for the presence of cells in which cleavage furrow ingression was occurring at the posterior end or at both extremities.

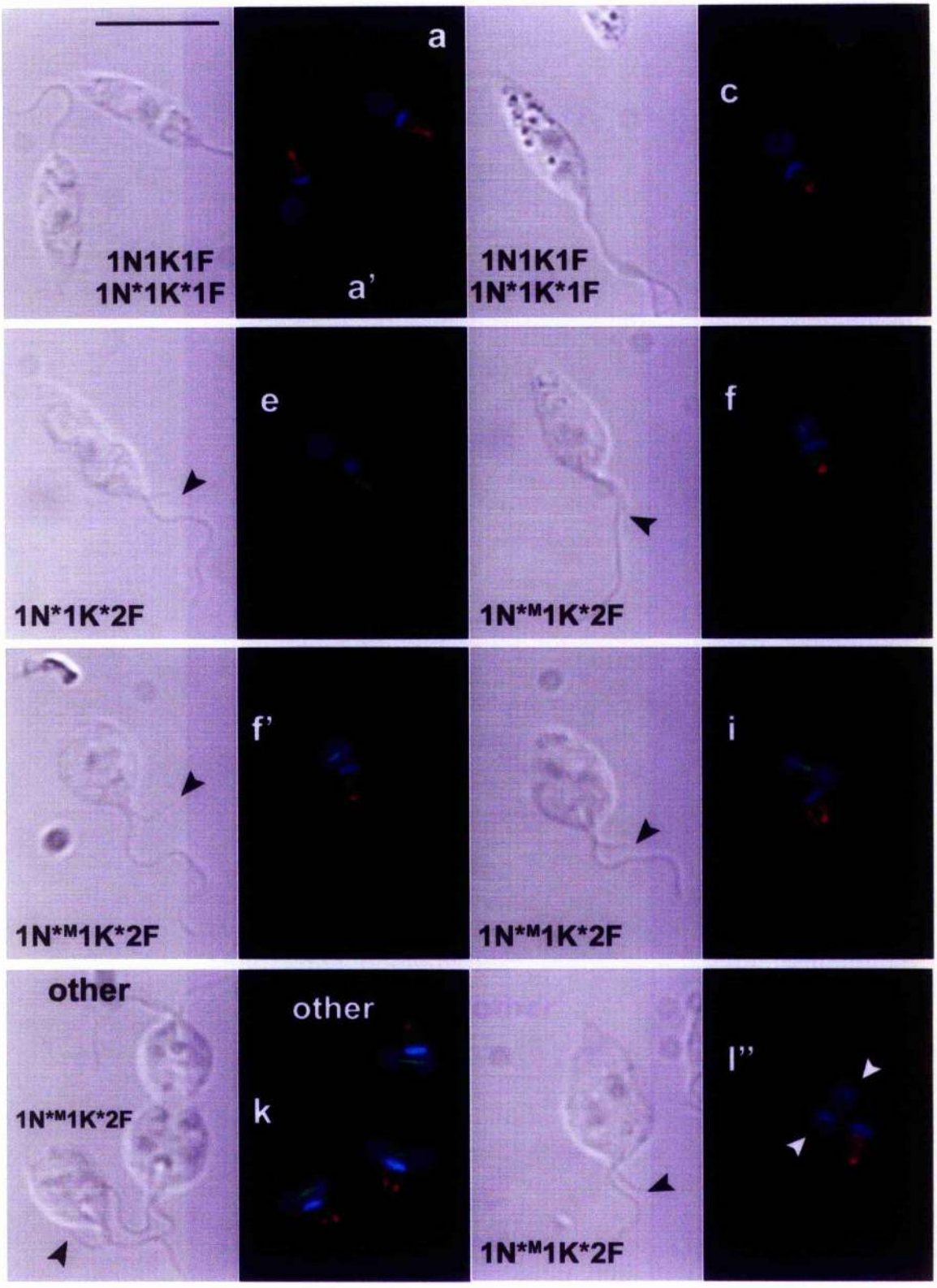
a
1N1K1F
1N*1K*1F
a'
1N1K1F
1N*1K*1F
c
e
1N*1K*2F
1N*M1K*2F
f
f'
1N*M1K*2F
1N*M1K*2F
i
other
1N*M1K*2F
other
k
1N*M1K*2F
l''

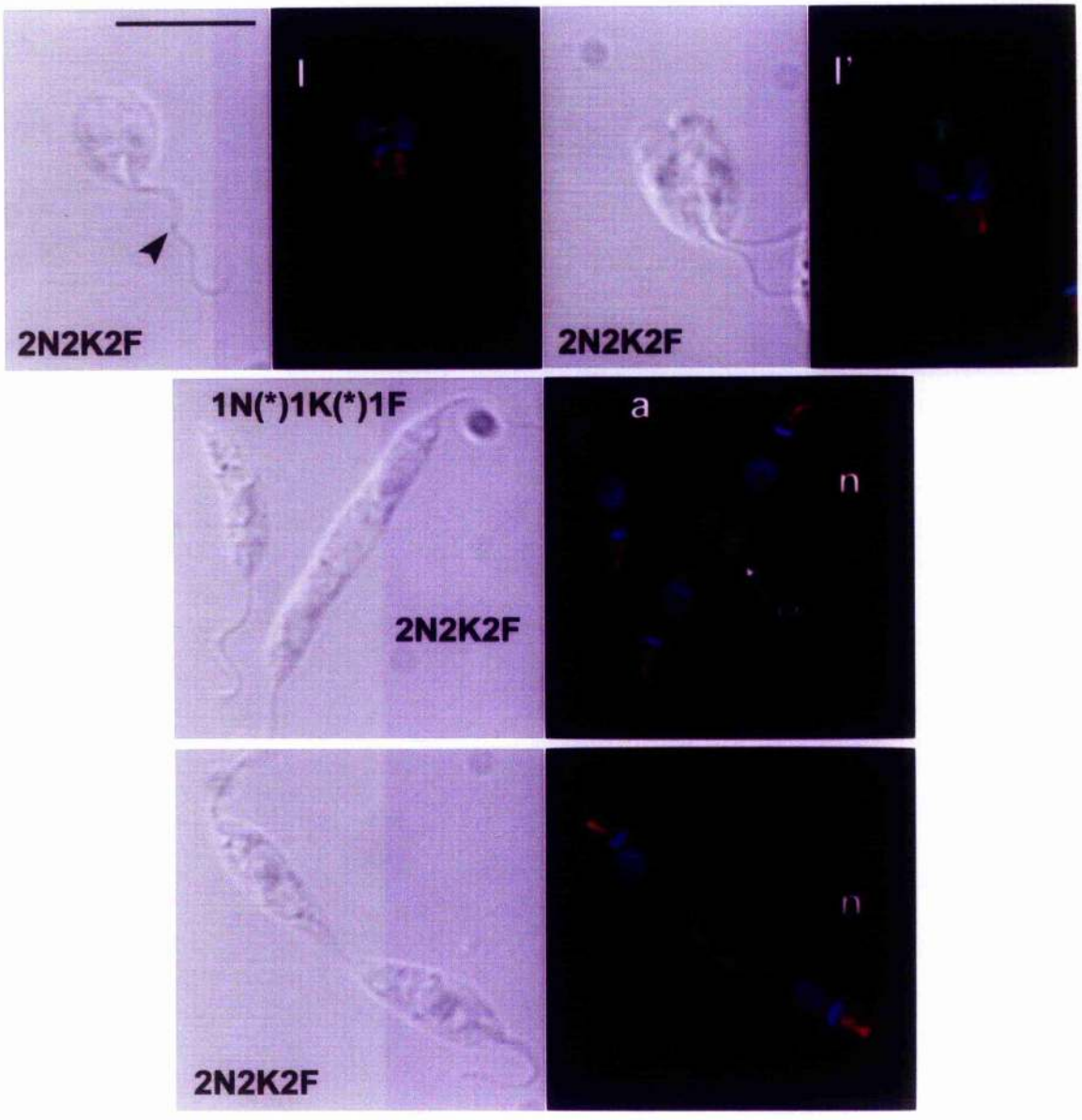

Figure 3.7: Observation by immunofluorescence of the events leading to cell division in *L. major* promastigotes

Nuclear and kinetoplast DNA of the fixed cells were stained with DAPI (blue). The microtubular events associated with nuclear division and shape remodelling were visualised with anti-β-tubulin and Alexa 488-conjugated anti-mouse (green) antibodies. Events associated with kinetoplast segregation and daughter flagellum growth were visualised with anti-RAB11 and Alexa 548-conjugated anti-rabbit (red) antibodies. These three labellings are merged in the pictures on the right. The letter code refers to the nomenclature in **figure 3.8.** On the left, the DIC image of the corresponding cell is shown. The black arrow heads indicate the growing daughter flagellum. For each cell, the number of nuclei (N), kinetoplasts (K) and flagella (F) are shown. The presence of an asterisk after N or K indicates that the DNA of this organelle is duplicated. The white arrow heads indicate a disassembling mitotic spindle. A structure similar to the contractile ring is arrowed with "cr". Scale bar = 10 μm.

Thus, using these two morphological markers, I was able to establish a list for the successive processes leading to cell division in *L. major* promastigotes (see **figure 3.7.** for additional illustrations). I subsequently used the created data to quantify the proportion of cells harbouring such morphological configurations. **Figure 3.8** summarises these findings. Cells with one nucleus, one kinetoplast and one flagellum (1N1K1F) were grouped with those that had duplicated their DNA content (1N*1K*1F) as this study could not accurately discriminate them. However, the presence of a daughter flagellum was indicative that DNA replication had occurred and thus, the 1N*1K*2F cells were pooled separately. About two thirds of the cells with one nucleus, one kinetoplast and two flagella had a mitotic spindle, indicating ongoing mitosis. These cells were identified as $1N^{*M}1K^{*}2F$. Cells where the kinetoplast segregated before ($1N^{*M}2K2F$) or after (2N1K*2F) completion of mitosis are also represented. Note that most of the 2N2K2K cells were undergoing cytokinesis. Therefore, termination of organelle division seems to trigger the start of cell partitioning. The cleavage furrow formed at the anterior end (2.30%) but was also found to be present at the posterior part of the cell (1.54%) or at both ends (0.77%). Finally, I classified as "others" the configurations observed in less than 0.5% of the total cells (mostly these were clumps of dividing cells like those shown in **figure 3.7**).

3.4. Discussion

It has previously been reported that, in their insect vector *Lutzomyia longipalpis*, *L. mexicana* and *L. infantum* are mainly present under seven morphologically distinct promastigote forms (Rogers *et al.*, 2002; Gossage *et al.*, 2003). Of these, only two cell types, the procyclic promastigotes and the leptomonad promastigotes (during the sandfly bloodmeal and sugar meal phases, respectively) are able to replicate (Gossage *et al.*, 2003). Their multiple differentiation steps will ultimately lead the cells to the non-replicative infectious form of the parasite, the metacyclic promastigote. In *L. mexicana*, both procyclic and leptomonad promastigotes possess a body length of about 6.5-11.5 μm but for the procyclics the flagellum length is shorter than the cell body while the leptomonads have a longer flagellum (Rogers *et al.*, 2002). When lesion amastigotes were used to initiate an *in vitro* culture of *L. mexicana* or *L. infantum* promastigotes, the differentiation processes and the sequential appearance of the various promastigote forms followed the same order as in the sandfly host. In freshly differentiated cultures, dividing procyclic and leptomomad promastigotes, defined by their possession of two nuclei and/or kinetoplasts, were found to respectively represent 56.5% and 12.0% of the *L. mexicana* promastigotes or 9.9% and 4.8% of the *L. infantum* promastigotes (Gossage *et al.*, 2003). These

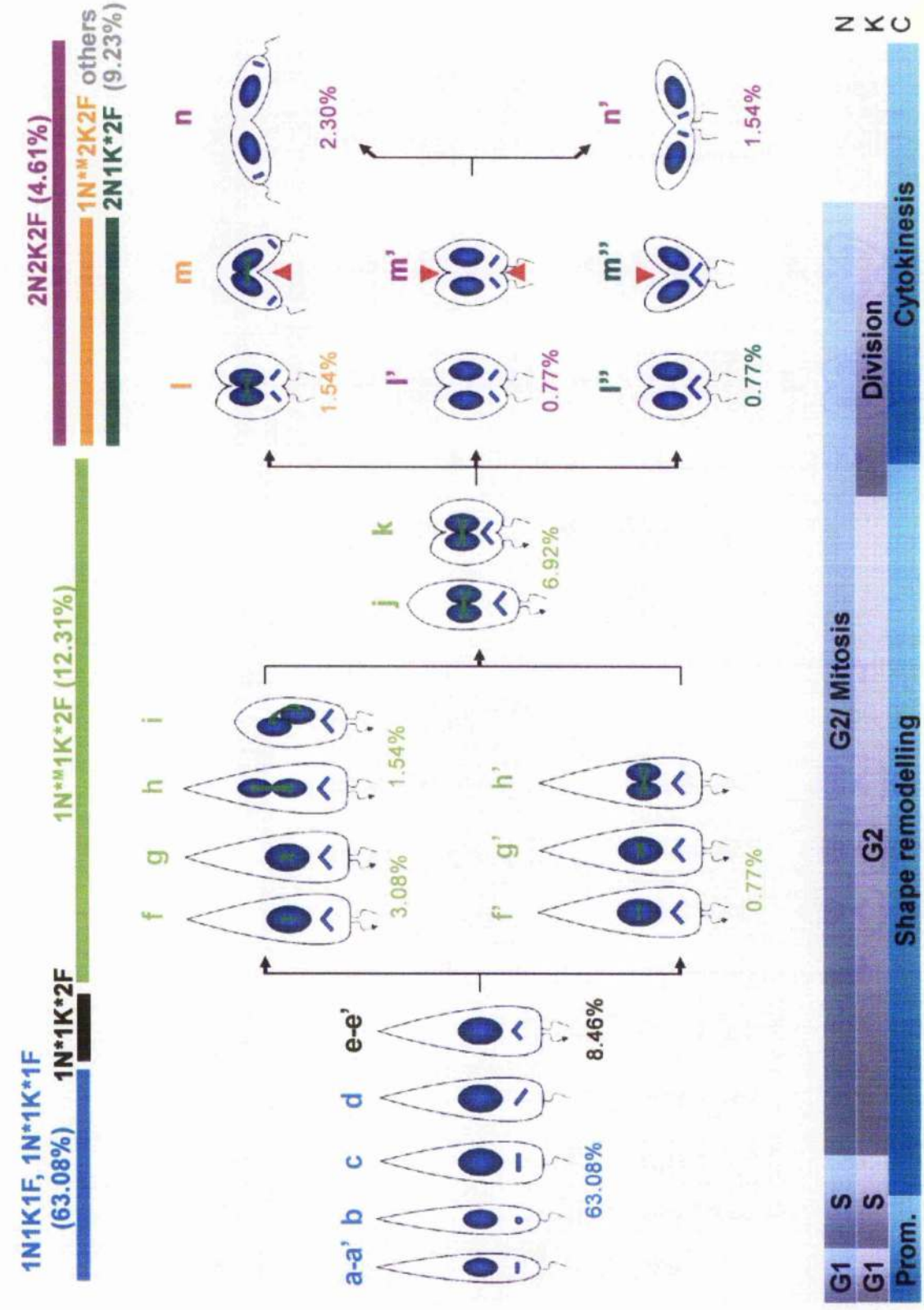

Figure 3.8: Schematic representation of the configurations observed through the *L. major* promastigote cell cycle and their relative abundance

130 cells were counted for this analysis. For each cell, the number of nuclei (N), kinetoplasts (K) and flagella (F) were scored. Cells with similar configuration were then

grouped (colour codes). The percentage of each of these populations over the total cell number are showed. The asterisk after the N or K indicates that the replication of the DNA of the specified organelle has occurred. Cells classified in "others" possess unique configurations. On the right, the chronology of the cell cycle phases of the nucleus, kinetoplast and the associated morphological events are shown. Please note that this time frame is not to scale.

differences were attributed to the observation that fresh *in vitro* cultures of *L. mexicana* cells were growing at faster rates than those of *L. infantum*. However, it was noted that, for both *Leishmania* species, the synchronicity and timing of the appearance of the different forms of promastigotes was lost after several sub-passages in culture (Gossage *et al.*, 2003). Thus, *in vitro*, it is commonly accepted that cells in their logarithmic phase of growth are principally procyclic promastigotes while non-replicative cells in their stationary phase are metacyclic promastigotes.

The cell cycle studies presented here were performed on cultures of *L. major* promastigotes at low number of sub-passages. Promastigotes in their early logarithmic phase of growth ($0.3x10^7$ cells ml^{-1}) were observed but no distinction was made between the possible different forms of the parasites. Indeed, while the morphological characteristics of the various types of *L. major* promastigote remain unclear, they are anyway most likely to be modified during progression within the cell cycle. When using the same classification as Gossage *et al.*, the percentage of dividing cells within culture of *L. major* promastigotes was found to be of 15.38% (part of $1N^{*M}1K^{*}2F$, $1N^{*M}2K2F$, 2N1K*2F and 2N2K2F). In a report characterising the effect of anti-tubulin inhibitors on *L. donovani*, it was roughly estimated that, under normal growth conditions, about 10 to 20% of the wild type cells were in dividing process (Havens *et al.*, 2000). However, it is difficult to directly compare the different sets of data, as the experiments were either performed in different conditions and/or on different *Leishmania* species. The study presented here represents one of the first descriptions of the cell cycle in *L. major* promastigotes. Many interesting observations were made, but the collected data need to be strengthened by the analysis of a larger number of cells. For their determination of the timing of the nuclear and kinetoplast phases of the cell cycle, Woodward and Gull analysed between 1,000 and 2,000 *T. brucei* cells (Woodward and Gull, 1990).

As discussed previously, differences in the chronology of cell cycle events were observed not only between different *Leishmania* species but also among different life stages of the parasite. The data accumulated in this study suggest that differing patterns of division could occur within the same population of promastigote cells. Indeed, it was first observed that during the nuclear mitosis, the mitotic spindle was able to form either longitudinally or laterally within the cell (**figures 3.4 and 3.8**). This tightly packed array of interpolar and kinetochore microtubules is involved in the

segregation of the 36 chromosomes of the *L. major* genome (ranging in size from 0.28 to 2.8 Mb) (Wincker et al., 1996; Ivens et al., 2005). Unlike in mammalian cells, in *Leishmania*, the number of kinetochore structures (only six) does not match the number of chromosomes (Urena, 1986; Urena, 1988). Therefore, it was speculated that, like in *T. brucei*, the interpolar microtubules of the mitotic spindle could participate to the division of the smaller chromosome pairs (Gull *et al.*, 1998). The ultrastructure of the dividing nucleus has been studied in detail in *T. brucei*. In addition to electron microscopy, the structure of the mitotic spindle was observed by immunofluorescence using the KMX anti-β-tubulin antibodies (Ogbadoyi *et al.*, 2000). As observed in the present study, the mitotic spindle was found to form within the intact nucleus. There it elongates between the opposing ends of the nucleus, being anchored at the intranuclear spindle poles. Meanwhile, the nuclear membrane contracts at the centre of the nucleus, until the constriction zone extends along the central spindle. At this point, it is difficult, without the labelling of the mitotic spindle to distinguish between dividing and divided nuclei. The ingression of the nuclear envelope constriction ultimately results in the completion of karyokinesis. Also, the present study revealed that while at the mitosis onset the majority of the *Leishmania* cells had a longitudinal mitotic spindle, after mitosis completion most of the parent and daughter nuclei were arranged laterally within the dividing cell. Therefore, it seems likely that this latter orientation results from the rotation of the two nuclei. Interestingly, this 90° clock or anti-clockwise movement is apparently happening during mitosis, as most of the rotating nuclei possessed a mitotic spindle (**figures 3.4E and 3.7i**). Also, it is interesting to note that radical body shape changes are timely associated with nuclear mitosis. Thus, these morphological modifications might be attributed to the spatial re-organisation necessary for nuclei re-positioning.

Meanwhile, most of the cells had completed the segregation of their duplicated kinetoplast. This finding contradicts previous observations indicating that the division of the kinetoplast was mainly occurring after the partitioning of the daughter and parent nuclei (Milligan, 1996; Havens *et al.*, 2000). Also, as these studies were performed on *L. mexicana and L. donovani*, it is possible that the order in which kinetoplast division and mitosis happen varies between different species, as previously suggested. However, these older studies were based on observations of DAPI staining, so it is possible that an elongated nucleus that had not completed the division process was considered as divided nuclei. This bias would therefore suggest that kinetoplast division occurs after mitosis. Thus methods like the one presently used, allowing the visualisation of the mitotic spindle, can more accurately indicate whether mitosis has or not reached completion. Indeed, while in most mammalian cells remnants of the mitotic spindle are still present after completion of karyokinesis (Scholey *et al.*, 2003) (**figure 3.2f**), in *T.*

brucei (Ogbadoyi *et al.*, 2000) but also here in *L. major* (**figure 3.7 l''**), the disassembly of the mitotic spindle seems to be concomitant with the end of nuclear division. Furthermore, the observation that cytokinesis was mainly starting at the anterior part of the cell, between the two flagella, and was following a longitudinal axis toward the posterior end of the cell, fits with the kinetoplast segregation occurring before the end of mitosis. Therefore, apparently, the succession of events leading to the division of *Leishmania* kinetoplast and nucleus resemble the one observed in *T. brucei* cells.

A major difference, however, was observed during cytokinesis. While in *T. brucei*, the cleavage furrow has to progress in a helical fashion to adapt to the presence of the attached flagella, in *Leishmania*, its ingression follows a longitudinal axis. Interestingly, it was observed that a structure closely similar to the mammalian contractile ring was visualised with the anti-β-tubulin antibodies (**figures 3.4G and 3.7n**). So far there are no published reports of the detection of a contractile ring in trypanosomatids. In most eukaryotes, this structure is composed of an array of actin and myosin II filaments (Field *et al.*, 1999). However, RNAi studies performed in *T. brucei* failed to establish the necessity of actin for the creation of a contractile ring and cytokinesis progression (Garcia-Salcedo *et al.*, 2004). Thus, it is possible that kinetoplastids possess a contractile ring with an unusual composition. In bacteria as well as in many eukaryotic organelles (e.g. mitochondrion), a tubulin-like protein, FtsZ, is the main constituent of a ring-like structure, the Z ring, which mediate cytokinesis or organellokinesis through its contraction (Errington *et al.*, 2003).The trypanosomatids β-tubulin might have retained some of the properties of this ancestral tubulin and might share a role in cytokinesis (de Pereda et al., 1996; Addinall and Holland, 2002). Furthermore the fact that the mitotic spindle and contractile ring are both composed of β-tubulin could explain why both mitosis and cytokinesis are blocked by tubulin inhibitors (Havens *et al.*, 2000).

Apart from the detection of β-tubulin in a ring-like structure potentially involved in *L. major* cytokinesis, another intriguing finding was the localisation of RAB11 within this parasite. Although RAB11 apparently remains associated with the endosomal system like in other organisms, the shape of the RAB11-positive compartment in *Leishmania* is most peculiar. Anchored at the flagellar pocket, this compartment then ramifies toward the mitochondrion membrane and the kinetoplast. The observed two pronged forked structure might result from the spatial hindrance caused by the tripartite attachment complex (TAC). Characterised in *T. brucei* but not yet in *L. major*, this complex, composed of series of filaments, connects the kinetoplast DNA network to the mitochondrial membrane and the basal body from which originates the flagellum (Ogbadoyi *et al.*, 2003). The TAC constitutes a mechanical link by which kinetoplast segregation is associated to the division of the basal body and the flagellum. Tightly

anchored at the base of the flagellum, the flagellar pocket follows a division cycle that is intimately correlated to the one of the flagellum. The formation of the daughter flagellar pocket starts with the appearance of the daughter flagellum and its development is linked to the growth of the new flagellum. Also the presence of RAB11 at the site of the flagellar pocket allowed us to follow the development and positioning of this organelle in relation to kinetoplast division and flagellum extension. However the reason why the RAB11-positive compartment adopts such a two pronged forked structure remain obscure and its function in the cell remain uncertain. In mammalian cells, RAB11-positive recycling endosomes were recently characterised for their role in membrane trafficking during cytokinesis (Wilson et al., 2005; Matheson et al., 2005; Fielding et al., 2005). Also, because of the close association of the RAB11-positive compartment with the *Leishmania* mitochondrion, and because this organelle needs to acquire new membranes before its division to allow its equal partitioning between parent and daughter cells, then we might wonder whether the RAB11-positive compartment might promote membrane trafficking between the flagellar pocket and the mitochondrion. Nevertheless, such a process has never been characterised and membrane vesicles are classically derived from the endoplasmic reticulum and the Golgi apparatus. In mammalian cells, traffic of lipids to the mitochondrion involves ER-like mitochondrion-associated membranes (MAMs) (Vance and Shiao, 1996). But the existence of such membranes in *Leishmania* remains unknown. Therefore the mechanisms by which the mitochondrion acquires the new membrane required for division are, in *Leishmania*, largely uncharacterised and an involvement of the RAB11-positive compartment can not be excluded. Furthermore, during mammalian cytokinesis, the RAB11-positive recycling endosomes uses motor proteins to move along microtubules to the site of the cleavage furrow (Fielding *et al.*, 2005), also we might wonder whether in *Leishmania*, the RAB11-positive compartment could interact with some of the TAC filaments to mediate exchanges between the flagellar pocket and the mitochondrion. This would explain the shape adopted by this compartment and its structural modulation during kinetoplast division. However, the immunofluorescence data suggest that this compartment is more likely a continuous and defined structure rather than an association of multiple vesicles moving along a filament. In *T. cruzi* insect forms (epimastigotes), RAB11 is present in a pre-lysosomal compartment composed of multiple organelles termed reservosomes (Mauricio de Mendonca et al., 2000). In addition to the flagellar pocket, *T. cruzi* possess an additional site involved in nutrient endocytosis, the cytostome, which is connected to a vesicular-tubular network of early endosomes (the cytopharynx) that ultimately deliver their content to the reservosomes for storage. In *Crithidia fasciculata*, the cytostome appears to be connected to the flagellar pocket and not directly to the external medium like in *T.*

cruzi (Brooker, 1971; Clayton et al., 1995). Although *Leishmania* appears to a lack cytostome, cytopharynx or reservosomes, it cannot be excluded that in this organism RAB11 might be present in a yet uncharacterised type of structure connecting the flagellar pocket to the lysosomal compartment. Thus, further ultrastructural analyses need to be performed, by electron microscopy, to answer this point and most importantly to clearly identify the nature of this RAB11-positive compartment in *Leishmania* and its intriguing function in the cell.

Chapter 4:
Structural and biochemical properties of trypanosomatid metacaspases

4.1. Presentation of the trypanosomatid metacaspases

Little is known about metacaspases in trypanosomatids. Five metacaspase genes have been identified in the *Trypanosoma brucei* genome, encoding for proteins (TbMCA1 to TbMCA5) that have different features and levels of sequence identity (**table 4.1**). Interestingly, although the meaning of this observation remains obscure, *Trypanosoma cruzi* and *Leishmania*, which spend part of their life cycle as intracellular forms, in the mammalian host, possess fewer metacaspases. It was recently reported that *T. cruzi* possesses only two metacaspases. These proteins, TcMCA3 and TcMCA5, were named after the *T. brucei* metacaspases with which they share closest sequence identity (Kosec *et al.*, 2006). The parasites responsible for cutanous (*L. major*) and visceral (*L. infantum*) leishmaniasis were both found to contain a single metacaspase gene, which were named *LmajMCA* and *LinfMCA*, respectively.

	TbMCA2	TbMCA3	TbMCA4	TbMCA5	LmajMCA	LinfMCA	TcMCA3	TcMCA5
TbMCA1	40.8	42.4	41.9	26.2	26.2	25.5	42.1	28.8
TbMCA2		88.2	48.4	32.0	36.0	34.5	58.9	36.0
TbMCA3			48.5	30.5	33.5	32.3	61.5	34.6
TbMCA4				26.6	28.6	27.7	46.4	30.4
TbMCA5					48.1	49.7	31.0	55.8
LmajMCA						93.5	33.1	54.4
LinfMCA							32.3	53.8
TcMCA3								36.1

Table 4.1: Percentage of identity between *Trypanosoma brucei*, *Leishmania major*, *L. infantum* and *T. cruzi* metacaspase proteins.

These two metacaspases share about 94% identity at the amino acids level (**table 4.1**) and are both most closely related to TbMCA5 (48.1% and 49.7%, respectively) and TcMCA5 (54.4% and 53.8%). Large scale comparative genomics recently performed with trypanosomatids showed that *T. brucei*, *T. cruzi* and *L. major* exhibit a striking conservation of gene order (termed synteny) (Ghedin *et al.*, 2004). Indeed, comparison of the *LmajMCA*, *TbMCA5* and *TcMCA5* loci revealed that these genes are syntenic orthologues.

Furthermore, these three metacaspases share a structural peculiarity, compared to the other trypanosomatids metacaspases, in the form of a proline-, glutamine- and tyrosine-rich C-terminal extension. While divergent between the metacaspases, repetitive motives have been identified in these regions (**figure 4.3, light blue underlined letters**). The presence of homologous repetitive modules in other proteins (wheat gliadin, human rhodopsin) suggests that these domains might fulfil specialised roles within the cells.

Further analysis of the properties of the metacaspases was performed by reconstruction of the phylogenetic relationships between the trypanosomatid metacaspases and those of other representative organisms (**figure 4.1**). The full lengths of the selected proteins were used for this analysis. The reconstructed tree shows that the metacaspases from *T. brucei*, *T. cruzi* and *L. major* cluster together, well separated from the other metacaspases. However, it has to be noted that the trypanosomatid metacaspases seem more similar to the type I metacaspase group. As expected, the syntenic orthologues of LmajMCA, TbMCA5 and TcMCA5 form a distinct clade. Interestingly, examination of the genomes of the yeasts *Saccharomyces cerevisiae* and *Schizosaccharomyces pombe* and the filamentous fungus *Aspergillus nidulans*, revealed the presence of a single metacaspase with closer sequence identity to *MCA5* than any other trypanosomatid metacaspases, suggesting that *MCA5* might represent the basal metacaspase gene.

4.2. Focus on TbMCA1 and TbMCA4

Two (TbMCA1 and TbMCA4) of the five *T. brucei* metacaspases have substitutions in their predicted active site residues. Indeed, while the active site of most metacaspases has a pair of histidine and cysteine residues, TbMCA1 possesses a tyrosine residue instead of the conserved predicted catalytic histidine and, like in TbMCA4, the predicted active site cysteine is replaced by a serine residue (**figure 4.2, red arrow heads**). Phylogenetic analysis revealed that TbMCA1 and TbMCA4 proteins are clearly separated from the other metacaspases (**figure 4.1**). Indeed, the branch that leads to these atypical proteins departed from the apparently ancestral MCA before the split that gave rise to the other trypanosomatids metacaspases, thus suggesting that TbMCA1 and TbMCA4 have evolved independently. Also, as the histidine-cysteine dyad is predicted to be essential for clan CD cysteine peptidase activity, then TbMCA1 and TbMCA4 potentially lack cysteine peptidase activity (Mottram et al., 2003).

Indeed, due to the replacement of putative active site histidine by a tyrosine residue, which lacks the imidazolium group essential for the stabilisation of the thiolate ion involved in the nucleophilic attack of the peptide bond, it is highly unlikely that

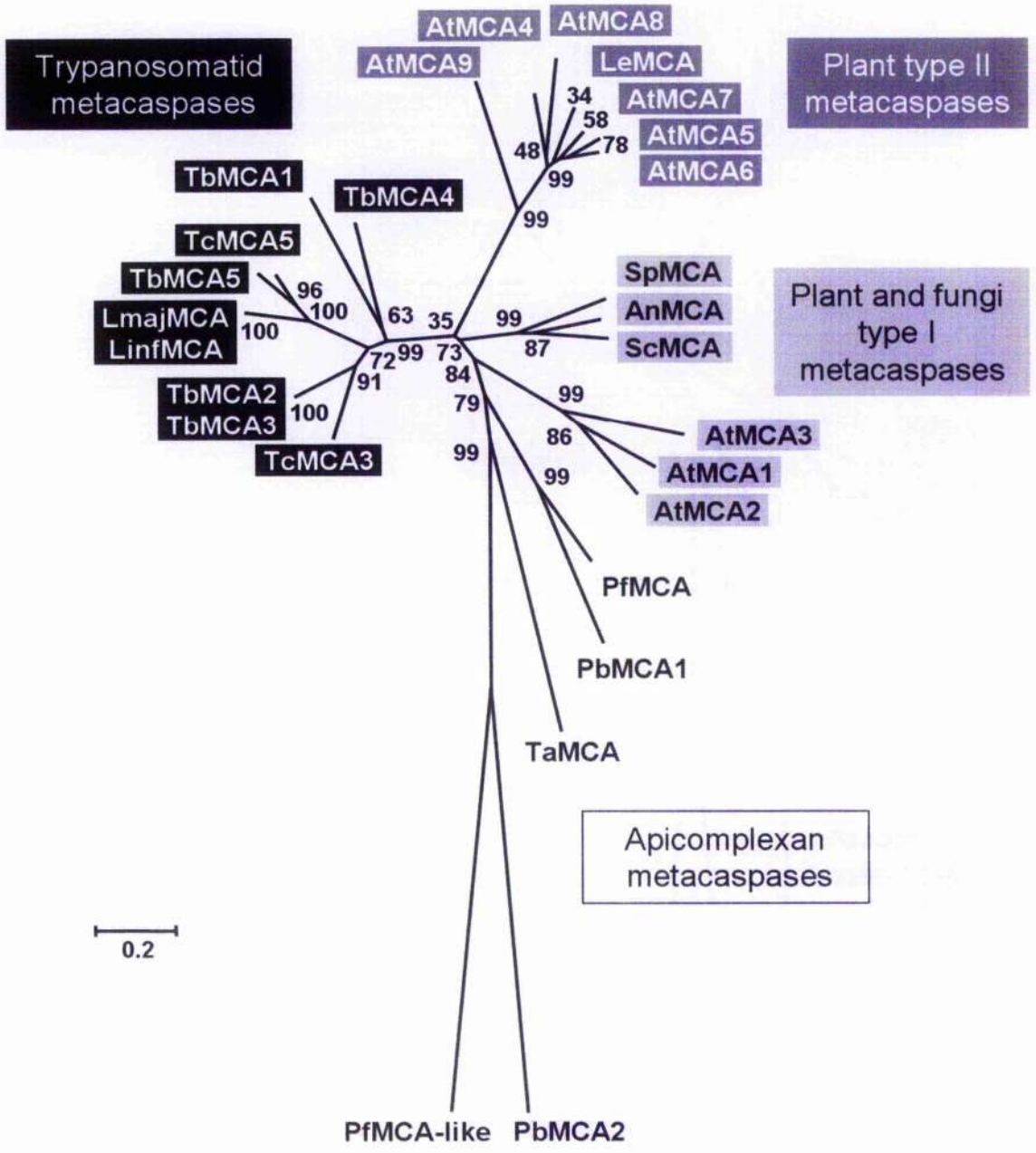

Figure 4.1: Phylogenetic analysis of selected metacaspases from trypanosomatids, plants, fungi and apicomplexan parasites.

Metacaspases in the tree are from *Arabidopsis thaliana* (At), *Aspergillus nidulans* (An), *Leishmania major* (Lmaj), *Lycopersicon esculentum* (Le), *Plasmodium berghei* (Pb), *P. falciparum* (Pf), *Saccharomyces cereviciae* (Sc), *Schizosaccha-romyces pombe* (Sp), *Theileria annulata* (Ta), *Trypanosoma brucei* (Tb) and *Trypanosoma cruzi* (Tc). Bootstrap values from 10,000 pseudoreplicates are shown on the nodes. The scale bar represents a distance of 0.2 substitutions per site. AnMCA (AAO13381.1), AtMCA1 (AAP84706.1), AtMCA2 (AAP84707.1), AtMCA3 (AAP84708.1), AtMCA4 (AAP84709.1), AtMCA5 (AAP84713.1), AtMCA6 (AAP84714.1), AtMCA7 (AAP84710.2), AtMCA8 (AAP84711.1), AtMCA9 (AAP84712.1), LmajMCA (AAZ14381, LmjF35.1580), LeMCA (AY114141), PbMCA1 (CAD88480.1, PB001074.02.0), PbMCA2 (CAD88481.1, PB000485.03.2), PfMCA (ABC84559, PF13_0289), PfMCA-like (PF14_0363) SpMCA (AAG38593.1), ScMCA (NP_014840), TbMCA1 (CAD24802.1, Tb11.02.0730), TbMCA2 (CAD24803.1, Tb927.6.940), TbMCA3 (CAD24804.1, Tb927.6.930), TbMCA4 (CAD24805.1,

Tb10.70.5250), TbMCA5 (CAD55946, Tb09.211.4760), TcMCA3 (e.g. XP_818074, Tc00.1047053509399.20) and TcMCA5 (XP_816130, Tc00.1047053510759.160) are represented (EMBL accession number, genedb designation (www.genedb.org)).

TbMCA1 will be an active peptidase (Barrett A.J. *et al.*, 2003). Markedly, one of the two metacaspases encoded by the *Plasmodium falciparum* genome possesses the predicted active site histidine and cysteine residues while the other has tyrosine and threonine substitutions at these respective positions (**figure 4.2, red arrow heads**). Thus, for the reasons previously discussed for TbMCA1, this latter protein is predicted to be a "dead" metacaspase. That two divergent protozoa have maintained apparently inactive proteins suggests that these "dead" metacaspases might have a specialised role within the cell. Interestingly, the human FLIP, an inactive structural homologue of caspases-8 and -10, which contain two death effector domains and an entire caspase domain mutated in the catalytic residues as well as the residues forming the substrate-binding S1 subsite, has been shown to act as a dominant negative inhibitor of apoptosis (Thome et al., 1997; Irmler et al., 1997). Indeed, FLIPs, which still possess their ability to bind to active caspases-8 and caspases-10, were hypothesized to act as competitive inhibitors preventing the binding of these caspases to adapter molecules and, consequently, the activation of death receptor-induced apoptosis (Hu *et al.*, 1997). Whether the potentially catalytically inactive TbMCA1 might act in a similar way remains an open question. *TbMCA1* might only be a pseudogene. However, it seems less likely that TbMCA4 might act as a "dead" metacaspase.

Indeed, in TbMCA4 the active site histidine residue is intact. Also, even though the active site cysteine residue has been replaced by a serine, a similar substitution is present in the single *Theileria annulata* metacaspase, TaMCA. Furthermore, in TbMCA4, a cysteine residue (**figure 4.2, orange arrow head**) is immediately adjacent to the substituted active site serine (**figure 4.2, second red arrow head**). This second cysteine residue is conserved in all trypanosome and *Leishmania* metacaspases but not in the yeast and plant metacaspases which possess a serine residue at this position. Therefore, TbMCA4 might have retained its peptidase activity by either using this adjacent cysteine as the active site residue or by being a mixed type peptidase. This would be similar to the situation with the serine repeat antigen 5 (SERA5) from *P. falciparum*, a protein with a high level of sequence identity to papain and potentially a Clan CA, C1 family cysteine peptidase, which has been shown to possess a catalytic activity even though it has a serine residue at the position of the active site cysteine (Hodder *et al.*, 2003).

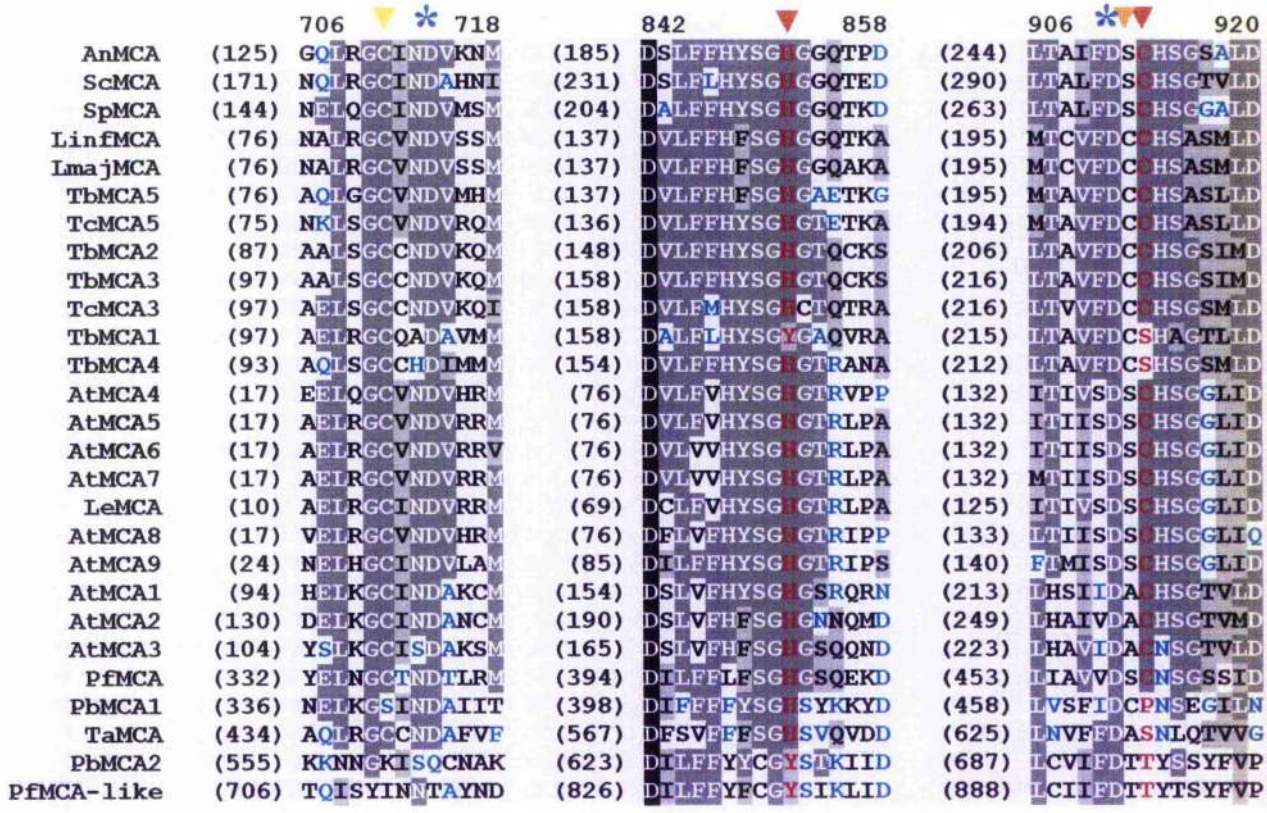

Figure 4.2: Alignments of selected domains of the active site region between several metacaspase proteins

Identical and conserved amino acids are shown in white on a black or dark grey background, respectively. Weakly similar amino acids are shown in black on a clear grey backgroung. Groups of similar amino acids are shown in blue. Catalytic residues from the active site are shown in red. Sequences were aligned using the Clustal W algorithm of the Align X program (Vector NTI Advance 10 package, http://www.informaxinc.com/). For details of the sequences used in this alignment, refer to **figure 4.1**. The red arrow heads indicate the position of the predicted catalytic residues while the orange and yellow arrow heads indicate potential alternative active site residues. The blue asterisks indicate the aspartate residue involved in the coordination of the substrate P1 residue.

Also, it cannot yet be excluded that, maybe, within the metacaspase active site, additional catalytic residue(s) still remain(s) to be characterised. Indeed, whereas the cysteine-histidine catalytic dyad is sufficient for cysteine peptidases of clans CK and CJ, other cysteine peptidases possess an additional highly conserved amino acid that is involved in the catalytic mechanism (Mottram *et al.*, 2003). The third amino acid residue of the catalytic triad differs between clans. In clan CA cysteine peptidase, it is either an asparagine or aspartic acid residue, and serves to orientate the active site histidine. The catalytic dyad of clan CD cysteine peptidases was predicted to be sufficient for their activity. Nevertheless, analysis of the catalytic activity of the human clan CD paracaspase revealed that an additional residue (cysteine-539) might be playing a role in the protein activity (Snipas *et al.*, 2004). Thus we cannot rule out that the

same might be true in metacaspases. Indeed, Szallies et al. reported that all trypanosomatid metacaspases possess, between the first strand and helix motifs of their predicted secondary structures, a conserved cysteine residue (**figure 4.2, yellow arrow head**), which, by superposition of the predicted metacaspase secondary structures upon the known structures of caspase-1 and gingipain, was found to be in the spatial proximity to the catalytic dyad (Szallies *et al.*, 2002). As these structure comparisons were not accessible online, we conducted a similar analysis with selected trypanosomatid metacaspases and caspases and concluded that, indeed, an additional cysteine residue might interact with the catalytic dyad of the metacaspases (refer to **section 4.5.**).

Consistent with these various observations concerning the TbMCA4 putative enzymatic activity, it was observed that heterologous expression of TbMCA4 in the yeast *Saccharomyces cerevisiae* led to a petite phenotype due a complete abolishment of respiration competence (Szallies *et al.*, 2002). This phenotype was abrogated when the predicted TbMCA4 active site residue histidine-164 was mutated to an alanine. Furthermore, the phenotypes induced by TbMCA4 expression in yeast were completely lost when the cysteine-218, the residue flanking the substitutive active site serine residue (**figure 4.2, orange and red arrow heads, respectively**), was mutated. Even more unexpected was the finding that mutation of the cysteine-98 (**figure 4.2, yellow arrow head**), together with the flanking cysteine-99, which, in the predicted secondary fold, are in the close proximity of the catalytic dyad, also resulted in the disappearance of the expression phenotype. Consequently, it seems that the atypical TbMCA4 possess an enzymatic activity when expressed in yeast cells. However, the nature of this activity remains to be established. More importantly, similar analyses remains to be performed in *T. brucei* to assess whether the phenotypes observed in yeast are physiologically relevant.

4.3. Focus on TbMCA2, TbMCA3 and TcMCA3

TbMCA2 and TbMCA3 share a very high level of sequence identity (88.2%). TbMCA3 possesses a 10 amino acids N-terminal extension compared to TbMCA2, a region that might contain a signal peptide (**figure 4.3, blue letters**). This is suggestive that the N-terminal domain may be important for selective targeting of the two proteins or some differential function(s). However, the fact that *T.cruzi* possesses a TbMCA3 but no TbMCA2 homologue suggests that these two proteins might be playing a similar role in the cell or that TbMCA2 might possess a *T. brucei*-specific role. However, as both TbMCA2 and TbMCA3 share almost 100% sequence identity over the remainder of their sequences, we can speculate that they will have very similar, if not identical, substrate

specificity. Furthermore, the tandem positioning of *TbMCA2* and *TbMCA3* on chromosome 6 of *T. brucei* is consistent with a gene duplication event and suggests that these genes might have similar functions. *In T. cruzi, TcMCA3* is present in approximately 16 copies, distributed in at least two clusters of tandemly repeated genes and located on two different-sized chromosomes (Kosec *et al.*, 2006). It was observed that the intergenic region of the *TcMCA3* tandem copies was composed of the 3'-end of the cysteinyl-tRNA synthetase gene and a truncated retrotransposon-like element. Upstream of at least one the tandem repeats, a complete cysteinyl-tRNA synthetase gene is present. Therefore it is likely that the increased copy number of *TcMCA3* results from the activity of transposable elements. Indeed, despite over hundreds of millions of years of independent evolution, *T. cruzi*, *T. brucei* and *L. major* exhibit a high level of gene synteny and the very few sites of genome rearrangement are all marked by the presence of retroposon-like sequences (Ghedin *et al.*, 2004). In accordance to this, the closely related *TbMCA2* and *TbMCA3* genes are located, like their *T. cruzi* homologue *TcMCA3*, downstream of the cysteinyl-tRNA synthetase gene (in the chromosome 6 of *T. brucei*) (www.genedb.org). Henceforth, gene synteny between *T. cruzi* and *T. brucei* was probably disrupted by, on *T. cruzi* side, extensive retrotransposon activity and, on *T. brucei* side, duplication of the original *MCA3* gene to give rise to *TbMCA2*. The reason why these two parasites would replicate a metacaspase that is absent from *L. major* remains obscure. As *L. major* does not possess a similar metacaspase, we can postulate that this function might be *Trypanosoma*-specific.

4.4. Metacaspases interactions

Mammalian caspases have protein interaction modules within their prodomains. Caspases with large prodomains are thought to be involved in the initiation of the apoptotic response (hence they are termed initiator caspases) while those with short prodomains are apparently activated by the initiator caspases and thus are termed effector caspases. Within these prodomains, related motifs have been identified. The death effector domain (DED)(Chinnaiyan et al., 1995) is found in caspases 8 and 10 and appears to be involved in interactions with DEDs of signaling adapter proteins such as MORT1/FADD (Chinnaiyan et al., 1995; Boldin et al., 1995) and TRADD (Hsu *et al.*, 1995). The CAspase REcruitment Domain (CARD) (Hofmann *et al.*, 1997) is found in caspases 1, 2, 4, and 9 and appears to be important in promoting interactions of these caspases with one another and with a range of other regulatory and adapter proteins. CARD and DED motifs, together with the Death Domain (DD), the recently characterized PYRIN domain (Fairbrother *et al.*, 2001) as well as many others (Aravind *et al.*, 1999), are members of the death domain-fold superfamily and are well established mediators

of protein-protein interactions in many proteins. Interestingly, the plant metacaspases are divided in two groups (termed type I and II) that might be analogous to the mammalian initiator and effector caspases (Vercammen *et al.*, 2004). The *Arabidopsis thaliana* type I metacaspases (AtMCA1, AtMCA2 and AtMCA3) possess N-terminal extensions ranging from approximately 80 to 120 amino acids in length that could represent prodomains similar to those found in mammalian upstream initiator caspases. However, instead of harboring interaction modules of the Death Domain-superfamily, the prodomains of the type I *A. thaliana* metacaspases are rich in proline (AtMCA1 and AtMCA2) or glutamine (AtMCA3) and all contain two putative CxxC-type zinc-finger structures, similar to the lesion-simulating disease-1 protein (LSD1), a negative regulator of the hypersensitive response with homology to GATA-type transcription factors (Dietrich *et al.*, 1997; Uren *et al.*, 2000) **(figure 4.3, light blue and underlined pink letters, respectively)**. While none of the trypanosomatid metacaspases possess any Death Domain-like motifs or zinc-finger structure, it is possible that the proline rich domain present in the C-terminal of LmajMCA, TbMCA5 and TcMCA5 might be involved in protein-protein interactions **(figure 4.3, light blue letters)**.

In yeast, many large-scale two-hybrid screens were undertaken to identify protein-protein interactions between full-length open reading frames predicted from the *Saccharomyces cerevisiae* genome (Uetz et al., 2000; Drees et al., 2001; Ito et al., 2001; Tong et al., 2002; Hazbun et al., 2003; Krogan et al., 2006). Interestingly, many potential partners of yeast metacaspase, ScMCA, were thus discovered. Among others, a physical interaction between ScMCA and Wwm1p (YFL010p), a potential hydrophilin which has been implicated in osmotic stress responses (Garay-Arroyo *et al.*, 2000), was identified. Overexpression of Wwm1p led to phenotypes closely related to the ones observed during TbMCA4 expression, nevertheless these effects were independent of ScMCA (as a Δ*ScMCA* harboured the same phenotype during Wwm1p overexpression). Simultaneous expression of Wwm1p and ScMCA resulted in the suppression of the phenotypes observed with the former alone, even when the ScMCA active site histidine and cysteine residues were mutated. However, a truncated form of ScMCA lacking its proline-rich N-terminus was not able to suppress the Wwm1p overexpression phenotype. It is established that WW domains, characterized by two signature tryptophan residues located 20-23 amino acids apart (Andre and Springael, 1994; Bork and Sudol, 1994), are protein-protein interaction modules that bind to short proline-rich motifs (termed WW binding domains), in proteins, in a variety of signalling pathways (Sudol and Hunter, 2000). Wwm1p possess one such WW domain. Consequently, the suppression of the Wwm1p overexpression phenotype by ScMCA overexpression could be explained by a titration of these two proteins mediated by their WW domain and proline-rich region, respectively. The physiological significance of this interaction remains uncharacterised.

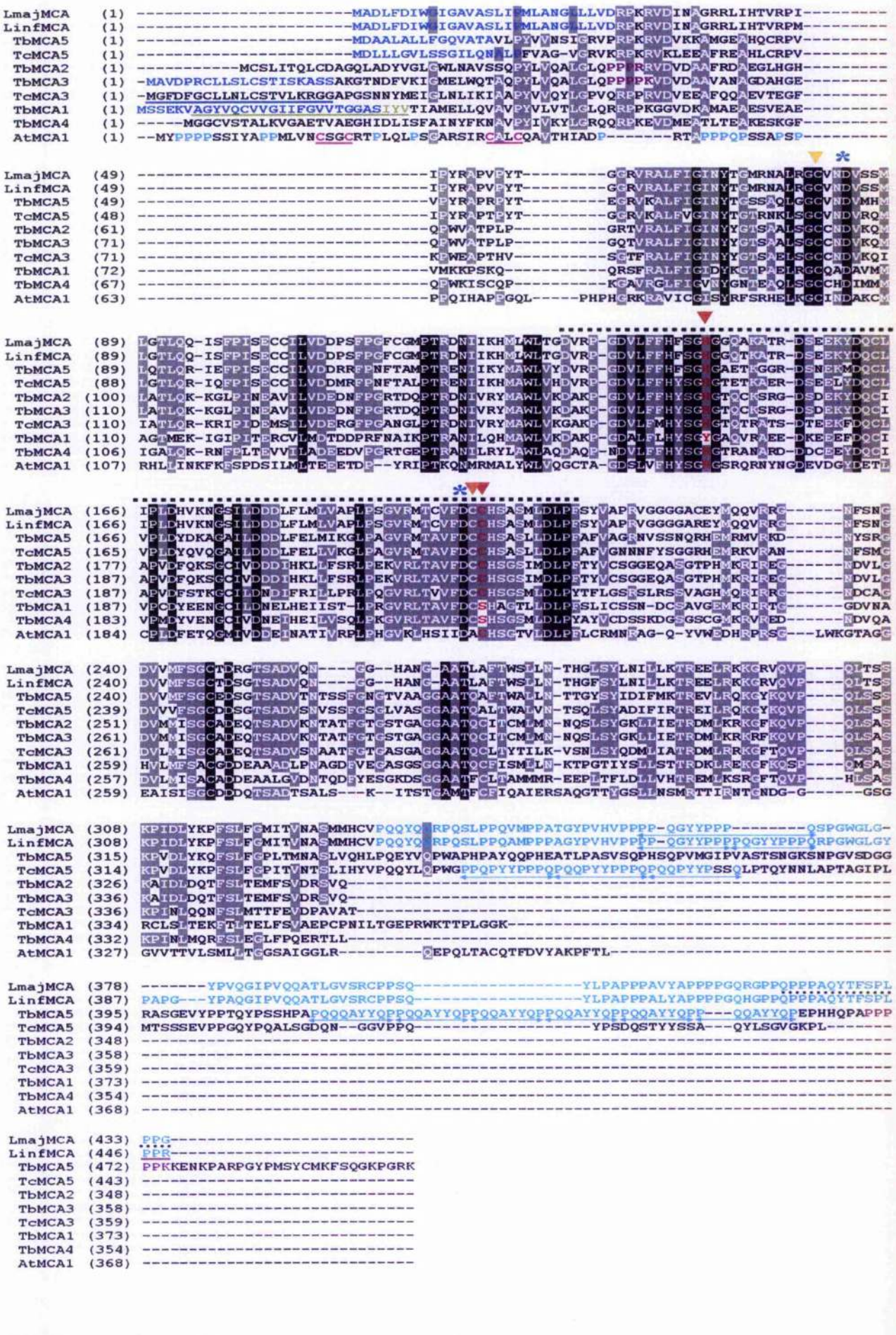
LmajMCA
LinfMCA
TbMCA5
TcMCA5
TbMCA2
TbMCA3
TcMCA3
TbMCA1
TbMCA4
AtMCA1

Figure 4.3: Sequence alignment of selected metacaspases

Identical and conserved amino acids are shown on a black or grey background, respectively. Sequences were aligned using the Clustal W algorithm of the Align X program (Vector NTI Advance 10 package, http://www.informaxinc.com/). Signal peptides predicted by SignalP 2.0 HMM are in dark blue (predicted cleavage site between residue 28 and 29 for LmajMCA, 26 and 27 for TbMCA1, 20 and 21 for TbMCA3, 15 and 16 for TbMCA5, 18 and 19 for TcMCA5). A signal peptide is predicted for TcMCA3 but with a low level of probability (blue line, cleavage between residues 20 and 21). A probable transmembrane helix was predicted for TbMCA1 by TMHMM2.0 at amino acids 7-29 (green letters and green line). The zinc finger domains of AtMCA1 are shown in pink. Proline-rich domains are in light blue and repetitive motifs are underlined by double headed arrows. The predicted Class III WW binding domain of TbMCA5 is shown in purple; a potential similar domain is underlined in purple in LinfMCA. The active site histidine and cysteine residues are shown in red and are marked with red arrow heads. Putative alternative active site cysteines are indicated by orange and yellow arrow heads. The blue asterisks indicate the aspartate residue involved in substrate P1 coordination. The 80-mer peptide used to generate anti-TbMCA2/3 antibodies is lined by a discontinuous black line. The 15-mer peptide used for the generation of the LmajMCA antibodies is lined by a dotted black line.

Interestingly, possible Class III WW binding domain motifs were identified within the *T. brucei* metacaspases. Class III WW binding domains are characterised by motifs of at least two proline residues flanked by arginine or lysine residues (Macias *et al.*, 2002). Such motifs were identified in the N-terminal regions of TbMCA1, TbMCA2 and TbMCA3 and the C-terminal extension of TbMCA5 **(figure 4.3, purple letters)** and potentially of LinfMCA **(figure 4.3, purple line)**. Meanwhile, LmajMCA and TbMCA4 do not seem to possess identifiable WW binding domains. However, ScMCA does not possess any classifiable WW binding domains but nevertheless interacts with Wwm1p through its proline-rich N-terminus (Szallies *et al.*, 2002). Indeed, while the amino acid composition of the WW binding domains could differ considerably from one protein to the other, there are also many other modules that can bind proline-rich ligands and mediate protein-protein interactions (Kay *et al.*, 2000).

In an attempt to characterise any potential metacaspase partners, searches of proteins harbouring WW motif(s) were performed (using Pfam search, www.genedb.org). Within *T. brucei*, eight proteins are predicted to possess WW domains. Most of them possess *L. major* orthologues. Three of these are hypothetical proteins (Tb11.01.3520 - LmjF17.2390, Tb927.1.3560 - LmjF12.0510 and Tb927.4.158 - LmjF34.3140), while two are putative myosin heavy chain proteins (Tb927.4.3380 and Tb927.5.2440 - LmjF17.1140), one possesses similarities to the yeast ubiquitin-ligase Rsp5p (Tb927.8.5290 - LmjF161140) and the last two are the zinc finger protein 2 (ZFP2, Tb11.01.6590 - LmjF32.1740) and a putative isoform (Tb927.3.720 - LmjF27.01). While most of the functions of these proteins remain obscure, TbZFP2 is, in *T. brucei*, among

the very few published examples of protein with a WW domain (Hendriks et al., 2001). In addition to its CCCH zinc finger, and it WW domain, TbZFP2 possess an E3 ubiquitin ligase domain in its N-terminal region. While protein(s) interacting with TbZFP2 remain(s) to be characterised, this protein belonging to the CCCH zinc finger family plays a major role in the *T. brucei* bloodstream to procyclic forms differentiation process by principally mediating extension of the posterior end-cytoskeletal microtubules (Hendriks et al., 2001). Type I plant metacaspases have proline-rich proregions with zinc finger domains (Uren *et al.*, 2000). The paracaspase possess a proregion mediating protein-protein interactions through a Death Domain (DD) but surprisingly harbour a functional E3 ubiquitin ligase domain in its C-terminus (Uren *et al.*, 2000). It is thus tempting to postulate that trypanosomatid metacaspases, and notably the WW binding domain harbouring-TbMCA5 might interact with this TbZFP2 to acquire, as a complex, the biological functions that other members of their protein family or clan would later obtain during evolution (Koonin and Aravind, 2002).

Many datasets for protein-protein interactions have now been produced in various organisms. Two of them, BioGRID (Stark *et al.*, 2006) (http://www.thebiogrid.org) and DIP (Xenarios *et al.*, 2000) (http://dip.doe-mbi.ucla.edu), were browsed to observe the experimentally characterised protein-protein interactions with the yeast metacaspase YOR197w (ScMCA). A compilation of the proteins found to associate with ScMCA is shown in **table 4.2**. Potential partners for the metacaspase are proteins involved in signal transduction (kinases), control of transcription, intracellular transport, and regulation of the actin cytoskeleton. It is thus tempting to postulate that the trypanosomatid metacaspases might be involved in similar networks. However, Blast searches revealed that most of the ScMCA partners identified are absent from the *T. brucei*, *L. major* and *T. cruzi* genomes (**table 4.2**). Furthermore, it was observed that different screens gave different interactions, thus lowering the probability that these are real interactions. In trypanosomatids, methods such as immunoprecipitation or affinity-purification, together with immuno-colocalisation, might help identify interacting partners and further aid in the understanding of metacaspase functions.

Name	Aliases	Description	Evi-dences	Reference	Tryps
TFB1	*YDR311W*	Subunit of TFIIH and nucleotide excision repair factor 3 complexes, required for nucleotide excision repair, target for transcriptional activators.	Two-hydrib	(Ito *et al.*, 2001)	NO
SRB4	*MED17 YER022W*	Subunit of the RNA polymerase II mediator complex; associates with core polymerase subunits to form the RNA polymerase II holoenzyme; essential for transcriptional regulation.			NO
KRE11	*TRS65 YGR166W*	Protein involved in biosynthesis of cell wall beta-glucans; subunit of the TRAPP (transport protein particle) complex, which is involved in the late steps of endoplasmic reticulum to Golgi transport.			NO
YAK1	*YJL141C*	Serine-threonine protein kinase that is part of a glucose-sensing system involved in growth control in response to glucose availability; translocates from the cytoplasm to the nucleus and phosphorylates Pop2p in response to a glucose signal.			YES?
JSN1	*PUF1 YJR091C*	Member of the Puf family of RNA-binding proteins, interacts with mRNAs encoding membrane-associated proteins; overexpression suppresses a tub2-150 mutation and causes increased sensitivity to benomyl in wild-type cells.			YES
SRO77	*SNI2 SOP2 YBL106C*	Protein with roles in exocytosis and cation homeostasis; functions in docking and fusion of post-Golgi vesicles with plasma membrane; homolog of Sro7p and *Drosophila* lethal giant larvae tumor suppressor; interacts with SNARE protein Sec9p.		(Drees *et al.*, 2001)	NO
SDC25	*YLL017W*	Ras protein signal transduction		(Tong *et al.*, 2002)	NO
PIN3	*LSB2 YPR154W*	Protein that induces appearance of [PIN+] prion when overproduced. Actin cytoskeleton organization and biogenesis.			YES?
ARC1	*YGL105W*	Protein that binds tRNA and methionyl- and glutamyl-tRNA synthetases (Mes1p and Gus1p), delivering tRNA to them, stimulating catalysis, and ensuring their localization to the cytoplasm; also binds quadruplex nucleic acids.	Affinity capture -MS	(Krogan *et al.*, 2006)	YES

Table 4.2: ScMCA potential protein partners and interacting pathways as predicted by various protein-protein interaction datasets

Data obtained from BioGRID (http://www.thebiogrid.org) and DIP (http://dip.doe-mbi.ucla.edu), while browsing for the yeast metacaspase ScMCA (YOR197w). Only first-order interactions are represented here. Blast searches were performed using GeneDB (www.genedb.org).

4.5. Predictions of structure, processing and post-translational modifications

Secondary structure predictions of the trypanosomatid metacaspases were performed with the PSIPRED software (McGuffin *et al.*, 2000) (http://bioinf.cs.ucl.ac.uk/psipred/psiform.html) and schematic representations of the results are shown in **figure 4.4.** While sharing little sequence identity at the primary amino acid level, similar secondary folds identified metacaspases as distant cousins of clan CD caspases (Uren *et al.*, 2000). Using the predicted secondary structure of LmajMCA to screen a database of proteins with experimentally characterised secondary fold (mGenTHREADER, http://bioinf.cs.ucl.ac.uk/psipred/ psiform.html), the best matches obtained were, as expected, caspases and, more precisely, caspase-3 (PDB ID: 1pauA0, score: 0.858, E value: 2e-04) and caspase-1 (PDB ID: 1bmqA0, score: 0.850, E value 3e-04). The secondary structure of the human caspase-3 is shown, as an example, in **figure 4.4,** to illustrate the similarities with the trypanosomatid metacaspases. At first glance, it can be noted that, due to their proline-, glutamine- and tyrosine-rich C-terminal domains (**figure 4.4, blue boxes**), TbMCA5, LmajMCA5 and TcMCA5 are bigger than caspase-3. While the C-terminal extensions of LmajMCA and TbMCA5 do not possess any α-helix or β-strand and are predicted to be coil regions, TcMCA5 C-terminus harbours two α-helixes and one β-strand. TbMCA4, which does not possess such C-terminal extension, has a size closer to caspase-3. Also, the trypanosomatid metacaspases all possess additional α-helixes in their N-terminus compared to the caspase-3 (**figure 4.4, green cylinders**). LmajMCA5, TbMCA5 and TcMCA5 are predicted to possess a signal peptide cleavage site after these structures (**figure 4.4, end of blue double arrows**). TbMCA3, which possesses a 10 amino acids extension in its N-terminus compared to TbMCA2, harbours an additional α-helix and is predicted to possess a signal peptide cleavage site, while TbMCA2 does not. TbMCA4, which possesses 3 β-strands upstream of its short first α-helix, is not predicted to possess such signal. Consequently, it is possible that the N-terminal α-helixes of the metacaspases might be involved in the targeting of these metacaspases to a specific compartment.

Nevertheless, as it is known that many cysteine peptidases are activated by cleavage of an N-terminal domain, it is also possible that this domain might act as a prodomain. Cysteine peptidases of the papain family (clan CA) undergo cleavage of N-terminal peptides of various lengths, which act as potent inhibitors of the full length enzyme, in order to enhance their enzymatic activity (Fox *et al.*, 1992). Caspase maturation also involves proteolytic removal of a prodomain together with cleavage into

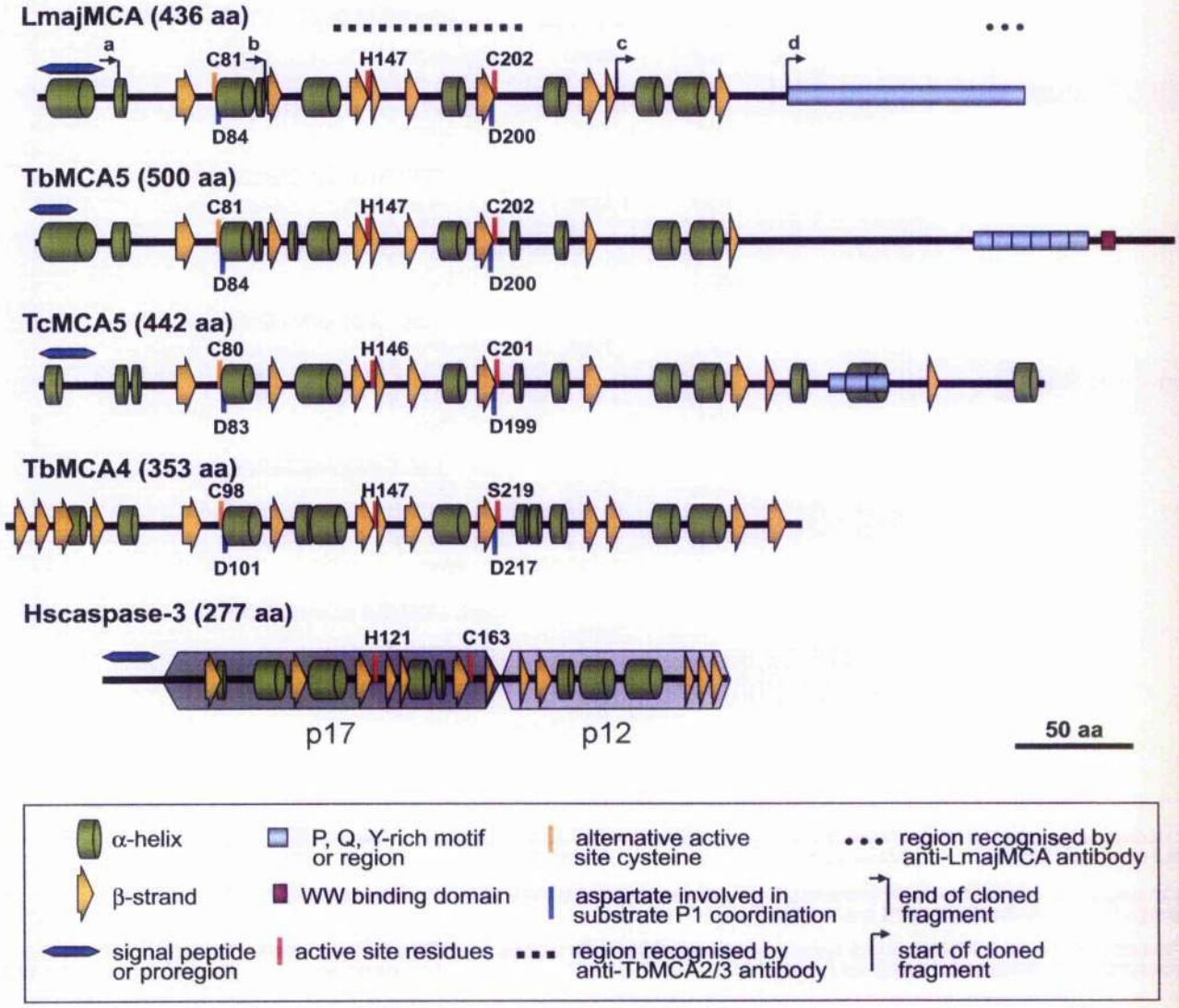

Figure 4.4: Comparison of the predicted secondary structures of some trypanosomatid metacaspases and the human caspase-3.

The schematics are based on the secondary structures predictions made with the PSIPRED software (McGuffin et al., 2000) (http://bioinf.cs.ucl.ac.uk/psipred /psiform .html). Amino acids (aa) of interest are labelled. Start or end of fragment used for the expression of Nterm-GFP (a), eNterm-GFP (b), GFP-eCterm (c) or Cterm-GFP (d) are indicated (refer to **chapters 2 and 6**).

two subunits; these subunits subsequently dimerise to form the active enzyme (Rotonda et al., 1996). The procaspase-3 is first cleaved at D175-S176 to remove the covalent connection between the large (17 kDa) and small (12 kDa) subunits (Nicholson et al., 1995) (**figure 4.4, p17 and p12**). The prodomain (**figure 4.4, blue double arrow**) is then removed after cleavage at D9-S10 and then at D28-S29 (Fernandes-Alnemri *et al.*, 1994). Therefore, all cleavages involved in caspase maturation occur on the carboxyl side of aspartate residues. So far, the only characterised eukaryotic peptidases with this

specificity are the caspases themselves and the cytotoxic T lymphocyte serine peptidase granzyme B (Earnshaw *et al.*, 1999). Also, activation of the caspases can occur either by auto-catalytic processing or by cleavage by an aspartate specific-peptidase.

Apart from in their N- and C-terminal regions, the secondary structures of the metacaspases are strikingly close to caspase-3. The active site region is particularly well conserved, with β-strand structures in close proximity of the histidine and cysteine (or serine for TbMCA4) residues (**figure 4.4, red bars**). The sequence context of the catalytic histidine residue in trypanosomatid metacaspases is H(Y/F)SGHG, suggesting an intermediate stabilizing role for the adjacent glycine, as in mammalian caspases (Earnshaw *et al.*, 1999). In caspases, the catalytic cysteine is contained in a QAC(R/Q)G context, with the glutamine residue shown to coordinate the substrate P1 aspartate. Interestingly, the trypanosomatid metacaspases have a DCCHSG signature, suggesting that this role is now played by an aspartate (D200 with LmajMCA numbering). This would imply that metacaspases are specific for a basic P1 amino acid such as arginine or lysine (Szallies *et al.*, 2002). Supporting this hypothesis, several recombinant plant metacaspases were shown to harbor such substrate specificity (Vercammen *et al.*, 2004; Watanabe and Lam, 2005) and lack caspase-like activity. It was postulated that D200 and D84 might together specify the substrate P1 scissile bond amino acid (for which Clan CD members appear to be highly specific) (**figure 4.4, blue bars**).

Interestingly, the 3D structure reconstruction of LmajMCA and TbMCA4 structure based on the tertiary structure of caspase-3, revealed that, while distant in the primary sequence, these two aspartate residues (D217 and D101 in TbMCA4) are in close association with the active site histidine and cysteine residues and contribute to the formation of the substrate pocket (the predicted 3D structure of LmajMCA is shown in **figure 4.5B**). As discussed previously, the substrate pocket seems also to be lined with another cysteine (C81 and C84 for LmajMCA and TbMCA4, respectively), which might participate in the catalytic activity.

By analogy to caspases, but consistent with their arginine/lysine specificity, production of the type II *A. thaliana* metacaspase 9 in *E. coli* resulted in autoprocessing of the proform, after an arginine residue (ITSR/ALPFKAV), into large and small subunits (Vercammen *et al.*, 2004). An additional lysine-specific processing was also observed to occur in the N-terminus of AtMCA9, leading in the removal of an 8 kDa peptide (LYKK/AGSTM). Thus, the type II metacaspases, like the executioner caspases in animals, appear strongly dependent on (auto)processing in order to be active. Also these observations raise the possibility that the trypanosomatid metacaspases might indeed be matured, having an argine/lysine-specific processing instead of the caspase aspartate-specific cleavage. Nevertheless, it has to be noted that, with their proline-rich domains, LmajMCA, TbMCA5 and TcMCA5 are more closely related to the type I

than the type II plant metacaspases. Indeed, the type I *A. thaliana* metacaspases possess large proline-rich N-terminal extensions that could represent prodomains analogous to those of the mammalian upstream initiator caspases. Also, bacterial overproduction of type I metacaspases failed to identified any processing pattern (Vercammen *et al.*, 2004), suggesting that, like for the mammalian initiator caspases, they might need oligomerization to be activated.

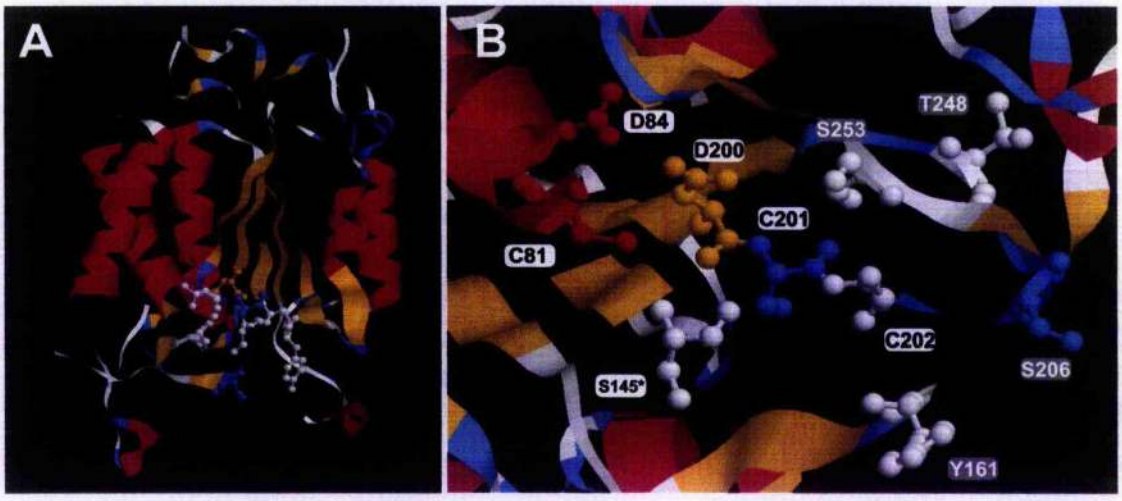

Sequence used for 3D reconstruction

```
1   MADLFDIWGI GAVASLIPML ANGLLLVDRP KRVDINAGRR LIHTVRPIIP YRAPVPYTGG
61  RVRALFIGIN YTGMRNALRG CVNDVSSMLG TLQQISFPIS ECCILVDDPS FPGFCGMPTR
121 DNIIKHMLWL TGDVRPGDVL FFHFSGHGGQ AKATRDSEEK YDQCLIPLDH VKNGSILDDD
181 LFLMLVAPLP SGVRMTCVFD CCHSASMLDL PFSYVAPRVG GGGACEYMQQ VRRGNFSNGD
241 VVMFSGCTDR GTSADVQNGG HANGAATLAF TWSLLNTHGL SYLNILLKTR EELRKKGRVQ
301 VPQLTSSKPI DLYKPFSLFG MITVNASMMH CVPQQYQQRP QSLPPQVMPP ATGYPVHVPP
361 PPQGYYPPPQ SPGWGLGYPV QGIPVQQATL GVSRCPPSQY LPAPPPAVYA PPPPGQRGPP
421 QPPPAQYTFS PLPPG
```

M: residue not aligning on cli4oa sequence
C: residue of the active site pocket
Y: residue potentially phosphorylated
S: residue potentially phosphorylated and glycosylated

Figure 4.5: Three dimensional structure prediction of LmajMCA based on caspase-3 tertiary fold.

Fold recognitions were obtained from the 3D-PSSM Web server V.2.6.0 (http://www.sbg.bio.ic.ac.uk/~3dpssm/index2.html). Snapshots of the proteins viewed in RasMol V2.6 are represented here. The different colours identify the various structural features (α-helix in pink, β-sheet in yellow and coiled domain in blue). Amino acids of the active site pocket are represented. The predicted 3D structure of LmajMCA (panel A) as well as a zoom on its active site region (panel B) are shown. Below, the sequence used for the 3D prediction is shown in bold within the full LmajMCA sequence. A colour code was applied to important residues as detailed in the legend (please note that this code does not apply to the Snapshots).

Another structural feature that might contribute to the differences in substrate specificity of the metacaspases is the predicted presence, in the tertiary fold, of a flaplike loop that projects over the active site (**figure 4.5A**). A similar flap is found in the caspase-3 and might explain their inability to cleave certain substrates even thought consensus cleavage sites are present (Rotonda et al., 1996; Mittl et al., 1997). Indeed, because of steric hindrance by the flap, certain potential substrates might fail to dock in the catalytic site. This flap is, in caspase-3, also a potential site for post-translational modifications, for example phosphorylation (Martins *et al.*, 1998), which could conceivably cause it to open or close further thereby providing a potential regulatory mechanism. LmajMCA is predicted to possess several potential serine, threonine and tyrosine phosphorylation sites (NetPhos 2.0, http://www.cbs.dtu.dk/services/NetPhos/), some of which being in close proximity of the active site pocket (Y161, S206, S253, T248, **figure 4.5B**). However, many glycosylation sites are also predicted and a few of them, present at potentially phosphorylatable serine or threonine residues, might actually prevent phosphorylation from occurring at these sites (YinOYang 1.2, http://www.cbs.dtu.dk/services /YinOYang/) and thus regulate the phosphorylation state of the metacaspase.

4.6. Discussion

The *in silico* analyses of the structural and biochemical properties of the trypanosomatid metacaspases reveals that although these proteins have a tertiary fold comparable to thoses of caspases, they are predicted to prefer susbtrates with, at their P1 positions, basic (such as arginine or lysine) rather than the acid residues (such as aspartate) favoured by caspases. Nevertheless, because of the presence of protein-protein interaction modules in some of the metacaspases (with the WW binding domains or the proline-, glutamine- and tyrosine rich-regions), it seems likely that the metacaspases might, as in the case for caspases, be involved in a cascade of events regulating a yet uncharacterised pathway. Whether these interactions are necessary for the regulation of the enzymatic activities of the metacaspases or of their bound partners remains to be determined. On the other hand, the role of these protein-protein interactions might be independent of any enzymatic activities. Indeed, the metacaspases might simply associate with other proteins to get trafficked throughout the cell. This idea is strengthened by the observation that some of the trypanosomatid metacaspases possess in their N-termini a predicted signal peptide, potentially targetting the protein to a special cellular compartment. One can thus assume that the metacaspases might play several roles in the cell, depending on their location and activation state. Metacaspases with differences in their active site dyad residues,

although likely enzymatically inactive, might nevertheless play important roles in the cell by, for example, binding natural inhibitors or substrates for the functional metacaspases and thus indirectly modulating the activity of these latter enzymes. The regulation of metacaspase activity might also be mediated by proteolytic processing, either performed autocatalytically or by upstream peptidases and by the addition of post-translational modifications. In the present study, I attempted to produce experimental evidence that the metacaspases possess indeed such properties.

Chapter 5:

Characterisation of *Leishmania major* metacaspase

5.1. Analysis of MCA expression in *L. major*

5.1.1. Antibodies

To elucidate the cellular function(s) of the metacaspase, its level of expression was assessed in the two life stages of *L. major* and at different time points of promastigote *in vitro* growth. In order to do so, antibodies were raised against a peptide covering the last 15 C-terminal amino acids of MCA. After affinity purification over the designed peptide, the rabbit antibody was used for Western blot analyses. In the first place, the experiment was performed on total protein lysates of wild type *L. major* promastigotes. The analysis allowed the detection of a protein with a molecular mass of about 50 kDa. This protein size was slightly higher than the one expected for MCA (~47 kDa) (**figure 5.1A, left panel**). Furthermore, at least two additional proteins, of about 40 and 30 kDa, were visualised, showing that detected protein might either be processed or degraded within the cells. To evaluate its specificity, the anti-MCA antibody was absorbed against the MCA peptide prior to Western blot analysis. The presence of the peptide was able to completely block the detection of the 50 kDa protein (**figure 5.1A, middle panel**). In addition, the anti-MCA antibody was tested with success on purified recombinant MCA and showed a protein profile similar to that observed in *Leishmania* (**figure 5.1A, right panel**).

However, the low sensitivity of this antibody impeded its use for further analyses. Therefore, antibodies raised against the full length TbMCA5 or the active site region of TbMCA2 and TbMCA3 were assessed. Intriguingly, even thought LmajMCA is more closely related to TbMCA5 than TbMCA2 and TbMCA3, only the antibody recognising these later two proteins was able to detect LmajMCA in promastigote cell extracts. The anti-TbMCA2/3 antibody was obtained by immunisation of rabbit with an 80-mer peptide encompassing the catalytic site histidine and cysteine residues (from D144 to T224, with TbMCA2 numbering), a region that is identical at 60.5% in LmajMCA (refer to **chapter 4, figures 4.3 and 4.5**). This antibody detected in promastigote cell extracts a protein of ~ 50 kDa (**figure 5.1B, left panel**). Nevertheless, several additional proteins were also detected, of about 38-40 kDa and 30 kDa. These proteins possess molecular masses comparable to the ones detected with the anti-LmajMCA antibody. The specificity of the anti-TbMCA2/3 antibody for LmajMCA was confirmed by its ability to detect purified recombinant LmajMCA and several variants of LmajMCA expressed exogenously in *L. major* promastigotes (refer to **chapter 6**). Interestingly, the anti-TbMCA2/3 antibody was able to detect LmajMCA in lysates of $1x10^7$ promastigotes, at a 1:10,000 dilution, thus showing a much greater sensitivity than the anti-LmajMCA

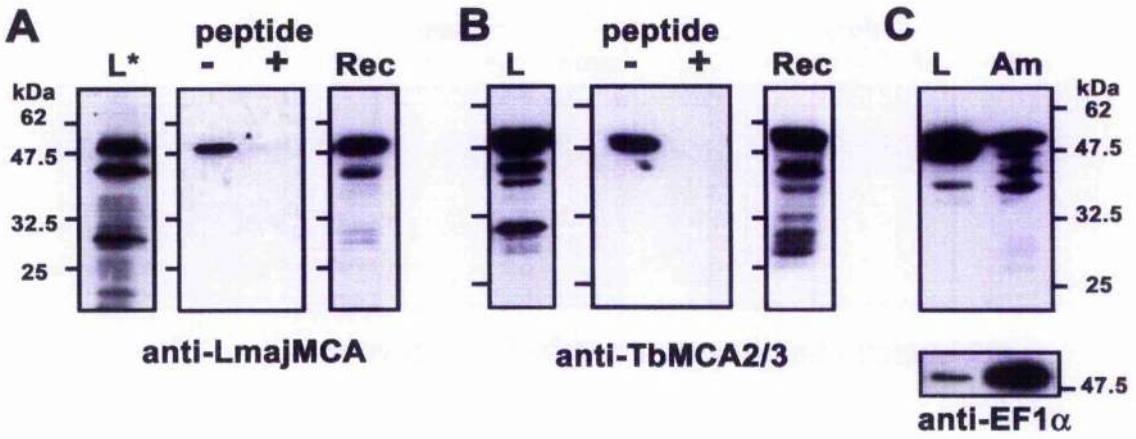

Figure 5.1: Antibodies specificity and expression profile of MCA

Western blot analyses performed on lysates of *Leishmania* promastigotes (L, L*) or amastigotes (Am) or on purified recombinant MCA-His (Rec).). Cells were lysed with 2% SDS in the presence of a mix of anti-peptidases.Total lysates were loaded on a 12% acrylamide gel and separated by SDS-PAGE. The gels were then transferred to PVDF membranes and hybridised with rabbit anti-LmajMCA antibodies (A), anti-TbMCA2/3 antibodies (B,C) or mouse anti-EF1α (C) at a 1:50, 1:10,000, and 1:20,000 dilutions, respectively. Revelation was performed using HRP-conjugated anti-rabbit or anti-mouse antibodies (Promega), at 1:5,000 dilutions, and the West Signal chemoluminescence detection system (Pierce). A,B) Peptide competition experiments carried out on promastigote extract (L). Anti-LmajMCA and anti-TbMCA2/3 were absorbed (+) or not (-) against 3 μg of the relevant peptide. L and L* promastigote extracts were done when cells were at a density of $1.5x10^7$ cells ml^{-1}.The equivalent to $1x10^7$ cells were loaded per lane except for L* where $1x10^8$ cells were used. Molecular weight markers are shown on the sides.

antibody. Consequently, the anti-TbMCA2/3 antibody was subsequently used for further analysis of LmajMCA expression level.

5.1.2. In the two life stages

The Western blot analysis previously performed on promastigote cells was repeated with *L. major* amastigotes extracted from mice lesions (**figure 5.1C**). In both stages of the parasite, the anti-TbMCA2/3 antibody was able to detect a major protein of ~ 50 kDa, thus suggesting that MCA was constitutively expressed. However, caution has to be exercised in the interpretation of the data collected on the amastigote cells. Indeed, while the amount of total protein from the promastigote and amastigote extracts was equalized by BCA quantification before loading on the SDS-PAGE gel, the subsequent Western blot analysis revealed that the protein used as a loading control, the elongation factor 1α (EF1α), was most abundant in the amastigote lysate. It is known that EF1α is expressed at equal level in both life stages of the parasite. Although

it should be possible to detect a size difference between the *Leishmania* and the macrophage EF1α (Nandan et al., 2003), the possibility that the amastigote preparation was contaminated with host EF1α could not be excluded. In that case, the protein detected with the anti-TbMCA2/3 antibody might be a cross-reacting protein from the mice macrophages. To exclude this hypothesis, an extract of non infected macrophages should have been probed, by Western blot, as a negative control.

5.1.3. During promastigote growth

Western blot analyses were performed on promastigotes at various stages during their *in vitro* growth (**figure 5.2**). Promastigote extracts were made when cells were at early (E) or late (L) time points of their logarithmic (L) or stationary (S) phases of growth (**figure 5.2A**). It was observed that a higher amount of MCA was detected in the early logarithmic phase of promastigote growth (**figure 5.2B, EL**) than in any of the subsequent phases (**figure 5.2B, LL, ES, LS**). Additional Western blot analyses performed on *L. major* metacyclic promastigotes, which were purified from a late stationary phase culture with peanut agglutinin (Da Silva and Sacks, 1987), revealed that the amount of MCA detectable in these cells was comparable to the one detected in late stationary phase promastigotes (data not shown). This decrease in the abundance of MCA within the cells could be the result of either a variation in the level of expression of the MCA during cell growth or a modification in the speed of its protein turn over.

In *Leishmania*, an approach combining proteomics and transcriptomics recently pointed out that there was little correlation between the messenger RNA expression and the level of protein detected in the promastigote cell (McNicoll et al., 2006). Consistent with this observation, expression profiling experiments using shotgun DNA libraries established that only about one percent of the analysed RNAs harboured two fold or greater expression changes and were differentially transcribed (Akopyants *et al.*, 2004). Therefore, in *Leishmania*, modification in the level of expression of a gene occurs mainly at the post-transcriptional, translational and post-translational levels (Clayton, 2002; Ivens et al., 2005; McNicoll et al., 2006). Stabilisation and /or activation of protein products involve modification by phosphorylation, glycosylation, lipidation, GPI-anchor addition, acylation or prenylation ... (Ivens et al., 2005). On the other hand, protein degradation is mediated, in *Leishmania*, by proteasomes (Robertson, 1999), eubacterial HslVU complexes (Couvreur *et al.*, 2002) and a specialised organelle termed the multivesicular tubule (MVT) /lysosome.

Interestingly, this lytic compartment undergoes major morphological and biochemical modifications during the promastigote growth and is particularly developed

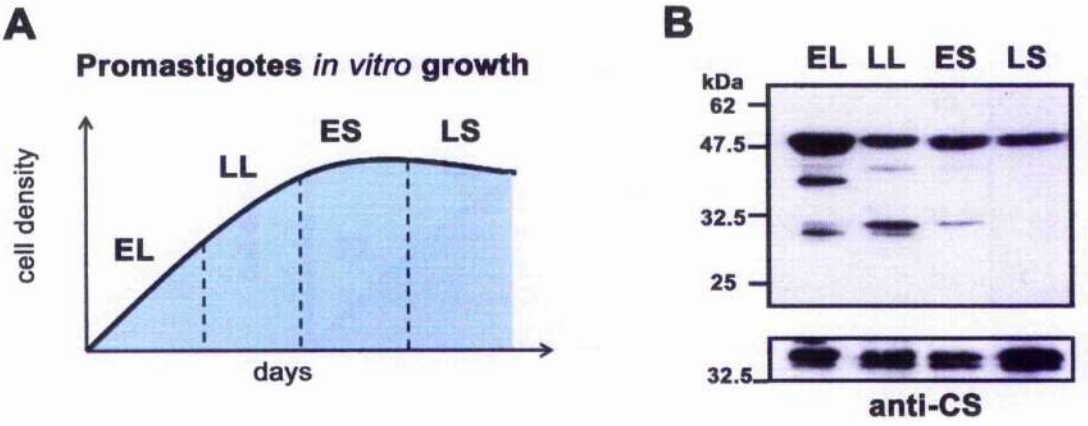

Figure 5.2: Analysis of MCA expression during promastigote *in vitro* growth

A) Schematic of the different phases of the promastigotes growth is shown. After a phase of exponential growth (dividing here in early and late logarithmic phases (EL,LL)), the cells enter a early stationary phase (ES) during which the cells progressively stop dividing, leading ultimately to a decline in the cell number as cells begin to die (late stationary, LS).

B) Promastigote extracts were made from cells at these various stages of growth (EL, $5x10^6$ cells ml^{-1}; LL, $1.8x10^7$ cells ml^{-1}; ES, $2.2x10^7$ cells ml^{-1}; LS, $2x10^7$ cells ml^{-1}). The amount of total protein loaded per lane was equalised after BCA quantification. Western blot analysis was performed using rabbit anti-TbMCA2/3 antibody and rabbit anti-cysteine synthase (CS) antibody (Williams, R.A., unpublished data) as a loading control.

and active in late stationary phase (Mullin *et al.*, 2001). Also, it can be assumed that proteins involved in cell growth and division and particularly essential for the early stages of the promastigote development will be unnecessary to the non-replicative metacyclic promastigotes and therefore actively degraded. While it remains unclear whether the various protein bands detected in promastigote extracts with the anti-TbMCA2/3 antibody are the results of MCA maturation or degradation, the concomitancy of the decrease, within the cell, of the MCA level and the progressive promastigote differentiation into non-dividing form pinpoints a possible involvement of MCA in cell replication. Interestingly, proteomics approaches recently revealed that the yeast metacaspase was probably ubiquinated and subsequently targeted for the proteasomal degradation (Peng *et al.*, 2003). Knowing the essential involvement of the proteasome in cell cycle control, this observation strengthens a potential role of the metacaspase in cell division (Robertson, 1999; Nakayama and Nakayama, 2006).

Leishmania development is non synchronous. At a given time point, cells at different phases of their division cycle can be observed within the same population. Nevertheless, cell cycle progression can be arrested by treatment with drugs such as hydroxyurea (Soto *et al.*, 2004) or flavopiridol (Hassan et al., 2001). While hydroxyurea

(HU) prevents DNA synthesis and blocks cell cycle progression at the boundary between the G1 and S phases, flavopiridol inhibits the mitotic kinase CRK3 and arrests the cells at the G2/M transition. However, the action of these two compounds is reversible and removal from the *Leishmania* culture medium results in a semi-synchronous release from the induced cell cycle block. Thus, with their ability to block and release cell cycle progression, HU or flavopiridol treatments enable the enrichment, within the population, of cells at a precise cell cycle phase. This method was used to analyse the potential variations in the amount of MCA present within the cell at precise time points of its division cycle.

Successful synchronisation of *L. major* promastigotes, as assessed by DNA content analyses performed by FACS, was achieved by treatment with either 5 mM HU (**figure 5.3A, second FACS panel**) or 2.5 μM flavopiridol for 12 hours. However, the synchronisation was only partial and even though cells in G1 or G2 phase were enriched, the rest of the population was composed of cells at various stages of their division cycle (**figure 5.3A, second FACS panel**, 46.4% cells in G1 phase, 15.6% in S phase and 17.9% in G2/M phase). The respective G1/S and G2/M blocks could be released after two successive washes of the cells and complete drug withdrawal. In the example of HU treatment shown in **figure 5.3A**, FACS analyses revealed that peaks in the number of cells in S or G2/M phases were reached at 1.5 hours or 4 hours after HU removal, respectively. Sample populations enriched in cells in G1, S and G2/M were thus collected and the cell lysates were analysed by Western blot to determine whether MCA protein level was cell cycle-regulated.

The Western blot membrane was probed with anti-TbMCA2/3 antibody and, in parallel, with anti-β-tubulin antibody as a loading control (**figure 5.3B**). After ECL revelation and relative quantification of the various proteins, it was concluded that there was no detectable variation in the cellular amount of the full length MCA during cell cycle progression. However, the difference in the amount of the ~ 30 kDa MCA product suggests that MCA might be processed, or degraded, at different rates during cell cycle progression. It is tempting to speculate that the regulation of the cellular function of MCA does not mainly involve translational controls but rather post-translational processes modulating its activation state. Nevertheless, biochemical data is needed to strengthen this hypothesis, as the changes in the ~ 30 kDa protein abundance were not consistently observed.

In the absence of a method to assay MCA activity within the cell, the role of the metacaspase was further investigated using immunolocalisation.

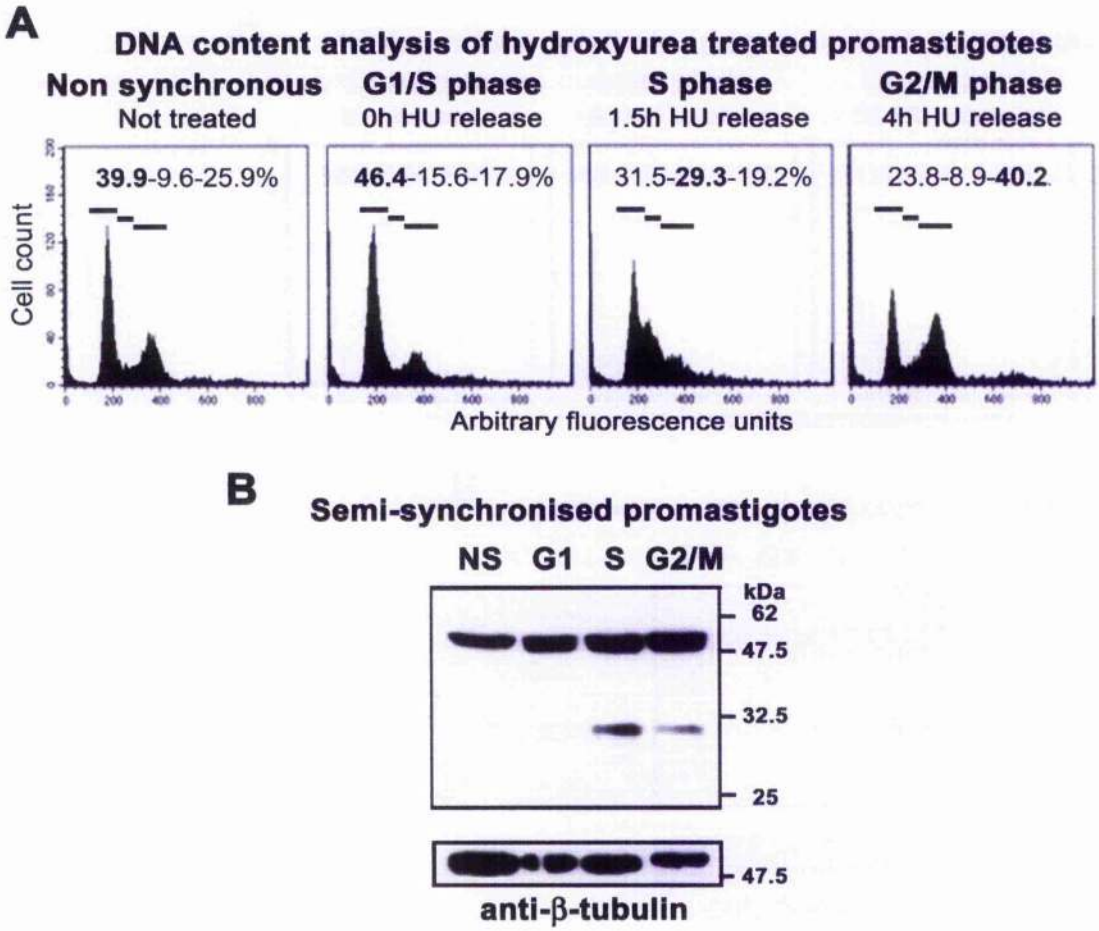

Figure 5.3: Analysis of MCA expression during cell cycle progression

Promastigote cells at $0.5x10^7$ cells ml^{-1} were partially synchronised at the G1/S phase boundary by treatment with 5 mM hydroxyurea (HU) for 12 hours and then released by drug removal.

A) Position within the cell cycle was determined by DNA content analysis using fluorescence activated cell sorting (FACS). The percentage of cells in G1, S and G2/M phase, respectively (numbers inside the FACS data frame) were determined before (not treated), during (0 h HU release) and after HU block (1.5 h and 4 h HU release). For each point, the most enriched cell population is indicated in bold.

B) Wild type population (NS) and HU treated populations enriched in cells in G1 phase, in S phase or G2/M phase were analysed by Western blot using rabbit anti-TbMCA2/3 antibody and mouse anti-β-tubulin antibody (KMX) (Birkett et al., 1985) as loading control (both at a 1:10,000 dilution). The Western blot was then revealed using anti-rabbit or anti-mouse HRP - conjugated secondary antibodies and the SuperSignal West Pico chemoluminescent system (Pierce).The equivalent of 10^7 parasites were loaded per lane. Equal loading was confirmed by BCA quantification (Pierce) and Coomassie staining of the corresponding SDS-PAGE gel. Molecular masses are indicated, in kDa, on the right.

5.2. Cellular localisation of MCA in promastigotes

5.2.1. Attempt to characterise MCA-positive compartment

The specific anti-TbMCA2/3 antibody was used to determine, by immunofluorescence, the subcellular localisation of MCA within the promastigote cells (**figure 5.4**).

The majority of the cells within a non synchronised *Leishmania* culture are found in the G1 phase (**figure 5.3A, first FACS frame**) and possess one nucleus, one kinetoplast, and one flagellum (1N1K1F). In those cells, MCA localised to punctate structures of heterogeneous size covering all of the cell body, with more of the structures in logarithmic phase promastigotes (**figure 5.4Aa**) than in stationary phase promastigotes (**figure 5.4Ab**). MCA-labelled structures did not co-localise with markers for known organelles such as the glycosome (glycosomal phosphofrutokinase (LdPFK,(Lopez *et al.*, 2002)) or the acidocalcisome (vacuolar pyrophophatase (TbVP1, (Lemercier et al., 2002)) (data not shown). Nevertheless, it was observed that the localisation of MCA changed during the cell cycle.

5.2.2. MCA relocates at various stages of the cell cycle

The temporal order of the events leading to division of *Leishmania* promastigote has been characterised and described in **chapter 3**. In summary, it was established that the 1N1K1F cell first enters S phase and duplicates its DNA content (1N*1K*1F). Then the growth of the second flagella starts (1N*1K*2F) and initiate the segregation of the duplicated kinetoplast. The nuclear mitosis then begins ($1N^{*M}1K^{*}2F$) and terminates mainly after completion of kinetoplast segregation ($1N^{*M}2K^{*}2F$, 2N2K2F). Cytokinesis ultimately leads to the separation of the parent and daughter cells.

While in 1N1K1F cells, the MCA signal was distributed throughout the cell, upon the beginning of the segregation of the kinetoplast (as suggested, in 1N*1K*2F cells, by the growth of the second flagellum), MCA was found to be associated with the kinetoplast, suggesting an involvement in segregation of this organelle (**figure 5.4Ac**). In $1N^{*M}1K^{*}2F$ cells MCA relocated to the nucleus (**figure 5.4Ad, e**). Immuno-colocalisation with anti-β-tubulin antibodies (**figure 5.4B**) revealed that MCA was associated with the mitotic spindle within the nucleus (Ersfeld and Gull, 1997; Ogbadoyi *et al.*, 2000). These studies also revealed that separation of the duplicated nuclei starts before and ends after kinetoplast segregation, as DAPI staining, coupled to anti-β-tubulin staining of the mitotic spindle, showed the presence of one (**figure 5.4Ba**) and

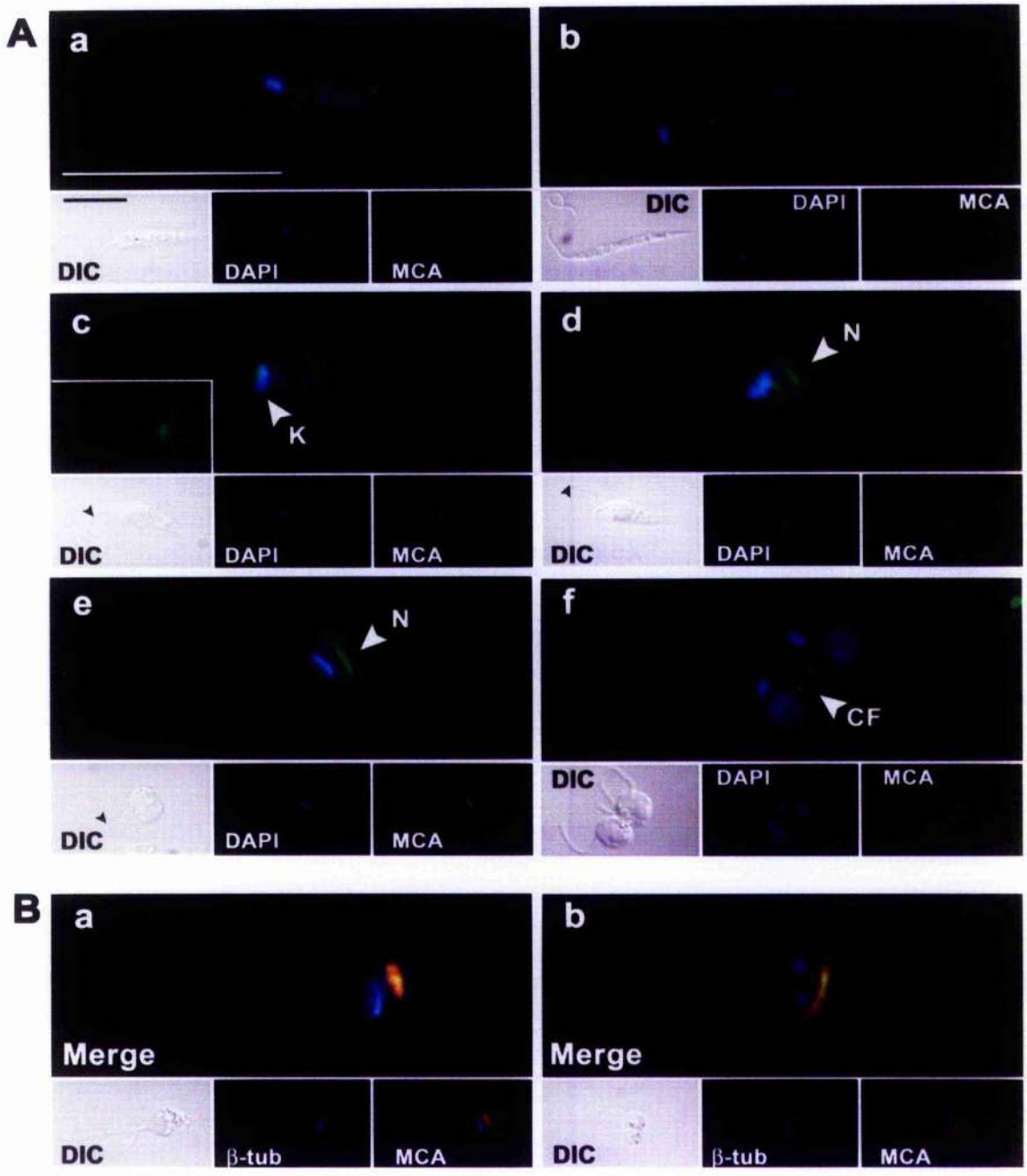

Figure 5.4: Changes in MCA localisation during cell cycle progression.

Fixed wild type cells were labelled with rabbit anti-TbMCA2/3 and Alexa Fluor 488 (green) or 548 (red) - conjugated anti-rabbit antibodies. Anti-β-tubulin antibodies (KMX,(Birkett et al., 1985)) were used together with Alexa Fluor 488- conjugated anti-mouse antibodies (green). DAPI staining of the nucleus (N) and kinetoplast (K) is shown in blue. Differential Interference Contrast (DIC) images are shown in the inset panels. Merged pictures are magnified. The scale bars apply to all pictures and equal10 μm.
A) Immunolocalisation of MCA in logarithmic phase (a) and stationary phase (b) promastigotes. Examples of fluorescent staining observed for cells in G1 (a, b) and G2/M (c, d, e) phases as well as in late cytokinesis (f) are shown. The black arrow heads (in c, d and e) indicate the presence of a second growing flagellum. The white arrow heads point the regions where the MCA signal is the strongest. K: kinetoplast; N: nucleus; CF: cleavage furrow. B) MCA relocates to the mitotic spindle during mitosis. Co-localisation of MCA (red) with β-tubulin (β-tub, green) was observed by immunofluorescence (yellow

in merged picture). The mitotic spindle starts to appear before (a) and disassembles after (b) kinetoplast segregation.

then two (**figure 5.4Bb**) kinetoplasts in cells undergoing nuclear division. MCA appears to associate with the mitotic spindle for the complete duration of this process. Upon the disassembly of the mitotic spindle and start of cytokinesis, MCA was found to be randomly distributed throughout the cell into the previously observed punctate structures. MCA accumulated near the cleavage furrow at a late stage of cytokinesis (**figure 5.4Af**).

The various changes in location of MCA during the *L. major* cell cycle, as well as its association with mitotic spindles, suggested that MCA might interact with microtubules.

5.2.3. MCA association with microtubules

Samples of semi-synchronised cells were fractionated following various extraction methods. First, the cells were lysed in 0.5% Triton X-100 for 15 mins at room temperature. The extracts were then centrifuged for 15 mins at 20,000g to separate the soluble protein fractions from the insoluble fractions. These latter protein pellets were then washed twice before resuspension in SDS-PAGE loading buffer. The various samples were then resolved by SDS-PAGE and processed for Western blot analyses using anti-TbMCA2/3 and anti-β-tubulin antibodies (**figure 5.5A**). It was observed that, independently of the various cell cycle phases, MCA was mainly present in the insoluble fraction together with the microtubule constituent, β-tubulin. This finding indicates that MCA is not a cytosolic protein and hinted that it might be associated with the microtubular network. Nevertheless, this method of extraction enriches for all Triton X100-insoluble constituents of the cell, not just microtubules.

Therefore two additional extraction protocols were assessed. The first one was based on a microtubule-stabilising buffer used on mammalian cells and previously used in *L.tropica* (Kratzerova et al., 2001), while the second was derived from formerly published methods on the preparation of trypanosome cytoskeletons (Woods et al., 1989; Robinson et al., 1991). Both protocols use non-ionic detergents to solubilise the plasma membrane and the internal membranous organelles while the intact microtubule cytoskeleton is stabilised by the presence of EGTA and magnesium ions in the buffers. The soluble and cytoskeletal fractions obtained were analysed by Western blot. While the anti-β-tubulin antibody confirmed that the microtubules were indeed in the insoluble fractions, the anti-TbMCA2/3 antibody revealed that these new extraction methods largely solubilised MCA (**figure 5.5B and C**). Nevertheless, a small proportion

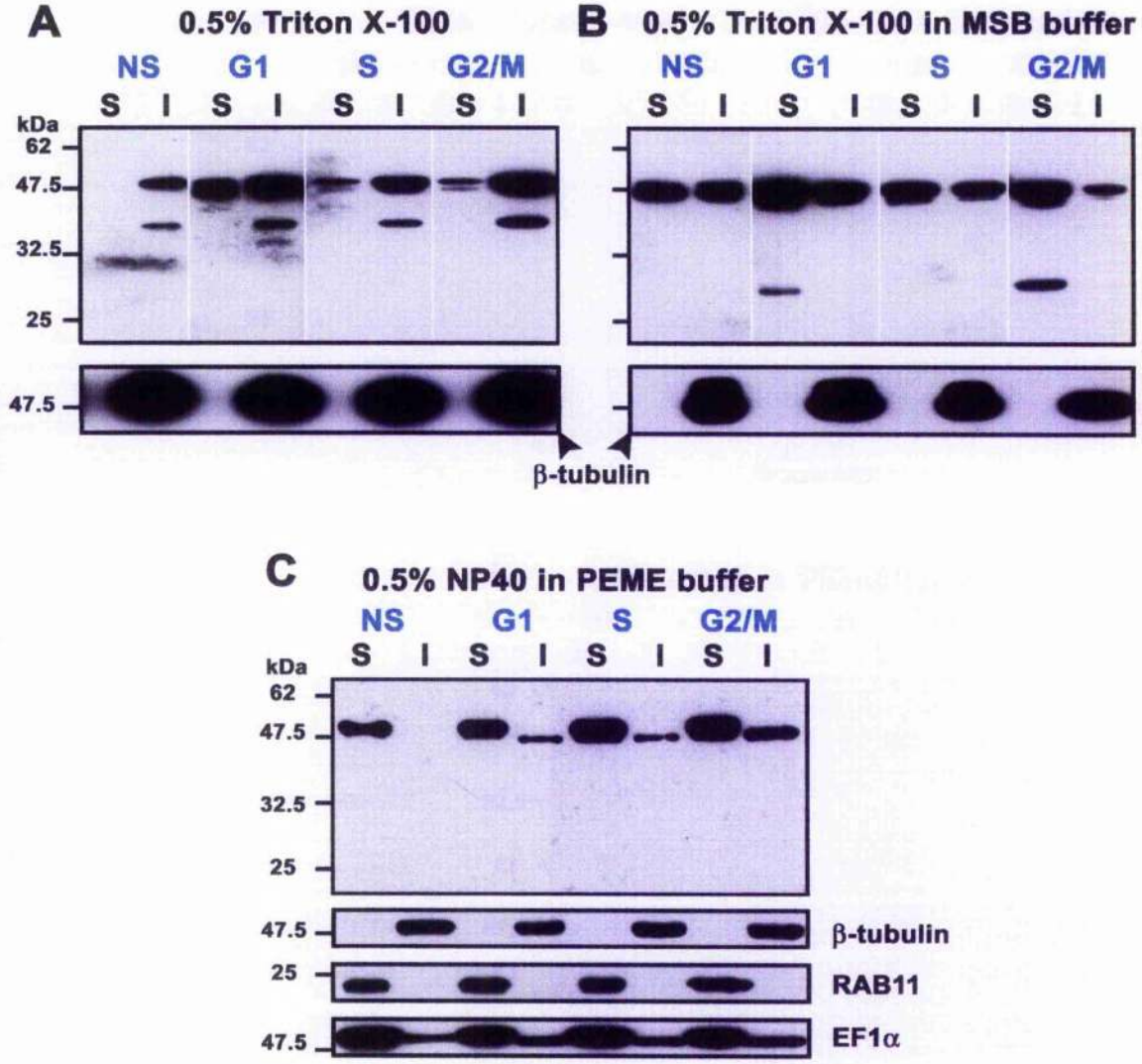

Figure 5.5: Cellular distribution of MCA along cell cycle progression

Non synchronised culture (NS) as well as promastigotes partially synchronised, by HU treatment, in G1, S or G2/M phase were analysed (blue labels). Cells were lysed in 0.5% Triton X-100 (v/v) in either water or microtubule-stabilising buffer (MSB, 20 mM Mes, pH 6.9, 2 mM EGTA, 2 mM $MgCl_2$, (Kratzerova et al., 2001)), in the presence of a cocktail of peptidase inhibitors for 15 mins at room temperature (panels A and B, respectively). Alternatively cells were lysed in 0.5% Nodinet P40 in PEME buffer (100 mM Pipes, pH 6.9, 2 mM EGTA, 1 mM $MgSO_4$, 0.1 mM EDTA), on ice for 5 mins (modified from (Woods et al., 1989; Robinson et al., 1991)) (panel C). The preparations were then centrifuged at 20,000g for 15 mins or at 250g for 30 mins, for the latter, at 4°C. The supernatants (S, soluble fractions) were collected for analysis. The pellets were washed twice in either water, MSB or PEME and then resuspended in T, TMSB or NP40-PEME (I, insoluble fraction). The S and I fractions were separated by SDS-PAGE in a 12% (w/v) acrylamide gel. The proteins were then transferred to a PVDF membrane and immunoblotted with rabbit anti-TbMCA2/3, anti-RAB11 and mouse anti- β-tubulin or anti-EF1α. The Western blots were then revealed using anti-rabbit or anti-mouse HRP-conjugated secondary antibodies and the SuperSignal West Pico chemoluminescent system (Pierce). Equal loading within the S fractions or P fractions group was confirmed by BCA quantification (Pierce) and Coomassie staining of the SDS-PAGE gels. Molecular masses are indicated, in kDa.

of MCA co-fractionated with β-tubulin. Also it can be said that depending of the method of extraction used, different amounts of MCA were detected in the microtubule fractions (**figure 5.5A, B and C**).

To determine more precisely the protein content of the detergent fractions, additional Western blot analyses were performed on cell extracts following 0.5% NP40 lysis in PEME buffer (**figure 5.5C**). RAB11, a protein found on the membrane of endosomes (Jeffries et al., 2001), and thus not associated with the cytoskeleton, was absent from the cytoskeleton fraction, demonstrating the effectiveness of the detergent extraction. Interestingly, elongation faction 1 alpha (EF1α) was also detected in the cytoskeleton fraction (**figure 5.5C**). In mammalian cells, EF1α has been shown to stabilise microtubules in a calcium/calmodulin-dependent manner *in vitro* and is thus recognised as a microtubule-associated protein (MAP) (Moore et al., 1998). EF1α in *T. brucei* (TbEF1α) similarly binds to calmodulin *in vitro* (Kaur and Ruben, 1994). Little is known about the physical properties of *Leishmania* EF1α - although it has been reported to occur in a Triton-X100 insoluble fraction (at 100,000g) (Nandan et al., 2003). These findings now suggest that LmajEF1α may also be a MAP. Surprisingly, LmajEF1α and MCA only partially associate with the cytoskeletal microtubules and most of the proteins are solubilised by the detergent extraction (**figure 5.5C**).

While most of the methods for identifying MAPs rely on their ability to bind microtubules *in vitro*, immunofluorescence analysis was important in demonstrating that these proteins were associated with microtubules *in vivo* (Olmsted, 1986). Interestingly, the immunolocalisation of MCA corroborates the detergent extraction findings. Indeed, the association of MCA with the mitotic spindle observed *in vivo* (**figure 5.4B**) confirms that a least a part of the MCA pool interacts with microtubules. Also, it seems that a higher proportion of the MCA pool is associated with microtubules during the G2/M phase (**figure 5.5C**). It is tempting to speculate that this observation reflects the presence of MCA on the mitotic spindle during nuclear mitosis. However, it is unclear whether the method of extraction used in this experiment is conservative of this intranuclear structure and it might have been solubilised. Furthermore, the cell fractionation protocol using 0.5% Triton X-100 in microtubule-stabilising buffer failed to confirm this transitory increased association between MCA and the cytoskeletal microtubules (**figure 5.5B**).

5.3. Genetic manipulation of the *MCA* chromosomal locus

The studies of MCA expression and localisation suggested that the metacaspase might play an essential role during *Leishmania* division. To gain further insights into MCA function, gene knock-out was attempted.

5.3.1. In wild type cells

5.3.1.1. By gene replacement

In order to obtain *MCA* null mutants, targeted gene replacement was undertaken. pGL842 and pGL849, two plasmids containing the 5' flanking region (FR) and the 3' FR of *MCA* were designed to replace *MCA* by homologous recombination with an antibiotic resistance marker (blasticidin or hygromycin, respectively) (**figure 5.6A**). Multiple attempts to knock-out the first *MCA* allele were made, with each construct, but no transfectant was obtained. Consequently, the transfection protocol was adapted, in the following ways, to try to optimise its efficiency. First, two different batches of *L. major* wild type cells were used, one coming from stabilates (WUMP 1815) and the other freshly isolated from mouse lesions (WUMP 3888). Then, various different amount of plasmid DNA were used for the transfection. The conditions of electroporation were modified, e.g. the 0.2 cm electroporation cuvettes were replaced by 0.4cm ones (Robinson and Beverley, 2003). And finally, different antibiotics concentrations were assessed to favour the selection of the transfectant cells. Unfortunately, all these adaptations had no effect on the outcome of the *MCA* knock-out attempts.

In trypanosomatids, it is well documented that even though the 5' and 3' FRs of a given gene are untranslated regions (UTRs), they contain essential information for the polyadenylation and the trans-splicing of the genes in 5' and 3' of the gene of interest, respectively (LeBowitz et al., 1993). Any interference with these processes would impede the maturation of the transcribed messenger RNA and subsequently their translation into protein. While the identity on the gene in 3' of MCA remains unknown, the gene in 5' of *MCA*, LmjF35.1570, encodes a putative methyltransferase (www.genedb.org). In case the 5' and 3' UTRs used in the *MCA* knock-out constructs disrupted somehow the regulation of the transcription of these genes and affected the cell survival, a new approach was tackled.

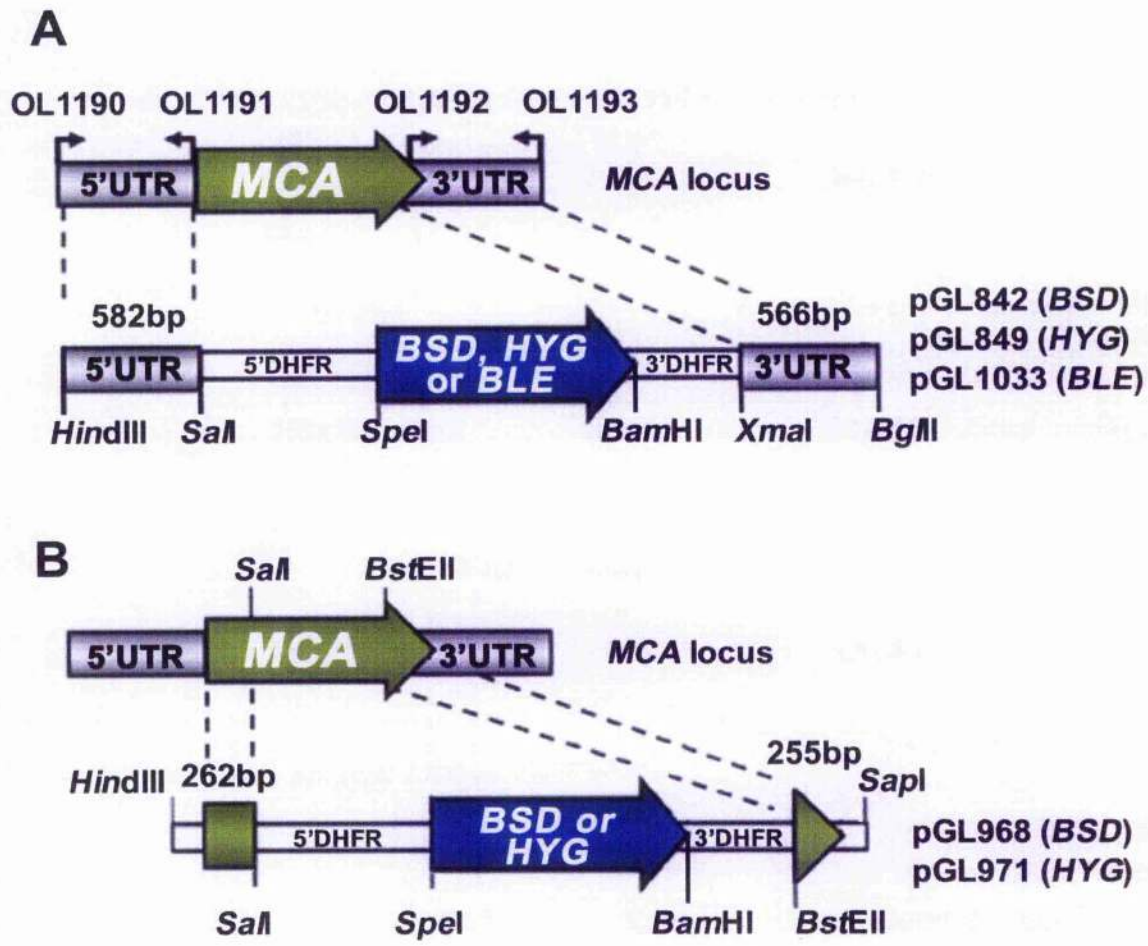

Figure 5.6: Schematics of *MCA* knock-out strategies

ORFs are shown as arrows, intergenic and flanking DNA sequences are shown as boxes. A) Gene replacement approach. The 5' and 3' untranslated flanking regions (5'UTR and 3'UTR) of *MCA* were amplified by PCR using the primer pairs OL1190-OL1191 and OL1192-OL1193, respectively. The 582 bp and 566 bp fragment were cloned, using the *Hin*dIII/*Sal*I and *Xma*I/*Bgl*II restriction sites, respectively, into pGL896 to generate pGL842. The blasticidin cassette (*BSD*) was then removed by *Spe*I/*Bam*HI digestion and replaced by either a hygromycin (*HYG*) or a phleomycin (*BLE*) resistance genes, to give pGL849 and pGL1033, respectively.

B) Gene disruption approach. The regions used for the homologous recombination are parts of *MCA* gene itself. The fragment covering the 262 first base pairs of *MCA* was obtained by PCR amplification of *MCA* with OL1397-OL1216, subcloning into the pPCR-Script and digestion by *Hin*dIII/*Sal*I (Note that the *Hin*dIII site comes from the pPCR-Script backbone). The last 255 bp were obtained by *Bst*EII/*Bam*HI digestion of OL1188-OL1189 amplified *MCA*. The two fragments were cloned into the pGL842 using its *Hin*dIII/*Sal*I and *Bst*EII/*Bgl*II restriction sites, respectively (Note that the *Bgl*II site being lost, the *Sap*I site was consequently used for the linearization of the recombination cassette). DHFR, dihydrofolate reductase gene.

5.3.1.2. By gene disruption

New gene knock-out constructions were designed. Instead of using the 5' and 3' UTRs of *MCA* for the double cross-over recombination, the first 262 bp and last 255 bp of the *MCA* gene were used (**figure 5.6B**). This new strategy therefore allowed gene knock-out by gene disruption thus ensuring that the genomic environment of *MCA* was not modified and that the expression of genes upstream and downstream of *MCA* was not affected.

Unfortunately, this new strategy did not yield to successful gene knock-out either. Again, the removal of the first allele of *MCA* was impossible. No report of incapacity to delete the first allele of a gene in *Leishmania* has been reported. Generally, the first allele of an essential gene can be successfully deleted (e.g. CRK3 (Hassan et al., 2001)), only the disruption of the second allele induces lethal phenotypes or genome rearrangements (triploid chromosomes, tetraploidy, aneuploidy (Cruz et al., 1993; Mottram et al., 1996a; Dumas et al., 1997; Tandon and Fraser, 2002)). One possible explanation could be that *MCA* locus is present at only one copy per genome. However, locus-specific haploidy has never been observed in *Leishmania* so far. Therefore, it seems likely that the incapacity to delete *MCA* first allele underlines a tight control of the level of expression of this gene and pinpoints its essential role in cell survival (Cruz et al., 1993).

5.3.2. In cell lines containing an additional copy of *MCA*

To confirm that recombination was possible in the *MCA* locus but also establish the primary function of MCA for *Leishmania* growth, the gene knock-out experiments were repeated in cell lines expressing an extra copy of *MCA*.

5.3.2.1. $P_{\beta TUB}$ MCA-TAP

A cell line allowing the expression of tandem affinity purification (TAP) tagged-MCA was previously created in the laboratory, by integration of a linearised *MCA-TAP* construct (pGL958) into the *L. major* β-tubulin locus (Besteiro, S. unpublished data). These parasites were transfected with the knock-out cassettes excised from pGL842 (*BSD*) and pGL1033 (*BLE*). The replacement of both chromosomal copies of *MCA* was surprisingly straightforward. Double resistant parasites were obtained and correct integration of the knock-out constructs was confirmed by PCR. A Southern blot analysis using a part of the *MCA* open reading frame as a probe and performed on the genomic DNA of the mutant parasites corroborated the PCR data and proved that the targeted replacement of *MCA* chromosomal copies had indeed been successful. Indeed, no copy

of the chromosomal *MCA* was detected (1.2kb DNA fragment) in the $P_{\beta TUB}$ MCA-TAP *Δmca::BSD/Δmca::BLE* cell line **(figure 5.7, light green arrow head, line 4)**.

Surprisingly, the number of copies of the *MCA-TAP* appeared to be fluctuating between the parental, heterozygote and chromosomal null cell lines **(figure 5.7, dark green arrow head, lanes 2, 3 and 4, respectively)**. This variable amount of *MCA-TAP* between cell lines could be explained by a possible maintenance of non-linearised *MCA-TAP* construct within the cell. In this case, the level of expression of MCA-TAP would not solely be regulated by the β-tubulin promoter, as desired, but mainly by modulation of the cellular number of *MCA-TAP* episome. The decrease of *MCA-TAP* copy number in $P_{\beta TUB}$ MCA-TAP *Δmca::BSD/Δmca::BLE* compared to the parental cell lines could thus indicate a physiological need to tightly regulate MCA-TAP expression. Indeed, as detailed previously, the level of expression of the wild type MCA seems to be securely adjusted during cell growth. It is then possible that, upon removal of both wild type copy of *MCA*, this stringent control was assigned to MCA-TAP expression.

5.3.2.2. MCA-His

To assess whether MCA was essential for *L. major* survival and infectivity in mice, attempts to remove both chromosomal copies of *MCA* were made in a cell line expressing a His- tagged variant of MCA, from an episomal construct. Indeed, once in the animal and upon removal of antibiotic pressure, *Leishmania* tend to lose their episomes unless the exogenously expressed protein is essential to the parasite persistence within the mammalian host (Vergnes et al., 2005a). If a successful infection occurred, the amastigotes would then be extracted from the lesion and the number of episomes per cell determined.

Wild type *L. major* cells were transfected with pGL981 to allow the episomal expression of MCA-His (from the pNUS-HcN vector (Tetaud *et al.*, 2002)). While populations of drug resistant mutants grew fine, clones were impaired in their growth and were tetraploid (see **chapter 6**). As the populations were expressing detectable amount of MCA-His, one of them was chosen to attempt the deletion of *MCA* chromosomal copies. The insert from pGL842 was transfected into this selected cell line, to replace one allele of *MCA* with a blasticidin selectable marker. Mutants resistant to blasticidin were obtained. While successful integration of the gene replacement cassette was confirmed by PCR, at least one additional *MCA* locus was detected and DNA content analyses revealed that the obtained transfectants were actually tetraploid. Therefore, removal of the chromosomal copies of *MCA* could not be achieved.

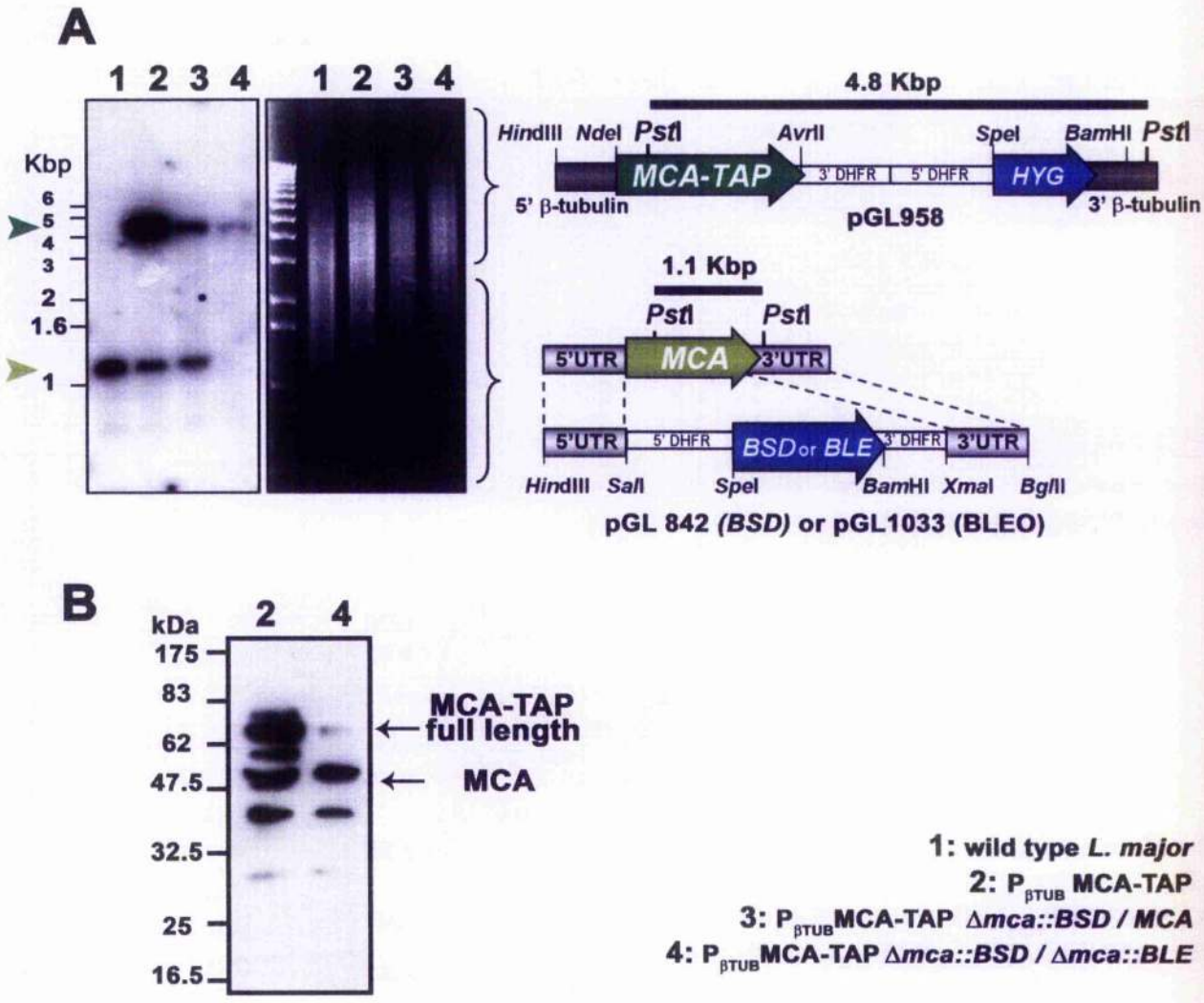

Figure 5.7: Removal of *MCA* locus in a cell line expressing a TAP-tagged copy of *MCA* under the control of the β-tubulin promoter.

A) Southern blot analysis and schematic representation of the wild type *MCA* locus and the plasmid constructs used for expression of MCA-TAP (pGL958) or for *MCA* gene replacement (pGL842, pGL1033). ORFs are shown as arrows, intergenic and flanking DNA sequences are shown as boxes. Genomic DNA was digested with *Pst*I, separated on a 0.8% agarose gel, blotted on a nylon membrane and hybridised with ^{32}P-labelled *Pst*I digested MCA ORF as a probe. The sizes of the DNA fragments labelled are indicated. Restriction enzymes of particular interest are shown. BSD, blasticidin resistance gene; DHFR, dihydrofolate reductase gene; HYG, hygromycin resistance gene; BLE: phleomycin resistance gene. B) Western blot analysis. Lysates corresponding to 10^7 promastigotes were, after transfer onto a PVDF membrane, hybridised with rabbit anti-TbMCA2/3 antibody at a 1:10,000 dilution. Revelation was performed using an anti-rabbit-HRP conjugated secondary antibody (Promega) and West Signal chemoluminescence detection system (Pierce). Lane 1: wild type *L. major*; Lane 2: $P_{\beta TUB}$ MCA-TAP; Lane 3: $P_{\beta TUB}$ MCA-TAP *Δmca:: BSD / MCA* ; Lane 4: $P_{\beta TUB}$ MCA-TAP *Δmca:: BSD / Δmca::BLE*. The molecular mass size markers are shown on the left.

Whether the tetraploidy results from the cloning of the transfected cell line, or from the attempt to delete the genomic *MCA*, remains uncertain. Possible ways to solve this issue would involve an improvement of the transfection efficiency to avoid the selection of clonal transfectants and a removal of the antibiotic pressure to reduce the episome copy number. Indeed, if the episomally-drived expression of MCA-His is essential to the removal of the chromosomal *MCA*, then it is very likely that the cells would conserve their episomes even in the absence of antibiotic selection. Furthermore, in such conditions, the level of expression of MCA-His would be minimal and would potentially tightly match the cellular requirements for the metacaspase. Consequently, the tetraploidy phenotype associated with the overexpression of MCA-His might be abrogated and new *MCA* knock-out attempts would be possible.

5.3.2.3. P_{rRNA} MCA and P_{rRNA} MCA^{H147A}

MCA and an MCA^{H147A} active site mutant were integrated independently into the 18S rRNA locus of wild type *L. major*. Integration was confirmed by PCR (**figure 5.8Aa, b**). A single *MCA* allele could be removed successfully from both cell lines (**figure 5.8Ac, d, e, f**), but it was not possible to remove both MCA alleles; in all cases an additional copy of the MCA locus was detected (**figure 5.8Ag, h**).

DNA content analyses were performed on the various cell lines (**figure 5.8B**). It is established that cells in G1 phase of the cell cycle are diploid (2C) while those in G2/M are tetraploid (4C) and the ones in S phase are between both. Within a given culture, *Leishmania* cells can be at different phases of the cell cycle. Nevertheless, even during the early periods of *Leishmania* promastigotes growth, when the growth rate is at its highest, cells in the G1 phase represent about 65% of the population. While the ploidy of the P_{rRNA} MCA and the single MCA allele deletion cell line P_{rRNA} MCA *Δmca::BSD* was found to be normal, the removal of the second allele of the chromosomal MCA resulted in the duplication of the cellular DNA content (**figure 5.8B2, 3 and 4, respectively**). These cells also exhibited a slower growth rate than wild type (**figure 5.8C, compare 4 with 1**), and had similar defects in cell cycle progression as observed with WT[MCA] type 2 transfectants (refer to **chapter 6**).

Surprisingly, the P_{rRNA} MCA *Δmca::BLA/Δmca::HYG/MCA* cell line showed a growth defect whereas the $P_{\beta TUB}$ MCA-TAP *Δmca::BSD/Δmca::BLE* cell line did not. One possible explanation, which could also account for the tetraploidy phenotype, is that the expression of the exogenous MCA is in P_{rRNA} MCA *Δmca::BLA/Δmca::HYG/MCA* controlled by the 18S rRNA promoter while in $P_{\beta TUB}$ MCA-TAP *Δmca::BSD/Δmca::BLE* is episomal and thus potentially reaching higher levels and producing an overexpression phenotype (refer to **chapter 6**).

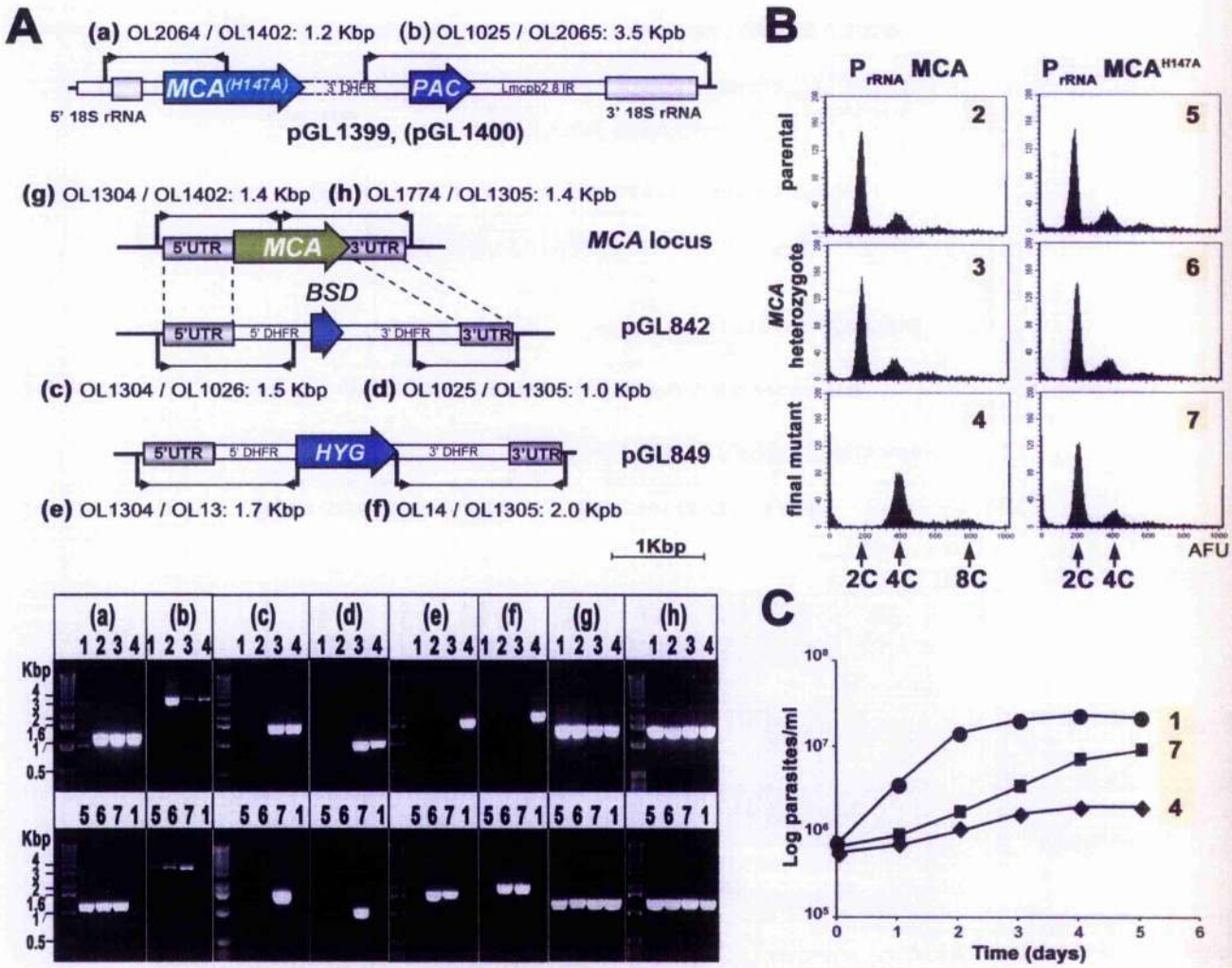

1: WT **2:** P_{rRNA} MCA **3:** P_{rRNA} MCA *Δmca::BSD* **4:** P_{rRNA} MCA *Δmca::BSD/Δmca::HYG/MCA*
5: P_{rRNA} MCA^{H147A} **6:** P_{rRNA} MCA^{H147A} *Δmca::HYG* **7:** P_{rRNA} MCA^{H147A} *Δmca::HYG/Δmca::BSD/MCA*

Figure 5.8: Removal of *MCA* locus in cell lines expressing an additional copy of *MCA* or MCA^{H147A}, under the control of the *18S rRNA* promoter.

A) Upper panel. Schematic representation of the *18S rRNA* locus, the wild type *MCA* locus and the plasmid constructs used for integrative ectopic expression of *MCA* (pGL1399), MCA^{H147A} (pGL1400) or *MCA* gene replacement (pGL849, pGL842). ORFs are shown as arrows, intergenic and flanking DNA sequences are shown as boxes. BLA, blasticidin resistance gene; DHFR, dihydrofolate reductase gene; HYG, hygromycin resistance gene; PAC: puromycin resistance gene. The pairs of oligonucleotides used for PCR amplifications, as well as the sizes of the fragments generated are indicated. Lower panel. The PCR reactions were performed to assess the integration of pGL1399 or pGL1400 inserts into the *18S rRNA* locus (a, b), the integration of pGL849 insert (c, d) and pGL842 insert (e, f) in the wild type *MCA* locus, and the integrity of the wild type *MCA* locus (g, h). Integration or integrity in the 5' (a, c, e, g) and the 3' (b, d, f, h) of the loci were tested.

B) DNA content analysis performed by FACS. The peaks representative of the cell count per arbitrary fluorescence units (AFU) indicates diploid (2C), tetraploid (4C) or octaploid (8C) cells.

C) Representative growth curves performed on the wild type (1), P_{rRNA} MCA *Δmca::BLA/Δmca::HYG/MCA* (4) and P_{rRNA} MCA^{H147A} *Δmca::HYG/Δmca::BLA/MCA* (7) cells.

Attempts to remove the second MCA allele in the P_{rRNA} MCA^{H147A} *Δmca::HYG* cell line lead to a duplication of MCA locus, but not of the entire DNA content, as the cell line was still diploid (**figure 5.8B7**). This finding suggests that firstly, MCA^{H147A} might indeed be a catalytically inactive mutant, and secondly that MCA exhibits an essential enzymatic activity that is indispensable for cell survival.

5.4. Phenotype analysis of the P_{rRNA} MCA^{H147A} *Δmca::HYG/Δmca::BSD/MCA* mutant

Less pronounced than during MCA overexpression, a slow growth phenotype was nevertheless observed for P_{rRNA} MCA^{H147A} *Δmca::HYG/Δmca::BLA/MCA* (**figure 5.8C, compare 7 to 1**). The slow growth rate could be explained by observation of the nucleus and kinetoplast configurations (**figure 5.9A**). A build up of cells in 2N2K2F (12.9% compared to 4.6% in the WT) and a decrease of cells in G1 phase (1N1K1F and 1N*1K*1F, "$1N^{(*)}1K^{(*)}1F$" from 63.1% to 52.1%) was observed suggesting a defect in cytokinesis (**figure 5.9A, left panel**). The increase in 2N2K2F cells was due to an accumulation of cells engaged in cytokinesis (11.9% compared to only 3.8% in the WT). Similarly, a detailed analysis of the additional cells with other configurations (16.5% against 10.0% for the WT) revealed the presence of aberrant cells in which cytokinesis was impaired (**figure 5.9A, right panel**). Most of those cells had started cytokinesis but were delayed in its completion by improper organelle segregation, inaccurate organelle positioning or aberrant axis of progression of the cleavage furrow (**figure 5.9B**). In parallel, the reduction in the number of cells in $1N^{*M}2K2F$ (from 12.3% to 6.7%) underscored a potential delay in the onset of mitosis, which might subsequently account for impaired nuclear partitioning.

5.5. Discussion

In the present chapter, Western blot analyses performed on *L. major* extracts firstly showed that MCA was slightly bigger than the predicted molecular weight. This size difference might be due to post-translational modifications such as glycosylation, phosphorylation, ubiquitination, ... (Ivens et al., 2005) and therefore underpins that the stability/degradation of MCA might be stringently adjusted. Furthermore, the presence of additional proteins of mainly ~38-40 kDa and ~ 30 kDa suggest that MCA might be processed and that its biological function might be regulated by this mechanism. For caspases, processing leads to the formation of large and small sub-units which remain tightly associated through covalent interactions and to the subsequent dimerisation and catalytic activation of the protein complex. Also, active caspases being involved in

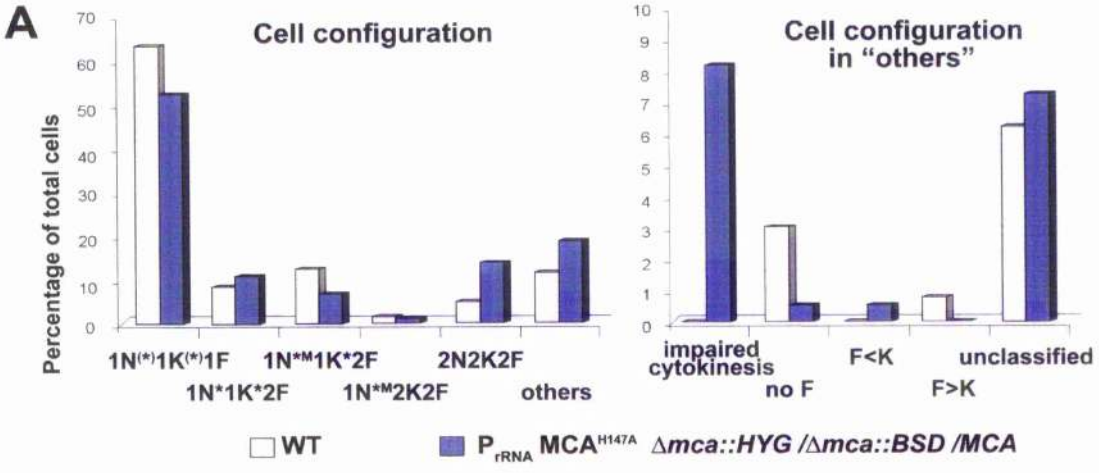

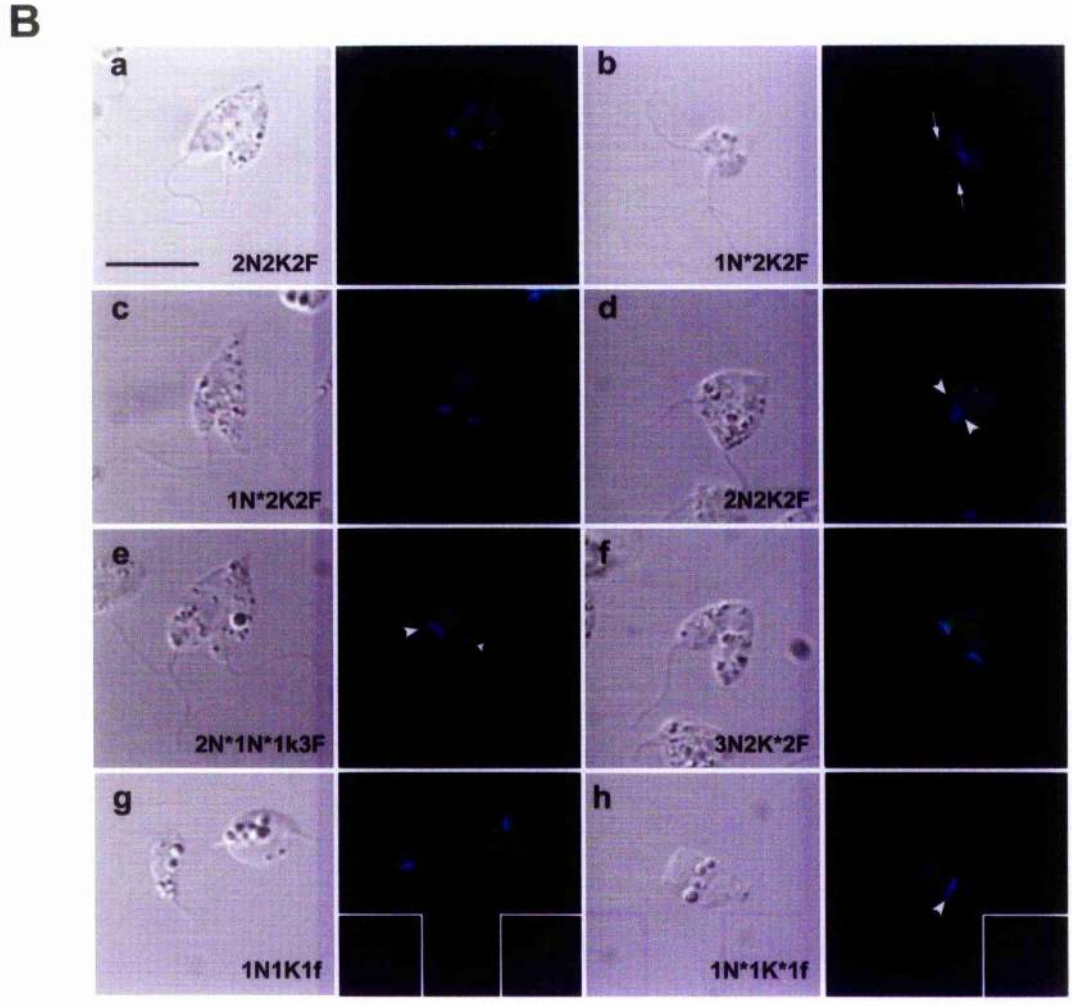

Figure 5.9: The P_{rRNA} MCA^{H147A} *Δmca:: HYG / Δmca::BSD / MCA* mutant shows a delay in kinetoplast segregation, nuclear division and cytokinesis.

A) Classification of the various cell configurations observed in the wild type (white bars) and mutant (blue bars) based on DAPI staining and cell morphology. Sub-groups of the cells classified in "others" are shown on the right panel. N: nucleus; K: kinetoplast; F: flagellum. Impaired cytokinesis refers to a group of cells having an ingressing cleavage furrow. F<K and F>K correspond to the cells with a number of nuclei different from the

number of flagella and where the number of flagella was either smaller or bigger than the number of kinetoplasts.
B) Immunolocalisation of MCA and /or MCA^{H147A} in various types of aberrant cells.
Fixed cells were labelled with rabbit anti-TbMCA2/3 and anti-rabbit Alexa Fluor 488-conjugated antibodies (green). DAPI staining of the nuclear and kinetoplast DNA is shown in blue. An example of a 2F2K2F is shown in (a). Pictures of cells classified in the "impaired cytokinesis" or "unclassified" groups are presented in b-f and g-h, respectively. The white arrows highlight structures at the base of the flagellum that were labelled by the antibodies. The white arrow heads point the kinetoplasts.

apoptotic cell death, their processing is closely controlled by mammalian cells (Earnshaw *et al.*, 1999). Interestingly, it was observed that, to gain their full enzymatic activity and exert their biological functions, caspases undergo (auto)processing and intracellular translocation (Kamada *et al.*, 2005). Indeed, nuclear degradation, one of the main features of apoptosis, is triggered by the translocation of several cytoplasmic caspases into the nucleus and the subsequent cleavage of nuclear proteins such as the lamins, the poly (ADP-ribose) polymerase (PARP), DNA-dependant protein kinase, DNA topoisomerase I, DNA replication factor RFC-140, RAD51 and members of the cohesion complex (e.g.RAD21) (Earnshaw et al., 1999; Porter, 1999; Fuentes-Prior and Salvesen, 2004).

In *L. major*, immunofluorescence analyses revealed that MCA was transiently present in the nucleus. However, this nuclear "translocation" occurred upon mitosis onset rather than, like in mammalian cells, after initiation of apoptosis. Also, MCA was not randomly distributed in the nucleus but was mainly associated with the mitotic spindle. Interestingly, some of the substrates cleaved by caspase during apoptosis play, in mammalian cells, crucial roles in cell division. Indeed, some of the PARP family members localise to the mitotic apparatus (Schreiber *et al.*, 2006).While PARP-1 and PARP-2 are mainly associated with the chromosome centromeres, vPARP bind to the kinetochore microtubules of the mitotic spindle. Thus, the presence of MCA on the mitotic spindle might underscore an interaction with its potential substrate. Although no gene encoding for vPARP was identified in *L. major*, other members of the PARP family are present. Thus it can not be excluded that some of these proteins might resume vPARP functions and that MCA might mediate its processing. However as the intracellular targets of MCA remain unknown, these remarks are highly speculative and the exact function of MCA on the mitotic spindle still awaits elucidation.

The restricted intranuclear localisation of MCA argues against an involvement in programmed cell death and rather suggests functions in cell proliferation. Also, while programmed cell death occurs principally in aging cells (Lee et al., 2002; Herker et al., 2004), MCA is present at a higher level in actively dividing logarithmic phase cells than in quiescent stationary phase cells, providing evidence for a role for the metacaspase in

cell division. Consistent with this observation was the finding that MCA intracellular localisation changes at different time points during cell cycle progression. Indeed, immunofluorescence experiments showed that initially distributed throughout the cell in punctuate structures of unknown nature, some MCA relocates to the kinetoplast at the onset of kinetoplast segregation, then later to the mitotic spindle during mitosis and, finally, close to the cleavage furrow at a late stage of cytokinesis. Therefore, MCA might not only be involved in mitosis but also in kinetoplast segregation and cytokinesis as strengthened by the phenotypical analyses of the P_{rRNA} MCA^{H147A} *Δmca:: HYG / Δmca::BLA / MCA* mutant. Indeed, in this cell line, the reduction in the amount of active MCA in the cell led to an impairment of kinetoplast and nucleus division and a delay in cytokinesis. Moreover, all the failed attempts to produce a *MCA* chromosomal null mutant underscore the essential role played by MCA in the cell.

Also, as we were unable to remove the first allele of *MCA* from *L. major* genome without expression of an *MCA* transgene, it suggests that the level of expression of MCA is very tightly regulated. Indeed, we observed that *L. major* adapted so as to keep at least one active copy of *MCA*. Removal of the two chromosomal copies of *MCA* was achieved successfully in a cell line containing episomal copies of the gene, but was accompanied by modulation of the number of *MCA*-bearing plasmids within the cell. When an extra copy of *MCA* was integrated in the genome, the first allele of *MCA* locus could be disrupted, but attempts to replace the second allele led to tetraploidy. This duplication of the genome could be explained by the fact that in this cell line the extra copy of *MCA* was integrated into the 18S rRNA locus and the regulation of the level of expression of the protein was perturbed and ultimately led to an accumulation of MCA in the cell and a phenotype previously observed during MCA overexpression. While tetraploidy has previously been reported to occur when attempting to knock-out an essential gene (Cruz et al., 1993), it was unlikely that the genome duplication observed during MCA overexpression and in the present case resulted from such process. Indeed, attempts to remove the two chromosomal alleles of *MCA* from a cell line containing a catalytically inactive extra copy of *MCA* (MCA^{H147A}) led to duplication of the *MCA* wild type locus, but not of the entire genome. This provides evidence that MCA function is linked to genome replication and that the cysteine peptidase catalytic activity of MCA is essential for cell survival.

In eukaryotic cells the cytoskeleton is involved in multiple vital processes such as cell growth and division, motility, intracellular organelle trafficking and morphogenesis. Intimately linked together, three main types of filaments form the backbone of the cytoskeleton. First, the actin filaments (microfilaments) give the cell its surface shape, its polarity, its ability to move and mediate cytokinesis. Second, the intermediate filaments confer mechanical strength to the cell and mediate crosstalk between

cytoskeletal proteins. And last but not least, the microtubules regulate intracellular traffic of proteins, vesicles and organelles as well as their positioning and are required for execution of mitosis (e.g. mitotic spindle formation) (Goode et al., 2000; Rodriguez et al., 2003; Chang and Goldman, 2004). The observation that MCA co-localise at least transiently with β-tubulin and its partial association with the cytoskeleton underpins the potential interaction of MCA with various types of cytoskeletal filaments.

Microfilaments are poorly characterised in *Leishmania*, but genes encoding actin and myosin are present in this parasite. In *L. donovani*, actin was shown to be present in the nucleus, kinetoplast and in a plasma-membrane associated network that co-localised with the sub-pellicular microtubules (Sahasrabuddhe *et al.*, 2004). While *L. major* apparently lacks genes coding for the intermediate filament proteins vimentin and desmin, epitopes common to the mammalian proteins can be detected in *Leishmania* promastigotes with anti-vimentin antibodies (Draberova et al., 1986; Kratzerova et al., 2001). The detected 57 kDa protein was located only on cell poles and was most marked during cell division. A 210 kDa microtubule-associated protein (MAP) was found to co-distribute with the vimentin/desmin-like 57 kDa protein at the anterior and posterior poles of cells, in a cell-cycle-dependent manner (Kratzerova et al., 2001). Direct fluorescence observation of MCA^{H147A}-GFP revealed that, similarly, this protein accumulated at the posterior end of *L. major* suggesting that MCA might, like the previously reported 210 kDa *L. donovani* MAP, interact with intermediate filament-like proteins. In mammalian cells intermediate filaments such as the nuclear lamins, keratins and vimentin were found to be substrates of caspase-3 (Prasad *et al.*, 1999), so we can postulate that MCA might act on intermediate filament-like proteins and participate in cellular remodelling during the cell cycle. Most importantly, in addition to its association with the mitotic spindle, we were able, after detergent extraction, to demonstrate by Western blot that MCA partially associates with cytoskeletal microtubules. Therefore, through its association with the sub-pellicular microtubules of the cytoskeleton, MCA may play a crucial role in cell division.

Indeed, overexpression of *MCA* led to a rapid growth arrest due to defect in kinetoplast segregation, mitotis and cytokinesis. In *T. brucei* kinetoplast segregation and cytokinesis are mediated by sub-pellicular microtubules (Robinson *et al.*, 1995). *T. brucei* procyclic cells overexpressing the sub-pellicular proteins CAP15 and CAP17 duplicate but fail to segregate their kinetoplast and lose their kinetoplast duplication/cytokinesis coordination (Vedrenne *et al.*, 2002). An association of MCA with filaments of the cytoskeleton provides an explanation of the phenotype when MCA is overexpressed, such as a severe impairment of cell division.

Remarkably, while caspases have mainly been reported to mediate cell death, recent findings suggest that they also possess fundamental apoptosis-independent

functions, their crucial tasks paradoxically also favouring cell survival, differentiation, proliferation, receptor internalisation, cytokine maturation and cell spreading (Algeciras-Schimnich *et al.*, 2002). In the present work, we showed that MCA plays an essential role in the *Leishmania* cell cycle but no role for MCA in *L. major* programmed cell death has been identified. Yet MCA has recently been shown to complement the programmed cell death-inducing function of the yeast metacaspase (Gonzalez et al., 2006). In mammals, cell proliferation and cell death are essential yet opposing cellular processes, but an essential function for programmed cell death in parasitic protozoa remains controversial. Nevertheless, we can postulate that MCA might mediate crosstalk between these processes and promote a balance between proliferation and death. Also, knowing the crucial role played by the microtubules and other cytoskeletal filaments on the spatial organisation of signal transduction, then maybe, MCA, which associate with this network, also plays a role in transmission of signals to downstream targets (Gundersen and Cook, 1999). The biochemical characterisation of the *L. major* metacaspase and the identification of its *in vivo* substrates should provide new insights into its function.

Chapter 6:
Expression of MCA in *L. major*, *E. coli* and *P. pastoris*

6.1. Expression in *Leishmania major*

6.1.1. Constructs generated

Previous experiments had showed that the removal of the chromosomal copies of *MCA* could not be achieved in wild type *L. major*, so the possible functions of MCA within the cell were assessed by episomal expression of several variants of the protein. Alignments between metacaspases and caspases were performed (**chapter 4**) and protein residues or domains for which functional analyses would be most revealing were chosen.

Within the MCA active site region, the catalytic cysteine was predicted to be C202. A mutant of the *L. major* metacaspase was created by changing C202 into a glycine, a residue lacking the sulfhydryl group predicted to be involved in MCA catalytic mechanism. The generated MCA^{C202G} was thus theoretically catalytically inactive.

Furthermore, MCA is predicted to possess either a signal peptide cleavage site or a proregion processing site between residue 28 and 29 (refer to **chapter 4**). To analyse the putative role of this particular domain, a 35 amino acid long N-terminal region was removed from the potentially catalytically active and inactive variants of MCA (to give ΔproMCA and $\Delta proMCA^{C202G}$). In addition, to allow the visualisation by fluorescence and immuno-detection of these proteins, Green Fluorescent Protein (GFP) or polyhistidine (His) tags were fused to their C-terminus. Two expression vectors were used for this purpose, the pNUS-GFPcN and the pNUS-HcN (Tetaud et al., 2002), both using a neomycin (G418) resistance gene as the selection marker.

The plasmid constructs encoding the various proteins of interest were then transfected and expressed in *L. major* promastigotes. Surprisingly, while generally 50 μg ml^{-1} of G418 is used for the selection of *L. major* transfectants, in this case no transfectant was obtained until the G418 concentration was lowered to 15 μg ml^{-1}. Even so, most of the transfectants obtained had a severe growth phenotype and an abnormal shape (**table 6.1**). The presence and expression of the plasmid constructs within the transfectants was confirmed by PCR and Western blot analyses (**figure 6.1.**), respectively. The exogenous expression of the full length active MCA, the potentially catalytically inactive, as well as the N-terminally truncated MCA all seemed to be toxic for the cells. As all the MCA variants had GFP or histidine tags at their C-terminus (**table 6.1**), it was thought that the tags might be interfering with the function(s) of the episomally expressed proteins and thus leading to the prevalence of the phenotype observed. Indeed, the steric hindrance created by the tags might induce the expressed proteins to misfold or might inhibit/promote physical interactions with other proteins. So, new

Cell lines	His-tag		GFP fusion		No tag	
	pGL	P/T (P%)	pGL	P/T (P%)	pGL	P/T (P%)
WT [MCA]	981	4/6 (67%)	985	5/6 (83%)	1128	1/4 (25%)
WT [MCA^{C202G}]	982	2/4 (50%)	986	5/6 (83%) 1/15* (7%)	1129	2/4 (50%)
WT [ΔproMCA]	983	1/6 (17%)	987	5/6 (83%)	1130	0/1
WT [$\Delta proMCA^{C202G}$]	984	2/5 (40%)	988	5/6 (83%)	1131	1/4 (25%)
WT [MCA^{C201G}]	-		1293	0/16	1294	0/3
WT [$MCA^{C201-202G}$]	-		1295	0/16	1296	0/0
WT [MCA^{H147A}]	1401	3/9 (33%)	1402	2/8 (25%)	(1406)	-
WT [Nterm-GFP]	-		1109	0/2	-	
WT [Cterm-GFP]	-		1108	0/3	-	
WT [MCAΔCterm]	-		1110	3/8** (37%)	-	
WT [ΔproMCAΔCterm]	-		1111	0/10	-	
WT [eNterm-GFP]	-		1403	1-4***/5 (20-80%)	-	
WT [GFP-eCterm]	-		1404	0/10	-	
WT [eNterm-GFP-Cterm]	-		1405	1/7 (14%)	-	

Table 6.1: Summary of the MCA variants expressed in *L. major* and the proportion of cells showing a phenotype

The constructs generated as well as their matching pGL numbers are show. For each construct, the total number of transfectants is indicated (T, second number) as well as the number of cells showing a phenotype (P, first number). The percentage of transfectants with a phenotope over the total number of transfectants is indicated (P%). (-) indicates variants that were not created or transfected into *L. major*. (*) Western blot analysis revealed that of the 15 transfectants, only the one with a phenotype was expressing detectable amount of the MCA variant. (**) Note that the transfectants with a phenotype expressed the expected size MCA variant while the others have a N-terminally truncated variant (see text). (***) While initially growing well immediately after selection, 3 transfectants showed a phenotype after less than two weeks in culture.

constructions were generated to allow the expression of the multiple MCA variants without any tags.

However, transfectants expressing the non-tagged MCA variants were also difficult to obtain. Only by decreasing the antibiotic pressure could plasmid-bearing cells be isolated. And still many of the created cell lines experienced difficulties in multiplying and developing properly (**table 6.1**); a phenotype strikingly comparable to the one observed upon expression of the C-terminally tagged MCA variants. Therefore, the growth phenotype could not be attributed to the presence of the C-terminal tags, but rather suggested the involvement of the metacaspase itself. However, as the WT [MCA^{C202}] cell line had a similar phenotype as the WT [MCA] cell line (**table 6.1**), it seemed that the phenotype was not due to the metacaspase enzymatic activity. Nevertheless, as an additional cysteine residue is immediately adjacent to the predicted active site cysteine, we could not rule out that this neighbouring residue, C201, might be involved in the catalytic activity of the metacaspase. In that case, what was thought to be a catalytically inactive mutant might instead still be functional.

Thus, to establish whether the observed growth phenotype was linked with the proteolytic function of the metacaspase, additional active site mutants were generated. C201 alone or together with C202 was mutated to a glycine residue (MCA^{C201G} and $MCA^{C201-202G}$). It was previously postulated that C81, or even several other cysteines, might be involved in catalysis (see **chapter 4**), so instead of mutating all these potentially important residues, the inactivation strategy was shifted toward the active site histidine (H147). Indeed, by replacing H147 with an alanine residue (MCA^{H147A}), the de-protonation and esterification of the active site cysteine will be prevented and the catalytic mechanism will subsequently be ineffective. Surprisingly, while WT [MCA^{C201G}] and WT [$MCA^{C201-202G}$] cell lines grew at a rate comparable to the wild type cells, some cell lines carrying the MCA^{H147A} construct had impaired growth (**table 6.1**). Thus whether the enzymatic activity of the metacaspase is involved in the observed growth phenotype remains an open question.

The WT [ΔproMCA] and transfectants expressing N-terminally truncated MCA variants were slightly less affected in their survival ability than the ones expressing the full length MCA variants. A potential involvement of the N-terminal domain in the correct targeting of the metacaspase was therefore suspected. To confirm this hypothesis, the first 21 amino acids of MCA were fused to GFP (to give Nterm-GFP). At the same time, I evaluated the possible role of the C-terminal domain in MCA trafficking by generating a GFP fusion of the last 108 amino acids (Cterm-GFP). Upon transfection into the parasite, the expression of Nterm-GFP or Cterm-GFP was confirmed and their respective intracellular localisations were determined. Like the GFP within the control cell line, Nterm-GFP and Cterm-GFP were found to be present in the cytosol of the cell.

Therefore it was deduced that these domains were unlikely to mediate the targeting or trafficking of MCA to a special compartment or organelle. Nevertheless, Western blot analysis of these overexpressing cell lines revealed that Cterm-GFP was extensively processed in the cell (**figure 6.1G**), suggesting it was degraded. Also, it was impossible to determine whether the observed fluorescent signal was due to Cterm-GFP or some of its cleavage products. However, even if no growth phenotype were associated with the expression of Cterm-GFP, its intensive degradation within the cells suggested that this domain of MCA might be somehow not properly folded or detrimental to the cells. Interestingly, this observation overlapped with the previous finding that transfectants expressing C-terminally GFP-fused MCA variants were more susceptible to growth impairment then the ones expressing non-tagged variants. Both sets of data suggested that the C-terminal domain of MCA might possess a defined function and that any interference with it was detrimental for the cell. The MCA C-terminal domain is rich in proline, glutamine and tyrosine residues that potentially could be involved in protein-protein interactions (refer to **chapter 4**), so it is conceivable that the contiguous presence of a bulky 25 kDa GFP protein might impede this function.

To investigate the role of the C-terminal extension several variants of MCA lacking their last 108 amino acids were created (constructs MCAΔCterm-GFP and ΔproMCAΔCterm-GFP) and expressed in *L. major*. Interestingly most of the transfectants grew normally, suggesting that the previously observed slow growth phenotype was probably linked to the presence of the MCA C-terminal domain within the cells. Nevertheless, a few WT[MCAΔCterm-GFP] transfectants had a growth defect. Western blot analysis with anti-GFP antibodies revealed that one of these slow growing transfectants was expressing the expected size MCAΔCterm-GFP, while the transfectants which grew normally contained a shorter protein that was most likely N-terminally truncated (**figure 6.1H**). Also, the WT[ΔproMCAΔCterm-GFP] transfectants were all found to express the expected size protein. However, the anti-GFP antibodies also detected a ~30 kDa protein (**figure 6.1H**), suggesting that ΔproMCAΔCterm-GFP was processed near its C-terminus. Taken together, these data indicate that the metacaspase is processed in both its N- and C-termini and that the N-terminal domain of MCA might be associated with the growth phenotype. Furthermore, it seemed that the cleaved domains, and the C-terminal one in particular, might be slightly larger that the ones predicted initially (**chapter 4**). To assess if the previously generated Nterm-GFP and Cterm-GFP constructs were too short to be able to target the protein properly or allow its interaction with other proteins, new constructions encoding extended N- and C-terminal domains of MCA (101 and 179 amino acids, respectively) were generated (to give eNterm-GFP and GFP-eCterm). In addition, in case both the N- and C-terminal

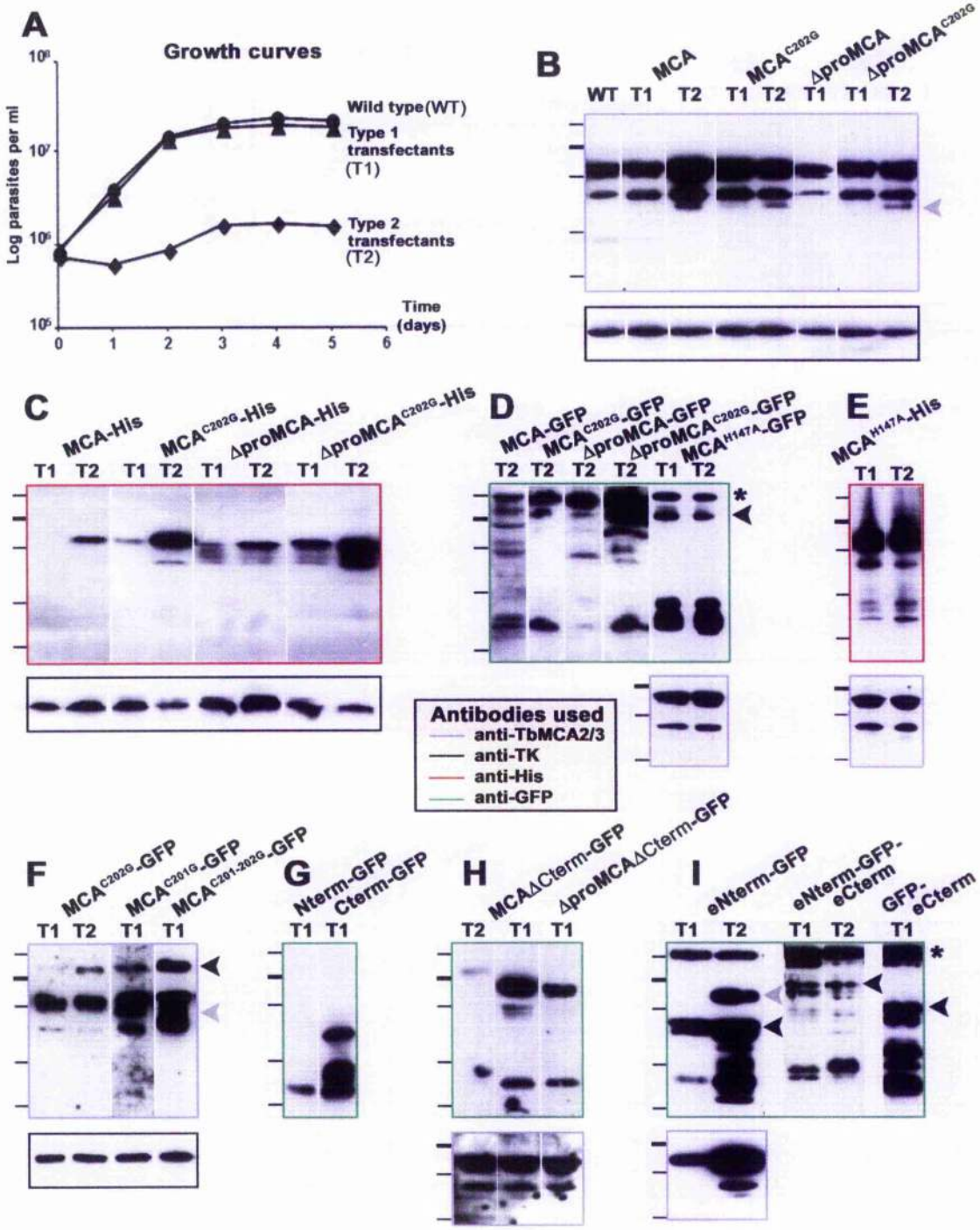

Figure 6.1: Analyses of *L. major* transfectants expressing MCA variants

Transfectants showing (Type 2, T2) or not (Type 1, T1) an impaired growth phenotype and a tetraploid DNA content were analysed. A) Representative growth curves. B-I) Western blot data. For each blot, a colour code indicates the antibodies that were used (legend in the yellow box). TK refers to *L. mexicana* transketolase (70kDa). Molecular masses are indicated on the left and show, from top to bottom: 83, 62 (thicker band), 47.5, 32.5 and 25 kDa control proteins. Proteins of interest are indicated with a black arrow head, those of unknown identity are shown with a grey arrow head. (*): cross-reacting band of ~83 kDa seen with the anti-GFP antibodies.

domains of MCA are needed for the protein's proper targeting, an additional construct with both domains was produced (eNterm-GFP-eCterm). The plasmids encoding these MCA variants were then transfected and expressed in *Leishmania*. Surprisingly, while initially growing at a rate comparable to the wild type, the cell lines expressing the construct with the extended N-terminal domain of MCA started to be impaired in their growth after about two weeks in culture (**table 6.1.**). Thus, this domain of MCA seems to be able to mediate the appearance of the overexpression growth phenotype. Western blot analyses were performed (**figure 6.1I.**) and are detailed in the section below. In addition, the cellular localisation of these last MCA variants was assessed and unexpectedly gave new insights into the potential functions of MCA (**section 6.1.3**).

6.1.2. Phenotype analyses

6.1.2.1. Altered growth rate

In the previous section, I described the different constructs that were generated for the study of MCA function as well as the rationale behind their design. Also, to make the analysis of the results easier, I only referred to the primary screen of the transfectants isolated, which was based on their growth rate compared to the wild type. Many growth experiments were performed, but again, to simplify, I decided to present a single example (expressors of non-tagged MCA, WT[MCA], **figure 6.1A**). Also it should be noted that the expression of the different variants of MCA being based on episomal systems (Kelly et al., 1992; Tetaud et al., 2002), thus the plasmid copy numbers and subsequently the levels of protein expression could vary from one cell to the another. Therefore, it was impossible to compare the growth rate of the developmentally-affected transfectants between one MCA variant and another, as there were already some growth rate variations within groups of transfectant expressing the same MCA variant. Accordingly, transfectants expressing the same MCA variant were classified in two groups. Type 1 refers to the transfectants that were growing at a rate comparable to the wild type cells while type 2 included all those that had an impaired growth rate (**figure 6.1A**). It was observed that while the transfectants coming from populations were generally growing like the wild type cells, most of those that were clonal were classified as type 2. Whether this finding results from the prolonged selection time of the clone compared to the population or reflects MCA involvement in growth from a single cell remains unclear.

Also, Western blot analyses were performed to detect any possible correlation between the level of expression of the MCA variants and the severity of the growth phenotype observed.

6.1.2.2. Western blot analysis

For most cell lines obtained there was a relationship between the level of expression of the MCA variants and the occurrence of a type 2 phenotype. Indeed, type 2 transfectants in the main expressed more MCA variant than the type 1 cell lines (**figure 6.1B, C, D**). Thus the evidence suggested that the observed phenotype was not due to the presence of the shuttle vectors within the cell or to the transfection procedure but truly to the expression of the protein of interest.

However, in some particular cases it was impossible to establish such a correlation. Indeed, for MCA^{C202G}, $\Delta proMCA^{C202G}$ (**figure 6.1B**), MCA^{H147A} (**figure 6.1D, E**) and eNterm-GFP-eCterm (**figure 6.1I**), there was no obvious difference in the level of expression of either the variant MCA and the wild type MCA between the type 1 (**T1**) and type 2 (**T2**) transfectants. While the type 2 phenotype remains unexplained for cells expressing MCA^{H147A}, the detection of additional protein products (**figure 6.1B, grey arrow head**) in type 2 transfectants expressing MCA^{C202G} and $\Delta proMCA^{C202G}$ compared to the type 1 transfectant expressing the same MCA variants suggest that alternative processing/degradation might be occurring in those former cells. Nevertheless, it was also observed that the expression of particular MCA variants was somehow affecting the expression of the wild type MCA. For example, expression of the GFP-fused extended N-terminal domain of MCA (eNterm-GFP), resulted in a considerable augmentation of the expression level of the wild type MCA (**figure 6.1I**).

The expression of various truncated forms of MCA allowed us to unravel some aspect of the processing of the protein *in vivo*. Indeed, removal of ~ 5 kDa and ~ 15 kDa peptides in the N- and C-terminal region of most of the MCA variants was observed. This was particularly distinguishable when performing Western blot using anti-GFP antibodies on the cell lines expressing MCAΔCterm-GFP and ΔproMCA ΔCterm-GFP (**figure 6.1H**). Interestingly, the wild type MCA seems indeed to be processed as a consistent pattern of protein products was observed (**chapter 5**). Furthermore, expression of non-tagged variants of MCA confirmed that the full length protein as well as the observed processing products, detected in the wild type with the anti-TbMCA2/3 antibodies, was indeed the *L. major* metacaspase (**figure 6.1B**). Nevertheless, it was impossible to clearly identify the positions within the peptide sequences where the cleavages occur.

Meanwhile, some MCA variants, MCA^{C201G} and $MCA^{C201-202G}$ for example, showed alternative processing with the appearance of additional protein band(s) on Western blots (**figure 6.1F, grey arrow head**). Whether this was due to break-down products or an impairment of their autoprocessing ability is still obscure. However, it is tempting to speculate that this alternative processing might impede the function of these MCA

variants, as none of the corresponding transfectants were found to be impaired in their growth and all were expressing a detectable amount of the protein of interest.

6.1.2.3. Tetraploidy

In my attempt to identify the cause of the lowered growth rate, a FACS analysis of the cellular DNA content was performed. While the type 1 transfectants had a diploid 2C-4C DNA content comparable to the wild type cells, all the type 2 transfectants had a tetraploid 4C-8C content (**figure 6.2A**). In several cases, an increase in the antibiotic pressure induced the appearance of a type 2 phenotype in transfectant previously classified as type 1. Therefore, concomitant with the growth impairment, the level of expression of the MCA variants is also linked with the tetraploidy phenotype. DAPI staining of representative type 2 cells showed that they had normal nuclear and kinetoplast configurations, but with twice the DNA content (**figure 6.2Cb**), indicating that the synchronisation between DNA duplication and its subsequent segregation is somehow impaired.

6.1.2.4. Defect in kinetoplast and nuclear division and cytokinesis impairment

In order to explain the tetraploidy phenotype, I decided to investigate whether cell cycle progression was somehow affected in the type 2 transfectants. To do so, a particular cell line was selected, in the present case, a type 2 transfectant expressing MCA without any tag (WT [MCA] type 2) was used, and a DAPI staining -based analysis of its nuclear and kinetoplast configurations was undertaken.

Comparison of the various cell configurations in WT [MCA] type 2 transfectant and wild type cells, revealed a reduction in cells in early mitosis ($1N^{*M}1K^{*}2F$, from 12.3% in WT to 0.9% in WT [MCA]), a moderate reduction of cells with two nuclei, two kinetoplasts and two flagella (2N2K2F, from 4.6% to 1.9%) and a doubling of cells with other configurations (from 10.0% to 20.6%) (**figure 6.2B, left panel**). Consistent with the decrease in the number of cells undergoing mitosis, an accumulation of aberrant cells with one or several mitotic nuclei (as indicated be the presence of a mitotic spindle, **figure 6.2Cd**) and multiple kinetoplasts and flagella were observed, indicating that mitosis was delayed in the WT[MCA] type 2 transfectants ("impaired mitosis", **figure 6.2B, right panel**). Additionally, most of the 2N2K2F cells had an aberrant positioning of the nuclei and kinetoplasts (**figure 6.2Cc**) and only very few were found to be undergoing cytokinesis (**figure 6.2B, left panel**). In WT [MCA] type 2 transfectants a high number of aberrant cells with differing configurations of nucleus,

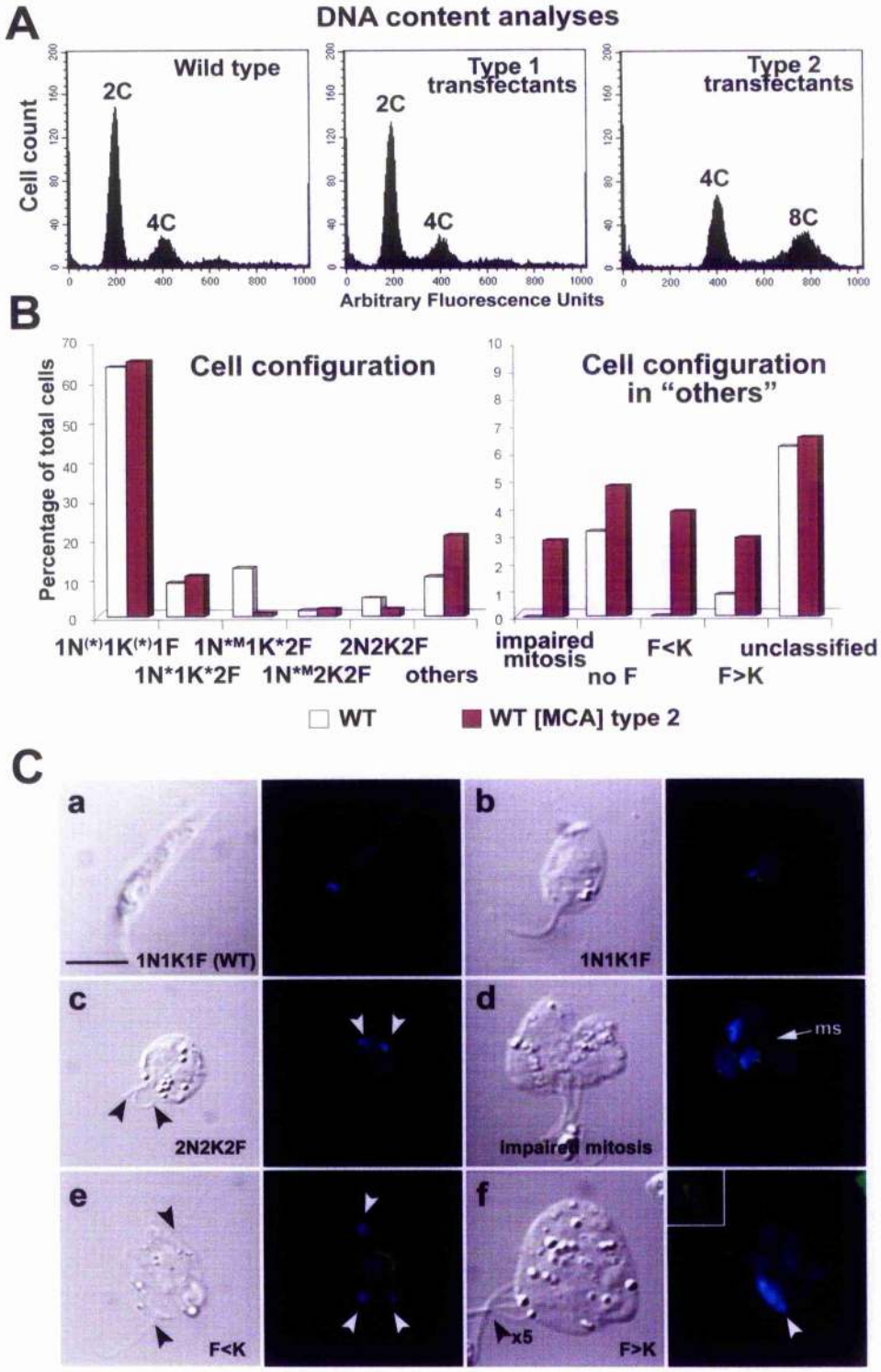

Figure 6.2: Phenotypes associated with the overexpression of MCA in *Leishmania*

A) FACS analysis of the cellular DNA content. Cell lines expressing MCA variants were classified as type 1 when growing at the same rate as wild type cells or as type II when showing an impaired growth rate. A representative example of the DNA content analysis performed on each of these groups is showed.

B) Classification of the various cell configurations observed in the wild type (yellow bars) and WT[MCA] type 2 (purple bars) cells, based on DAPI staining and cell morphology. Sub-groups of the cells classified in "others" are shown on the right panel.

N: nucleus; K: kinetoplast; F: flagellum; N^{*M}: nucleus in mitosis; F<K and F>K correspond to the cells with a number of nuclei different from the number of flagella and where the number of flagella was either smaller or bigger than the number of kinetoplasts.
C) Immunofluorescence performed on *L.major* wild type (a) and WT[MCA] type 2 cells (b-f). Fixed cells were labelled with rabbit anti-TbMCA 2/3 antibodies and Alexa Fluor 488-conjugated anti-rabbit antibodies (green). DAPI staining of the nuclear and kinetoplast DNA is shown in blue. Examples of a wild type and a WT[MCA] type 2 cells with one nucleus, one kinetoplast, and one flagellum (1F1K1F) are shown in a and b, respectively. Note the cell in b has a larger nucleus and kinetoplast than the wild type cell, due to its tetraploidy. Picture (c) shows a 2N2K2F cell in which the kinetoplasts and nuclei are not properly positioned within the cell. Aberrant cells with mitotic nucleus (ms, mitotic spindle in d), and fewer (F<K, e) or more (F>K, f) flagella than kinetoplasts are shown. White arrow heads identify kinetoplasts.

kinetoplast and flagellum were observed (**figure 6.2B, left panel and Cd-f**), suggesting a severe defect that caused de-regulation of cell cycle control.

6.1.3. Direct fluorescence localisation

Traditional immunolocalisation methods necessitate the fixation of the cells, which can alter the sub-cellular compartments and compromise the observation of the localisation of the protein of interest. Indeed, organelles such as the multivesicular tubule (MVT)/lysosomes in *Leishmania* are known to be particularly sensitive to fixation and tend to disintegrate under such conditions (Mullin et al., 2001; Besteiro et al., 2004). These restrictions were overcome by the use of the *Aequorea victoria* green fluorescent protein (GFP) as a localisation marker. The advantages of the GFP are that, once fused to the protein of interest, it allows the following of its movement within live cells and also the monitoring of dynamic cellular events (Gerdes and Kaether, 1996). Thus, data collected with GFP fusions are very likely to closely relate to the physiological behaviour of the corresponding wild type proteins.

GFP fusions of multiple MCA variants were designed to visualise the localisation of these proteins within the cell and establish whether differently processed proteins were trafficked to different intracellular compartment. I also wanted to assess whether the catalytic activity of MCA was necessary for its correct targeting and whether active and inactive MCA were present in distinct compartments. Furthermore, the existence within the MCA sequence of a predicted signal peptide suggested that this particular domain of MCA might play an important role in the localisation of the metacaspase. Also, as the proline-, glutamine- and proline- rich C-terminal extension of MCA might mediate protein-protein interactions, I wished to determine the intracellular localisation(s) of the MCA with this domain.

6.1.3.1. Full length protein and N-terminally truncated mutants

Theoretically a powerful tool, the use of the GFP as a fluorescent marker for the localisation of MCA rapidly showed its limitations. Indeed, as previously detailed, the expression of MCA-GFP and ΔproMCA-GFP was toxic for most of the transfectants and they had abnormalities such as an aberrant shape and DNA content and an impaired growth rate. For both protein variants, the only transfectant that was still behaving similarly to the wild type cells was actually expressing a barely detectable level of the protein of interest. Therefore, the intensity of the GFP signals, in those transfectants, was too low to be able to visualise the localisation of MCA-GFP and ΔproMCA-GFP.

6.1.3.2. N-terminal domain

Secondary structure software predictions suggested that MCA might contain a signal peptide in its N-terminus. A part of MCA N-terminus was fused to GFP (Nterm-GFP) to see if this region of the protein was targeting the protein to a specialised compartment/organelle within the cell. Nterm-GFP was found to be present in the cytoplasm of the transfectant cells. However, *in vivo* removal of a N-terminal fragment of MCA was confirmed by Western blot (see **section 6.1.2.2**) although there were doubts about the nature and the length of removed domain. Indeed, it was unclear whether this domain was acting as predicted as a target signal or if it was acting as a proregion. Experiments performed with plant type I metacaspases revealed that they were autocatalytically-processed after arginine/lysine residues, both in their N- and C-termini (Vercammen et al., 2004). Also, these metacaspases were found to possess a preference for GRR substrates. Thus, the MCA peptide sequence was analysed for the presence of similar residues. Three GR motifs were identified, two present in the MCA N-terminus, at positions 38 and 60, and one in MCA C-terminus (G297). The sizes of the potentially removed fragments based on these cleavage sites could fit with the molecular mass of the MCA processing products identified by Western blot. Furthermore, MCAΔCterm-GFP and ΔproMCAΔCterm-GFP, which still contained these GR motifs, were also processed in their N- and C-termini (refer to **section 6.1.2.2.**). Therefore it was probable that these motifs were genuine processing sites.

To determine where these cleavage events were occurring in the cell, extended regions of MCA N- and C-termini, of 101 and 179 amino acids respectively, were fused to the GFP (eNterm-GFP, GFP-eCterm and eNterm-GFP-eCterm) and expressed in *Leishmania*. Fluorescence observations performed on the live transfectants revealed that eNterm-GFP and eNterm-GFP-eCterm were located in a reticulated structure extending throughout the cell body. Co-localisation experiments with MitoTracker Red

CMXRos (Molecular Probes) indicated that both MCA variants were located in the mitochondrion (**figure 6.3Aa**). However, the wild type MCA does not seem to be present within the mitochondrial matrix (**figure 6.3Ab**). The data collected with GFP-eCterm are detailed below.

6.1.3.3. Catalytic mutants and C-terminal domain

Even though the expression of various catalytic mutants of MCA was inducing type 2 phenotypes in clonal transfectants, viable cell lines expressing lower level of those protein variants were obtained. Thus the localisations of MCA^{C202G}-GFP, $\Delta proMCA^{C202G}$-GFP and MCA^{H147A}-GFP could be assessed. The fluorescent signals observed for the three protein variants were strikingly similar to each other and those detected for GFP-eCterm. An example of these observations is shown in **figure 6.3B**. While the majority of the detected GFP signal was cytosolic, various discrete localisations within the cell were also labelled. Fluorescent punctate structures were seen mainly at the tip of the cell (**white arrow heads**) but also moving along the cell body and the flagellum (**white arrow**). A tubular structure was also visualised in some cases (**grey arrow**). However, the use of various dyes such as the FM4-64 and the MitoTracker Red CMXRos (Molecular Probes), respective markers of the MVT-lysosome and the mitochondrion, failed to identify the nature of these compartments. The dynamics of the GFP labellings lead us to postulate a potential association of these MCA variants with the microtubular network.

Interestingly, the extended C-terminal domain of MCA fused to GFP (GFP-eCterm) showed similar localisations within the cells. It could be argued that the punctate signals might actually reflect the trafficking of GFP degradation products. However such labelling was not visible in cell lines expressing the GFP only or Cterm-GFP, a MCA protein variant that was extensively processed as determined by Western blot (**figure 6.1G**). This finding raises the possibility that MCA interacts with microtubules trough its C-terminal proline-, glutamine- and tyrosine-rich domain.

MCA^{C201G}-GFP and $MCA^{C201-202G}$-GFP were found to be present in the cytosol of the overexpressing cells. No motile punctate structures could be detected.

6.1.4. Association with the cytoskeleton

Consistent with these observations, I previously characterised the wild type MCA as a protein partially associated with cytoskeletal microtubules (see **chapter 5**). However, basic proteins (such as MCA is predicted to be) have been reported to bind to tubulin in a non-specific manner (Robinson *et al.*, 1991). Nevertheless, the fact that several GFP-fused MCA variants, which possessed lower predicted pIs, were present

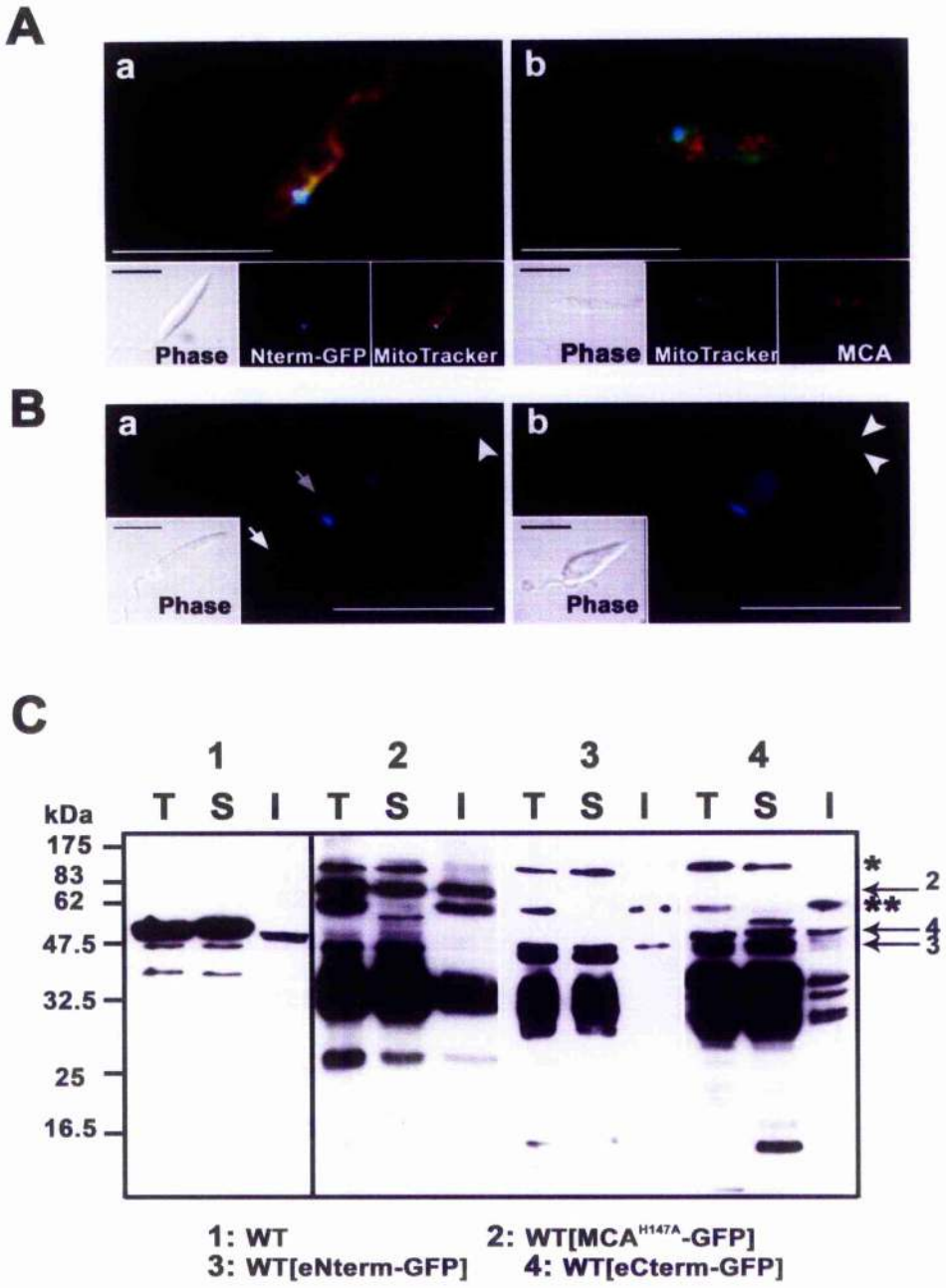

Figure 6.3: Localisation of several MCA variants within the cells.

Panel A. (a) Live fluorescence observation of eNterm-GFP (green). The mitochondrion was labelled in red with the MitoTracker Red CMXRos (Molecular Probes). Co-localisation is shown in yellow. (b) Immunolocalisation of MCA in wild type cells. The mitochondrion was labelled in green (MitoTracker Green, Molecular Probes) before fixation.
Panel B. Examples of the fluorescent signals observed in cells expressing MCA^{C202G}-GFP, $\Delta proMCA^{C202G}$-GFP, MCA^{H147A}-GFP and eCterm-GFP (green). The kinetoplast and nuclear DNA were stained with DAPI (blue). Scale bar =10 μm. C) Association of MCA and other variants with the cytoskeleton microtubules. Promastigotes were extracted with 0.5% Nodinet P40 in PEME buffer. The total (T), soluble (S) and insoluble (I) fractions were analysed by SDS-PAGE, transferred to a PVDF membrane and immunoblotted with rabbit anti-TbMCA2/3 (panel 1) or mouse anti-GFP (Clontech) antibodies. (*) and (**) indicate soluble and insoluble cross reacting protein bands, respectively, on panels 2,3 and 4.

within motile sub-cellular structures, suggested that MCA interaction with microtubules was real. To confirm this finding, experiments previously performed with the wild type MCA were repeated with diverse MCA variants.

6.1.4.1. Overexpressors of MCA^{H147A}-GFP

After extraction in PEME buffer with 0.5 % NP-40, while most of MCA^{H147A}-GFP processing products were present in the soluble fraction, a large part of the full length protein variant remained associated with the cytoskeletal microtubules (**figure 6.3C, panel 2, arrow 2**). It was previously observed that the wild type MCA was also able to associate with the cytoskeleton (**chapter 5** and **figure 6.3C, panel 1**). However, the proportion of protein interacting with these microtubules seems to be lower for the wild type MCA than for MCA^{H147A}-GFP. It is still unclear whether this accumulation of MCA^{H147A}-GFP with the cytoskeletal network results from the overexpression of the protein or the fact that it is potentially catalytically inactive. This experiment will have to be repeated with overexpressors of active MCA variants.

6.1.4.2. Overexpressors of eNterm-GFP

To exclude the possibility that the association of MCA^{H147A}-GFP with the cytoskeleton might be an artefact due to the presence of the GFP, the experiment was repeated with a cell line expressing eNterm-GFP. Consistent with its presence in the mitochondrial matrix, eNterm-GFP was found to be present mainly in the soluble fraction of the detergent-treated cell extracts (**figure 6.3C, panel 3, arrow 3**). Therefore, the GFP does not seem able to mediate interactions with the microtubular network.

6.1.4.3. Overexpressors of eCterm-GFP

Direct fluorescence observations revealed that the localisation within the cell of eCterm-GFP was comparable to that of MCA^{H147A}-GFP. Therefore, detergent extractions were performed on cells expressing eCterm-GFP to assess whether the C-terminal domain of MCA was promoting interaction with the cytoskeleton. While most of the protein was processed, only a very small portion of eCterm-GFP remained associated with the sub-pellicular microtubules (**figure 6.3C panel 4, arrow 4**). Therefore, it seems unlikely that this C-terminal region of MCA would, by itself, be able to mediate the binding of MCA to the cytoskeleton.

As observed for the wild type MCA (**chapter 5**), the proportion of MCA^{H147A}-GFP, eNterm-GFP or eCterm-GFP associated with the cytoskeleton does not seem to change with cell cycle progression (data not shown).

6.2. Expression in *Escherichia coli*

I initially attempted to produce recombinant MCA for two reasons. First, to immunise rabbits and induce the production of anti-MCA polyclonal antibodies. Secondly, to assess the potential *in vitro* enzymatic activity of MCA toward a range of substrates and its sensitivity to inhibitors.

The pET28a (+) vector was used to generate N- and/or C-terminally polyhistidine tagged variants of MCA. Constructs allowing the expression of MCA-His, His-ΔproMCA, and MCA^{C202G}-His were produced and transformed into *E. coli* BL21(DE3) cells. Initial expression trials and the subsequent sample analyses revealed that these protein variants were expressed at a low level and were mainly present in inclusion bodies. We tried to optimise the expression conditions by increasing the induction time, lowering the induction temperature or using a different bacterial host (BL21(DE3)pLys), but none yielded satisfactory expression. Therefore, we were unable to achieve either of the two initial aims of this part of the project. However, even when expressed at a low level, processing of the different MCA variants was observed. Like in *L. major* cells, Western blot using antibodies against MCA or against the histidine tag revealed a pattern of multiple protein bands and suggested proteolytic cleavage was occurring in both the N- and C-termini of MCA (data not shown).

6.3. Expression in *Pichia pastoris*

The low level of expression and the extreme insolubility of different MCA variants in *E. coli* suggested the proteins were toxic for the bacteria. Therefore, a different expression host, *Pichia pastoris*, was evaluated.

As a yeast, *P. pastoris* has many of the advantages of higher eukaryotic expression systems such as protein processing, protein folding, and post-translational modifications but is easier and less expensive to use than other eukaryotic expression systems such as baculovirus or mammalian tissue culture, and generally gives higher expression levels. Furthermore, in association with the pPIC9 vector, this system allows the secretion of the expressed recombinant protein in the culture medium, thus limiting the potential toxicity of the protein for the cell and facilitating its purification process.

As a methylotrophic yeast, *P. pastoris* is capable of metabolizing methanol as its sole carbon source. The methanol metabolism initiates with the oxidation of methanol into formaldehyde and hydrogen peroxide, a process mediated by alcohol oxidase (AO).

Also, to avoid hydrogen peroxide toxicity, methanol metabolism takes place within the peroxisome, a specialized organelle that sequesters toxic by-products from the rest of the cell. Furthermore, as the alcohol oxidase has a poor affinity for oxygen it is expressed at a high level by the cell. Thus, the *Pichia* system uses the promoter of the AO to drive the expression of heterologous protein. After integration of the gene of interest into the alcohol oxidase (*AO*) locus, the expression of the recombinant protein starts upon addition of methanol into the yeast culture medium and activation of the methanol-inducible *AO* promoter. For more detail about the *Pichia* system, please refer to the Material and Methods section (**chapter 2**).

The principal aim of this approach being the production of active MCA to facilitate biochemical characterization of its enzymatic properties, constructs allowing the expression of the full length active MCA, but also truncated variants ΔproMCA, MCAΔCterm, ΔproMCAΔCterm, were generated. All of them were fused in their N-termini with the α-factor secretion signal. The linearised plasmids were then transfected into *Pichia*. After verification by PCR of the correct integration of the expression cassette into the *Pichia* genome, expression trials were performed. In parallel, a control cell line expressing and secreting bovine albumin was used. After about 10 days of methanol induction, 24 hours time point samples were analysed by SDS-PAGE, Coomassie staining and Western blot.

While in the control cell line the production of albumin was easily detectable, expression of the various MCA variants could not be visualized. Western blot analysis revealed that the MCA variants were probably expressed, but at a very low level and within the cell. This finding was most unexpected and suggested both that the multiple MCA variants were not efficiently translated and that they were somehow not properly secreted and so retained within the cell. The weak expression of the MCA variants could be explained by the poor codon bias for *Pichia* (Sinclair and Choy, 2002). As for the absence of recombinant protein secretion, one possible explanation was that the N-terminal signal sequence of MCA was interfering with the α-factor secretion factor, thwarting its correct trafficking and liberation into the culture medium. However, ΔproMCA and ΔproMCAΔCterm constructs, which lacked the first 21 N-terminal residues of MCA, also lacked significant expression and were not secreted. Thus, the secretion problem was either not due to the N-terminal domain of MCA or the domain removed was too short and there was still, in ΔproMCA, a conflicting region. Therefore a new expression construct was generated where a bigger part of the N-terminus of MCA was removed (the first 73 amino acids, ΔeproMCA and ΔeproMCAΔCterm). Attempts to produce these MCA variants were made and the results are presented in **figure 6.4**. A cell line previously created, ΔproMCAΔCterm, was used as a negative expression

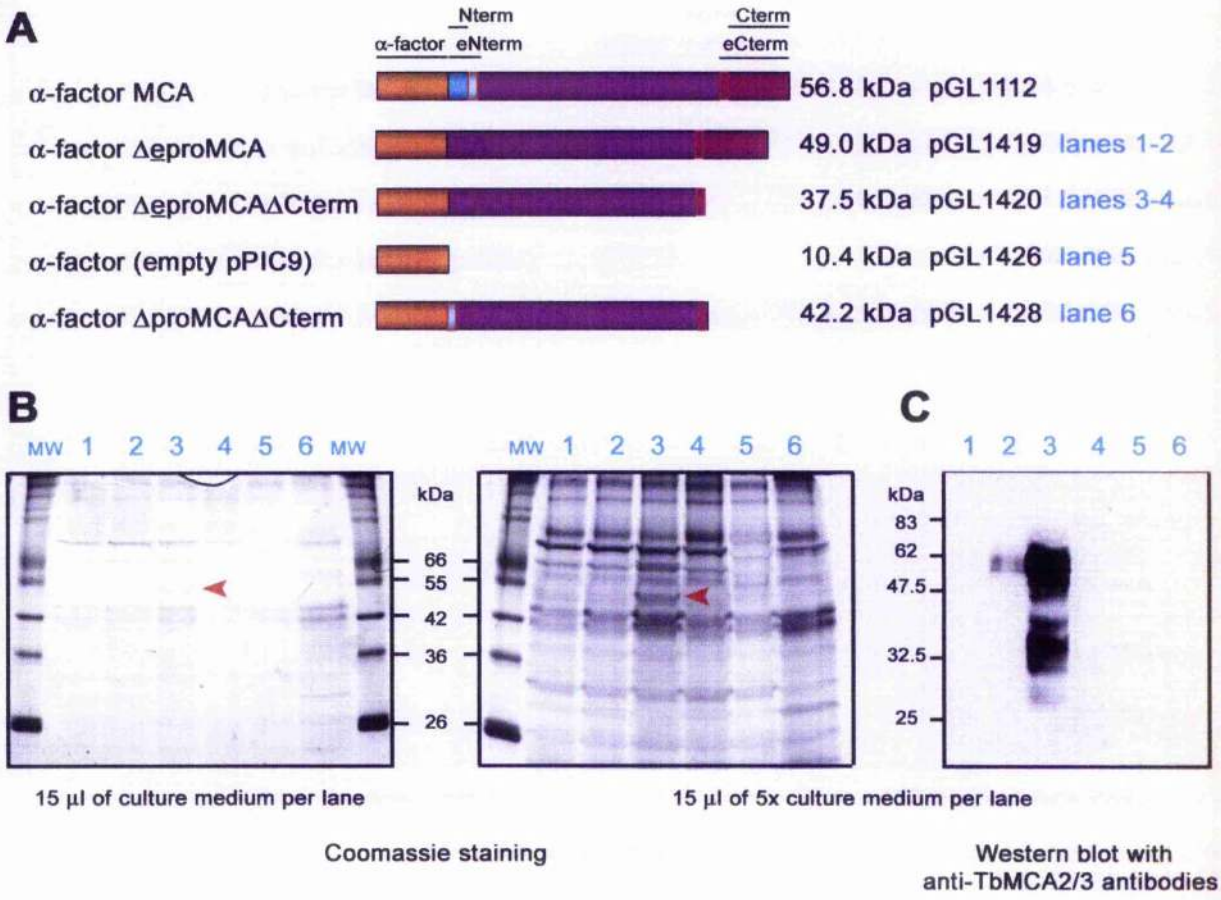

Figure 6.4: Expression of several MCA variants in *P. pastoris*.

A) Schematic representations of the MCA variants expressed.
B) SDS-PAGE analyses of culture medium samples after induction with methanol for 217 hours. Secreted proteins were visualised by Coomassie staining. The red arrow head indicates the presence of an additional protein. On the right panel, culture medium samples were concentrated 5 times.
C) Western blot analysis performed using anti-TbMCA2/3 rabbit antibodies. The experiment was performed on concentrated culture medium samples.

control. Culture media of the different *Pichia* transfectants, concentrated (**figure 6.4B, right panel**) or not (**figure 6.4B, left panel**) were analyzed, by SDS-PAGE and/or Western blot, for the presence of the secreted MCA variants. As indicated in **figure 6.4B** by a **red arrow head** there was, in the culture medium of one (**lane 3**) of the transfectants expressing ΔeproMCAΔCterm, an additional protein compared to the secretion pattern of the other transfectants. However the size of the protein detected (~50 kDa) was much bigger than the expected size of ΔeproMCAΔCterm (37.5 kDa) (**figure 6.4A**). Therefore, a Western blot was carried out and probed with anti-TbMCA2/3 antibodies to check the identity of the additional secreted protein (**figure 6.4C**). The additional protein was thus recognized as the metacaspase variant. One possible explanation for the increased molecular weight of ΔeproMCAΔCterm is the

addition of bulky glycans to the protein by *Pichia*. Indeed, the *Pichia* expression system was initially chosen because it allows eukaryotic post-transcriptional modifications, and glycosylation is one of them. Also, *Pichia* is known to add N-linked oligosaccharides that are larger than the ones used by *Leishmania* for its post-translational modifications (Grinna and Tschopp, 1989; Parodi, 1993; Montesino et al., 1998). There are 7 glycosylation sites predicted in MCA (**chapter 4**) and so it is reasonable to expect that the MCA variant would be glycosylated in *Pichia*. It is still unknown whether such modifications occur in *Leishmania*.

6.4. *In vitro* translation

I previously reported the advantages of the *Pichia* expression system and although it proved to be relatively efficient, many aspects of this method of production render its utilisation unaccommodating. The need to check for the integration of the expression constructs, the long induction periods and the heavy glycosylation that might compromise the functionality of the expressed protein are many of the factors that restrict its use. We tried to overcome these limitations by using a cell-free protein biosynthesis system (or *in vitro* translation system). The method chosen (EasyExpress, Qiagen) generates proteins by coupled or successive transcription and translation, in cell-free extract of prokaryotic cells. It possesses many advantages, among which are its rapidity (as it is theoretically possible to use PCR product templates for protein synthesis), the possibility to produce toxic protein and the simplification of the purification process.

Having already generated constructs for the expression of various MCA variants in *E. coli*, the *in vitro* translation was performed using one of these plasmid DNAs as a template (pET28a(+)-MCA (pGL1421)), in order to express a C-terminal His-tagged full length MCA (MCA-His). In parallel, the reaction was performed with a control DNA that encodes the elongation factor EF-Ts with a C-terminal His-tag (32 kDa). After a 1 hour incubation at 37°C, the protein production was stopped and the His-tagged proteins were purified by Nickel-affinity. The samples were then further analysed by SDS-PAGE (**figure 6.5, left panels**). While the positive control protein was easily detectable on a Coomassie stained gel (**figure 6.5B, black arrow head**), it was difficult to determine whether MCA-His was expressed (**figure 6.5A**). Therefore, a Western blot using anti-TbMCA2/3 antibodies was performed (**figure 6.5, right panels**). The production of the protein of interest was thus confirmed and the efficiency of its purification validated.

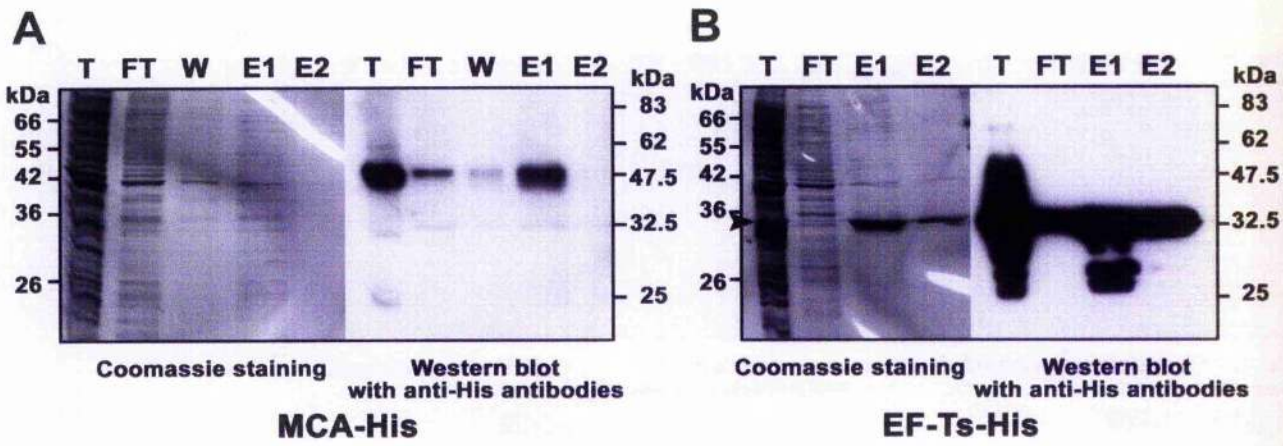

Figure 6.5: Purification of His-tagged proteins expressed using an *in vitro* translation kit.

His-tagged MCA (A) or elongation factor-Ts (B) were affinity purified by Nickel chelate affinity chromatography under native conditions, from 50 µl of an Easy Express Protein Synthesis Mini Kit (Qiagen) *in vitro* translation reaction. Protein samples were then analysed by SDS-PAGE and visualised by Coomassie staining (left panels) or by Western bot, using anti-polyhistidine mouse antibodies (Qiagen) (right panels). T: total fraction; FT: flow through; W: wash; E1 and E2: first and second elution fractions.

6.5. Discussion

6.5.1. Metacaspases locatisations and functions

In the yeast *S. cerevisiae*, heterologous expression of TbMCA4 resulted in a petite phenotype. In these cells, mitochondria had a reduced thiol content compared to mitochondria from wild type cells. Thus, TbMCA4 expression seems, in yeast, to be acting on the metabolic state of the mitochondrion (Szallies *et al.*, 2002). TbMCA1, TbMCA3, TbMCA5 and LmajMCA, but not TbMCA2 and TbMCA4, are predicted to possess a signal peptide at their N-terminus, indicative of a possible specific intracellular targeting (**chapter 4**). While little is known of the nature of the predicted signal peptide at the N-terminus of the *T. brucei* metacaspases, we observed here that this region of LmajMCA was targeting the GFP to the mitochondrion (**figure 6.3Aa**). The fact that a short region of the LmajMCA N-terminal sequence was not able to target the GFP (Nterm-GFP) to the mitochondrion, while a longer domain (eNterm-GFP) could, shows that at least 21 amino acids of the domain are required for targeting. In the absence of the complete signal peptide sequence, interaction with the translocon apparently did not occur and Nterm-GFP was left in the cytoplasm.

In mammalian cells, a consensus sequence of a few amino acids is enough to target a protein to the mitochondrion. No such signal was predicted to be present in LmajMCA using algorithms based on mammalian mitochondrial targeting sequences, such as MITOPROT (http://ihg.gsf.de/ihg/mitoprot.html). Also, it was possible that the observed mitochondrial targeting of eNterm-GFP was an artefact and did not reflect the behaviour of the wild type LmajMCA. However, another construct, much larger and likely to possess a different tertiary fold, eNterm-GFP-eCterm, was also found in the mitochondrion. Furthermore, phylogenetic analyses indicate that metacaspases might have been introduced into eukaryotes by their mitochondrial endosymbiont (Koonin and Aravind, 2002), thus the metacaspases might still possess a physiological function within the mitochondrion, as suggested by TbMCA4 expression in yeast and the localisation of the extended N-terminal domain of LmajMCA. Consistent with these observations, immunolocalisation of the wild type LmajMCA, revealed that it temporally associates with the mitochondrial DNA during kinetoplast segregation (**chapter 5**). It is likely that, to be able to access this organelle, the metacaspase will need to be translocated into the mitochondrion first. In *T. brucei*, a kinetoplast protein overexpressed as a GFP fusion was shown to be present throughout the mitochondrion and not only its DNA (Klingbeil *et al.*, 2002). Therefore, it is possible that the fluorescence detected throughout the mitochondrion for eNterm-GFP and eNterm-GFP-eCterm are some overexpression artefacts and that the N-terminal domain of LmajMCA actually targets the protein to the kinetoplast. Nevertheless, other yet uncharacterised regions of LmajMCA might also target LmajMCA to the kinetoplast after its entry into the mitochondrion via its N-terminal domain.

The N-termini of caspases and plant metacaspases were shown to contain prodomains whose removal was required for acquisition of full enzymatic activity (Earnshaw et al., 1999; Vercammen et al., 2004). The plant metacaspase AtMCA9 is able to process its small N-terminal prodomain through its R/K substrate specificity (Vercammen et al., 2004). Substrate profiling experiments revealed that this enzyme preferred GRR (Vercammen et al., 2004) but also VRPR/I (Vercammen *et al.*, 2006) peptide substrates. Interestingly, GRR and VRPI motifs were found in MCA N-terminus at positions 38-40 and 45-48, respectively, thus namely between the regions used for the construction of Nterm-GFP (residues 1-21) and eNterm-GFP (residues 1-101). Thus, although data are missing to confirm this hypothesis, either of these motifs could be sites for autocatalytic processing of MCA. Therefore, LmajMCA might contain in its N-terminus not only a targeting signal but also a prodomain and consequently might possess a preprodomain. This LmajMCA N-terminal preprodomain would present the advantages of not only controlling the intracellular localisation of the metacaspase but also of regulating its activity. After targeting into the mitochondrion, the pre-domain

would be removed by signal peptidase and the pro-domain autoprocessed to ultimately obtain a fully functional LmajMCA. The protein ΔeproMCAΔCterm, which starts at residue 74, lacks this predicted preprodomain. Interestingly, it was the only LmajMCA variant that was successfully expressed by *Pichia* and secreted in the culture medium. Unfortunately, we were unable at the time to determine the substrate specificity of LmajMCA and thus determine if it was capable of autoprocessing. Consequently, it is still unclear whether the processing of the N-terminal prodomain of LmajMCA can be done autocatalytically.

For caspases, interacting peptidases such as Granzyme B have been shown to be necessary for their processing and activation (Stennicke and Salvesen, 2000). If such a process applies to LmajMCA then the compartment in which the metacaspase will become active would depend on the location of the activating enzyme(s). Thus, a LmajMCA protein activated in the cytoplasm would not translocate to the mitochondrion, whereas a non-processed protein would enter the mitochondrion and become active after removal of the N-terminal preprodomain. Both of these situations might be occurring in the cell as LmajMCA was found to be present in different compartments. Constitutively present in punctate structures throughout the cell, LmajMCA transiently relocates to the kinetoplast and then to the mitotic spindle during nuclear division (see **chapter 5**). Also, in the event where LmajMCA becomes active in the cytoplasm, the removal of the N-terminal preprodomain might expose a second targeting signal and thus promote LmajMCA translocation into the nucleus. The presence of LmajMCA in this organelle can also be achieved by either direct or indirect (thought motor protein) association of the active metacaspase with microtubules. These different intracellular locations suggest that metacaspases play several roles in the cell, some in the kinetoplast and others in the nucleus, and that these functions might be interconnected. Indeed, analysis of the phenotypes associated with the overexpression of LmajMCA variants showed that LmajMCA was likely involved in kinetoplast and nuclear segregation and cell cycle progression.

In *T. brucei*, it is well established that kinetoplast division and cytokinesis are cytoskeletal microtubule-mediated events (Robinson *et al.*, 1995; Vedrenne *et al.*, 2002). We showed previously that LmajMCA associates partially with the cytoskeleton. Here we found that several MCA variants (mostly GFP-fusions) associated with subpellicular microtubules. Live fluorescence observations suggested that the MCA C-terminal domain (eCterm-GFP) might be involved in these interactions, although fractionation experiments failed to confirm this hypothesis. Although many aspects of LmajMCA processing remain obscure, it seems that the N- and C-terminal domains of this protein are likely to be important for its function.

6.5.2. Expression of MCA variants in different systems

One initial aims of my thesis project was to determine whether MCA functions as a peptidase and to identify the residues involved in its catalytic activity. Unfortunately, expression of various MCA variants, in both bacterial and eukaryotic systems, failed to provide sufficient amount of recombinant protein to perform biochemical studies. However, one promising lead remains. Although it needs scaling up, the *in vitro* translation method proved to be moderately efficient and easy to perform. Thus additional constructs were created to allow the expression of potentially catalytically inactive MCA variants (MCA^{C201G}, $MCA^{C201-202G}$, MCA^{C202G} and MCA^{H147A} with C-terminal His tags). Hopefully, future work using these constructs together with *in vitro* translation will lead to a better understanding of MCA catalytic processes.

Meanwhile, the various phenotypes observed, in *Leishmania*, upon expression of MCA^{C202G}-GFP and MCA^{H147A}-GFP might be explained by: i) these MCA variants being still catalytically active and their expression being toxic for the cell when above a certain threshold; ii) the fact that MCA function is conferred by its structural properties but not by any enzymatic activity; iii) the possibility that if MCA is present in the cell as homo-oligomers or within a complex then the overexpressed MCA^{C202G}-GFP and MCA^{H147A}-GFP would take part to these complexes and therefore cause the same phenotype as when overexpressing MCA-GFP (via a dominant negative effect). However, several observations suggest that the latter two hypotheses are more likely to be true. First, we have so far no evidence that the enzymatic activity of MCA is directly responsible of the observed overexpression phenotypes. While WT [MCA^{C202G}-GFP] and WT [MCA^{H147A}-GFP] overexpressors had a growth defect, most of the WT [MCA^{C201G}-GFP] and WT [$MCA^{C201-202G}$-GFP] overexpressors lacked such phenotype. Also, it was observed that MCA^{C201G}-GFP and $MCA^{C201-202G}$-GFP were processed differently than MCA^{C202G}-GFP and MCA^{H147A}-GFP, with the appearance of an additional protein (**figure 6.1F, grey arrow**). Thus it seems likely that the absence of phenotype in the WT [MCA^{C201G}-GFP] and WT [$MCA^{C201-202G}$-GFP] overexpressors was not likely to be linked with an alteration of the catalytic activity of the proteins, but rather due to their alternative processing and a modification of some of their properties. In addition, it appeared that overexpression of MCA variants lacking the 102 C-terminal amino-acids gave, in most cases, no particular phenotype. Although it is tempting to postulate that the MCA C-terminal extension might be involved in the observed overexpression phenotype, it was impossible to establish whether the disappearance of such phenotype in WT [MCAΔCterm-GFP] and WT [ΔproMCAΔCterm-GFP] transfectants was due to the removal of the C-terminal interaction module or to the expression of severely shortened and therefore incomplete and non functional

proteins. However, evidence that the function of MCA within the cell relies on its structural properties rather than solely on its enzymatic activity were given by the observation that the expression of eNterm-GFP was in itself able to reproduce a phenotype induced by the expression of full length MCA.

Indeed, although eNterm-GFP lacks the catalytic domain of MCA, it seems able to influence the level of expression of the wild type MCA therefore suggesting a potential interaction between these two proteins. Also it is possible that in complex with MCA, eNterm-GFP might facilitate the translocation of this protein into the mitochondrion. The possibility that the growth phenotypes observed upon expression of various MCA variants resulted from their aberrant accumulation within the mitochondrion was considered. However, cell fractionation experiments revealed that while eNterm-GFP was mainly soluble, most of the MCA variants were associated with the sub-pellicular microtubules fraction, thus excluding their possible gathering in the mitochondrion. Nevertheless, it was shown previously that the accumulation of eNterm-GFP in the matrix of the mitochondrion was probably an overexpression artefact and that MCA was likely associated with the mitochondrial DNA. Therefore, the MCA variants being expressed at a lower level than eNterm-GFP might also be associated with the kinetoplast. Thus, the growth defect observed during the expression of these multiple MCA variants could be the result of the accumulation of MCA in the kinetoplast. However, direct fluorescence observations failed to confirm this hypothesis. On the other hand, the N-terminal domain of MCA might be able to mediate protein-protein interactions and association with MCA partners. In that case, expression of eNterm-GFP but also all the MCA variants carrying this domain would induce a dominant negative effect and the appearance of the type 2 phenotype.

To understand the mechanisms by which MCA generates this defined overexpression phenotype, it is essential to characterize the proteins interacting with MCA within the cell. Indeed, the identification of protein partners might give some clue about not only the substrate specificity of the metacaspase but also about its function within the cell.

Chapter 7:
Characterisation of *Trypanosoma brucei* metacaspases

I also attempted to determine the biological function(s) of metacaspases in trypanosomatids by investigating the role of three metacaspases of *T. brucei*, TbMCA2, TbMCA3 and TbMCA5. Also, before presenting the data produced by Matthew J. Helms in the context of his PhD thesis (2004) as well as the new set of findings concerning these proteins, I would like to introduce some relevant aspects of *T. brucei* biology.

7.1. *Trypanosoma brucei* and Trypanosomiasis

Although *Leishmania* spp. and the African trypanosome *Trypanosoma brucei* are both parasitic protozoa from the Kinetoplastidae order and Trypanosomatidae family, there is a vast genetic distance between them (Vickerman, 1994). While both possess a diphasic life cycle, alternating between an insect and a mammalian host, the nature and the spectrum of the diseases they cause differ profoundly.

In contrast to *Leishmania*, which spends most of its mammalian stage as an intracellular form, *T. brucei* procyclic forms (PCF), transmitted during the bloodmeal of an infected tsetse fly (*Glossina spp.*), will remain as free living forms within the mammalian host blood, rapidly adapting and differentiating into the bloodstream forms (BSF). BSFs will divide and spread up to the point where their number will overtake the number of red blood cells, leading to severe anemia, one symptom of the sleeping sickness in human (for *Trypanosoma brucei rhodesiense* and *T. b. gambiense* infections) or Nagana in livestock (for *T. b. brucei*). After developing in the blood, lymph and peripheral organs, the parasites cross the blood-brain barrier and enter the central nervous system, where they cause serious neurological disorders, leading to coma and, if left untreated, death. It is estimated that sleeping sickness (or Human African Trypanosomiasis, HAT) causes 66,000 deaths each year, with 300,000 to 500,000 new cases reported annually. HAT is known to occur in 36 countries in sub-saharan Africa. *T. b. gambiense*, which causes chronic form of HAT, is found in central, west and some parts of Eastern Africa while *T. b.rhodesiense*, responsible of acute HAT, is present in Southern and Eastern Africa. Treatment has always been difficult, especially when the disease has reached an advanced stage with central nervous system involvement, as few effective drugs are available. Pentamidine is not effective against late-stage disease and some parasite strains are resistant to it. Suramin has to be administered intravenously and can have adverse side-effects. Melarsoprol, an arsenical drug developed over 50 years ago, is used against late-stage disease, but often induces serious - sometimes fatal side-effects. Eflornithine, originally developed as an anticancer agent, has shown promising results against the gambiense form but treatment is expensive and most of the time unaffordable for the affected patients.

After over 100 years of research in the field, trypanosomiasis is still highly prevalent. (www.who.int/tdr)

7.2. Introduction to *T. brucei* metacaspases

Antibodies raised against TbMCA2/3 or TbMCA5 were used to determine the expression profiles of these proteins in *T. brucei*. It was observed that TbMCA2 and TbMCA3 are exclusive to the mammalian bloodstream form (BSF) parasites, while TbMCA5 is expressed in both BSF and procyclic trypomastigote forms (PCF) at approximately equal levels. In addition, proteomic analyses (Mascot score: 126, peptides matched: 8) suggested that TbMCA4 is expressed in bloodstream form parasites (personal communication to genedb, M.A.J. Ferguson, D. Martin and I. Nett, http://www.genedb.org/genedb/FreeTextSearch?searchText=Full+Content+Search&q=MCA4&org=tryp). Finally, messenger RNA transcripts of *TbMCA1* to *TbMCA5* have successfully been amplified by reverse transcription-based PCR from *T. brucei* bloodstream forms (Szallies *et al.*, 2002).

Gene knock-out experiments demonstrated that *TbMCA2* and *TbMCA3* genes are non-essential *in vitro* within BSF parasites. Gene deletion of *TbMCA5* was done on wild type and *ΔTbmca2/3* bloodstream forms. *ΔTbmca2/3ΔTbmca5* cells showed a reduced growth rate compared to the wild type and while their morphology appeared normal, their movement was sluggish. This reduction in growth rate was not permanent however, as after several passages the growth rate returned to wild-type levels. This suggests that the *ΔTbmca2/3ΔTbmca5* mutants might be undergoing some form of adaptation to the loss of *TbMCA5* in the *ΔTbmca2/3* background. The fact that this phenomenon was not observed during *TbMCA5* knockout into BSF wild-type background does suggest that there is redundancy within the metacaspase gene family. *TbMCA5* was also shown to be non-essential for PCF. Nevertheless, as the expression patterns and functions of TbMCA1 and TbMCA4 remain uncharacterised, we can not rule out that these metacaspases could compensate for the loss of the others.

Cells lines allowing the silencing, by RNA interference (RNAi), of *TbMCA2*, *TbMCA3* and/or *TbMCA5* were also generated. RNAi is a mechanism of gene silencing which, after introduction of specific double stranded RNA (dsRNA) within the cell, leads to the selective down-regulation of the expression of the targeted gene. In *T. brucei*, production of dsRNA can be achieved by insertion of the chosen nucleic sequence between the two opposing T7 RNA polymerase promoters of the p2T7^{Ti} vector (LaCount *et al.*, 2000). Present downstream of the T7 promoters, a tetracycline operator allows the expression of dsRNA to be tetracycline-inducible. Meanwhile, T7 polymerase terminators ensure that only the inserted gene sequence is transcribed into dsRNA.

After linearization, the RNAi cassette integrates into the transcriptionally silent ribosomal DNA (rDNA) spacer regions of the *T. brucei* genome. A bleomycin resistance gene allows the selection of the vector within the transfected cells. For the system to work, transgenic BSF and PSF cell lines expressing the bacterial T7 RNA polymerase and the tetracycline repressor protein (TetR) were engineered (427 pLew13pLew90-6 and 427 pLew13pLew29, respectively) (Wirtz et al., 1999). The produced TetR protein binds to the tetracycline operator and blocks T7 RNA polymerase transcription of the targeted gene, until addition of tetracycline to the parasite culture medium (Wirtz *et al.*, 1994). Indeed, TetR possesses a higher affinity for tetracycline than for the tetracycline operator, so it preferentially binds to the tetracycline and undergoes conformational changes that ultimately prevent its DNA binding affinity. This removal of repression allows the T7 RNA polymerase to begin the transcription of the RNAi DNA cassette and production of the specific dsRNA. A complex cellular machinery then process the synthesized dsRNA into 20-26 base-pair fragments (siRNA) and unwinds them, allowing specific recognition of and degradation of the target mRNA (LaCount and Donelson, 2001). In the case of *TbMCA2*, *TbMCA3* and/or *TbMCA5* silencing, the RNAi data suggested that *TbMCA2* and *TbMCA3* in the BSF and *TbMCA5* in both BSF and PCF are non essential to general parasite health or survival *in vitro*. Nevertheless, triple RNAi of *TbMCA2*, *TbMCA3* and *TbMCA5* led, in BSF, to a rapid growth arrest and a mutant morphology (enlarged, misshaped parasites with multiple flagella).

Localisation of TbMCA2 and TbMCA3 proteins was performed by immuno-fluorescence (IF), on BSF parasites, using a system of HA-tag and anti-HA antibodies. The IF images showed that the HA-tagged TbMCA2 and TbMCA3 proteins are located within several organelles found primarily between the nucleus and kinetoplast. How the trypanosome MCAs are directed to the compartments in which they reside is unclear. As seen in **chapter 4**, TbMCA3 and TbMCA5 have predicted signal peptides, whereas TbMCA2 does not. TbMCA3 and TbMCA5 are therefore likely to be sorted through the classic secretory pathway, whilst TbMCA2 might either be trafficked in association with TbMCA5, TbMCA3 or another ER-directed protein or via an unconventional secretory pathway. Double labelling with TbMCA5, using polyclonal anti-TbMCA5 sheep antibodies, showed that both TbMCA2HA and TbMCA3HA were mainly located within the same structures as TbMCA5. Co-localisations with various characterised protein markers were performed to identify the nature of these structures. TbMCA5 was found to be mainly present in a RAB11-positive compartment. RAB11 has been shown to be associated with the recycling endosomes in *T. brucei* (Grunfelder *et al.*, 2003), and most notably to be involved in the VSG recycling pathway and anti-VSG antibodies degradation (Jeffries *et al.*, 2001). In mammalian cells, RAB11 has also been localized in the Golgi complex (Wilcke *et al.*, 2000). Recently, RAB11- and FIP3-containing recycling endosomes were

shown to accumulate near the cleavage furrow and be required for successful completion of cytokinesis (Wilson *et al.*, 2005).

7.3. New results

In *T. brucei* BSF there was a major difference between the consequences of knocking down TbMCA2, TbMCA3 and TbMCA5 expression in the RNAi cell lines, which was lethal, and sequential deletion of *TbMCA2*, *TbMCA3* and *TbMCA5*, which was not lethal.

So far, prostaglandin D_2-induced cell death is the best characterised form of programmed cell death in *T. brucei* BSF (Figarella *et al.*, 2005; Figarella *et al.*, 2006). In order to test if the metacaspases are involved in prostaglandin D_2-induced cell death in BSF, wild type BSF parasites and *ΔTbmca2/3ΔTbmca5* mutants were treated with prostaglandin D_2 and their growth characteristics assessed. However, as the growth phenotype of the *ΔTbmca2/3ΔTbmca5* mutants was lost after several weeks in culture, suggesting an adaptation (**section 7.2.2**), the experiments were carried out on freshly selected transfectants.

TbMCA2, TbMCA3 and TbMCA5 were found, in BSF, to partially co-localise with RAB11-positive vesicles. The RAB11 compartment in *T. brucei* BSF has been shown to contain recycling receptors and their cargo, such as transferrin receptor/transferrin and VSG/anti-VSG antibody (Jeffries *et al.*, 2001). A significant level of co-localisation between internalised anti-VSG 221 antibodies and TbMCA5 was previously reported by Matthew John Helms. These data provide evidence that a proportion of metacaspases of *T. brucei* are in close association with RAB11-positive recycling endosomes and their cargo. Therefore the efficiency of VSG recycling and anti-VSG antibodies degradation were assessed in wild type, *ΔTbmca2/3ΔTbmca5* and triple RNAi cell lines.

Finally, as the growth rates of triple RNAi-induced BSF cells and to a lesser extent *ΔTbmca2/3ΔTbmca5* cells were significantly slower than wild type, analysis of kinetoplasts and nuclei configuration was performed to follow the progression of the parasites through their cell cycle. The potential modification of the metacaspases localisation during cell division was also investigated.

7.3.1. Prostaglandin D_2 treatment

Wild type and non adapted *ΔTbmca2/3ΔTbmca5* BSF cells were treated with either 0, 2.5, 5 or 7.5 μM of prostaglandin D_2 (PGD_2) (**figure 7.1**). In the absence of treatment, the non adapted *ΔTbmca2/3ΔTbmca5* cells have a slower growth rate than the wild type cells (refer to **7.2.2**).

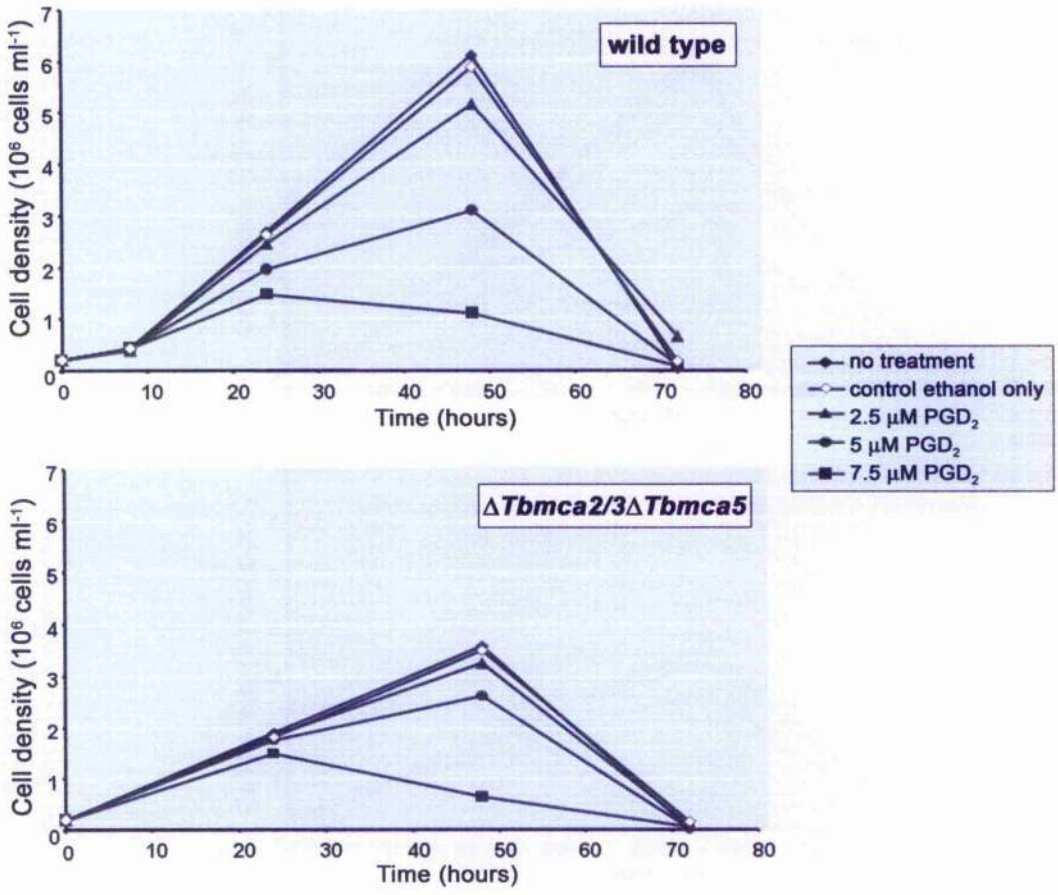

Figure 7.1: Prostaglandin D_2-induced cell death in wild type and Δ*Tbmca2/3ΔTbmca5 T. brucei* bloodstream forms.

Wild type (upper panel) and non adapted Δ*Tbmca2/3ΔTbmca5* cells (lower panel) were treated with either 0 (open diamond), 2.5 (triangle), 5 (round) or 7.5 µM (square) of prostaglandin D_2 (PGD_2) and the growth rates were compared to the non-treated cells (close diamond).

Prostaglandin D_2 caused death as previously reported (Figarella *et al.*, 2005; Figarella *et al.*, 2006). Nevertheless, no obvious difference in the kinetics of cell death was noted between the wild type and Δ*Tbmca2/3ΔTbmca5* (**figure 7.1**), demonstrating that TbMCA2, TbMCA3 and TbMCA5 are not required as effectors of prostaglandin D_2-induced cell death in BSF *T. brucei*.

7.3.2. Assessment of VSG recycling *in vivo*

To establish if the metacaspases are involved in the VSG recycling process in bloodstream form trypanosomes, wild type parasites were compared with Δ*Tbmca2/3ΔTbmca5* and triple RNAi-induced cells. Surface VSG was biotinylated at 4°C prior to 5 minutes of endocytosis at 37°C. Non-internalised biotin was cleaved from the

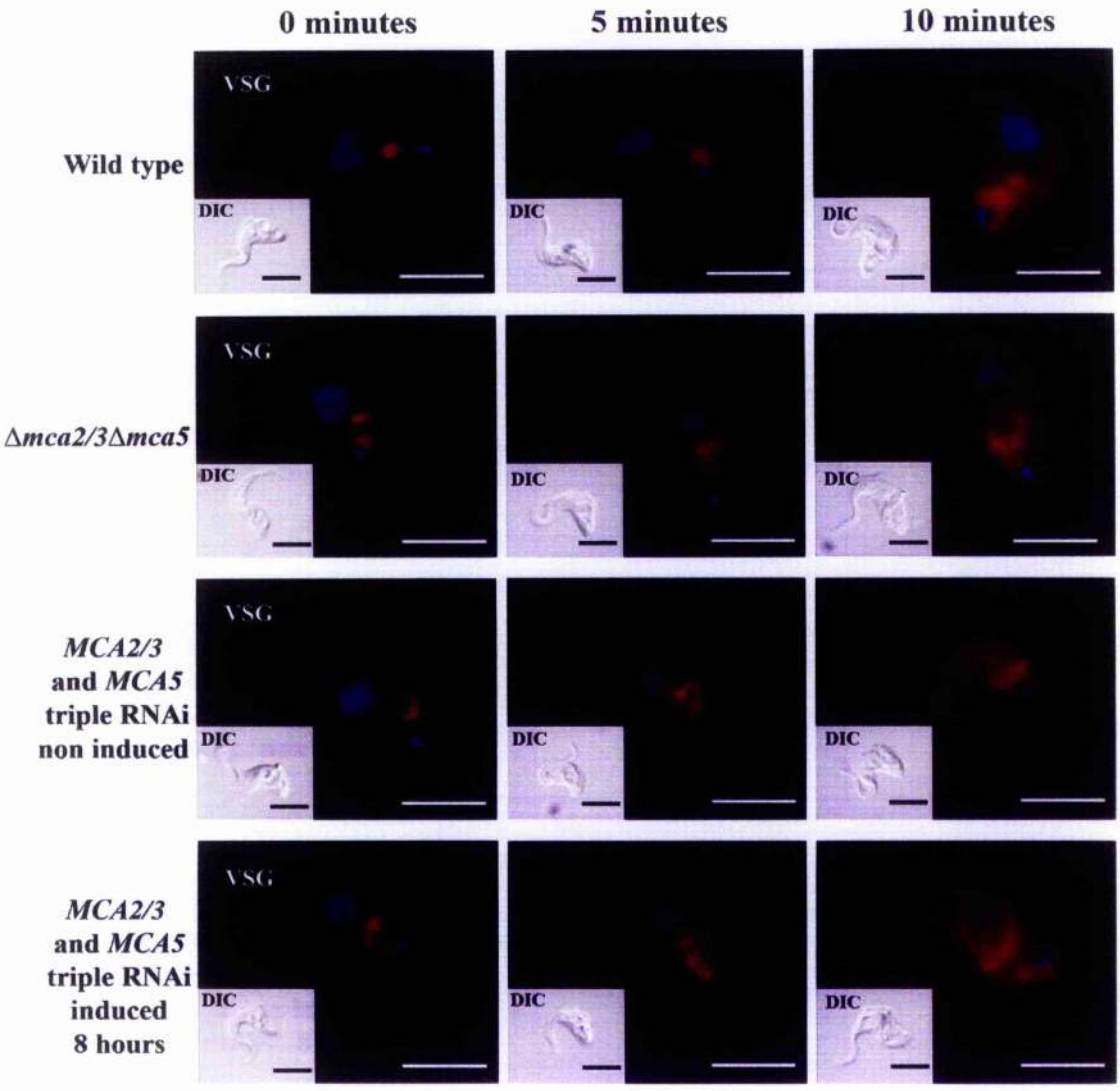

Figure 7.2: Recycling of VSG.

Wild type, Δ*Tbmca2/3*Δ*Tbmca5* and triple RNAi lines (+/- induction with tetracycline for 8 hours) parasites were biotinylated at 4°C prior to incubation at 37°C for 5 minutes in HMI-9 medium. Remaining surface label was then cleaved by incubation with 50 mM glutathione at 4°C. Cells were then prepared for IFA both immediately after the glutathione incubation and following a 5 or 10 minutes chase period in HMI-9 medium at 37°C. Parasites were stained with streptavidin-Texas Red conjugate (red). DNA was visualised with DAPI (blue). DIC images of the parasite are shown. Scale bar = 10 μm.

parasite surface and cells resuspended in medium for 0 to 10 minutes to allow time for recycling to occur.

Immuno-fluorescence analysis of parasites showed that internalised biotin-VSG co-localised with RAB11-positive structures (Helms et al., 2006) and that, following 5 minutes and 10 minutes chase periods, wild type, ΔTbmca2/3ΔTbmca5 and induced triple RNAi parasites were able to recycle this internalised VSG and return it to the cell

surface (**figure 7.2**). Therefore, it appears that the loss of TbMCA2, TbMCA3 and TbMCA5 does not prevent endocytosis of VSG, the trafficking through RAB11-positive vesicles, or its subsequent return to the cell surface.

7.3.3. Assessment of the degradation of anti-VSG antibodies

It has been documented previously that IgG-VSG immune complexes are internalised by *T. brucei* and that whilst the VSG is recycled to the surface, the IgG is degraded intracellularly (O'Beirne et al., 1998; Jeffries et al., 2001; Pal et al., 2003). Anti-VSG IgG has been localised to RAB11-positive vesicles, but the peptidases involved in the degradation of IgG and their location within the cell have not been identified. The finding that the metacaspases are present within recycling endosomes, which traffic anti-VSG IgG, raised the possibility that they might be involved in the degradation of the internalised IgG. To investigate this hypothesis, parasites were labelled with a polyclonal rabbit anti-VSG221 IgG at 4°C for 30 minutes, washed extensively and incubated at 37°C for a further 5 or 10 minutes. Following this period, parasites were examined by IFA. The ability to internalise and degrade antibody was unimpaired in Δ*Tbmca2/3*Δ*Tbmca5* and the triple RNAi mutant 8 hours after induction (**figure 7.3**). Whole cell lysates from wild type and Δ*Tbmca2/3*Δ*Tbmca5* and TCA precipitations of the culture medium were then subjected to SDS-PAGE, transferred to PVDF membrane and probed with an anti-rabbit HRP conjugate to determine the fate of the internalised antibodies (Helms et al., 2006). Examination of cell-associated anti-VSG221 IgG illustrated that there was no build up of it within Δ*Tbmca2/3*Δ*Tbmca5* parasites compared with wild type parasites. A single protein, corresponding to rabbit heavy chain IgG, was detected at equivalent levels in both cell lines (Helms et al., 2006). Analysis of the secreted products illustrated that the degradation of the anti-VSG IgG was very similar in Δ*Tbmca2/3*Δ*Tbmca5* parasites as in wild type parasites (Helms et al., 2006). These data show that the Δ*Tbmca2/3*Δ*Tbmca5* parasites are still functional with regard to anti-VSG antibody internalisation, degradation and secretion and show that the absence of TbMCA2, TbMCA3 and TbMCA5 from recycling endosomes does not affect this process.

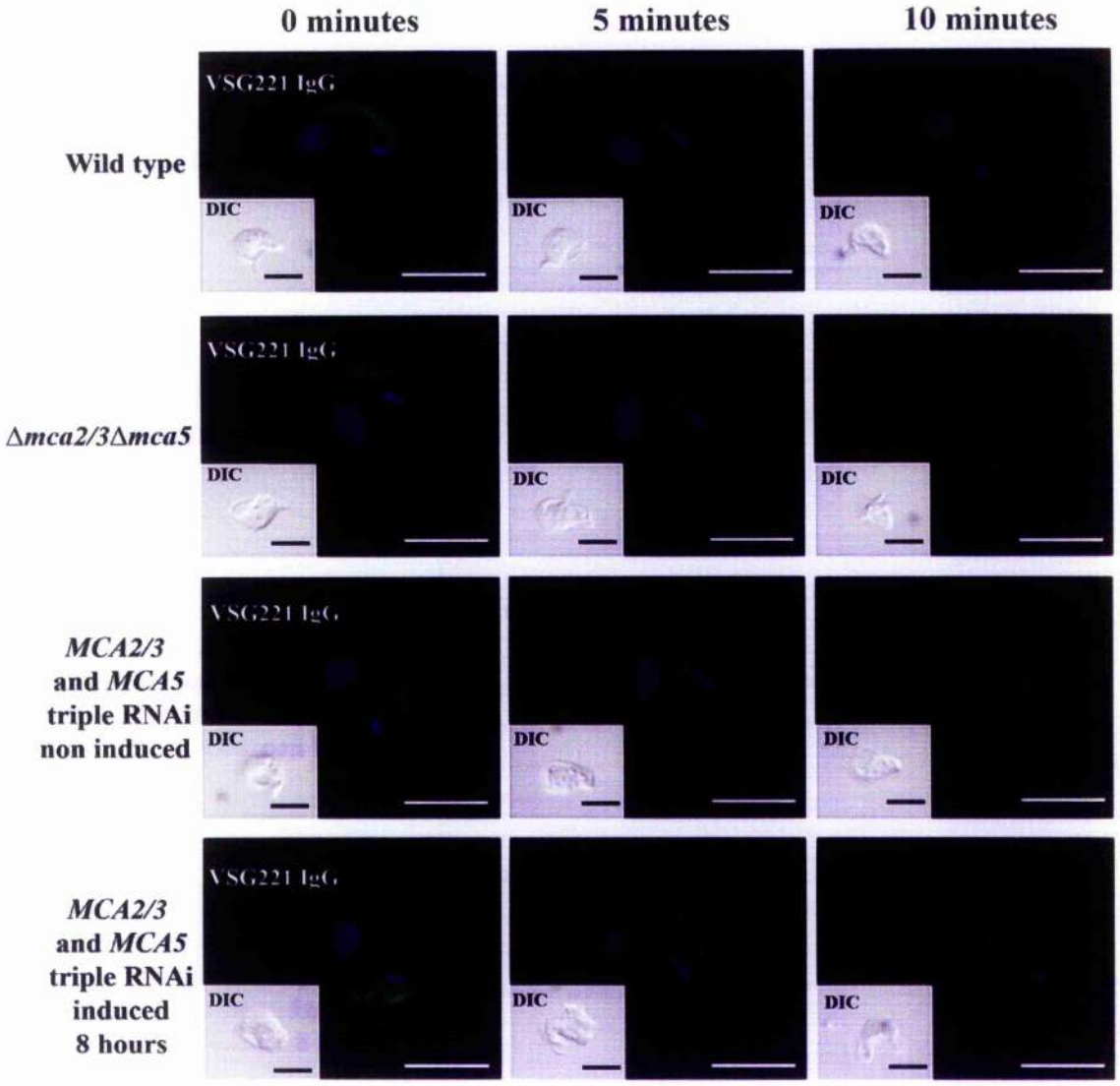

Figure 7.3: Degradation of anti-VSG IgG.

BSF wild type, Δ*Tbmca2/3*Δ*Tbmca5* and triple RNAi lines (+/- induction with tetracycline for 8 hours) were labelled with anti-VSG221 rabbit IgG at 4°C in HMI-9 prior to incubation at 37°C for 10 and 30 minutes in HMI-9. Parasites were fixed and stained with anti-rabbit-FITC conjugate (green) and DAPI (blue). Scale bar = 10 μm.

7.3.4. Growth curves and cell cycle analysis

While a proportion of metacaspases of *T. brucei* are in close association with RAB11-positive recycling endosomes and their cargo, we demonstrated that TbMCA2, TbMCA3 and TbMCA5 are not required for efficient recycling of VSG or the degradation of anti-VSG antibodies. To pursue our attempts in elucidating the function(s) of these metacaspases in the cell, we decided to analyse in more detail the phenotypes associated with the simultaneous gene silencing of *TbMCA2*, *TbMCA3* and *TbMCA5* by RNA interference.

As described previously, triple RNAi of *TbMCA2*, *TbMCA3* and *TbMCA5* resulted in a rapid growth arrest (**figure 7.4A, left panel**). Western blot analysis confirmed almost total down-regulation of TbMCA2, TbMCA3 and TbMCA5 after induction with tetracycline for 24 hours (**figure 7.4A, right panels**), whilst the level of the cross-reacting protein of 48 kDa (marked *) remained constant. Analysis of kinetoplast and nuclei configuration in induced cells was performed in order to analyse the progression of the parasites through the cell cycle in comparison to wild type (**figure 7.4B**). At 4 hours post-induction, a significant increase was observed in the number of cells with one nucleus and one kinetoplast (1N1K) (**figure 7.4B, lower panel**). This increase was attributed to an accumulation of cells with a bone-shaped kinetoplast (41% of the 1N1K cells vs 27% in the non-induced, **figure 7.4C, upper panel**) indicating that kinetoplast segregation was impaired. The concomitant appearance of aberrant cells with two nuclei and a single big kinetoplast (2N1K, **figure 7.4B**), not normally found in wild type cells as kinetoplast division typically occurs before mitosis, confirmed the delay in kinetoplast segregation. By 8 hours post-induction, many 1N1K cells had belatedly managed to divide their kinetoplast leading to a slight increase of 1N2K cells (**figure 7.4B**). Most marked, however, was an accumulation of 2N2K cells, suggesting a post-mitotic block prior to the start of furrow ingression at cytokinesis. Cells appeared to be unable to escape this pre-cytokinesis block, as by 12 hours post-induction the number of cells with multiple nuclei and kinetoplasts was almost four times higher than in the non-induced control, showing that DNA replication and mitosis still occurred but cell division invariably failed (**figure 7.4B**). These data suggest that TbMCA2, TbMCA3 and TbMCA5 expression is required for multiplication of BSF *T. brucei*, but it is known that these proteins can individually compensate for the loss of each other (Helms, 2004).

Furthermore, progressive gene knock-out of these three metacaspases, in BSF, suggests that alternative biochemical pathways could balance for the lack of TbMCA2, TbMCA3 and TbMCA5. Indeed, while shortly after selection, Δ*Tbmca2/3*Δ*Tbmca5* parasites were impaired in their growth compared to the wild type cells, after several weeks in culture, the growth rate of the mutants was back to wild type level, suggesting that adaptation had taken place. Interestingly, it has to be noted that, at early stages of selection, the Δ*Tbmca2/3*Δ*Tbmca5* parasites showed a higher number of cells at the pre-cytokinesis stage of the cell cycle than wild type parasites (wild type: 71% 1N1K, 18% 1N2K, 9% 2N2K; Δ*Tbmca2/3*Δ*Tbmca5*: 54% 1N1K, 24% 1N2K, 17% 2N2K) suggesting a pre-cytokinesis cell cycle block. This phenotype mirrors, at a lesser extend, the one

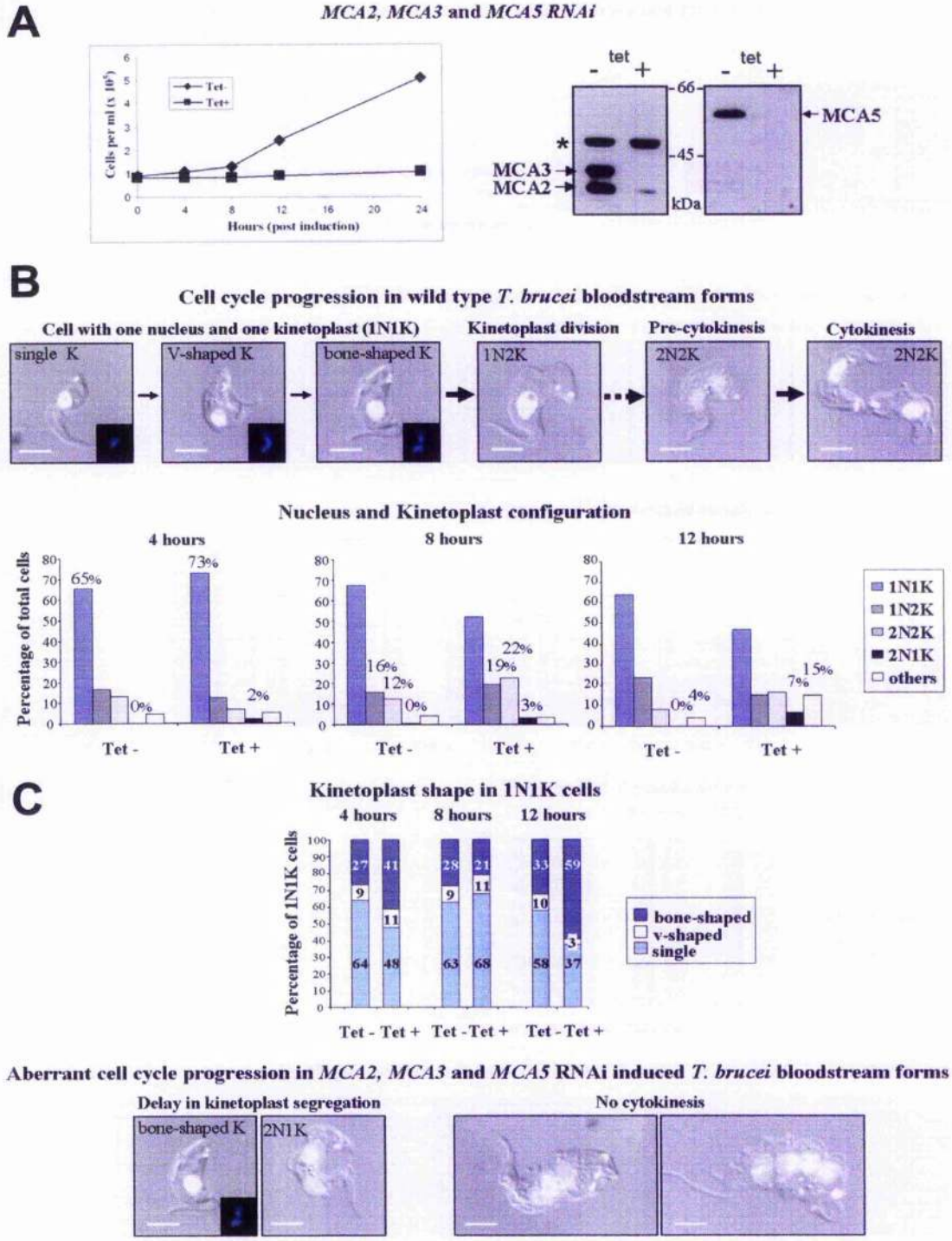

Figure 7.4: RNAi of metacaspases in bloodstream form *T. brucei*.

(A) Left panel: growth curve of a *TbMCA2/3* and *TbMCA5* triple RNAi clone + or - induction with tetracycline (tet). Right panels: Western blot of cell extracts from a *TbMCA2/3* and *TbMCA5* clone, + or - tet, probed with anti-TbMCA2/3 (left) or anti-TbMCA5 antibodies (right). * cross-reacting 48 kDa protein. (B) Upper panel: normal cell cycle progression in BSF. The kinetoplast division occurs before nuclear division, ultimately followed by cytokinesis. Pictures illustrating various cell stages are shown (DAPI, stained nucleus (N) and kinetoplast(K), in white) In the bottom right corner of the 1N1K pictures an enlargement of the kinetoplast is shown (blue). Lower panel: N and K configurations determined by DAPI staining post-induction with tet. "Others"

indicates cells with an abnormal configuration excluding 2N1K cells. For each time point, 200 cells were analysed. (C) Upper panel: analysis of kinetoplast configuration in 1N1K cells after tet induction. Images of representative triple RNAi induced BSF are shown below. The Western blots in Panel A were performed by Matthew J. Helms.

observed rapidly after triple RNAi induction. Also it can be postulated that it is the rapid removal of all three metacaspase genes at once that resulted in the RNAi lethal effect, the parasite could not adapt to overcome this.

7.3.5. Metacaspase localisation during cytokinesis of bloodstream forms

In *T. brucei* bloodstream forms, TbMCA5 was previously shown to co-localise partially with RAB11-positive endosomes. Also, in view of the finding that RNAi of *TbMCA2*, *TbMCA3* and *TbMCA5* induces a pre-cytokinesis block, we decided to investigate further the role of these metacaspases during cell division. To do so, we followed, during the process of cytokinesis, the localisation of TbMCA5 and RAB11. As cells undergoing cytokinesis represent only a small percentage of the total cell population (about 5%), we used a cell line that, upon RNAi induction, accumulate at a post-mitotic state (2N2K) and harbour a defect in cytokinesis progression (Hammarton *et al.*, 2005). 8 hours after RNAi induction of the kinase activator MOB1, 60% of the 2N2K bloodstream form cells displayed a visible cleavage furrow, indicating that furrow ingression was somehow impaired by the downregulation of this protein. This phenotype was used to investigate whether TbMCA5 and RAB11 were associated with the cleavage furrow during cytokinesis. In 2N2K cells with a visible furrow, these two proteins were found to mainly co-localise in a compartment close to the kinetoplast (data not shown), comparable to the one observed in 1N1K cells (**figure 7.5, left panel**).

In mammalian cells, RAB-11 recycling endosomes are known to accumulate at the cleavage furrow during the ultimate stage of cytokinesis, when the cells undergoes abscission (Wilson et al., 2005; Fielding et al., 2005). Therefore, the observation of TbMCA5 and RAB11 localization was then focused on cell-cell scission. However, upon completion of daughter cells separation, TbMCA5 and RAB11 were not present at the cleavage furrow and instead maintained their peri-kinetoplast localization (**figure 7.5, right panel**). Thus, it seems that TbMCA5 is not directly involved in cleavage furrow ingression and cytokinesis completion.

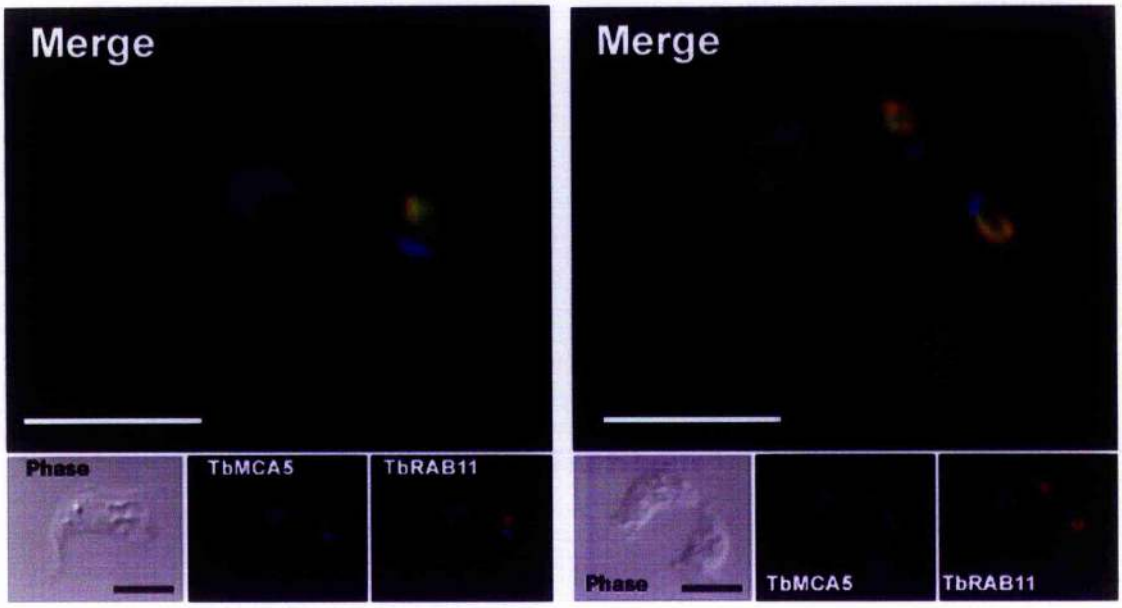

Figure 7.5: TbMCA5 localisation during cytokinesis of bloodstream forms

Bloodstream form parasites were fixed and stained using sheep anti-TbMCA5 (green) and rabbit anti-TbRAB11 (red). Nuclear and kinetoplast DNA were visualised by DAPI staining (blue). Co-localisation of the signals appears in yellow. The panel on the left shows a 1N1K cell, while the one on the right shows a 2N2K cell at a late stage of cytokinesis (abscission). Scale bar = 10 μm

7.4. Discussion

7.4.1. Features of *T. brucei* metacaspases

This study concentrated on TbMCA2, TbMCA3 and TbMCA5 of *T. brucei*. The parasite's genome encodes two other metacaspases, TbMCA1 and TbMCA4, although they lack the predicted active site cysteine and so presumably are not active as cysteine peptidases. TbMCA1 and TbMCA4 have extensive sequence identity with TbMCA2, TbMCA3 and TbMCA5, including within the catalytic centres (**figure 4.2**), even though both proteins have substitutions at the predicted essential catalytic positions (Szallies et al., 2002; Mottram et al., 2003). Recent analysis has shown that inactive enzyme homologues are abundant in a variety of enzyme families, including peptidases (Pils and Schultz, 2004). It has been proposed that some of these "dead" peptidases, by adapting existing protein modules, have evolved new regulatory functions. This could be the case for TbMCA1 and TbMCA4 of *T. brucei*. However, it can not be excluded that these proteins might possess an enzymatic activity (see **chapter 4**). Active or not, the fact that TbMCA1 and TbMCA4 possess different active site residues from the one present in TbMCA2, TbMCA3 and TbMCA5 strongly suggests that the two sets of proteins

have different functions within the cell. Furthermore, the fact that TbMCA4 is expressed in bloodstream forms (see **section 7.2.1**), and that simultaneous RNAi of TbMCA2, TbMCA3 and TbMCA5 affects the growth rate of those parasites, this could be taken as evidence that TbMCA4 is not able to compensate for the loss of these three metacaspases and that they have separate functions within the cell. At the same time it seems that there is some level of functional redundancy between TbMCA2, TbMCA3 and TbMCA5 as sequential deletion of these genes led to no obvious phenotype, while deletion of all three genes induced a reduction of the growth rate of the mutant bloodstream forms compared to the wild type cells. However, the apparent adaptation of the Δ*Tbmca2/3*Δ*Tbmca5* parasites is intriguing. Indeed, while initially growing more slowly than the wild type, the growth rate of the triple null mutant gradually increased, with the time spent in culture, to finally match the wild type level. Selection of faster growing parasites might explain this adaptation. However, the mechanism behind this recovery is uncertain. The most obvious explanation would be for TbMCA1 and TbMCA4 to be able to complement the loss of TbMCA2, TbMCA3 and TbMCA5. Indeed it will be interesting to determine if TbMCA1 or TbMCA4 are up-regulated in the Δ*Tbmca2/3*Δ*Tbmca5* line but no antibodies are available at present to investigate this possibility. It would also be interesting to determine whether these metacaspases co-localise with TbMCA2, TbMCA3 and TbMCA5 within the cell.

7.4.2. TbMCA2, TbMCA3 and TbMCA5 localisation in the cell

Immunofluorescence observations, performed in bloodstream forms, revealed that TbMCA2 and TbMCA3 are co-localising almost completely in a compartment that was identified as RAB11-positive (Helms et al., 2006). As previously discussed (**chapter 4**), TbMCA2 and TbMCA3 have significant divergence only in their N-terminal domain, a region that in TbMCA3 is predicted to contain a putative signal peptide. Also, it was initially believed that the small extension present on TbMCA3 might have been involved in differential targeting of TbMCA2 and TbMCA3. However, this does not seem to be the case, as these two proteins are found in the same compartment. Furthermore, TbMCA5, which is also predicted to possess a signal peptide at its N-terminus but does not show any homology with TbMCA3 in this region, is also found in the RAB11-positive compartment that contains TbMCA2 and TbMCA3. Therefore, the N-terminal domain may not be involved in the targeting of TbMCA3 and TbMCA5 to the RAB11-positive compartment. However, we can not exclude the possibility that this domain might, through some secondary structure peculiarities, be able to target these metacaspases to another cellular compartment. Indeed, immunofluorescence observations revealed that

the co-localisation between TbMCA5 and RAB11 was not total, and that at least a small part of the TbMCA5 protein pool is distinct from RAB11 (Helms et al., 2006).

Secondary structure predictions suggest that the extension at the N-terminus of TbMCA3 contains an α-helix domain. Also this additional structural feature might participate in the shielding of the nearby WW binding domain and might therefore modulate the ability of the protein to associate with its partners. However, as TbMCA2 possesses a similar WW binding domain, but no additional N-terminal helix structure to modulate its interaction capacity, then the benefit of TbMCA3 adopting such a regulatory strategy is unclear. We could also say that, by modifying the structural environment of the WW binding domain, the N-terminal region of TbMCA3 might confer some binding specificity to this interaction module. Thus, although both proteins possess a WW binding domain, TbMCA2 and TbMCA3 might have two distinct sets of protein partners. On balance it is unlikely that the N-terminal domain of TbMCA3 modulates protein-protein interactions, however, it can not be excluded that this domain might contain, like in LmajMCA, an atypical mitochondrial targeting signal. In the *L. major* metacaspase, this region was postulated to enable the entry into the mitochondrion and the subsequent interaction with the mitochondrial DNA, the kinetoplast. In *T. brucei*, immunofluorescence observations seem to indicate that TbMCA2, TbMCA3 and TbMCA5 do not associate with the kinetoplast. Nevertheless, the N-terminal domains of TbMCA5 and TbMCA3 might mediate a transient relocation to this organelle during the cell-cycle. This might correlate with the observation that LmajMCA relocates to the kinetoplast upon the start of the mitochondrial DNA segregation (**chapter 5**). Thus the premature entry or exit of the metacaspases from the mitochondrion would then presumably interfere with the kinetoplast division. And indeed, overexpression in *L. major* and RNAi in *T. brucei* bloodstream forms of the metacaspase(s) induce a defect in kinetoplast segregation. Consequently it is possible that the N-terminal domain of LmajMCA, TbMCA3 and TbMCA5 mediate the transient relocalisation of these metacaspases to the mitochondrion and more precisely the kinetoplast DNA. We might then postulate that metacaspases trafficking to this alternative location might represent a part of the metacaspase pool not co-localising with RAB11.

Meanwhile, it is still unclear how TbMCA2, TbMCA3 and TbMCA5 are targeted to the RAB11-positive recycling endosomes. In eukaryotic cells, the secretory and endocytic pathways consist of multiple compartments, each with a unique set of proteins and lipids. Also, to ensure their identities and functions, these various compartments are required to direct molecules to defined locations. Various signals responsible for targeting proteins to different intracellular locations have been described (van Vliet et al., 2003). One of the main platforms where protein targeting is

performed is the trans-Golgi network (TGN). At this site, cytosol-oriented sorting signals direct protein cargo to the appropriate export compartment (Traub and Kornfeld, 1997). However, it is difficult to predict if there are any such sorting signals in the metacaspases. It is probable that a yet uncharacterised conserved motif within TbMCA2, TbMCA3 and TbMCA5 is responsible for their targeting to the same compartment.

7.4.3. *T. brucei* metacaspases putative functions

The reasons why these three metacaspases accumulate in a RAB11- positive compartment remain obscure. Rab proteins are small GTPases belonging to a sub-group of the Ras superfamilly which are involved in the speciation and regulation of vesicular traffic (Novick and Brennwald, 1993; Nuoffer and Balch, 1994). In *T. brucei*, RAB11 is highly expressed in bloodstream form and mediates recycling of glycosylphosphatidyl-inositol-anchored proteins, including the variant surface glycoprotein (VSG) and the transferrin receptor, plus trafficking of internalized anti-VSG antibody and transferrin. *T. brucei* expresses around 10^7 copies of the VSG on the external surface of the plasma membrane (Jackson *et al.*, 1985). This surface coat molecule is proposed to act primarily as a steric barrier preventing antibody and complement binding to invariant surface determinants. VSG is highly immunogenic, and a robust anti-VSG immune response can eliminate parasites from the bloodstream with high efficiency. However, a process of antigenic variation, consisting in a rapid switching of the expressed VSG gene to an immunologically non-cross reactive VSG (Cross *et al.*, 1980) ensure that host anti-VSG antibodies do not reach levels sufficient to clear the infection (Pays *et al.*, 1994). Nevertheless, host antibodies may be generated faster than the switching of VSGs. Also, it is believed that the rapid trafficking and recycling of the VSGs plays an important role for the defence against the immune system (O'Beirne *et al.*, 1998). Indeed, in the bloodstream forms, it has been demonstrated that the total surface pool is being, *in vitro*, turned over in 12 minutes (Engstler *et al.*, 2004). Also, it is very likely that this rapid membrane turn over could allow the removal of anti-VSG antibodies, thus ensuring the parasite's escape from the host immune response. In trypanosomatids, the endo- and exocytosis are highly polarised processes occurring exclusively at the site of the flagellar pocket (McConville *et al.*, 2002). Upon their endocytosis, the VSGs enter the endosomal system. Also, as VSGs are very stable molecules, the majority of the internalised VSGs are being recycled back to the surface (Seyfang *et al.*, 1990), while in contrast, the anti-VSG antibodies are extensively degraded (O'Beirne *et al.*, 1998). It has been established that the internalisation of the VSG and the anti-VSG antibodies is mediated by the Rab5-positive early endosomes while their recycling occurs through the RAB11-positive recycling endosomes (Jeffries *et al.*, 2001; Pal *et al.*, 2003). However,

immunofluorescence experiments failed to establish the lasting presence of TbMCA2, TbMCA3 and TbMCA5 in early endosomes while revealing their co-localisation with the RAB11-posivite recycling endosomes.

To assess whether the metacaspases were involved in recycling processes in *T. brucei* bloodstream forms, we followed, by immunofluorescence analyses, the trafficking of internalised biotinylated VSGs through the endocytic pathway and their subsequent return to the cell surface via RAB11-positive recycling endosomes in *ΔTbmca2/3ΔTbmca5* and triple RNAi induced parasites and compared it with the wild type cells. As expected, in the wild type BSF, a rapid turn over of the surface VSG pool was observed and within 15 minutes, most of the internalised biotinylated VSGs were back on the cell surface. However, even in the absence of TbMCA2, TbMCA3 and TbMCA5, the rate of the VSG recycling was comparable to the wild type, indicating that these proteins are unlikely involved in this process. The analysis then shifted to the pathway of the removal and degradation of the host anti-VSG antibodies. It is still unclear whether the dissociation of the antibodies from the VSGs occurs via a proteolytic clipping event or via a pH reduction, during their shifting from one endosomal compartment to the next. Additionally, the peptidases involved in the degradation of these antibodies and the compartment(s) where this occurs are still elusive. However, it was observed that TbMCA5 is partially co-localising with anti-VSG antibodies (Helms et al., 2006). Also it was initially thought that the metacaspases might play a role in the degradation of these IgGs. However, our analysis revealed that the *ΔTbmca2/3ΔTbmca5* and triple RNAi- induced parasites were not displaying any marked build up of internalised anti-VSG antibodies, thus suggesting that the metacaspases were not responsible for anti-VSG antibodies processing. Furthermore, it has recently been established that the *A. thaliana* metacaspases possess a strict substrate specificity, with a preference for arginine or lysine residues at the P1 position of their substrates (Vercammen et al., 2004; Watanabe and Lam, 2005). Also, if the same is true for the *T. brucei* metacaspases, it is very unlikely that they would be effective general degradative enzymes. Rather, the metacaspase would be predicted to specifically cleave and process protein substrates to allow their activation. Also, even though the metacaspases are present in RAB11-positive recycling endosomes, we failed to establish any involvement of TbMCA2, TbMCA3 and TbMCA5 in the recycling processes themselves.

In *Drosophila* cells, the endocytic and secretory pathways are postulated to converge in Rab-11 positive recycling endosomes (Pelissier *et al.*, 2003; Strickland and Burgess, 2004). Also, even if this has not been experimentally established yet, it is possible that, in trypasomatids, the RAB11-positive recycling endosomes are also a constitutive part of the traditional secretory pathway. In that case, the metacaspases

might be involved in the activation of a secreted protein. The comparison of the secretion profiles of wild type, *ΔTbmca2/3ΔTbmca5* and triple RNAi-induced bloodstream form parasites may be able to address this possibility. However, the very rapid cell cycle arrest induced, in bloodstream forms, upon RNAi of TbMCA2, TbMCA3 and TbMCA5, suggest that the metacaspases are more likely involved in the control of cell division.

It has recently been shown that, in mammalian cells, RAB11-positive recycling endosomes recruit, during cytokinesis, various proteins and membrane constituents on the site of cleavage furrow ingression (Wilson et al., 2005; Fielding et al., 2005). In most eukaryotic cells, mitosis ends with the start of cytokinesis, a process by which the plasma membrane is dramatically constricted and ultimately leading to the production of two daughter cells. Cytokinesis is mediated by the contraction of an actin/myosin ring that forms perpendicular to and midway between the nuclear mitotic spindle and creates an ingressing cleavage furrow (Fishkind and Wang, 1995; Glotzer, 1997a; Glotzer, 1997b; Field et al., 1999; Robinson and Spudich, 2000; Glotzer, 2001; Robinson and Spudich, 2004; Glotzer, 2005) **(figure 3.2e, f)**. In mammalian cells, it has recently been suggested that the increased surface area necessary for the production of two daughter cells is supplied, during cytokinesis, by insertion of additional membrane at the cleavage furrow (Finger and White, 2002). Interestingly, at this site, the plasma membrane seems to possess a distinct lipidid and protein content (Emoto et al., 1996; Umeda and Emoto, 1999; Emoto and Umeda, 2000). This unique composition might explain the malleability of cleavage furrow plasma membrane during ingression and its ability to be pinched in two, but might also mediate the creation of transduction signals necessary for progression through cytokinesis. Thus, membrane traffic during cytokinesis not only promotes the expansion of the plasma membrane surface but also mediates the delivery of key proteins involved in cleavage furrow ingression and abscission. Also, work in *Xenopus* indicates that the additional membrane does not come from the expansion of the preexisting surface membrane but from the insertion of internally-stored membrane (Bluemink and de Laat, 1973; Byers and Armstrong, 1986; Bielíavsky et al., 1992). In plant cells, it is well established that, during cytokinesis, membrane expansion is induced by delivery of Golgi-derived exocytic vesicles (Bednarek and Falbel, 2002). Also, it has been suggested that the endocytic machinery and more precisely the endosomes are likely to be a source of membrane during cytokinesis. Indeed, dynamin, a protein involved in clathrin coat-dependent endocytosis, and α-adaptin, a component of coat proteins involved in receptor-mediated endocytosis, are both known to be present in the cleavage furrow and to be required for cell division (Swanson and Poodry, 1980; Dornan *et al.*, 1997). Even if the dynamics of endosomes during cell division are still elusive, it was proposed that RAB11 may regulate the

delivery of endocytic vesicles to the cleavage furrow (Riggs *et al.*, 2003, Strickland and Burgess, 2004). While playing a key role in the regulation of plasma membrane receptor trafficking, RAB11-positive recycling endosomes were indeed found to accumulate near the cleavage furrow and implicated in regulating membrane delivery to the cleavage furrow, an essential requirement for successful completion of cytokinesis in mammalian cells. In *Caenorhabditis elegans* ovaries, RNAi of RAB11 causes cytokinesis defects including furrow regression and scission (Skop *et al.*, 2001) indicating that vesicular transport through the RAB11-recycling endosomes is indeed required for supplying the extra membrane necessary for furrow ingression. In mammalian cells, RAB11 interacts, between others, with at least six RAB11- Family Interacting Proteins (RAB11-FIPs) (Hobdy-Henderson *et al.*, 2003). Also, in those cells, the complex of RAB11 and RAB11-FIP3 has been shown to be essential for cytokinesis completion, but not cytoplasm furrowing and midbody formation, and is suggested to play a role in the last stage of cytokinesis, abscission (Wilson et al., 2005; Fielding et al., 2005). Therefore, RAB11-recycling endosomes deliver not only membrane but also essential proteins that control the ingression of the cleavage furrow and completion of cytokinesis.

Cytokinesis in trypanosomatids remains an obscure process. Particularly, it is still unknown whether additional membranes are being recruited to the cleavage furrow. Furthermore, no proteins localising to the cleavage furrow have been characterised yet. We therefore decided to determine the localisation of RAB11 and the associated metacaspases during cytokinesis and more precisely during the abscission process (**figure 7.5**). Immunofluorescence observations performed on dividing *T. brucei* bloodstream forms revealed that RAB11 and TbMCA5 were not directly associated with the cleavage furrow. Nevertheless, while data for the other four *T. brucei* metacaspases are lacking, the same experiment performed in *L. major* suggested that LmajMCA, might be present at that site upon the cell-cell scission (**figure 5.4f**). In *T. brucei* bloodstream forms, RNAi of RAB11 leads to a immediate and complete growth arrest (Hall *et al.*, 2005), suggesting that somehow, RAB11 might play a role in cell cycle progression. However, as genome database searches failed to identify any homologue of the RAB11-FIP family in *T. brucei* and *L. major*, it is still unclear if RAB11 might be involved in the control of cytokinesis. However it is tempting to postulate that it might be the case and that the metacaspases might be somehow linked to this process. Nevertheless, as the TbMCA2, TbMCA3 and TbMCA5 RNAi lead to a complete pre-cytokinesis block, then it is more likely that these metacaspases would be involved in the early cytokinesis events. In addition, as the phenotypes observed during the triple RNAi induction, namely the delay in kinetoplast segregation and the complete block in cytokinesis, are known to be microtubule-mediated events (Robinson *et al.*, 1995), then TbMCA2, TbMCA3 and TbMCA5 might be involved in the control of microtubules

dynamics. Recently, in *Drosophila* embryos, RAB11-containing recycling endosomes were characterised as mediators of actin cytoskeleton remodelling during the early stages of furrow formation (Riggs *et al.*, 2003). Even if actin is still poorly characterised in trypanosomatids, but knowing how intrinsically the microtubular and actin networks are connected in mammalian cells (Rodriguez *et al.*, 2003), it will then be tempting to speculate that the metacaspases might be involved in cytoskeleton remodelling during cell cycle progression.

Clearly, further analysis of the metacaspases in *T. brucei* is necessary to elucidate their roles and to provide insights into the networks to which they contribute. Whether these might involve PCD-like phenomena is an open question. Whilst it has been proposed that metacaspases of yeast (Madeo et al., 2002b; Herker et al., 2004; Wadskog et al., 2004), plants (Hoeberichts et al., 2003; Watanabe and Lam, 2005; Bozhkov et al., 2005), and *L. major* (Gonzalez et al., 2006) have functions associated with PCD, we have not been able to find any evidence for similar functions in BSF *T. brucei*. Indeed, the observations that TbMCA2 and TbMCA3 are stage-regulated, and, with TbMCA5, do not undergo any caspase-like processing, that the absence of the metacaspases does not prevent prostaglandin D_2-induced programmed cell death, and that these three metacaspases are co-located mainly in RAB11-positive vesicles, argue against a caspase-like involvement in PCD. Although it cannot yet be ruled out that metacaspases are involved in apoptotic-like cell death in BSF *T. brucei*, the data presented here suggest that metacaspases may have PCD-independent functions that could be associated with RAB11-positive endosomes and play crucial roles for the cell.

Chapter 8:
General discussion

At the beginning of this study nothing was known about the role of the metacaspase in *Leishmania*. During these three years, I have managed to answer some of our initial questions. First I demonstrated that the metacaspase is expressed in both the insect and the mammalian forms of the parasite. Surprisingly, I identified a role for LmajMCA in DNA segregation during mitosis and kinetoplast division and an involvement in cytokinesis. These finding were most unexpected as to date metacaspases had principally been found to be involved in the induction of defined forms of programmed cell death in yeast and plants (Madeo et al., 2002b; Suarez et al., 2004; Bettiga et al., 2004; Watanabe and Lam, 2005; Weinberger et al., 2005; Mazzoni et al., 2005; Bozhkov et al., 2005). Recently, Gonzalez *et al.* showed that the *L. major* metacaspase was able to complement the programmed cell death-inducing function of the yeast metacaspase (Gonzalez et al., 2006). Therefore, many aspects of the multiple functions of this metacaspase still remain to be investigated.

In this study I tried to produce recombinant LmajMCA, in order to establish the biochemical properties of this enzyme. Unfortunately, many problems were encountered and success was achieved only towards the end of the project. The *Pichia* system seemed to be the most promising expression system. Unfortunately the yields of the recombinant protein were not reproducible and impeded any biochemical characterisation. In the meantime, our collaborators managed to establish optimised conditions for the expression of LmajMCA in yeast and solved in part the mystery of LmajMCA substrate specificity (Gonzalez et al., 2006). They found that, like its plant counterparts, LmajMCA cleaves substrate after arginine residues and possesses an affinity for peptide substrates of GGR composition. An N- and C-terminally truncated version of LmajMCA, mainly containing its catalytic domain (termed cd-LmajMCA), showed a higher activity toward this substrate than the full length LmajMCA, indicating that, like caspases, LmajMCA needs to be processed to become active. Cleavage that seems to occur in a caspase-like fashion, between large and small sub-units, apparently depends on the catalytic dyad C202 and H147, indicating that LmajMCA is likely subject to auto-processing (Gonzalez et al., 2006). Although the exact location of the cleavage site remains to be determined, it seems that LmajMCA is processed in both its N-and C-terminus, with the removal of an N-terminal domain and the C-terminal proline-, glutamine- and tyrosine-rich extension. In addition, the N-terminal signal peptide is apparently removed independently of LmajMCA auto-cleavage (Gonzalez et al., 2006). Interestingly, the present study showed that similar processing was occurring in *L. major* promastigotes for LmajMCA and also most of the other LmajMCA variants expressed. It is possible that LmajMCA possesses a preprodomain in its N-terminus involved in both the targeting of the peptidase and the regulation of its catalytic activity. Recently, a cysteine residue conserved in all metacaspases (C29 in AtMCA9,

C98 in TbMCA4 or C81 in LmajMCA), present apparently in close proximity to the catalytic dyad in the tertiary fold, and previously identified as playing a role in the toxicity of TbMCA4 when expressed in yeast (Szallies et al., 2002), was found to be, in the plant metacaspase AtMCA9, involved in the processing of an N-terminal peptide (Belenghi et al., 2006). The removal of the N-terminus appears to be essential for the production of a fully functional AtMCA9, as mutation of C29 to an alanine residue resulted in 90% reduction of the enzyme activity toward its favoured substrate Ac-VRPR-AMC. Nevertheless, it was observed that in this mutant processing between the large and small sub-units of the enzyme still occurred and that this process was dependent on the active site cysteine C147 (Belenghi et al., 2006). Taken together these data suggest that LmajMCA, like AtMCA9, might need two steps of activation. First the protein is cleaved between large and small sub-units by removal of N-and C-terminal fragments and then the enzyme is further processed at its N-terminus to gain optimal activity.

Interestingly, it was established that the full length AtMCA9 is S-nitrosylated on C147 (Belenghi et al., 2006). S-nitrosylation, which consists of the covalent attachment of a nitrogen monoxide group to the thiol side chain of a cysteine, is a post-translational modification mediating nitric oxide (NO) signalling (Hess et al., 2005). As for caspases (e.g. caspase-3), S-nitrosylation of the AtMCA9 zymogen resulted in inhibition of the enzyme activity, thus providing a mechanism by which caspase/metacaspase activity could be regulated (Mannick et al., 2001). However, once processed between its large and small sub-units, the S-nitrosylation of AtMCA9 resulted in an increased proteolytic activity of this enzyme toward its favoured substrate. Therefore it seems that S-nitrosylation can control both steps of the activation process of the metacaspase, first by blocking the initiation of the protein auto-processing and then later by activating the second step and favouring the action of the S-nitrosylation-insensitive C29 and the removal of the N-terminal peptide, which would result in the production of a fully functional enzyme. It will be interesting, therefore, to test whether LmajMCA is subjected to S-nitrosylation and whether this post-translational modification regulates the catalytic activity of LmajMCA. This finding could be of physiological significance as, within the mammalian host, *Leishmania* promastigotes and amastigotes are subject to high level of NO, one of the main antimicrobial agents produced by the infected macrophages (Basu and Ray, 2005).

The potential involvement of C81 in the enzymatic activity of LmajMCA needs to be investigated further. If this cysteine residue can, as suggested for AtMCA9, replace in part the function of the active site cysteine (C202) in the catalytic centre, then this might provide a possible explanation for the phenotype observed during the overexpression of LmajMCA^{C202G} in *L. major*, LmajMCA^{C202G} being still active. By analogy, C81 would only be involved in the final step of the metacaspase activation process, a

step that would take place after the C202-mediated auto-processing. Therefore, the only possible mechanism by which LmajMCA^{C202G} could become active would involve other peptidases carrying out the first processing step. Belenghi *et al.* showed that the active site mutated metacaspase variants AtMCA9^{C147A} and AtMCA^{C29A} possessed a VRPRase activity that was more than twice that of the wild type enzyme when processed correctly by *in vitro* incubation with the wild type AtMCA9 (Belenghi et al., 2006). Also, in the context of the LmajMCA^{C202G} overexpressors, the wild type LmajMCA is still present in the cell and thus would be able to process LmajMCA^{C202G}. The second step of activation could then be mediated by either the additional cysteine residue C81 or maybe again by the wild type LmajMCA. This would mean that mutations in crucial residues in LmajMCA active site would not interfere with the processing of the mutant protein during its overexpression in cells with a wild type background. Therefore, LmajMCA^{C202G}, LmajMCA^{C201G}, LmajMCA$^{C201-202G}$ and LmajMCA^{H147A} are all likely to be processed by the wild type LmajMCA in their respective overexpressors. However, only enzymes with available alternative active site residues would be able to become catalytically active. If the cysteine C81 is indeed involved in the catalytic centre, LmajMCA^{C202G}, LmajMCA^{C201G} and LmajMCA$^{C201-202G}$ could theoretically become active enzymes. However, while the overexpression of LmajMCA^{C202G} induced in *L. major* a phenotype comparable to the one induced by overexpression of the wild type LmajMCA, suggesting that LmajMCA^{C202G} is indeed still active, no such phenotype was detected in the LmajMCA^{C201G} and LmajMCA$^{C201-202G}$ overexpressors. With the current state of knowledge available, I cannot explain why the overexpression of LmajMCA^{C201G} and LmajMCA$^{C201-202G}$ are not toxic for the cell when the overexpression of LmajMCA^{C202G} is. One could predict that the C201G active site mutation might interfere with the catalytic centre configuration and thus modify somehow the catalytic mechanism of LmajMCA^{C201G} and LmajMCA$^{C201-202G}$. Alternative processing/degradation of these proteins might also occur. As for LmajMCA^{H147A}, only the existence of an additional histidine residue able to substitute for the active site histidine would explain the phenotype associated with the overexpression of this variant. Surprisingly, even though the recombinant cd-LmajMCA^{H147A} lacked catalytic activity toward GGR substrate *in vitro*, LmajMCA^{H147A} was found to still be able to partially complement the PCD-inducing function of the yeast metacaspase (Gonzalez et al., 2006), suggesting that this mutant enzyme might possess some residual activity. This might account for the reduced number of transfectants possessing a type 2 phenotype in the LmajMCA^{H147A} overexpressors compared to the WT[MCA] or WT[MCA^{C202G}] cells. However it can not be excluded that some of the phenotypes observed during overexpression of LmajMCA and its several variants, in *Leishmania* promastigotes, might be independent from the metacaspase activity. Therefore it can be concluded that the identity of the active site residues essential for

LmajMCA function remain to some extent cryptic and need to be fully elucidated. Hopefully, further biochemical studies on the recombinant LmajMCA and several of its active site variants will clarify this point. In addition, the positions of LmajMCA processing sites need to be determined. Based on the latest findings on the substrate specificity of the plant and *L. major* metacaspases (Vercammen et al., 2006; Gonzalez et al., 2006), the processing of LmajMCA N-terminus might occur at any of positions 38-40, 45-48, or 59-61, where GRR, VRPI and GGR sites are respectively present. Also it will be interesting to determine whether the removal of this peptide actually affects LmajMCA activity and whether C81 plays a role in this process.

Interestingly, applying the AtMCA9 findings to the *T. brucei* metacaspases suggests that even though TbMCA4 might be unable to auto-process because of a substitution of its active site cysteine by a serine residue, it could theoretically acquire enzymatic activity through processing mediated by the successive action of an upstream peptidase and of the alternative active site cysteine C98. Processing of TbMCA2, TbMCA3 or TbMCA5 has so far not been observed *in vivo* (Helms et al., 2006), but we can not rule out that autocatalytic cleavage or activation by an upstream peptidases might occur under special circumstances. The potential for an active TbMCA4 might thus explain the progressive recovery from the initial slow growth phenotype of the *ΔTbMCA2/3ΔTbMCA5* bloodstream forms, with the active TbMCA4 compensating for the loss of the other metacaspases activities. Also, as sequential RNAi of TbMCA2, TbMCA3 or TbMCA5 in *T. brucei* bloodstream forms (Helms et al., 2006) revealed that these three metacaspases possess overlapping functions, the same might occur for TbMCA4, which is also apparently expressed in this stage of the parasite (see **section 7.2.1**). Futures investigations should now focus on the functional characterisation of the remaining two metacaspases of the *T. brucei* family, TbMCA1 and, most importantly, TbMCA4. Determination of their expression pattern, intracellular localisation, possible processing and substrate specificity should complete the previous (Helms, 2004) and present studies and will hopefully provide new insights into the roles of these proteins in the parasites.

TbMCA2 has recently been expressed and purified from *E. coli* and a sufficient amount of active enzyme has been obtained to start a biochemical characterisation of its properties (Gareth Westrop and Cathy Moss, unpublished data). Interestingly, induction of TbMCA2 expression resulted in an endogenous protein from *E. coli* being cleaved. This processing was specific to TbMCA2 enzymatic activity, as a catalytic mutant (C213G) of this protein failed to produce a comparable cleavage. Mass spectrometry analysis identified the *E. coli* protein cleaved by TbMCA2 as being the elongation factor Tu (EF-Tu). Since then, *in vitro* assays confirmed that EF-Tu but not EF-G was cleaved by TbMCA2. N-terminal peptide sequencing revealed that TbMCA2

cleaved EF-Tu at two different sites, distant by only 5 amino acids, after an arginine and then a lysine residue (VR/GSALK/ALEG). Therefore, TbMCA2 seems to possess a substrate specificity comparable to the plant metacaspases AtMCA9 and AtMCA4 and the *L. major* metacaspase (Vercammen et al., 2004; Watanabe and Lam, 2005; Gonzalez et al., 2006). Also, EF-Tu might represent an *in vivo* substrate of the metacaspases as homologues of this protein are found in both *T. brucei* (Tb10.389.0070) and *L. major* (LmjF18.0740). It is assumed that EF-Tu and EF-G diverged from a common ancestral GTPase and then gave rise to the eukaryotic elongation (EF1α, EF2) and release (eRF1, eRF3) factors (Inge-Vechtomov et al., 2003). These proteins were initially characterised for their role in protein translation. Except for eRF1 (which is derived from EF-G), all of them possess potential orthologues in trypanosomatids. More recently, EF1α was found to interact with the cellular actin network (Izawa et al., 2000) and to stabilise microtubules (Moore et al., 1998) and thus seem to be involved in cytoskeleton organisation. This protein was found to be up-regulated during the early stages of serum deprivation- and hydrogen peroxide-induced apoptosis (Duttaroy et al., 1998; Chen et al., 2000; Talapatra et al., 2002). In *T. cruzi*, EF1α relocates to the nucleus upon programmed cell death-induction (Billaut-Mulot et al., 1996). In *L. donovani* EF1α was identified as a virulence factor essential for the parasite survival in the mammalian host through its modulation of host cell apoptosis (Nandan et al., 2003; Olivier et al., 2005). In sea urchin embryos, EF1α appears to associate with the mitotic apparatus (Ohta et al., 1990). Therefore, with these multiple functions, EF1α acts on processes associated with both the survival and the death of the cell. Assuming that EF1α possesses such varied roles in trypanosomatids, then any possible modulation of EF1α activity by metacaspase cleavage will have dramatic consequences for the cell. The same might be said of EF2 which, in mammalian cells, is indirectly controlled by the extracellular signal-regulated kinase (ERK) pathway promoting entry and progression through mitosis (Roberts et al., 2006) and is involved in cytokinesis and initiation of differentiation in *Dictyostelium* (Watanabe et al., 2003). Possessing C-termini comparable to that of EF1α, two yeast orthologues of the mammalian release factor eRF1 and eRF3 (encoded by *SUP45* and *SUP35*, respectively), initially characterised for their involvement in the termination of protein translation, were found to participate not only to cytoskeleton organisation but also in cell cycle regulation (Valouev et al., 2002). Deletion of the *SUP35* gene in *S. cerevisiae* resulted in cells with aberrant morphology in which the actin cytoskeletal structures had disappeared and where mitosis was impeded by an impairment in mitotic spindle formation. The EF1α–like C-terminal domain of eRF3 was found to be responsible of these phenotypes. Cells lacking eRF1 accumulated with 2C and more DNA content, indicating that DNA replication was somehow uncoupled from

cell division. Strikingly, the phenotypes observed in yeast upon deletion of eRF3 and eRF1 were similar to the ones observed during the overexpression of LmajMCA in *L. major* (impairment in kinetoplast segregation, mitosis and cytokinesis, aberrant shape and tetraploidy). Although no homologue of eRF1 has been identified in the *L. major* genome, a putative orthologue of eRF3 is present (LmjF11.1170). Interestingly, this protein possesses, in its EF1α-like C-terminal, a VRGIDENDIH sequence that could potentially work as a cleavage site for LmajMCA (in case it has a substrate specificity similar to TbMCA2). Therefore it is tempting to speculate that eRF3 might be an *in vivo* target for LmajMCA. To gain further insights into this exciting finding, a determination of LmajMCA *in vivo* partners in now needed. This could be achieved by either expressing, in *L. major* cells, LmajMCA at a low level, or in an inactive form, with a tag optimised for protein purification (see **section 6.5.2**) or by doing a two-hybrid screen in yeast. Such an approach has recently been successfully followed with a catalytically inactive variant of the plant metacaspase AtMCA9 (Vercammen et al., 2006). Initially found to bind to AtMCA9 *in vitro*, a serine peptidase inhibitor termed AtSerpin1 was subsequently identified as a suicide inhibitor of AtMCA9 (Vercammen et al., 2006). No orthologue of AtSerpin1 is present in trypanosomatids, but such a strategy of investigation if performed with the parasite metacaspases could lead to a better understanding of the functions of these proteins. Indeed, the identification of metacaspase specific inhibitors might provide leads for the development of much needed new anti-trypanosomatid drugs.

References

A

Addinall, S.G. and B. Holland. 2002. The tubulin ancestor, FtsZ, draughtsman, designer and driving force for bacterial cytokinesis. *J. Mol. Biol.* 318:219-236.

Akopyants, N.S., R.S. Matlib, E.N. Bukanova, M.R. Smeds, B.H. Brownstein, G.D. Stormo, and S.M. Beverley. 2004. Expression profiling using random genomic DNA microarrays identifies differentially expressed genes associated with three major developmental stages of the protozoan parasite *Leishmania major*. *Mol. Biochem. Parasitol.* 136:71-86.

Alberio, S.O., S.S. Dias, F.P. Faria, R.A. Mortara, C.L. Barbieri, and H.E. Freymuller. 2004. Ultrastructural and cytochemical identification of megasome in *Leishmania (Leishmania) chagasi*. *Parasitol. Res.* 92:246-254.

Alexander, J., G.H. Coombs, and J.C. Mottram. 1998. *Leishmania mexicana* cysteine proteinase-deficient mutants have attenuated virulence for mice and potentiate a Th1 response. *J. Immunol.* 161:6794-6801.

Algeciras-Schimnich, A., B.C. Barnhart, and M.E. Peter. 2002. Apoptosis-independent functions of killer caspases. *Curr. Opin. Cell Biol.* 14:721-726.

Alzate, J.F., A. Alvarez-Barrientos, V.M. Gonzalez, and A. Jimenez-Ruiz. 2006. Heat-induced programmed cell death in *Leishmania infantum* is reverted by Bcl-X(L) expression. *Apoptosis.* 11:161-171.

Ameisen, J.C. 1996. The origin of programmed cell death. *Science* 272:1278-1279.

Ameisen, J.C., T. Idziorek, O. Billaut-Multo, M. Loyens, J.P. Yissier, A. Potentier, and A. Ouaissi. 1996. Apoptosis in a unicellular eukaryote (*Trypanosoma cruzi*): Implications for the evolutionary origin and role of programmed cell death in the control of cell proliferation, differentiation and survival. *Parasitol. Today* 12:49.

Andre, B. and J.Y. Springael. 1994. WWP, a new amino acid motif present in single or multiple copies in various proteins including dystrophin and the SH3-binding Yes-associated protein YAP65. *Biochem. Biophys. Res. Commun.* 205:1201-1205.

Aravind, L., V.M. Dixit, and E.V. Koonin. 1999. The domains of death: evolution of the apoptosis machinery. *Trends Biochem. Sci.* 24:47-53.

Aravind, L., V.M. Dixit, and E.V. Koonin. 2001. Apoptotic molecular machinery: vastly increased complexity in vertebrates revealed by genome comparisons. *Science* 291:1279-1284.

Arnoult, D., K. Akarid, A. Grodet, P.X. Petit, J. Estaquier, and J.C. Ameisen. 2002. On the evolution of programmed cell death: apoptosis of the unicellular eukaryote *Leishmania major* involves cysteine proteinase activation and mitochondrion permeabilization. *Cell Death. Differ.* 9:65-81.

Asgian, J.L., K.E. James, Z.Z. Li, W.Carter, A.J. Barrett, J. Mikolajczyk, G.S. Salvesen, and J.C. Powers. 2002. Aza-peptide epoxides: a new class of inhibitors selective for clan CD cysteine proteases. *J. Med. Chem.* 45:4958-4960.

Assuncao, G.C. and R. Linden. 2004. Programmed cell deaths. Apoptosis and alternative deathstyles. *Eur. J Biochem.* 271:1638-1650.

B

Barrett A.J., N.D.Rawlings and J.F. Woessner. The Handbook of Proteolytic Enzymes. [2nd ed.]. 2003. Academic Press.

Barrett, A.J. and N.D. Rawlings. 2001. Evolutionary lines of cysteine peptidases. *Biol. Chem.* 382:727-733.

Barrett, M.P., J.C. Mottram, and G.H. Coombs. 1999. Recent advances in identifying and validating drug targets in trypanosomes and leishmanias. *Trends Microbiol.* 7:82-88.

Bastin, P., T.J. Pullen, F.F. Moreira-Leite, and K. Gull. 2000. Inside and outside of the trypanosome flagellum: a multifunctional organelle. *Microbes. Infect.* 2:1865-1874.

Basu, M.K. and M. Ray. 2005. Macrophage and *Leishmania*: an unacceptable coexistence. *Crit Rev. Microbiol.* 31:145-154.

Bednarek, S.Y. and T.G. Falbel. 2002. Membrane trafficking during plant cytokinesis. *Traffic.* 3:621-629.

Belenghi, B., M. Carmen Romero-Puertas, D. Vercammen, A. Brackenier, D. Inze, M. Delledonne, and F. Van Breusegem. 2006. Metacaspase activity of *Arabidopsis thaliana* is regulated by S-nitrosylation of a critical cysteine residue. *J. Biol. Chem.*

Benne, R., B.J. Van den, J.P. Brakenhoff, P. Sloof, J.H. Van Boom, and M.C. Tromp. 1986. Major transcript of the frameshifted *coxII* gene from trypanosome mitochondria contains four nucleotides that are not encoded in the DNA. *Cell* 46:819-826.

Benzel, I., F. Weise, and M. Wiese. 2000. Deletion of the gene for the membrane-bound acid phosphatase of *Leishmania mexicana*. *Mol. Biochem. Parasitol.* 111:77-86.

Besteiro, S., G.H. Coombs, and J.C. Mottram. 2004. A potential role for ICP, a *Leishmanial* inhibitor of cysteine peptidases, in the interaction between host and parasite. *Mol Microbiol* 54:1224-1236.

Bettiga, M., L. Calzari, I. Orlandi, L. Alberghina, and M. Vai. 2004. Involvement of the yeast metacaspase Yca1 in ubp10[Delta]-programmed cell death. *FEMS Yeast Research* 5:141-147.

Bieliavsky, N., M. Geuskens, M. Goldfinger, and R. Tencer. 1992. Isolation of plasma membranes, Golgi bodies and mitochondria of *Xenopus laevis* morulae. Identification of plasma membrane proteins. *J. Submicrosc. Cytol. Pathol.* 24:335-349.

Billaut-Mulot, O., R. Fernandez-Gomez, M. Loyens, and A. Ouaissi. 1996. *Trypanosoma cruzi* elongation factor 1-alpha: nuclear localization in parasites undergoing apoptosis. *Gene* 174:19-26.

Birkett, C.R., K.E. Foster, L. Johnson, and K. Gull. 1985. Use of monoclonal antibodies to analyse the expression of a multi-tubulin family. *FEBS Lett.* 187:211-218.

Bluemink, J.G. and S.W. de Laat. 1973. New membrane formation during cytokinesis in normal and cytochalasin B-treated eggs of *Xenopus laevis*. I. Electron microscope observations. *J. Cell Biol.* 59:89-108.

Boatright, K.M. and G.S. Salvesen. 2003. Mechanisms of caspase activation. *Curr. Opin. Cell Biol.* 15:725-731.

Boldin, M.P., E.E. Varfolomeev, Z. Pancer, I.L. Mett, J.H. Camonis, and D. Wallach. 1995. A novel protein that interacts with the death domain of Fas/APO1 contains a sequence motif related to the death domain. *J. Biol. Chem.* 270:7795-7798.

Borges, V.M., U.G. Lopes, W. de Souza, and M.A. Vannier-Santos. 2005. Cell structure and cytokinesis alterations in multidrug-resistant *Leishmania (Leishmania) amazonensis*. *Parasitol. Res.* 95:90-96.

Bork, P. and M. Sudol. 1994. The WW domain: a signalling site in dystrophin? *Trends Biochem. Sci.* 19:531-533.

Bozhkov, P.V., L.H. Filonova, M.F. Suarez, A. Helmersson, A.P. Smertenko, B. Zhivotovsky, and S. Von Arnold. 2003. VEIDase is a principal caspase-like activity involved in plant programmed cell death and essential for embryonic pattern formation. *Cell Death. Differ.*11:175-182

Bozhkov, P.V., M.F. Suarez, L.H. Filonova, G. Daniel, A.A. Zamyatnin, Jr., S. Rodriguez-Nieto, B. Zhivotovsky, and A. Smertenko. 2005. Cysteine protease mcII-Pa executes programmed cell death during plant embryogenesis. *Proc. Natl. Acad. Sci. U. S. A* 102:14463-14468.

Broadhead, R., H.R. Dawe, H. Farr, S. Griffiths, S.R. Hart, N. Portman, M.K. Shaw, M.L. Ginger, S.J. Gaskell, P.G .McKean, and K. Gull. 2006. Flagellar motility is required for the viability of the bloodstream trypanosome. *Nature* 440:224-227.

Brooker, B.E. 1971. The fine structure of Crithidia fasciculata with special reference to the organelles involved in the ingestion and digestion of protein. *Z. Zellforsch. Mikrosk. Anat.* 116:532-563.

Bursch, W., A. Ellinger, C. Gerner, U. Frohwein, and R. Schulte-Hermann. 2000. Programmed cell death (PCD). Apoptosis, autophagic PCD, or others? *Ann. N. Y. Acad. Sci.* 926:1-12.

Byers, T.J. and P.B. Armstrong. 1986. Membrane protein redistribution during *Xenopus* first cleavage. *J. Cell Biol.* 102:2176-2184.

C

Calero, M., C.Z. Chen, W. Zhu, N. Winand, K.A. Havas, P.M. Gilbert, C.G. Burd, and R.N. Collins. 2003. Dual prenylation is required for Rab protein localization and function. *Mol. Biol. Cell* 14:1852-1867.

Chang, L. and R.D. Goldman. 2004. Intermediate filaments mediate cytoskeletal crosstalk. *Nat. Rev. Mol. Cell Biol.* 5:601-613.

Chen, E., G. Proestou, D. Bourbeau, and E. Wang. 2000. Rapid up-regulation of peptide elongation factor EF-1alpha protein levels is an immediate early event during oxidative stress-induced apoptosis. *Exp. Cell Res.* 259:140-148.

Chen, J.M., N.D. Rawlings, R.A. Stevens, and A.J. Barrett. 1998. Identification of the active site of legumain links it to caspases, clostripain and gingipains in a new clan of cysteine endopeptidases. *FEBS Lett.* 441:361-365.

Cheng, J., T.S. Park, L.C. Chio, A.S. Fischl, and X.S. Ye. 2003. Induction of apoptosis by sphingoid long-chain bases in *Aspergillus nidulans*. *Mol. Cell Biol.* 23:163-177.

Chinnaiyan, A.M., K. O'Rourke, M. Tewari, and V.M. Dixit. 1995. FADD, a novel death domain-containing protein, interacts with the death domain of Fas and initiates apoptosis. *Cell* 81:505-512.

Choi, D.W. 1988. Calcium-mediated neurotoxicity: relationship to specific channel types and role in ischemic damage. *Trends Neurosci.* 11:465-469.

Chowdhury, A.R., S. Mandal, A. Goswami, M. Ghosh, L. Mandal, D. Chakraborty, A. Ganguly, G. Tripathi, S. Mukhopadhyay, S. Bandyopadhyay, and H.K. Majumder. 2003. Dihydrobetulinic acid induces apoptosis in *Leishmania donovani* by targeting DNA topoisomerase I and II: implications in antileishmanial therapy. *Mol. Med.* 9:26-36.

Clarke, A., R. Desikan, R.D. Hurst, J.T. Hancock, and S.J. Neill. 2000. NO way back: nitric oxide and programmed cell death in *Arabidopsis thaliana* suspension cultures. *Plant J.* 24:667-677.

Clayton, C., T. Hausler, and J. Blattner. 1995. Protein trafficking in kinetoplastid protozoa. *Microbiol. Rev.* 59:325-344.

Clayton, C.E. 2002. Life without transcriptional control? From fly to man and back again. *EMBO J.* 21:1881-1888.

Cohen, G.M. 1997. Caspases: the executioners of apoptosis. *Biochem. J.* 326 (Pt 1):1-16.

Coombs, G.H., L. Tetley, V.A. Moss, and K. Vickerman. 1986. Three dimensional structure of the *Leishmania amastigote* as revealed by computer-aided reconstruction from serial sections. *Parasitology* 92 (Pt 1):13-23.

Coombs, G.H., K. Vickerman, M.A. Sleigh, and A. Warren. 1998. Evolutionary Relationships Among Protozoa. Kluver Academic Publishers, London.

Couvreur, B., R. Wattiez, A. Bollen, P. Falmagne, D. Le Ray, and J.C. Dujardin. 2002. Eubacterial HslV and HslU subunits homologs in primordial eukaryotes. *Mol. Biol. Evol.* 19:2110-2117.

Croft, S.L. and G.H. Coombs. 2003. Leishmaniasis--current chemotherapy and recent advances in the search for novel drugs. *Trends Parasitol.* 19:502-508.

Croft, S.L., K. Seifert, and M. Duchene. 2003. Antiprotozoal activities of phospholipid analogues. *Mol. Biochem. Parasitol.* 126:165-172.

Cross, G.A., A.A. Holder, G. Allen, and J.C. Boothroyd. 1980. An introduction to antigenic variation in trypanosomes. *Am. J. Trop. Med. Hyg.* 29:1027-1032.

Cruz, A.K., R. Titus, and S.M. Beverley. 1993. Plasticity in chromosome number and testing of essential genes in *Leishmania* by targeting. *Proc. Natl. Acad. Sci. U. S. A* 90:1599-1603.

Curtis, M.A., J. Aduse-Opoku, and M. Rangarajan. 2001. Cysteine proteases of *Porphyromonas gingivalis*. *Crit Rev. Oral Biol. Med.* 12:192-216.

D

D'Avino, P.P., M.S. Savoian, and D.M. Glover. 2005. Cleavage furrow formation and ingression during animal cytokinesis: a microtubule legacy. *J. Cell Sci.* 118:1549-1558.

Da Silva, R. and D.L. Sacks. 1987. Metacyclogenesis is a major determinant of *Leishmania* promastigote virulence and attenuation. *Infect. Immun.* 55:2802-2806.

Danon, A., V. Rotari, A. Gordon, N. Mailhac, and P. Gallois. 2003. UV-C overexposure induces a programmed cell death in *Arabidopsis*, which is mediated by caspase-like activities and can be suppressed by caspase inhibitors, p35 and defender against apoptotic death. *J. Biol. Chem.*279:779-787

Das, B.B., N. Sen, A. Ganguly, and H.K. Majumder. 2004. Reconstitution and functional characterization of the unusual bi-subunit type I DNA topoisomerase from *Leishmania donovani*. *FEBS Lett.* 565:81-88.

de Pereda, J.M., D. Leynadier, J.A. Evangelio, P. Chacon, and J.M. Andreu. 1996. Tubulin secondary structure analysis, limited proteolysis sites, and homology to FtsZ. *Biochemistry* 35:14203-14215.

Debrabant, A., N. Lee, S. Bertholet, R. Duncan, and H.L. Nakhasi. 2003. Programmed cell death in trypanosomatids and other unicellular organisms. *Int. J. Parasitol.* 33:257-267.

Debrabant, A. and H. Nakhasi. 2003. Programmed cell death in trypanosomatids: is it an altruistic mechanism for survival of the fittest? *Kinetoplastid. Biol. Dis.* 2:7.

del Pozo, O. and E. Lam. 1998. Caspases and programmed cell death in the hypersensitive response of plants to pathogens. *Curr. Biol.* 8:1129-1132.

Deolindo, P., A.S. Teixeira-Ferreira, E.J. Melo, A.C. Arnholdt, W. Souza, E.W. Alves, and R.A. DaMatta. 2005. Programmed cell death in *Trypanosoma cruzi* induced by *Bothrops jararaca* venom. *Mem. Inst. Oswaldo Cruz* 100:33-38.

Dickinson, D.P. 2002. Cysteine peptidases of mammals: their biological roles and potential effects in the oral cavity and other tissues in health and disease. *Crit Rev. Oral Biol. Med.* 13:238-275.

Dietrich, R.A., M.H. Richberg, R. Schmidt, C. Dean, and J.L. Dangl. 1997. A novel zinc finger protein is encoded by the Arabidopsis LSD1 gene and functions as a negative regulator of plant cell death. *Cell* 88:685-694.

Dornan, S., A.P. Jackson, and N.J. Gay. 1997. Alpha-adaptin, a marker for endocytosis, is expressed in complex patterns during *Drosophila* development. *Mol. Biol. Cell* 8:1391-1403.

Draberova, E., P. Draber, F. Havlicek, and V. Viklicky. 1986. A common antigenic determinant of vimentin and desmin defined by monoclonal antibody. *Folia Biol. (Praha)* 32:295-303.

Drees, B.L., B. Sundin, E. Brazeau, J.P. Caviston, G.C. Chen, W. Guo, K.G. Kozminski, M.W. Lau, J.J. Moskow, A. Tong, L.R. Schenkman, A. McKenzie, P. Brennwald, M. Longtine, E. Bi, C. Chan, P. Novick, C. Boone, J.R. Pringle, T.N. Davis, S. Fields, and D.G. Drubin. 2001. A protein interaction map for cell polarity development. *J. Cell Biol.* 154:549-571.

Dumas, C., M. Ouellette, J. Tovar, M.L. Cunningham, A.H. Fairlamb, S. Tamar, M. Olivier, and B. Papadopoulou. 1997. Disruption of the trypanothione reductase gene of *Leishmania* decreases its ability to survive oxidative stress in macrophages. *EMBO J.* 16:2590-2598.

Duttaroy, A., D. Bourbeau, X.L. Wang, and E. Wang. 1998. Apoptosis rate can be accelerated or decelerated by overexpression or reduction of the level of elongation factor-1 alpha. *Exp. Cell Res.* 238:168-176.

E

Earnshaw, W.C., L.M. Martins, and S.H. Kaufmann. 1999. Mammalian caspases: structure, activation, substrates, and functions during apoptosis. *Annu. Rev. Biochem* 68:383-424.

Edinger, A.L. and C.B. Thompson. 2004. Death by design: apoptosis, necrosis and autophagy. *Curr. Opin. Cell Biol.* 16:663-669.

Ellis, M., D.K. Sharma, J.D. Hilley, G.H. Coombs, and J.C. Mottram. 2002. Processing and trafficking of *Leishmania mexicana* GP63. Analysis using GP18 mutants deficient in glycosylphosphatidylinositol protein anchoring. *J. Biol. Chem.* 277:27968-27974.

Emoto, K., T. Kobayashi, A. Yamaji, H. Aizawa, I. Yahara, K. Inoue, and M. Umeda. 1996. Redistribution of phosphatidylethanolamine at the cleavage furrow of dividing cells during cytokinesis. *Proc. Natl. Acad. Sci. U. S. A* 93:12867-12872.

Emoto, K. and M. Umeda. 2000. An essential role for a membrane lipid in cytokinesis. Regulation of contractile ring disassembly by redistribution of phosphatidylethanolamine. *J. Cell Biol.* 149:1215-1224.

Engelberg-Kulka, H., S. Amitai, I. Kolodkin-Gal, and R. Hazan. 2006. Bacterial programmed cell death and multicellular behavior in bacteria. *PLoS. Genet.* 2:e135.

Engstler, M., L. Thilo, F. Weise, C.G. Grunfelder, H. Schwarz, M. Boshart, and P. Overath. 2004. Kinetics of endocytosis and recycling of the GPI-anchored variant surface glycoprotein in *Trypanosoma brucei*. *J. Cell Sci.* 117:1105-1115.

Errington, J., R.A. Daniel, and D.J.Scheffers. 2003. Cytokinesis in bacteria. *Microbiol. Mol. Biol. Rev.* 67:52-65

Ersfeld, K. and K. Gull. 1997. Partitioning of large and minichromosomes in *Trypanosoma brucei*. *Science* 276:611-614.

Ersfeld, K., S.E. Melville, and K. Gull. 1999. Nuclear and genome organization of *Trypanosoma brucei*. *Parasitol. Today* 15:58-63.

Esseiva, A.C., A.L. Chanez, N. Bochud-Allemann, J.C. Martinou, A. Hemphill, and A. Schneider. 2004. Temporal dissection of Bax-induced events leading to fission of the single mitochondrion in *Trypanosoma brucei*. *EMBO Rep.* 5:268-273.

F

Fairbrother, W.J., N.C. Gordon, E.W. Humke, K.M. O'Rourke, M.A. Starovasnik, J.P. Yin, and V.M. Dixit. 2001. The PYRIN domain: a member of the death domain-fold superfamily. *Protein Sci.* 10:1911-1918.

Feagin, J.E. 2000. Mitochondrial genome diversity in parasites. *Int. J. Parasitol.* 30:371-390.

Fernandes-Alnemri, T., G. Litwack, and E.S. Alnemri. 1994. CPP32, a novel human apoptotic protein with homology to *Caenorhabditis elegans* cell death protein Ced-3 and mammalian interleukin-1 beta-converting enzyme. *J. Biol. Chem.* 269:30761-30764.

Fernando, P., J.F. Kelly, K. Balazsi, R.S. Slack, and L.A. Megeney. 2002. Caspase 3 activity is required for skeletal muscle differentiation. *Proc. Natl. Acad. Sci. U. S. A* 99:11025-11030.

Field, C., R. Li, and K. Oegema. 1999. Cytokinesis in eukaryotes: a mechanistic comparison. *Curr. Opin. Cell Biol.* 11:68-80.

Fielding, A.B., E. Schonteich, J. Matheson, G. Wilson, X. Yu, G.R. Hickson, S. Srivastava, S.A. Baldwin, R. Prekeris, and G.W. Gould. 2005. Rab11-FIP3 and FIP4 interact with Arf6 and the exocyst to control membrane traffic in cytokinesis. *EMBO J.* 24:3389-3399.

Figarella, K., M. Rawer, N.L. Uzcategui, B.K. Kubata, K. Lauber, F. Madeo, S. Wesselborg, and M. Duszenko. 2005. Prostaglandin D2 induces programmed cell death in *Trypanosoma brucei* bloodstream form. *Cell Death Differ.* 12:335-346.

Figarella, K., N.L. Uzcategui, A. Beck, C. Schoenfeld, B.K. Kubata, F. Lang, and M. Duszenko. 2006. Prostaglandin-induced programmed cell death in *Trypanosoma brucei* involves oxidative stress. *Cell Death. Differ.*13:1802-1814

Finger, F.P. and J.G. White. 2002. Fusion and fission: membrane trafficking in animal cytokinesis. *Cell* 108:727-730.

Fischer, U., R.U. Janicke, and K. Schulze-Osthoff. 2003. Many cuts to ruin: a comprehensive update of caspase substrates. *Cell Death. Differ.* 10:76-100.

Fishkind, D.J. and Y.L. Wang. 1995. New horizons for cytokinesis. *Curr. Opin. Cell Biol.* 7:23-31.

Flower, T.R., L.S. Chesnokova, C.A. Froelich, C. Dixon, and S.N. Witt. 2005. Heat shock prevents alpha-synuclein-induced apoptosis in a yeast model of Parkinson's disease. *J Mol Biol* 351:1081-1100.

Fox, T., E. de Miguel, J.S. Mort, and A.C. Storer. 1992. Potent slow-binding inhibition of cathepsin B by its propeptide. *Biochemistry* 31:12571-12576.

Fuentes-Prior, P. and G.S. Salvesen. 2004. The protein structures that shape caspase activity, specificity, activation and inhibition. *Biochem. J.* 384:201-232.

Fujinaga, M., M.M. Cherney, H. Oyama, K. Oda, and M.N. James. 2004. The molecular structure and catalytic mechanism of a novel carboxyl peptidase from *Scytalidium lignicolum*. *Proc. Natl. Acad. Sci. U. S. A* 101:3364-3369.

G

Garami, A. and T. Ilg. 2001. The role of phosphomannose isomerase in *Leishmania mexicana* glycoconjugate synthesis and virulence. *J. Biol. Chem.* 276:6566-6575.

Garay-Arroyo, A., J.M. Colmenero-Flores, A. Garciarrubio, and A.A. Covarrubias. 2000. Highly hydrophilic proteins in prokaryotes and eukaryotes are common during conditions of water deficit. *J. Biol. Chem.* 275:5668-5674.

Garcia-Salcedo, J.A., D. Perez-Morga, P. Gijon, V. Dilbeck, E. Pays, and D.P. Nolan. 2004. A differential role for actin during the life cycle of *Trypanosoma brucei*. *EMBO J.* 23:780-789.

Gerdes, H.H. and C. Kaether. 1996. Green fluorescent protein: applications in cell biology. *FEBS Lett.* 389:44-47.

Ghedin, E., F. Bringaud, J. Peterson, P. Myler, M. Berriman, A. Ivens, B. Andersson, E. Bontempi, J. Eisen, S. Angiuoli, D. Wanless, A. Von Arx, L. Murphy, N. Lennard, S. Salzberg, M.D. Adams, O. White, N. Hall, K. Stuart, C.M. Fraser, and N.M. El Sayed. 2004. Gene synteny and evolution of genome architecture in trypanosomatids. *Mol. Biochem. Parasitol.* 134:183-191.

Ghedin, E., A. Debrabant, J.C. Engel, and D.M. Dwyer. 2001. Secretory and endocytic pathways converge in a dynamic endosomal system in a primitive protozoan. *Traffic.* 2:175-188.

Glotzer, M. 1997a. Cytokinesis. *Curr. Biol.* 7:R274-R276.

Glotzer, M. 1997b. The mechanism and control of cytokinesis. *Curr. Opin. Cell Biol.* 9:815-823.

Glotzer, M. 2001. Animal cell cytokinesis. *Annu. Rev. Cell Dev. Biol.* 17:351-386.

Glotzer, M. 2005. The molecular requirements for cytokinesis. *Science* 307:1735-1739.

Gonzalez, I.J., C. Desponds, C. Schaff, J.C. Mottram, and N.Fasel. 2006. *Leishmania major* metacaspase can replace yeast metacaspase in programmed cell death and has arginine-specific cysteine peptidase activity. *Int. J. Parasitol.* Epub ahead of print.

Goode, B.L., D.G. Drubin, and G. Barnes. 2000. Functional cooperation between the microtubule and actin cytoskeletons. *Curr. Opin. Cell Biol.* 12:63-71.

Gossage, S.M., M.E. Rogers, and P.A. Bates. 2003. Two separate growth phases during the development of *Leishmania* in sand flies: implications for understanding the life cycle. *Int. J. Parasitol.* 33:1027-1034.

Gozani, O., M. Boyce, L. Yoo, P. Karuman, and J. Yuan. 2002. Life and death in paradise. *Nat. Cell Biol.* 4:E159-E162.

Grinna, L.S. and J.F. Tschopp. 1989. Size distribution and general structural features of N-linked oligosaccharides from the methylotrophic yeast, Pichia pastoris. *Yeast* 5:107-115.

Grunfelder, C.G., M. Engstler, F. Weise, H. Schwarz, Y.D. Stierhof, G.W. Morgan, M.C. Field, and P. Overath. 2003. Endocytosis of a glycosylphosphatidylinositol-anchored protein via clathrin-coated vesicles, sorting by default in endosomes, and exocytosis via RAB11-positive carriers. *Mol. Biol. Cell* 14:2029-2040.

Guerin, P.J., P. Olliaro, S. Sundar, M. Boelaert, S.L. Croft, P. Desjeux, M.K. Wasunna, and A.D. Bryceson. 2002. Visceral leishmaniasis: current status of control, diagnosis, and treatment, and a proposed research and development agenda. *Lancet Infect. Dis.* 2:494-501.

Gull, K., S. Alsford, and K. Ersfeld. 1998. Segregation of minichromosomes in trypanosomes: implications for mitotic mechanisms. *Trends Microbiol.* 6:319-323.

Gundersen, G.G. and T.A. Cook. 1999. Microtubules and signal transduction. *Curr. Opin. Cell Biol.* 11:81-94.

H

Hall, B.S., E. Smith, W. Langer, L.A. Jacobs, D. Goulding, and M.C. Field. 2005. Developmental variation in Rab11-dependent trafficking in *Trypanosoma brucei*. *Eukaryot. Cell* 4:971-980.

Hall, D.H., G. Gu, J. Garcia-Anoveros, L. Gong, M. Chalfie, and M. Driscoll. 1997. Neuropathology of degenerative cell death in *Caenorhabditis elegans*. *J. Neurosci.* 17:1033-1045.

Hammarton, T.C., S.G. Lillico, S.C. Welburn, and J.C. Mottram. 2005. *Trypanosoma brucei* MOB1 is required for accurate and efficient cytokinesis but not for exit from mitosis. *Mol. Microbiol.* 56:104-116.

Hammarton, T.C., J.C. Mottram, and C. Doerig. 2003. The cell cycle of parasitic protozoa: potential for chemotherapeutic exploitation. *Prog. Cell Cycle Res.* 5:91-101.

Handman, E. 2001. Leishmaniasis: current status of vaccine development. *Clin. Microbiol. Rev.* 14:229-243.

Handman, E. and D.V. Bullen. 2002. Interaction of *Leishmania* with the host macrophage. *Trends Parasitol.* 18:332-334.

Hansen, G. 2000. Evidence for *Agrobacterium*-induced apoptosis in maize cells. *Mol. Plant Microbe Interact.* 13:649-657.

Harder, S., M. Bente, K. Isermann, and I. Bruchhaus. 2006. Expression of a mitochondrial peroxiredoxin prevents programmed cell death in *Leishmania donovani*. *Eukaryot. Cell* 5:861-870.

Hassan, P., D. Fergusson, K.M. Grant, and J.C. Mottram. 2001. The CRK3 protein kinase is essential for cell cycle progression of *Leishmania mexicana*. *Mol. Biochem. Parasitol.* 113:189-198.

Havens, C.G., N. Bryant, L. Asher, L. Lamoreaux, S. Perfetto, J.J. Brendle, and K.A. Werbovetz. 2000. Cellular effects of leishmanial tubulin inhibitors on *L. donovani*. *Mol. Biochem. Parasitol.* 110:223-236.

Hazbun, T.R., L. Malmstrom, S. Anderson, B.J. Graczyk, B. Fox, M. Riffle, B.A. Sundin, J.D. Aranda, W.H. McDonald, C.H. Chiu, B.E. Snydsman, P. Bradley, E.G. Muller, S. Fields, D. Baker, J.R. Yates and T.N.Davis. 2003. Assigning function to yeast proteins by integration of technologies. *Mol. Cell* 12:1353-1365.

Helms,M.J. Characterisation of *T. brucei* metacaspases. PhD thesis . 2004.

Helms, M.J., A. Ambit, P. Appleton, L. Tetley, G.H. Coombs, and J.C. Mottram. 2006. Bloodstream form *Trypanosoma brucei* depend upon multiple metacaspases associated with RAB11-positive endosomes. *J. Cell Sci.* 119:1105-1117.

Hendriks, E.F., D.R. Robinson, M. Hinkins, and K.R. Matthews. 2001. A novel CCCH protein which modulates differentiation of *Trypanosoma brucei* to its procyclic form. *EMBO J.* 20:6700-6711.

Hengartner, M.O. 2000. The biochemistry of apoptosis. *Nature* 407:770-776.

Herker, E., H. Jungwirth, K.A. Lehmann, C. Maldener, K.U. Frohlich, S. Wissing, S. Buttner, M. Fehr, S. Sigrist, and F. Madeo. 2004. Chronological aging leads to apoptosis in yeast. *J. Cell Biol.* 164:501-507.

Hess, D.T., A. Matsumoto, S.O. Kim, H.E. Marshall, and J.S. Stamler. 2005. Protein S-nitrosylation: purview and parameters. *Nat. Rev. Mol. Cell Biol.* 6:150-166.

Hirumi, H. and K. Hirumi. 1989. Continuous cultivation of *Trypanosoma brucei* blood stream forms in a medium containing a low concentration of serum-protein without feeder cell-layers. *J. Parasitol.* 75:985-989.

Hobdy-Henderson, K.C., C.M. Hales, L.A. Lapierre, R.E. Cheney, and J.R. Goldenring. 2003. Dynamics of the apical plasma membrane recycling system during cell division. *Traffic.* 4:681-693.

Hodder, A.N., D.R. Drew, V.C. Epa, M. Delorenzi, R. Bourgon, S.K. Miller, R.L. Moritz, D.F. Frecklington, R.J. Simpson, T.P. Speed, R.N. Pike, and B.S. Crabb. 2003. Enzymic, phylogenetic, and structural characterization of the unusual papain-like protease domain of *Plasmodium falciparum* SERA5. *J. Biol. Chem.* 278:48169-48177.

Hoeberichts, F.A., A. ten Have, and E.J. Woltering. 2003. A tomato metacaspase gene is upregulated during programmed cell death in *Botrytis cinerea*-infected leaves. *Planta* 217:517-522.

Hofmann, K., P. Bucher, and J. Tschopp. 1997. The CARD domain: a new apoptotic signalling motif. *Trends Biochem. Sci.* 22:155-156.

Holzmuller, P., R. Bras-Goncalves, and J.L. Lemesre. 2006. Phenotypical characteristics, biochemical pathways, molecular targets and putative role of nitric oxide-mediated programmed cell death in *Leishmania*. *Parasitology* 132:S19-S32.

Holzmuller, P., D. Sereno, M. Cavaleyra, I. Mangot, S. Daulouede, P. Vincendeau, and J.L. Lemesre. 2002. Nitric oxide-mediated proteasome-dependent oligonucleosomal DNA fragmentation in *Leishmania amazonensis* amastigotes. *Infect. Immun.* 70:3727-3735.

Hsu, H., J. Xiong, and D.V. Goeddel. 1995. The TNF receptor 1-associated protein TRADD signals cell death and NF-kappa B activation. *Cell* 81:495-504.

Hsu, S.L., C.T. Yu, S.C. Yin, M.J. Tang, A.C. Tien, Y.M. Wu, and C.Y. Huang. 2006. Caspase 3, periodically expressed and activated at G2/M transition, is required for nocodazole-induced mitotic checkpoint. *Apoptosis.* 11:765-771.

Hu, S., C. Vincenz, J. Ni, R. Gentz, and V.M. Dixit. 1997. I-FLICE, a novel inhibitor of tumor necrosis factor receptor-1- and CD-95-induced apoptosis. *J. Biol. Chem.* 272:17255-17257.

I

Ilg, T. 2000. Lipophosphoglycan is not required for infection of macrophages or mice by *Leishmania mexicana*. *EMBO J.* 19:1953-1962.

Inge-Vechtomov, S., G. Zhouravleva, and M. Philippe. 2003. Eukaryotic release factors (eRFs) history. *Biol. Cell* 95:195-209.

Irmler, M., M. Thome, M. Hahne, P.S chneider, K. Hofmann, V. Steiner, J.L. Bodmer, M. Schroter, K. Burns, C. Mattmann, D. Rimoldi, L.E. French, and J. Tschopp. 1997. Inhibition of death receptor signals by cellular FLIP. *Nature* 388:190-195.

Ito, T., T.Chiba, R. Ozawa, M. Yoshida, M. Hattori, and Y. Sakaki. 2001. A comprehensive two-hybrid analysis to explore the yeast protein interactome. *Proc. Natl. Acad. Sci. U. S. A* 98:4569-4574.

Ivanovska, I. and J.M. Hardwick. 2005. Viruses activate a genetically conserved cell death pathway in a unicellular organism. *J Cell Biol* 170:391-399.

Ivens, A.C., C.S. Peacock, E.A. Worthey, L. Murphy, G.Aggarwal, M.Berriman, E.Sisk, M.A.Rajandream, E.Adlem, R.Aert, *et al.* 2005. The genome of the kinetoplastid parasite, *Leishmania major*. *Science* 309:436-442.

Izawa, T., Y. Fukata, T. Kimura, A. Iwamatsu, K. Dohi, and K. Kaibuchi. 2000. Elongation factor-1 alpha is a novel substrate of rho-associated kinase. *Biochem. Biophys. Res. Commun.* 278:72-78.

J

Jackson, D.G., M.J. Owen, and H.P. Voorheis. 1985. A new method for the rapid purification of both the membrane-bound and released forms of the variant surface glycoprotein from *Trypanosoma brucei*. *Biochem. J.* 230:195-202.

Jayanarayan, K.G. and C.S. Dey. 2002. Microtubules: dynamics, drug interaction and drug resistance in *Leishmania*. *J. Clin. Pharm. Ther.* 27:313-320.

Jayanarayan, K.G. and C.S. Dey. 2005. Altered tubulin dynamics, localization and post-translational modifications in sodium arsenite resistant Leishmania donovani in response to paclitaxel, trifluralin and a combination of both and induction of apoptosis-like cell death. *Parasitology* 131:215-230.

Jeffries, T.R., G.W. Morgan, and M.C. Field. 2001. A developmentally regulated rab11 homologue in *Trypanosoma brucei* is involved in recycling processes. *J Cell Sci* 114:2617-2626.

Joshi, P.B., B.L. Kelly, S. Kamhawi, D.L. Sacks, and W.R. McMaster. 2002. Targeted gene deletion in *Leishmania major* identifies leishmanolysin (GP63) as a virulence factor. *Mol. Biochem. Parasitol.* 120:33-40.

K

Kamada, S., U. Kikkawa, Y. Tsujimoto, and T. Hunter. 2005. Nuclear translocation of caspase-3 is dependent on its proteolytic activation and recognition of a substrate-like protein(s). *J. Biol. Chem.* 280:857-860.

Kamhawi, S. 2006. Phlebotomine sand flies and *Leishmania* parasites: friends or foes? *Trends Parasitol.*

Kaur, K.J. and L. Ruben. 1994. Protein translation elongation factor-1 alpha from *Trypanosoma brucei* binds calmodulin. *J. Biol. Chem.* 269:23045-23050.

Kay, B.K., M.P. Williamson, and M. Sudol. 2000. The importance of being proline: the interaction of proline-rich motifs in signaling proteins with their cognate domains. *FASEB J* 14:231-241.

Kelly, J.M., H.M. Ward, M.A. Miles, and G. Kendall. 1992. A shuttle vector which facilitates the expression of transfected genes in *Trypanosoma cruzi* and *Leishmania*. *Nucleic Acids Res.* 20:3963-3969.

Kerr, J.F., A.H. Wyllie, and A.R. Currie. 1972. Apoptosis: a basic biological phenomenon with wide-ranging implications in tissue kinetics. *Br. J. Cancer* 26:239-257.

Khan, M.A., P.B. Chock, and E.R. Stadtman. 2005. Knockout of caspase-like gene, *YCA1*, abrogates apoptosis and elevates oxidized proteins in *Saccharomyces cerevisiae*. *Proc. Natl. Acad. Sci. U. S. A* 102:17326-17331.

Killick-Kendrick, R. 1990. The life-cycle of *Leishmania* in the sandfly with special reference to the form infective to the vertebrate host. *Ann. Parasitol. Hum. Comp* 65 Suppl 1:37-42.

Killick-Kendrick, R., D.H. Molyneux, and R.W. Ashford. 1974a. *Leishmania* in phlebotomid sandflies. I. Modifications of the flagellum associated with attachment to the mid-gut and oesophageal valve of the sandfly. *Proc. R. Soc. Lond B Biol. Sci.* 187:409-419.

Killick-Kendrick, R., D.H. Molyneux, and R.W. Ashford. 1974b. Ultrastructural observations on the attachment of *Leishmania* in the sandfly. *Trans. R. Soc. Trop. Med. Hyg.* 68:269.

Kim, M., K. Murphy, F. Liu, S.E. Parker, M.L. Dowling, W. Baff, and G.D. Kao. 2005. Caspase-mediated specific cleavage of BubR1 is a determinant of mitotic progression. *Mol. Cell Biol.* 25:9232-9248.

Klingbeil, M.M., S.A. Motyka, and P.T. Englund. 2002. Multiple mitochondrial DNA polymerases in *Trypanosoma brucei*. *Mol. Cell* 10:175-186.

Knight, R.A. 2002. The archaeology of apoptosis. *Cell Death. Differ.* 9:1-2.

Koonin, E.V. and L. Aravind. 2002. Origin and evolution of eukaryotic apoptosis: the bacterial connection. *Cell Death. Differ.* 9:394-404.

Kosec, G., V.E. Alvarez, F. Aguero, D. Sanchez, M. Dolinar, B. Turk, V. Turk, and J.J. Cazzulo. 2006. Metacaspases of *Trypanosoma cruzi*: possible candidates for programmed cell death mediators. *Mol. Biochem. Parasitol.* 145:18-28.

Kratzerova, L., E. Draberova, C. Juliano, V. Viklicky, P.L. Fiori, P. Cappuccinelli, and P. Draber. 2001. Cell cycle-dependent changes in localization of a 210-kDa microtubule-interacting protein in *Leishmania*. *Exp. Cell Res.* 266:270-278.

Kroemer, G., W.S. El Deiry, P. Golstein, M.E. Peter, D. Vaux, P. Vandenabeele, B. Zhivotovsky, M.V. Blagosklonny, W. Malorni, R.A. Knight, M. Piacentini, S. Nagata, and G. Melino. 2005. Classification of cell death: recommendations of the Nomenclature Committee on Cell Death. *Cell Death. Differ.* 12 Suppl 2:1463-1467.

Krogan, N.J., G. Cagney, H. Yu, G. Zhong, X. Guo, A. Ignatchenko, J. Li, S. Pu, N. Datta, A.P.Tikuisis, T.Punna, *et al.* 2006. Global landscape of protein complexes in the yeast *Saccharomyces cerevisiae*. *Nature* 440:637-643.

Kulkarni, M.M., W.R. McMaster, E. Kamysz, W. Kamysz, D.M. Engman, and B.S. McGwire. 2006. The major surface-metalloprotease of the parasitic protozoan, *Leishmania*, protects against antimicrobial peptide-induced apoptotic killing. *Mol. Microbiol.*

Kumar, S., K. Tamura, and M. Nei. 2004. MEGA3: Integrated software for Molecular Evolutionary Genetics Analysis and sequence alignment. *Brief. Bioinform.* 5:150-163.

L

LaCount, D.J., S. Bruse, K.L. Hill, and J.E. Donelson. 2000. Double-stranded RNA interference in *Trypanosoma brucei* using head-to-head promoters. *Mol. Biochem. Parasitol.* 111:67-76.

LaCount, D.J. and J.E. Donelson. 2001. RNA interference in African trypanosomes. *Protist.* 152:103-111.

LeBowitz, J.H., H.Q. Smith, L. Rusche, and S.M. Beverley. 1993. Coupling of poly(A) site selection and trans-splicing in *Leishmania*. *Genes Dev.* 7:996-1007.

Lecaille, F., J. Kaleta, and D. Bromme. 2002. Human and parasitic papain-like cysteine proteases: their role in physiology and pathology and recent developments in inhibitor design. *Chem. Rev.* 102:4459-4488.

Lee, N., S. Bertholet, A. Debrabant, J. Muller, R. Duncan, and H.L. Nakhasi. 2002. Programmed cell death in the unicellular protozoan parasite *Leishmania*. *Cell Death. Differ.* 9:53-64.

Lemercier, G., S. Dutoya, S. Luo, F.A. Ruiz, C.O. Rodrigues, T. Baltz, R. Docampo, and N. Bakalara. 2002. A vacuolar-type H+-pyrophosphatase governs maintenance of functional acidocalcisomes and growth of the insect and mammalian forms of *Trypanosoma brucei*. *J. Biol. Chem.* 277:37369-37376.

Leung, K.F., R. Baron, and M.C. Seabra. 2006. Thematic review series: lipid posttranslational modifications. geranylgeranylation of Rab GTPases. *J. Lipid Res.* 47:467-475.

Lewis, K. 2000. Programmed death in bacteria. *Microbiol. Mol. Biol. Rev.* 64:503-514.

Li, D.N., S.P. Matthews, A.N. Antoniou, D. Mazzeo, and C. Watts. 2003. Multistep autoactivation of asparaginyl endopeptidase in vitro and in vivo. *J. Biol. Chem.* 278:38980-38990.

Lillico, S., M.C. Field, P. Blundell, G.H. Coombs, and J.C. Mottram. 2003. Essential roles for GPI-anchored proteins in African trypanosomes revealed using mutants deficient in GPI8. *Mol. Biol. Cell* 14:1182-1194.

Lincoln, J.E., C. Richael, B. Overduin, K. Smith, R. Bostock, and D.G. Gilchrist. 2002. Expression of the antiapoptotic baculovirus *p35* gene in tomato blocks programmed cell death and provides broad-spectrum resistance to disease. *Proc. Natl. Acad. Sci. U. S. A* 99:15217-15221.

Lockshin, R.A. and Z. Zakeri. 2004a. Apoptosis, autophagy, and more. *Int. J Biochem. Cell Biol.* 36:2405-2419.

Lockshin, R.A. and Z. Zakeri. 2004b. Caspase-independent cell death? *Oncogene* 23:2766-2773.

Lopez, C., N. Chevalier, V. Hannaert, D.J. Rigden, P.A. Michels, and J.L. Ramirez. 2002. *Leishmania donovani* phosphofructokinase. Gene characterization, biochemical properties and structure-modeling studies. *Eur. J. Biochem.* 269:3978-3989.

Lukovic, D., A. Komoriya, B.Z. Packard, and D.S. Ucker. 2003. Caspase activity is not sufficient to execute cell death. *Exp. Cell Res.* 289:384-395.

M

Macias, M.J., S. Wiesner, and M. Sudol. 2002. WW and SH3 domains, two different scaffolds to recognize proline-rich ligands. *FEBS Lett.* 513:30-37.

Madeo, F., S. Engelhardt, E. Herker, N. Lehmann, C. Maldener, A. Proksch, S. Wissing, and K.U. Frohlich. 2002a. Apoptosis in yeast: a new model system with applications in cell biology and medicine. *Curr. Genet.* 41:208-216.

Madeo, F., E. Herker, C. Maldener, S. Wissing, S. Lachelt, M. Herlan, M. Fehr, K. Lauber, S.J. Sigrist, S. Wesselborg, and K.U. Frohlich. 2002b. A caspase-related protease regulates apoptosis in yeast. *Mol. Cell* 9:911-917.

Mannick, J.B., C. Schonhoff, N. Papeta, P. Ghafourifar, M. Szibor, K. Fang, and B. Gaston. 2001. S-Nitrosylation of mitochondrial caspases. *J. Cell Biol.* 154:1111-1116.

Martins, L.M., T.J. Kottke, S.H. Kaufmann, and W.C. Earnshaw. 1998. Phosphorylated forms of activated caspases are present in cytosol from HL-60 cells during etoposide-induced apoptosis. *Blood* 92:3042-3049.

Matheson, J., X.Yu, A.B. Fielding, and G.W. Gould. 2005. Membrane traffic in cytokinesis. *Biochem. Soc. Trans.* 33:1290-1294.

Maurer-Stroh, S. and F.Eisenhaber. 2005. Refinement and prediction of protein prenylation motifs. *Genome Biol.* 6:R55.

Mauricio de Mendonca, S.M., J.L. Nepomuceno da Silva, Cunha e-Silva, W. de Souza, and L.U. Gazos. 2000. Characterization of a Rab11 homologue in *Trypanosoma cruzi*. *Gene* 243:179-185.

Mazzoni, C., E. Herker, V. Palermo, H. Jungwirth, T. Eisenberg, F. Madeo, and C. Falcone. 2005. Yeast caspase 1 links messenger RNA stability to apoptosis in yeast. *EMBO Rep.* 6:1076-1081.

McConville, M.J., K.A. Mullin, S.C. Ilgoutz, and R.D. Teasdale. 2002. Secretory pathway of trypanosomatid parasites. *Microbiol. Mol. Biol. Rev.* 66:122-154.

McGuffin, L.J., K. Bryson, and D.T. Jones. 2000. The PSIPRED protein structure prediction server. *Bioinformatics.* 16:404-405.

McKean, P.G. 2003. Coordination of cell cycle and cytokinesis in *Trypanosoma brucei*. *Curr. Opin. Microbiol.* 6:600-607.

McNicoll, F., J. Drummelsmith, M. Muller, E. Madore, N. Boilard, M. Ouellette, and B. Papadopoulou. 2006. A combined proteomic and transcriptomic approach to the study of stage differentiation in *Leishmania infantum*. *Proteomics.* 6:3567-3581.

Meier, P., A. Finch, and G. Evan. 2000. Apoptosis in development. *Nature* 407:796-801.

Melino, G., R.A. Knight, and P. Nicotera. 2005. How many ways to die? How many different models of cell death? *Cell Death. Differ.* 12 Suppl 2:1457-1462.

Milligan,K. University of Glasgow. PhD thesis.1996.

Misslitz, A., J.C. Mottram, P. Overath, and T. Aebischer. 2000. Targeted integration into a rRNA locus results in uniform and high level expression of transgenes in *Leishmania* amastigotes. *Mol. Biochem. Parasitol.* 107:251-261.

Mittl, P.R., S. Di Marco, J.F. Krebs, X. Bai, D.S. Karanewsky, J.P. Priestle, K.J. Tomaselli, and M.G. Grutter. 1997. Structure of recombinant human CPP32 in complex with the tetrapeptide acetyl-Asp-Val-Ala-Asp fluoromethyl ketone. *J. Biol. Chem.* 272:6539-6547.

Mittra, B., A. Saha, A.R. Chowdhury, C. Pal, S. Mandal, S. Mukhopadhyay, S. Bandyopadhyay, and H.K. Majumder. 2000. Luteolin, an abundant dietary component is a potent anti-leishmanial agent that acts by inducing topoisomerase II-mediated kinetoplast DNA cleavage leading to apoptosis. *Mol. Med.* 6:527-541.

Mogi, M. and A. Togari. 2003. Activation of caspases is required for osteoblastic differentiation. *J. Biol. Chem.* 278:47477-47482.

Montesino, R., R. Garcia, O. Quintero, and J.A. Cremata. 1998. Variation in N-linked oligosaccharide structures on heterologous proteins secreted by the methylotrophic yeast *Pichia pastoris. Protein Expr. Purif.* 14:197-207.

Moore, R.C., N.A. Durso, and R.J. Cyr. 1998. Elongation factor-1alpha stabilizes microtubules in a calcium/calmodulin-dependent manner. *Cell Motil. Cytoskeleton* 41:168-180.

Moreira, M.E., H.A. Del Portillo, R.V. Milder, J.M. Balanco, and M.A. Barcinski. 1996. Heat shock induction of apoptosis in promastigotes of the unicellular organism *Leishmania (Leishmania) amazonensis. J. Cell Physiol* 167:305-313.

Mottram, J.C., D.R. Brooks, and G.H. Coombs. 1998. Roles of cysteine proteinases of trypanosomes and *Leishmania* in host-parasite interactions. *Curr. Opin. Microbiol.* 1:455-460.

Mottram, J.C., M.J. Helms, G.H. Coombs, and M.Sajid. 2003. Clan CD cysteine peptidases of parasitic protozoa. *Trends Parasitol.* 19:182-187.

Mottram, J.C., B.P. McCready, K.G. Brown, and K.M. Grant. 1996a. Gene disruptions indicate an essential function for the LmmCRK1 cdc2-related kinase of *Leishmania mexicana. Mol. Microbiol* 22:573-583.

Mottram, J.C., A.E. Souza, J.E. Hutchison, R. Carter, M.J. Frame, and G.H. Coombs. 1996b. Evidence from disruption of the *lmcpb* gene array of *Leishmania mexicana* that cysteine proteinases are virulence factors. *Proc. Natl. Acad. Sci. U. S. A* 93:6008-6013.

Mukherjee, S.B., M. Das, G. Sudhandiran, and C. Shaha. 2002. Increase in cytosolic Ca2+ levels through the activation of non-selective cation channels induced by oxidative stress causes mitochondrial depolarization leading to apoptosis-like death in *Leishmania donovani* promastigotes. *J. Biol. Chem.* 277:24717-24727.

Mullin, K.A., B.J. Foth, S.C. Ilgoutz, J.M. Callaghan, J.L. Zawadzki, G.I. McFadden, and M.J. McConville. 2001. Regulated degradation of an endoplasmic reticulum membrane protein in a tubular lysosome in *Leishmania mexicana*. *Mol. Biol. Cell* 12:2364-2377.

N

Nakayama, K.I. and K. Nakayama. 2006. Ubiquitin ligases: cell-cycle control and cancer. *Nat. Rev. Cancer* 6:369-381.

Nandan, D., A. Cherkasov, R. Sabouti, T. Yi, and N.E. Reiner. 2003. Molecular cloning, biochemical and structural analysis of elongation factor-1 alpha from *Leishmania donovani*: comparison with the mammalian homologue. *Biochem. Biophys. Res. Commun.* 302:646-652.

Nasmyth, K., J.M. Peters, and F. Uhlmann. 2000. Splitting the chromosome: cutting the ties that bind sister chromatids. *Science* 288:1379-1385.

Nguewa, P.A., M.A. Fuertes, B. Valladares, C. Alonso, and J.M. Perez. 2004. Programmed cell death in trypanosomatids: a way to maximize their biological fitness? *Trends in Parasitology* 20:375-380.

Nicholson, D.W., A. Ali, N.A. Thornberry, J.P. Vaillancourt, C.K. Ding, M. Gallant, Y. Gareau, P.R. Griffin, M. Labelle, and Y.A. Lazebnik. 1995. Identification and inhibition of the ICE/CED-3 protease necessary for mammalian apoptosis. *Nature* 376:37-43.

Nicholson, D.W. and N.A. Thornberry. 2003. Apoptosis. Life and death decisions. *Science* 299:214-215.

Novick, P. and P. Brennwald. 1993. Friends and family: the role of the Rab GTPases in vesicular traffic. *Cell* 75:597-601.

Nuoffer, C. and W.E. Balch. 1994. GTPases: multifunctional molecular switches regulating vesicular traffic. *Annu. Rev. Biochem.* 63:949-990.

O

O'Beirne, C., C.M. Lowry, and H.P. Voorheis. 1998. Both IgM and IgG anti-VSG antibodies initiate a cycle of aggregation-disaggregation of bloodstream forms of *Trypanosoma brucei* without damage to the parasite. *Mol. Biochem. Parasitol.* 91:165-193.

Ogbadoyi, E., K. Ersfeld, D. Robinson, T. Sherwin, and K. Gull. 2000. Architecture of the *Trypanosoma brucei* nucleus during interphase and mitosis. *Chromosoma* 108:501-513.

Ogbadoyi, E.O., D.R. Robinson, and K. Gull. 2003. A high-order trans-membrane structural linkage is responsible for mitochondrial genome positioning and segregation by flagellar basal bodies in trypanosomes. *Mol. Biol. Cell* 14:1769-1779.

Ohta, K., M. Toriyama, M. Miyazaki, H. Murofushi, S. Hosoda, S. Endo, and H. Sakai. 1990. The mitotic apparatus-associated 51-kDa protein from sea urchin eggs is a GTP-binding protein and is immunologically related to yeast polypeptide elongation factor 1 alpha. *J. Biol. Chem.* 265:3240-3247.

Olivier, M., D.J. Gregory, and G. Forget. 2005. Subversion mechanisms by which Leishmania parasites can escape the host immune response: a signaling point of view. *Clin. Microbiol. Rev.* 18:293-305.

Olmsted, J.B. 1986. Microtubule-associated proteins. *Annu. Rev. Cell Biol.* 2:421-457.

P

Pal, A., B.S. Hall, T.R. Jeffries, and M.C. Field. 2003. Rab5 and Rab11 mediate transferrin and anti-variant surface glycoprotein antibody recycling in *Trypanosoma brucei*. *Biochem. J.* 374:443-451.

Papadopoulou, B., G. Roy, M. Breton, C. Kundig, C. Dumas, I. Fillion, A.K. Singh, M. Olivier, and M. Ouellette. 2002. Reduced infectivity of a *Leishmania donovani* biopterin transporter genetic mutant and its use as an attenuated strain for vaccination. *Infect. Immun.* 70:62-68.

Parodi, A.J. 1993. N-glycosylation in trypanosomatid protozoa. *Glycobiology* 3:193-199.

Pays, E., L. Vanhamme, and M. Berberof. 1994. Genetic controls for the expression of surface antigens in African trypanosomes. *Annu. Rev. Microbiol.* 48:25-52.

Pearson, T.W., R.P. Beecroft, S.C. Welburn, S. Ruepp, I. Roditi, K.Y. Hwa, P.T. Englund, C.W. Wells, and N.B. Murphy. 2000. The major cell surface glycoprotein procyclin is a receptor for induction of a novel form of cell death in African trypanosomes *in vitro*. *Mol. Biochem. Parasitol.* 111:333-349.

Pelissier, A., J.P. Chauvin, and T. Lecuit. 2003. Trafficking through Rab11 endosomes is required for cellularization during *Drosophila* embryogenesis. *Curr. Biol.* 13:1848-1857.

Peng, J., D. Schwartz, J.E. Elias, C.C. Thoreen, D. Cheng, G. Marsischky, J. Roelofs, D.Finley, and S.P.Gygi. 2003. A proteomics approach to understanding protein ubiquitination. *Nat. Biotechnol.* 21:921-926.

Piacenza, L., G. Peluffo, and R. Radi. 2001. L-arginine-dependent suppression of apoptosis in *Trypanosoma cruzi*: contribution of the nitric oxide and polyamine pathways. *Proc. Natl. Acad. Sci. U. S. A* 98:7301-7306.

Piacenza, L., G.Peluffo, and R. Radi. 2002. L-arginine metabolism in *Trypanosoma cruzi* in the regulation of programmed cell death. *Methods Enzymol.* 359:286-302.

Pils, B. and J. Schultz. 2004. Inactive enzyme-homologues find new function in regulatory processes. *J. Mol. Biol.* 340:399-404.

Ploubidou, A., D.R. Robinson, R.C. Docherty, E.O. Ogbadoyi, and K. Gull. 1999. Evidence for novel cell cycle checkpoints in trypanosomes: kinetoplast segregation and cytokinesis in the absence of mitosis. *J Cell Sci* 112 (Pt 24):4641-4650.

Porter, A.G. 1999. Protein translocation in apoptosis. *Trends Cell Biol.* 9:394-401.

Prasad, S., V.A. Soldatenkov, G. Srinivasarao, and A. Dritschilo. 1999. Intermediate filament proteins during carcinogenesis and apoptosis (Review). *Int. J. Oncol.* 14:563-570.

Pupkis, M.F., L. Tetley, and G.H. Coombs. 1986. *Leishmania mexicana*: amastigote hydrolases in unusual lysosomes. *Exp. Parasitol.* 62:29-39.

R

Raina, P. and S. Kaur. 2006. Chronic heat-shock treatment driven differentiation induces apoptosis in *Leishmania donovani*. *Mol. Cell Biochem.* 289:83-90.

Rawlings, N.D., F.R. Morton, and A.J. Barrett. 2006. MEROPS: the peptidase database. *Nucleic Acids Res.* 34:D270-D272.

Ridgley, E.L., Z.H. Xiong, and L. Ruben. 1999. Reactive oxygen species activate a Ca2+-dependent cell death pathway in the unicellular organism *Trypanosoma brucei brucei*. *Biochem. J.* 340 (Pt 1):33-40.

Riggs, B., W. Rothwell, S. Mische, G.R. Hickson, J. Matheson, T.S. Hays, G.W. Gould, and W. Sullivan. 2003. Actin cytoskeleton remodeling during early *Drosophila* furrow formation requires recycling endosomal components Nuclear-fallout and Rab11. *J. Cell Biol.* 163:143-154.

Roberts, E.C., K. Hammond, A.M. Traish, K.A. Resing, and N.G. Ahn. 2006. Identification of G2/M targets for the MAP kinase pathway by functional proteomics. *Proteomics.* 6:4541-4553.

Robertson, C.D. 1999. The *Leishmania mexicana* proteasome. *Mol. Biochem. Parasitol.* 103:49-60.

Robinson, D., P. Beattie, T. Sherwin, and K. Gull. 1991. Microtubules, tubulin, and microtubule-associated proteins of trypanosomes. *Methods Enzymol.* 196:285-299.

Robinson, D.N. and J.A. Spudich. 2000. Towards a molecular understanding of cytokinesis. *Trends Cell Biol.* 10:228-237.

Robinson, D.N. and J.A. Spudich. 2004. Mechanics and regulation of cytokinesis. *Curr. Opin. Cell Biol.* 16:182-188.

Robinson, D.R. and K. Gull. 1991. Basal body movements as a mechanism for mitochondrial genome segregation in the trypanosome cell cycle. *Nature* 352:731-733.

Robinson, D.R., T. Sherwin, A. Ploubidou, E.H. Byard, and K. Gull. 1995. Microtubule polarity and dynamics in the control of organelle positioning, segregation, and cytokinesis in the trypanosome cell cycle. *J. Cell Biol.* 128:1163-1172.

Robinson, K.A. and S.M. Beverley. 2003. Improvements in transfection efficiency and tests of RNA interference (RNAi) approaches in the protozoan parasite *Leishmania*. *Mol. Biochem. Parasitol.* 128:217-228.

Rodriguez, O.C., A.W. Schaefer, C.A. Mandato, P. Forscher, W.M. Bement, and C.M. Waterman-Storer. 2003. Conserved microtubule-actin interactions in cell movement and morphogenesis. *Nat. Cell Biol.* 5:599-609.

Rogers, M.E., M.L. Chance, and P.A. Bates. 2002. The role of promastigote secretory gel in the origin and transmission of the infective stage of *Leishmania mexicana* by the sandfly *Lutzomyia longipalpis*. *Parasitology* 124:495-507.

Rogers, M.E., T. Ilg, A.V. Nikolaev, M.A. Ferguson, and P.A. Bates. 2004. Transmission of cutaneous leishmaniasis by sand flies is enhanced by regurgitation of fPPG. *Nature* 430:463-467.

Roisin-Bouffay, C., M.F. Luciani, G. Klein, J.P. Levraud, M. Adam, and P. Golstein. 2004. Developmental cell death in *Dictyostelium* does not require paracaspase. *J. Biol. Chem.* 279:11489-11494.

Rotonda, J., D.W. Nicholson, K.M. Fazil, M. Gallant, Y. Gareau, M. Labelle, E.P. Peterson, D.M. Rasper, R. Ruel, J.P. Vaillancourt, N.A. Thornberry, and J.W. Becker. 1996. The three-dimensional structure of apopain/CPP32, a key mediator of apoptosis. *Nat. Struct. Biol.* 3:619-625.

Ruefli-Brasse, A.A., D.M. French, and V.M. Dixit. 2003. Regulation of NF-{kappa}B-dependent lymphocyte activation and development by paracaspase. *Science.* 302:1581-1584.

S

Sacks, D.L., G. Modi, E. Rowton, G. Spath, L. Epstein, S.J. Turco, and S.M. Beverley. 2000. The role of phosphoglycans in *Leishmania*-sand fly interactions. *Proc. Natl. Acad. Sci. U. S. A* 97:406-411.

Sahasrabuddhe, A.A., V.K. Bajpai, and C.M. Gupta. 2004. A novel form of actin in *Leishmania*: molecular characterisation, subcellular localisation and association with subpellicular microtubules. *Molecular and Biochemical Parasitology* 134:105-114.

Sambrook J. and Russell D.W. 2001. Molecular Cloning, a laboratory manual. CSHL Press.

Sasse, R. and K. Gull. 1988. Tubulin post-translational modifications and the construction of microtubular organelles in *Trypanosoma brucei*. *J. Cell Sci.* 90 (Pt 4):577-589.

Scholey, J.M., I. Brust-Mascher, and A. Mogilner. 2003. Cell division. *Nature* 422:746-752.

Schreiber, V., F. Dantzer, J.C. Ame, and G. de Murcia. 2006. Poly(ADP-ribose): novel functions for an old molecule. *Nat. Rev. Mol. Cell Biol.* 7:517-528.

Selvapandiyan, A., A. Debrabant, R. Duncan, J. Muller, P. Salotra, G. Sreenivas, J.L. Salisbury, and H.L. Nakhasi. 2004. Centrin gene disruption impairs stage-specific basal body duplication and cell cycle progression in *Leishmania*. *J. Biol. Chem.* 279:25703-25710.

Selvapandiyan, A. , R. Duncan, A. Debrabant, N. Lee, G. Sreenivas, P. Salotra, and H.L.Nakhasi. 2006. Genetically modified live attenuated parasites as vaccines for leishmaniasis. *Indian J. Med. Res.* 123:455-466.

Sen, N., B. Banerjee, B.B. Das, A. Ganguly, T. Sen, S. Pramanik, S. Mukhopadhyay, and H.K. Majumder. 2006a. Apoptosis is induced in leishmanial cells by a novel protein kinase inhibitor withaferin A and is facilitated by apoptotic topoisomerase I-DNA complex. *Cell Death. Differ.*Epub ahead of print.

Sen, N., B. Banerjee, S.S. Gupta, B.B. Das, A. Ganguly, and H.K. Majumder. 2006b. *Leishmania donovani*: Dyskinetoplastid cells survive and proliferate in the presence of pyruvate and uridine but do not undergo apoptosis after treatment with camptothecin. *Exp. Parasitol.* 114:204-214.

Sen, N., B.B. Das, A. Ganguly, B. Banerjee, T. Sen, and H.K. Majumder. 2006c. *Leishmania donovani:* intracellular ATP level regulates apoptosis-like death in luteolin induced dyskinetoplastid cells. *Exp. Parasitol.* 114:204-214.

Sen, N., B.B. Das, A. Ganguly, T. Mukherjee, S. Bandyopadhyay, and H.K. Majumder. 2004a. Camptothecin induced imbalance in intracellular cation homeostasis regulates programmed cell death in unicellular hemoflagellate *Leishmania donovani*. *J Biol Chem.* 279:52366-52375.

Sen, N., B.B. Das, A. Ganguly, T. Mukherjee, G. Tripathi, S. Bandyopadhyay, S. Rakshit, T. Sen, and H.K. Majumder. 2004b. Camptothecin induced mitochondrial dysfunction leading to programmed cell death in unicellular hemoflagellate *Leishmania donovani*. *Cell Death. Differ.*18:924-936.

Sereno, D., P. Holzmuller, I. Mangot, G. Cuny, A. Ouaissi, and J.L. Lemesre. 2001. Antimonial-mediated DNA fragmentation in *Leishmania infantum* amastigotes. *Antimicrob. Agents Chemother.* 45:2064-2069.

Seyfang, A., D. Mecke, and M. Duszenko. 1990. Degradation, recycling, and shedding of *Trypanosoma brucei* variant surface glycoprotein. *J. Protozool.* 37:546-552.

Sherwin, T. and K. Gull. 1989. The cell division cycle of *Trypanosoma brucei brucei*: timing of event markers and cytoskeletal modulations. *Philos. Trans. R. Soc. Lond B Biol. Sci.* 323:573-588.

Silva, R.D., R. Sotoca, B. Johansson, P. Ludovico, F. Sansonetty, M.T. Silva, J.M. Peinado, and M. Corte-Real. 2005. Hyperosmotic stress induces metacaspase- and mitochondria-dependent apoptosis in *Saccharomyces cerevisiae*. *Mol. Microbiol.* 58:824-834.

Simpson, L. 1968. Effect of acriflavin on the kinetoplast of *Leishmania tarentolae*. Mode of action and physiological correlates of the loss of kinetoplast DNA. *J. Cell Biol.* 37:660-682.

Simpson, L. 1986. Kinetoplast DNA in trypanosomid flagellates. *Int. Rev. Cytol.* 99:119-179.

Simpson, L. 1987. The mitochondrial genome of kinetoplastid protozoa: genomic organization, transcription, replication, and evolution. *Annu. Rev. Microbiol.* 41:363-382.

Simpson, L. and F. Kretzer. 1997. The mitochondrion in dividing *Leishmania tarentolae* cells is symmetric and circular and becomes a single asymmetric tubule in non-dividing cells due to division of the kinetoplast portion. *Mol. Biochem. Parasitol.* 87:71-78.

Sinclair, G. and F.Y. Choy. 2002. Synonymous codon usage bias and the expression of human glucocerebrosidase in the methylotrophic yeast, *Pichia pastoris*. *Protein Expr. Purif.* 26:96-105.

Singh, G., K.G. Jayanarayan, and C.S. Dey. 2005. Novobiocin induces apoptosis-like cell death in topoisomerase II over-expressing arsenite resistant *Leishmania donovani*. *Mol. Biochem. Parasitol.* 141:57-69.

Skeiky, Y.A., R.N. Coler, M. Brannon, E. Stromberg, K. Greeson, R.T. Crane, J.R. Webb, A. Campos-Neto, and S.G. Reed. 2002. Protective efficacy of a tandemly linked, multi-subunit recombinant leishmanial vaccine (Leish-111f) formulated in MPL adjuvant. *Vaccine* 20:3292-3303.

Skop, A.R., D. Bergmann, W.A. Mohler, and J.G. White. 2001. Completion of cytokinesis in C. elegans requires a brefeldin A-sensitive membrane accumulation at the cleavage furrow apex. *Curr. Biol.* 11:735-746.

Snipas, S.J., H.R. Stennicke, S. Riedl, J. Potempa, J. Travis, A.J. Barrett, and G.S. Salvesen. 2001. Inhibition of distant caspase homologues by natural caspase inhibitors. *Biochem. J.* 357:575-580.

Snipas, S.J., E. Wildfang, T. Nazif, L. Christensen, K.M. Boatright, M. Bogyo, H.R. Stennicke, and G.S. Salvesen. 2004. Characteristics of the caspase-like catalytic domain of human paracaspase. *Biol. Chem.* 385:1093-1098.

Soto, M., S. Iborra, L. Quijada, C. Folgueira, C. Alonso, and J.M. Requena. 2004. Cell-cycle-dependent translation of histone mRNAs is the key control point for regulation of histone biosynthesis in *Leishmania infantum*. *Biochem. J.* 379:617-625.

Spath, G.F., L. Epstein, B. Leader, S.M. Singer, H.A. Avila, S.J. Turco, and S.M. Beverley. 2000. Lipophosphoglycan is a virulence factor distinct from related glycoconjugates in the protozoan parasite *Leishmania major*. *Proc. Natl. Acad. Sci. U. S. A* 97:9258-9263.

Sperandio, S., B. De, I, and D.E. Bredesen. 2000. An alternative, nonapoptotic form of programmed cell death. *Proc. Natl. Acad. Sci. U. S. A* 97:14376-14381.

Stark, C., B.J. Breitkreutz, T. Reguly, L. Boucher, A. Breitkreutz, and M. Tyers. 2006. BioGRID: a general repository for interaction datasets. *Nucleic Acids Res.* 34:D535-D539.

Stennicke, H.R. and G.S. Salvesen. 1999. Catalytic properties of the caspases. *Cell Death. Differ.* 6:1054-1059.

Stennicke, H.R. and G.S. Salvesen. 2000. Caspases - controlling intracellular signals by protease zymogen activation. *Biochim. Biophys. Acta* 1477:299-306.

Stierhof, Y.D., P.A. Bates, R.L. Jacobson, M.E. Rogers, Y. Schlein, E. Handman, and T. Ilg. 1999. Filamentous proteophosphoglycan secreted by *Leishmania* promastigotes forms gel-like three-dimensional networks that obstruct the digestive tract of infected sandfly vectors. *Eur. J. Cell Biol.* 78:675-689.

Strickland, L.I. and D.R. Burgess. 2004. Pathways for membrane trafficking during cytokinesis. *Trends Cell Biol* 14:115-118.

Suarez, M.F., L.H. Filonova, A. Smertenko, E.I. Savenkov, D.H. Clapham, S. Von Arnold, B. Zhivotovsky, and P.V .Bozhkov. 2004. Metacaspase-dependent programmed cell death is essential for plant embryogenesis. *Curr. Biol.* 14:R339-R340.

Sudhandiran, G. and C. Shaha. 2003. Antimonial-induced increase in intracellular Ca2+ through non-selective cation channels in the host and the parasite is responsible for apoptosis of intracellular *Leishmania donovani* amastigotes. *J. Biol. Chem.* 278:25120-25132.

Sudol, M. and T. Hunter. 2000. NeW wrinkles for an old domain. *Cell* 103:1001-1004.

Swanson, M.M. and C.A. Poodry. 1980. Pole cell formation in *Drosophila melanogaster*. *Dev. Biol.* 75:419-430.

Szallies, A., B.K. Kubata, and M. Duszenko. 2002. A metacaspase of *Trypanosoma brucei* causes loss of respiration competence and clonal death in the yeast *Saccharomyces cerevisiae*. *FEBS Lett.* 517:144-150.

T

Talapatra, S., J.D. Wagner, and C.B. Thompson. 2002. Elongation factor-1 alpha is a selective regulator of growth factor withdrawal and ER stress-induced apoptosis. *Cell Death. Differ.* 9:856-861.

Tandon, A. and P. Fraser. 2002. The presenilins. *Genome Biol.* 3:reviews3014.

Tetaud, E., I. Lecuix, T. Sheldrake, T. Baltz, and A.H. Fairlamb. 2002. A new expression vector for *Crithidia fasciculata* and *Leishmania*. *Mol. Biochem. Parasitol.* 120:195-204.

Thome, M., P. Schneider, K. Hofmann, H. Fickenscher, E. Meinl, F. Neipel, C. Mattmann, K. Burns, J.L. Bodmer, M. Schroter, C. Scaffidi, P.H. Krammer, M.E. Peter, and J. Tschopp. 1997. Viral FLICE-inhibitory proteins (FLIPs) prevent apoptosis induced by death receptors. *Nature* 386:517-521.

Thornberry, N.A. and Y. Lazebnik. 1998. Caspases: enemies within. *Science* 281:1312-1316.

Tian, R., G.Y. Zhang, C.H. Yan, and Y.R.Dai. 2000. Involvement of poly(ADP-ribose) polymerase and activation of caspase-3-like protease in heat shock-induced apoptosis in tobacco suspension cells. *FEBS Lett.* 474:11-15.

Tong, A.H., B. Drees, G. Nardelli, G.D. Bader, B. Brannetti, L. Castagnoli, M. Evangelista, S. Ferracuti, B. Nelson, S. Paoluzi, M. Quondam, A. Zucconi, C.W. Hogue, S. Fields, C. Boone, and G. Cesareni. 2002. A combined experimental and computational strategy to define protein interaction networks for peptide recognition modules. *Science* 295:321-324.

Traub, L.M. and S. Kornfeld. 1997. The trans-Golgi network: a late secretory sorting station. *Curr. Opin. Cell Biol.* 9:527-533.

Tsuda, A., W.H. Witola, K. Ohashi, and M. Onuma. 2005. Expression of alternative oxidase inhibits programmed cell death-like phenomenon in bloodstream form of *Trypanosoma brucei rhodesiense*. *Parasitol. Int.* 54:243-251.

Turco, S.J., G.F. Spath, and S.M. Beverley. 2001. Is lipophosphoglycan a virulence factor? A surprising diversity between Leishmania species. *Trends Parasitol.* 17:223-226.

U

Ueda-Nakamura, T., M. Attias, and W. de Souza. 2001. Megasome biogenesis in *Leishmania amazonensis*: a morphometric and cytochemical study. *Parasitol. Res.* 87:89-97.

Uetz, P., L. Giot, G. Cagney, T.A. Mansfield, R.S. Judson, J.R. Knight, D. Lockshon, V. Narayan, M. Srinivasan, P. Pochart, A. Qureshi-Emili, Y. Li, B. Godwin, D. Conover, T. Kalbfleisch, G. Vijayadamodar, M. Yang, M. Johnston, S. Fields, and J.M. Rothberg. 2000. A comprehensive analysis of protein-protein interactions in *Saccharomyces cerevisiae*. *Nature* 403:623-627.

Uhlmann, F. 2001. Secured cutting: controlling separase at the metaphase to anaphase transition. *EMBO Rep.* 2:487-492.

Umeda, M. and K. Emoto. 1999. Membrane phospholipid dynamics during cytokinesis: regulation of actin filament assembly by redistribution of membrane surface phospholipid. *Chem. Phys. Lipids* 101:81-91.

Uren, A.G., K. O'Rourke, L.A. Aravind, M.T. Pisabarro, S. Seshagiri, E.V. Koonin, and V.M.Dixit. 2000. Identification of paracaspases and metacaspases: two ancient families of caspase-like proteins, one of which plays a key role in MALT lymphoma. *Mol. Cell* 6:961-967.

Urena, F. 1986. Three-dimensional reconstructions of the mitotic spindle and dense plaques in three species of *Leishmania*. *Z. Parasitenkd.* 72:299-306.

Urena, F. 1988. Ultrastructure of the mitotic nuclei in *Leishmania mexicana* ssp. Tridimensional reconstruction of the mitotic spindle and dense plaques. *Rev. Biol. Trop.* 36:129-137.

Uzonna, J.E., G.F. Spath, S.M. Beverley, and P. Scott. 2004. Vaccination with phosphoglycan-deficient *Leishmania major* protects highly susceptible mice from virulent challenge without inducing a strong Th1 response. *J. Immunol.* 172:3793-3797.

V

Valouev, I.A., V.V. Kushnirov, and M.D. Ter Avanesyan. 2002. Yeast polypeptide chain release factors eRF1 and eRF3 are involved in cytoskeleton organization and cell cycle regulation. *Cell Motil. Cytoskeleton* 52:161-173.

van Oers, N.S. and Z.J. Chen. 2005. Cell biology. Kinasing and clipping down the NF-kappa B trail. *Science* 308:65-66.

van Vliet, C., E.C. Thomas, A. Merino-Trigo, R.D. Teasdale, and P.A. Gleeson. 2003. Intracellular sorting and transport of proteins. *Prog. Biophys. Mol. Biol.* 83:1-45.

van Zandbergen, G., A. Bollinger, A. Wenzel, S. Kamhawi, R. Voll, M. Klinger, A. Muller, C. Holscher, M. Herrmann, D. Sacks, W. Solbach, and T. Laskay. 2006. *Leishmania* disease development depends on the presence of apoptotic promastigotes in the virulent inoculum. *Proc. Natl. Acad. Sci. U. S. A* 103:13837-13842.

van Zandbergen, G., M. Klinger, A. Mueller, S. Dannenberg, A. Gebert, W. Solbach, and T. Laskay. 2004. Cutting edge: neutrophil granulocyte serves as a vector for *Leishmania* entry into macrophages. *J. Immunol.* 173:6521-6525.

Vance, J.E. and Y.J. Shiao. 1996. Intracellular trafficking of phospholipids: import of phosphatidylserine into mitochondria. *Anticancer Res.* 16:1333-1339.

Vardi, A., I. Berman-Frank, T. Rozenberg, O. Hadas, A. Kaplan, and A. Levine. 1999. Programmed cell death of the dinoflagellate *Peridinium gatunense* is mediated by CO(2) limitation and oxidative stress. *Curr. Biol.* 9:1061-1064.

Vedrenne, C., C. Giroud, D.R. Robinson, S. Besteiro, C. Bosc, F. Bringaud, and T. Baltz. 2002. Two related subpellicular cytoskeleton-associated proteins in *Trypanosoma brucei* stabilize microtubules. *Mol. Biol. Cell* 13:1058-1070.

Veitch, N.J., D.A. Maugeri, J.J. Cazzulo, Y. Lindqvist, and M.P. Barrett. 2004. Transketolase from *Leishmania mexicana* has a dual subcellular localization. *Biochem. J.* 382:759-767.

Vercammen, D., B. Belenghi, C.B. Van De, T. Beunens, J.A. Gavigan, R. De Rycke, A. Brackenier, D. Inze, J.L. Harris, and F. Van Breusegem. 2006. Serpin1 of *Arabidopsis thaliana* is a suicide inhibitor for metacaspase 9. *J. Mol. Biol.* 364:625-636.

Vercammen, D., C.B. Van De, G. De Jaeger, D. Eeckhout, P. Casteels, K. Vandepoele, I. Vandenberghe, J. Van Beeumen, D. Inze, and F. Van Breusegem. 2004. Type-II metacaspases Atmc4 and Atmc9 of *Arabidopsis thaliana* cleave substrates after arginine and lysine. *J Biol. Chem.* 279:45329-45336.

Vergnes, B., D. Sereno, N. Madjidian-Sereno, J.L. Lemesre, and A. Ouaissi. 2002. Cytoplasmic SIR2 homologue overexpression promotes survival of *Leishmania* parasites by preventing programmed cell death. *Gene* 296:139-150.

Vergnes, B., D. Sereno, J. Tavares, A. Cordeiro-da-Silva, L. Vanhille, N. Madjidian-Sereno, D. Depoix, A. Monte-Alegre, and A. Ouaissi. 2005a. Targeted disruption of cytosolic SIR2 deacetylase discloses its essential role in *Leishmania* survival and proliferation. *Gene* 363:85-96.

Vergnes, B., L. Vanhille, A. Ouaissi, and D. Sereno. 2005b. Stage-specific antileishmanial activity of an inhibitor of SIR2 histone deacetylase. *Acta Trop.* 94:107-115.

Verma, N.K. and C.S. Dey. 2004. Possible mechanism of miltefosine-mediated death of *Leishmania donovani*. *Antimicrob. Agents Chemother.* 48:3010-3015.

Vickerman, K. 1994. The evolutionary expansion of the trypanosomatid flagellates. *Int. J. Parasitol.* 24:1317-1331.

W- X- Z

Wadskog, I., C. Maldener, A. Proksch, F. Madeo, and L. Adler. 2004. Yeast lacking the SRO7/SOP1-encoded tumor suppressor homologue show increased susceptibility to apoptosis-like cell death on exposure to NaCl stress. *Mol. Biol. Cell* 15:1436-1444.

Waller, R.F. and M.J. McConville. 2002. Developmental changes in lysosome morphology and function *Leishmania* parasites. *Int. J. Parasitol.* 32:1435-1445.

Watanabe, N. and E. Lam. 2005. Two *Arabidopsis* metacaspases AtMCP1b and AtMCP2b are arginine/lysine-specific cysteine proteases and activate apoptosis-like cell death in yeast. *J Biol. Chem.* 280:14691-14699.

Watanabe, S., K. Sakurai, A. Amagai, and Y. Maeda. 2003. Unexpected roles of a *Dictyostelium* homologue of eukaryotic EF-2 in growth and differentiation. *J. Cell Sci.* 116:2647-2654.

Weinberger, M., L. Ramachandran, L. Feng, K. Sharma, X. Sun, M. Marchetti, J.A. Huberman, and W.C. Burhans. 2005. Apoptosis in budding yeast caused by defects in initiation of DNA replication. *J Cell Sci* 118:3543-3553.

Welburn, S.C., M.A. Barcinski, and G.T. Williams. 1997. Programmed cell death in trypanosomatids. *Parasitol. Today* 13:22-26.

Welburn, S.C., S. Lillico, and N.B. Murphy. 1999. Programmed cell death in procyclic form *Trypanosoma brucei rhodesiense* --identification of differentially expressed genes during con A induced death. *Mem. Inst. Oswaldo Cruz* 94:229-234.

Welburn, S.C. and I. Maudlin. 1997. Control of *Trypanosoma brucei brucei* infections in tsetse, Glossina morsitans. *Med. Vet. Entomol.* 11:286-289.

Welburn, S.C., I. Maudlin, and D.S. Ellis. 1989. Rate of trypanosome killing by lectins in midguts of different species and strains of *Glossina*. *Med. Vet. Entomol.* 3:77-82.

Welburn, S.C. and N.B. Murphy. 1998. Prohibitin and RACK homologues are up-regulated in trypanosomes induced to undergo apoptosis and in naturally occurring terminally differentiated forms. *Cell Death. Differ.* 5:615-622.

Wilcke, M., L. Johannes, T. Galli, V. Mayau, B. Goud, and J. Salamero. 2000. Rab11 regulates the compartmentalization of early endosomes required for efficient transport from early endosomes to the trans-golgi network. *J. Cell Biol.* 151:1207-1220.

Williams, R.A., L. Tetley, J.C. Mottram, and G.H. Coombs. 2006. Cysteine peptidases CPA and CPB are vital for autophagy and differentiation in *Leishmania mexicana*. *Mol. Microbiol.* 61:655-674.

Wilson, G.M., A.B. Fielding, G.C. Simon, X.Yu, P.D. Andrews, R.S. Hames, A.M. Frey, A.A. Peden, G.W. Gould, and R. Prekeris. 2005. The FIP3-Rab11 protein complex regulates recycling endosome targeting to the cleavage furrow during late cytokinesis. *Mol Biol. Cell* 16:849-860.

Wincker, P., C. Ravel, C. Blaineau, M. Pages, Y. Jauffret, J.P. Dedet, and P. Bastien. 1996. The *Leishmania* genome comprises 36 chromosomes conserved across widely divergent human pathogenic species. *Nucleic Acids Res.* 24:1688-1694.

Wirtz, E., C. Hartmann, and C. Clayton. 1994. Gene expression mediated by bacteriophage T3 and T7 RNA polymerases in transgenic trypanosomes. *Nucleic Acids Res.* 22:3887-3894.

Wirtz, E., S. Leal, C. Ochatt, and G.A. Cross. 1999. A tightly regulated inducible expression system for conditional gene knock-outs and dominant-negative genetics in *Trypanosoma brucei*. *Mol. Biochem. Parasitol.* 99:89-101.

Woods, A., A.J. Baines, and K. Gull. 1989. Evidence for a Mr 88,000 glycoprotein with a transmembrane association to a unique flagellum attachment region in *Trypanosoma brucei*. *J. Cell Sci.* 93 (Pt 3):501-508.

Woodward, R. and K. Gull. 1990. Timing of nuclear and kinetoplast DNA replication and early morphological events in the cell cycle of *Trypanosoma brucei*. *J. Cell Sci.* 95 (Pt 1):49-57.

Wu, Y., X. Wang, X. Liu, and Y. Wang. 2003. Data-mining approaches reveal hidden families of proteases in the genome of malaria parasite. *Genome Res.* 13:601-616.

Xenarios, I., D.W. Rice, L. Salwinski, M.K. Baron, E.M. Marcotte, and D. Eisenberg. 2000. DIP: the database of interacting proteins. *Nucleic Acids Res.* 28:289-291.

Zangger, H., J.C. Mottram, and N. Fasel. 2002. Cell death in *Leishmania* induced by stress and differentiation: programmed cell death or necrosis? *Cell Death. Differ.* 9:1126-1139.

Zermati, Y., C. Garrido, S. Amsellem, S. Fishelson, D. Bouscary, F. Valensi, B. Varet, E. Solary, and O. Hermine. 2001. Caspase activation is required for terminal erythroid differentiation. *J. Exp. Med.* 193:247-254.